Nitrogen-rich compounds as precursors to novel silicon nitrides:
hydrido(azido)silanes, low-valent silicon azides, pentazoles

Matthew M. Y. Crawford

A thesis submitted in partial fulfilment of the requirements for the degree of
Doctor of Philosophy

The University of Sheffield
Faculty of Science
Department of Chemistry

September 2023

Acknowledgements

First, I would like to thank my supervisor, Dr Peter Portius, for his guidance during this project. Prior to working in his research group, I had been told he was "quite the character", to which my confused response was: "what is that supposed to mean?". Having worked with him for four years, I can confidently say that his open-minded attitude and unwavering dedication to scientific principles is indeed what you would call "quite the character", and an inspiration to those of us who pursue scientific discovery. His considerable expertise has led to many valuable discussions from which this work has greatly benefited, and I am grateful to have had him as my supervisor for this project.

I owe considerable gratitude to the NMR support staff, Dr Sandra van Meurs and Dr Khalid Doudin, for training me on the use of NMR instruments. They generously allowed me to spend time on the NMR service instruments, without which the considerable number of ^{29}Si spectra and reaction monitoring experiments recorded during this work would not have been possible (seriously, I used an absurd amount of instrument time, thanks for always putting up with me). I would like to extend this gratitude to Dr Craig Robertson, who, in addition to also providing some NMR support, taught me on the operation of single-crystal X-ray diffractometers, and helped me with solving difficult structures. The technical support staff have been extremely friendly and helpful, from which I have learned much that was not only beneficial to this work but will also undoubtedly be valuable to me in the future.

I would also like to thank the other members of the Portius group, who have been alongside me throughout the project. Dr Thomas Speak, who taught me almost everything I know about computational chemistry, as well as performing much of the silanes calculations in this work. My fellow PhD students, Bradley Westwater (now with a Dr. title, congratulations), who's seemingly limitless motivation in the lab gave me inspiration to keep up my own work, and William Greenwood, who has been a friendly, much-needed source of conversation making my time in Sheffield more enjoyable. Finally, the MChem/MSc students whom I have supervised – Callum Evans, Zekun Han and Michael Jones, who have been learning along with me on what has been a challenging but enjoyable research project.

Abstract

Multiple hydrido(azido)silicon compounds have been synthesised as precursors for low-valent silicon azides. The conversion of $HSiCl_3$ to $HSi(N_3)_3$ with $TMS(N_3)$ (TMS = trimethylsilyl) has been monitored, affording NMR data on all species of the form $HSiX_3$, H_2SiX_2 and H_3SiX (X = Cl, N_3). $HSi(N_3)_3$ has been synthesised free of disproportionation for the first time, using the reagent $NaAl(N_3)_4$. The synthesis of the known complex $(^{Dipp}NCN)SiH(N_3)_2$ (NCN = amidinato ligand) has been greatly optimised, and the optimised methods used to make the new complexes $(^{tBu}NCN)SiH(N_3)_2$ and $(^{TMS}NCN)SiH(N_3)_2$. The reactivity of $(^{Dipp}NCN)SiH(N_3)_2$ towards $Na(^{Dipp}NCN)$ and $LiSi(TMS)_3$ has been tested, affording a hexacoordinate hydrido(azido)silicon complex, $(^{Dipp}NCN)_2Si(N_3)_2$, and a hydridosilaimine, $(^{Dipp}NCN)Si(H)=NSi(TMS)_3$. Another silaimine, $(^{Dipp}NCN)Si(N_3)=NSi(TMS)_3$ was also synthesised, starting from $(^{Dipp}NCN)Si(N_3)_3$. While synthesising $(^{Dipp}NCN)Si(N_3)_3$, $[(^{Dipp}NCN)H_2][Si(N_3)_5]$ was also obtained, containing a new homoleptic azidosilicon species, $Si(N_3)_5^-$. Thermal decomposition of $(^{Dipp}NCN)SiH(N_3)_2$ affords two distinct silicon-nitrogen binary compounds, with empirical formulae of SiN_2 and SiN_4. The latter of these contains an azido group and is thus hypothesised to be an amorphous azido(nitrido)silicon polymer, $[Si(N)(N_3)]_n$.

The reaction of $Si(N_3)_4$ with alkali metals does not afford low-valent azidosilicon products. This reduction mostly likely affords elemental silicon by analogy to known reductions of $SiCl_4$. In one case, traces of material with a matching infrared spectrum to $[Si(N)(N_3)]_n$ were observed. Reaction of $Si(N_3)_4$ with $LiN(TMS)_2$ affords $(TMS)_2N-Si(N_3)_3$. Catalytic decomposition of this product can be induced with $PPN(N_3)$ ($PPN^+ = [N(PPh_3)_2]^+$), affording $TMS(N_3)$ and, based on stoichiometry, $[Si(N)(N_3)]_n$. The material formed from this reaction matches the infrared spectrum of the $[Si(N)(N_3)]_n$ formed from the decomposition of $(^{Dipp}NCN)SiH(N_3)_2$.

Reaction of $IPrSiCl_2$ with azide-transfer reagents results in de-coordination of the IPr ligand from the silicon. In one case, $[Si(N)(N_3)]_n$ was observed by IR spectroscopy, which may result from the *in-situ* decomposition of $Si(N_3)_2$. Alternative low-valent silicon chlorides were investigated as precursors for low-valent silicon azides. The ligands 2,6-bis(N-(2,6-diisopropylphenyl)acetimino)pyridine (BIP) and 2,2';6',2''-terpyridine were found to react with Si_2Cl_6 to afford complexes of $SiCl_2$. In all cases, modification of the ligand took place

alongside coordination. Among these products, (^{SiCl3}BIP)SiCl$_2$ represents the first silicon complex containing a bis(imino)pyridine ligand. A selective synthesis for SiCl$_3^-$ in solution has been developed, however attempts to remove this ion from solution result in its decomposition.

As the pentazolyl group is an alternative nitrogen-rich functional group to the azido group, the synthesis of pentazole derivatives from neutral diazo compounds has been investigated. Diazocyclopentadiene, tetramethyldiazocyclopentadiene, phosphoryl azide and hyponitrous acid were found to be unreactive towards azide, attributed to them being insufficiently electrophilic. 2-diazoimidazole was observed to react with azide ions, but produced inextricable products. Sulphuryl azide (SO$_2$(N$_3$)$_2$) reacts with azide ions to afford SO$_2$(N$_3$)$^-$ with loss of N$_2$, which is predicted to proceed *via* a pentazole intermediate. Diazoquinone is observed to react with azide ions to afford the known pentazole compound, 4-pentazolylphenoxide.

Table of Contents

List of Abbreviations

Functional groups

iPr	isopropyl
tBu	tert-butyl
Ph	phenyl
Dipp	2,6-diisopropylphenyl
Mes*	2,4,6-tri-tert-butylphenyl
Ar	aryl (specifically 4-tert-butylphenyl for ^{Dipp}NCN)
Ac	acetyl
TMS	trimethylsilyl
Ts	tosyl (*para*-toluenesulphonyl)
Cp	cyclopentadienyl
Cp^x	tetramethylcyclopentadienyl
Cp*	pentamethylcyclopentadienyl
R	unspecified organic group
NCN	amidinato group with unspecified substituents
^{Dipp}NCN	N,N'-bis(2,6-diisopropylphenyl)-(4-tert-butylphenyl)amidinato group
^{tBu}NCN	N,N'-di(tert-butyl)phenylamidinato group
^{TMS}NCN	N,N'-bis(trimethylsilyl)phenylamidinato group
NacNac	pentan-1,3-diketimino group with unspecified substituents
^{Dipp}NacNac	N,N'-bis(2,6-diisopropylphenyl)pentan-1,3-diketimino group
^{Mes}NacNac	N,N'-bis(2,4,6-trimethylphenyl)pentan-1,3-diketimino group
PPN$^+$	bis(triphenylphosphine)iminium cation $[N(PPh_3)_2]^+$

Compounds

15c5	15-crown-5 (1,4,7,10,13-pentaoxacyclopentadecane)
18c6	18-crown-6 (1,4,7,10,13,16-hexaoxacyclooctadecane)
ATAC	2,4-diazido-2,4-di-tert-butyl-1,3-bis(azido(DippNacNac)aluminyl)cyclodisilazane
BIP	2,6-bis(N-(2,6-diisopropylphenyl)acetimino)pyridine
CpN$_2$	diazocyclopentadiene
Cp^{x}N$_2$	tetramethyldiazocyclopentadiene
DCM	dichloromethane
DIPEA	diisopropylethylamine
DME	dimethoxyethane
DMSO	dimethylsulphoxide
HMPA	hexamethylphosphoramide
HTTCT	1,1,1,4,4,4-hexakis(trimethylsilyl)-2,2,3,3-tetrachlorotetrasilane

HTTMT	1,1,1,4,4,4-hexakis(trimethylsilyl)-2,2,3,3-tetramethyltetrasilane
IPr	1,3-bis(2,6-diisopropylphenyl)imidazol-2-ylidene
ab-IPr	1,3-bis(2,6-diisopropylphenyl)imidazol-4-ylidene
ItBu	1,3-di-tert-butylimidazol-2-ylidene
ab-ItBu	1,3-di-tert-butylimidazol-4-ylidene
NHC	unspecified N-heterocyclic carbene
TABTC	2,2,4,4-tetraazido-1,3-bis(tris(trimethylsilyl)silyl)cyclodisilazane
Terpy	2,2';6',2''-terpyridine
THF	tetrahydrofuran

Analytical data

IR	infrared
NMR	nuclear magnetic resonance
SCXRD	single-crystal X-ray diffraction analysis
δ	chemical shift (NMR spectroscopy)
ν	wavenumber (IR spectroscopy)
ppm	parts per million
vs	very strong absorption (IR data)
s	strong absorption (IR data)
m	medium absorption (IR data)
w	weak absorption (IR data)
vw	very weak absorption (IR data)
s	singlet signal (NMR data)
d	doublet signal (NMR data)
t	triplet signal (NMR data)
q	quartet signal (NMR data)
sept	septet signal (NMR data)
m	complex multiplet signal (NMR data)
br	broad signal (IR and NMR data)
vbr	very broad signal (IR and NMR data)
$^3J_{H-H}$	three-bond ^1H-^1H coupling constant
$^1J_{Si-H}$	one-bond ^{29}Si-^1H coupling constant
$^2J_{Si-H}$	two-bond ^{29}Si-^1H coupling constant

Others

eq.	equivalents
~	approximately
Δ	heat applied (reaction diagrams)
hν	light applied (reaction diagrams)

1. Introduction

Silicon nitride has an important role in modern society, being used as an insulating and protective material in semiconductor manufacturing due to its durability and chemical resistance.[1] In addition, it sees extensive use in industrial tools due to its high hardness and durability at high temperatures.[2] Current synthetic methods to produce silicon nitride (Figure 1.1) rely on high temperature processes that are energy consuming. Additionally, the lower temperature vapour deposition methods use precursors which may introduce undesired chemical elements – notably hydrogen and chlorine.[1, 3]

$$3\,Si \ + \ 2\,N_2 \ \xrightarrow{\ 1300 - 1400\ ^\circ C\ } \ \alpha\text{-}Si_3N_4$$

$$3\,SiO_2 \ + \ 6\,C \ + \ 2\,N_2 \ \xrightarrow{\ 1450 - 1500\ ^\circ C\ } \ \alpha\text{-}Si_3N_4 \ + \ 6\,CO$$

$$3\,Si(NH)_2 \ \xrightarrow{\ 1000\ ^\circ C\ } \ Si_3N_4 \ + \ N_2 \ + \ 3\,H_2$$

$$3\,SiH_4 \ + \ 4\,NH_3 \ \xrightarrow{\ 700 - 900\ ^\circ C\ } \ Si_3N_4 \ + \ 12H_2 \quad \text{Atmospheric Pressure Chemical Vapour Deposition}$$

$$3\,SiH_2Cl_2 \ + \ 4\,NH_3 \ \xrightarrow{\ 700 - 800\ ^\circ C\ } \ Si_3N_4 \ + \ 6\,HCl \ + \ 6\,H_2 \quad \text{Low Pressure Chemical Vapour Deposition}$$

$$SiH_4 \ + \ NH_3 \ \xrightarrow{\ 200 - 550\ ^\circ C\ } \ Si_xN_yH_z \ + \ H_2 \quad \text{Plasma Enhanced Chemical Vapour Deposition}$$

Figure 1.1. Existing syntheses of silicon nitride.[3, 4]

Silicon azides have the potential to serve as alternative precursors to silicon nitride. Experimental studies have shown that azido-silicon complexes thermally decompose with elimination of N_2,[5, 6] which is backed up by calculations on a structurally similar phosphorous complex, hexaazidophosphate $(P(N_3)_6^-)$.[7] Additionally, these decomposition processes occur at relatively low temperatures of 200 – 300 °C. Hence, the formation of silicon nitrides could be envisioned by thermal decomposition of silicon azides with removal of the excess nitrogen content *via* N_2 elimination. Not only would this result in a less energy-intensive synthesis, this method may also allow for the isolation of novel silicon-nitrogen compounds that are not stable at the high temperatures of existing silicon nitride syntheses.

$$\text{Si(N}_3)_4 \xrightarrow{\Delta} x\text{N}_2 + \text{SiN}_{12\text{-}2x}$$

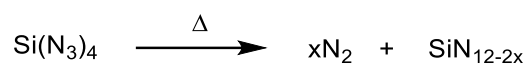**Figure 1.2.** Hypothetical thermal decomposition of silicon tetraazide ($\text{Si(N}_3)_4$).

Pure silicon tetraazide ($\text{Si(N}_3)_4$) is highly explosive,[8] which complicates the use of it as a reagent for experimental work. Thermal decomposition of pure $\text{Si(N}_3)_4$ would be hazardous outside of solution, while high-temperature decomposition of solution-phase $\text{Si(N}_3)_4$ may result in reaction with the solvent. As an alternative process to thermal decomposition, the conversion of an azide to a nitride can be viewed as a reduction, as per the half-equation in Figure 1.3.
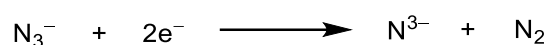
$$\text{N}_3^- + 2e^- \longrightarrow \text{N}^{3-} + \text{N}_2$$

Figure 1.3. Two-electron reduction of an azide ion to afford nitride with elimination of N_2.

Thus, in forming silicon nitrides from silicon azides, ways to facilitate the reduction of silicon azides must be considered. Plausible methods include treatment of silicon azides with strong reducing agents, reductive elimination of azido-silicon complexes, or the addition of azido groups to already reduced silicon species. Some of these methods may proceed via low-valent silicon azides as intermediates – a yet unreported class of compounds of great interest to the field of main-group chemistry.

1.1. Azide chemistry

1.1.1. Synthesis, structure, and coordination

The azide ion is a triatomic anion consisting of only nitrogen. Azides have been known for well over a century, with sodium azide (NaN_3) being reported in 1890 from the treatment benzoyl hydrazine with nitrous acid, followed by reaction of the resulting benzoyl azide with sodium hydroxide.[9] Modern syntheses of NaN_3 instead use either the reaction of sodium amide with nitrous oxide, or sodium hydroxide with hydrazine and a nitrite ester (Figure 1.4).[10-12] Other azide-containing compounds are then typically derived from NaN_3.

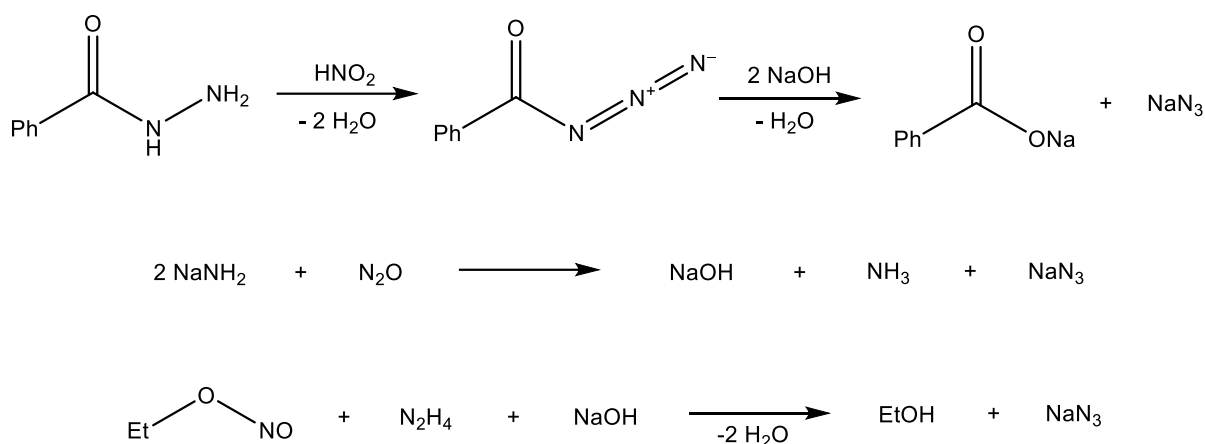$$2 \, NaNH_2 + N_2O \longrightarrow NaOH + NH_3 + NaN_3$$

Figure 1.4. Synthetic methods to produce sodium azide.

At the time of the original synthesis, it was believed that azide ions had a cyclic structure. However, it has since been proven that their structure is linear.[13] The linear structure of azide ions can be rationalised by the formal Lewis structure shown in Figure 1.5. This structure thus involves charge separation, with the central nitrogen atom having a formal positive charge, and the outer nitrogen atoms each having a formal negative charge.[14]
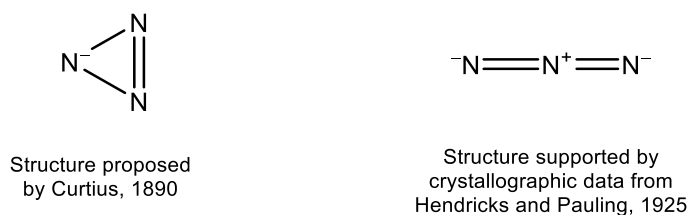

Structure proposed
by Curtius, 1890

Structure supported by
crystallographic data from
Hendricks and Pauling, 1925

Figure 1.5. Proposed and actual structures of the azide ion.

The concentration of negative charge on the terminal nitrogen atoms results in significant nucleophilicity at these positions, even in covalently bound azides. This nucleophilic nature allows for the formation of bridging complexes where both terminal nitrogen atoms of an azido group each coordinate to a different electrophilic centre.[15] The unusual electronic structure of azido groups also affects the manner of binding to different coordination centres, with important consequences to their stability that can be understood from an analysis of the resonance forms of a covalent azide. The azido group can act as both a π-donor and a π-acceptor, and in doing so weakens the bond between the adjacent (α) and central (β) nitrogen atoms. The extreme case of these interactions results in the formal reduction of the azido group to release N_2 (Figure 1.6).
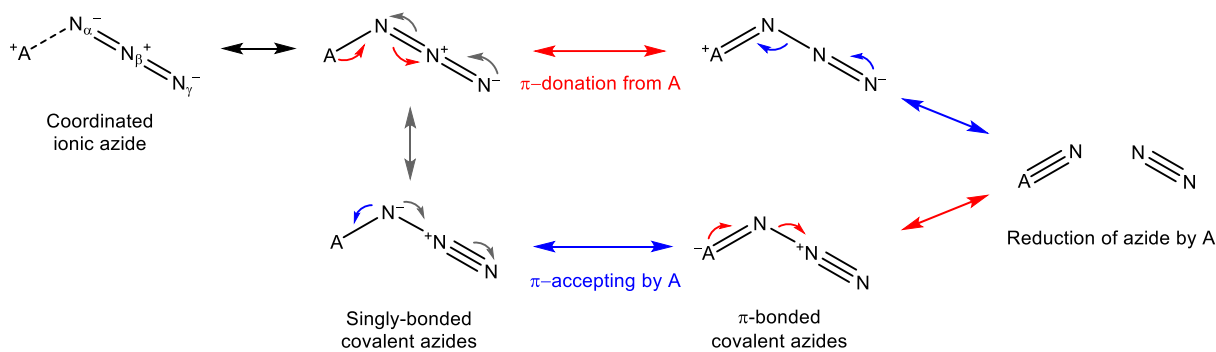
Figure 1.6. Resonance forms of azide coordinated to an undefined atom A, and the reduction of the azide by π-interactions to release N_2.

1.1.2. Applications

Aside from chemical transformations, NaN_3 is used for its release of N_2 upon decomposition. This dinitrogen release is utilised to inflate emergency slides in aircraft, and has also historically been used to inflate car airbags. Furthermore, NaN_3 is highly toxic, which also allows it to be used as a biocide.[16] Azides have considerable application in chemical synthesis, with a broad range of chemical transformations that utilise its unique chemistry.[17] Due to their nucleophilic nature, azido groups are readily incorporated into molecules by means of nucleophilic substitution using azide ions. Once incorporated, several known transformations utilise the elimination of N_2 from the azido groups, either by a concerted mechanism as seen in the Curtius rearrangement,[18, 19] or via thermally/photolytically generated nitrene intermediates.[20] Reaction of covalent azides with phosphines (the Staudinger reaction) also proceeds with N_2 elimination to form iminophosphoranes,[21] which can be hydrolysed to afford amines.[22] Other important reactions of azides include reduction with hydride reagents to afford amines,[23] and cycloaddition reactions to form nitrogen-containing heterocycles.[24] Examples of these reactions are shown in Figure 1.7.
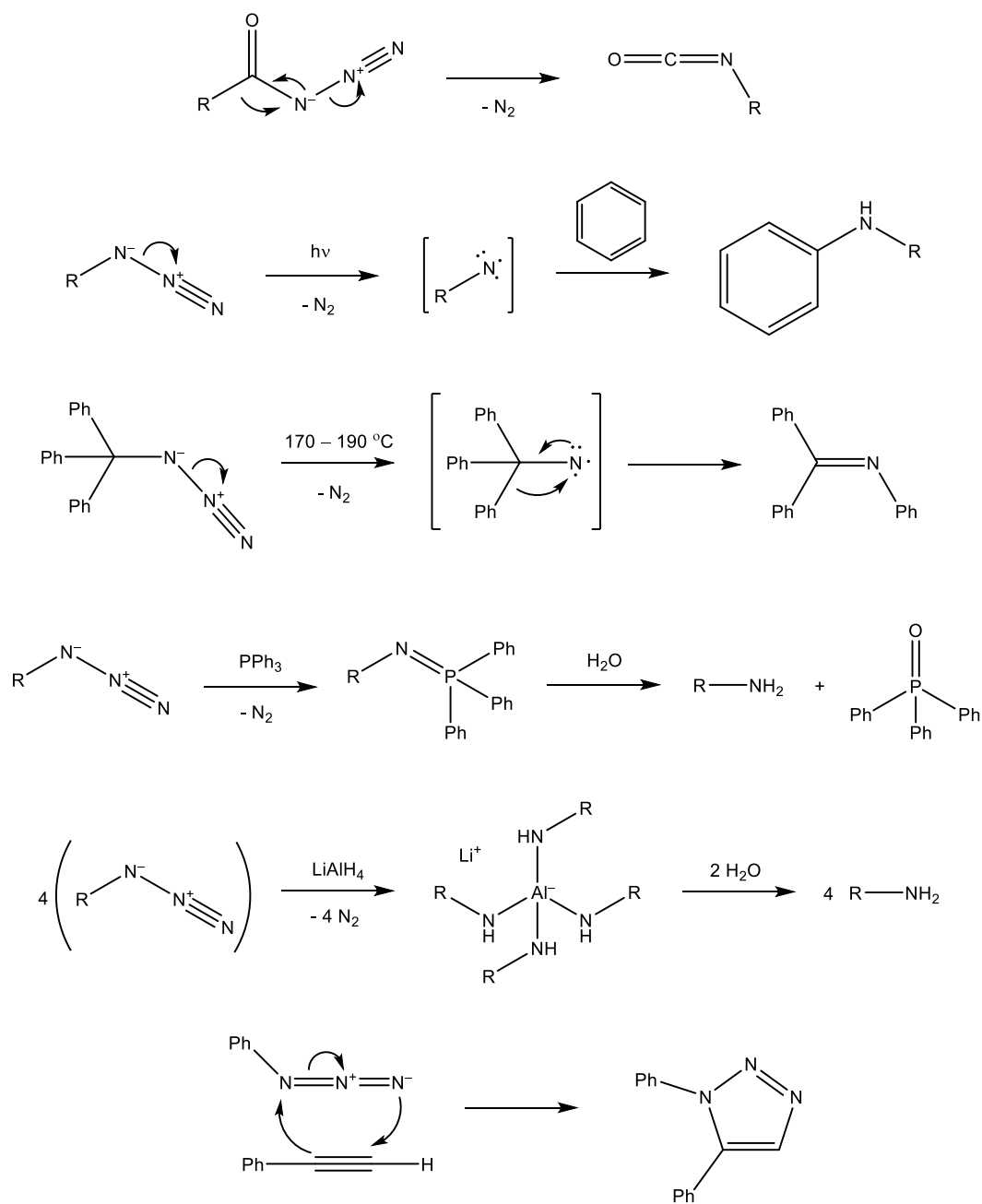
Figure 1.7. Selected examples of azido-group chemistry.

1.1.3. Silicon azides

Silicon azides have been known since 1954 with the synthesis of silicon tetraazide ($Si(N_3)_4$) from NaN_3 and $SiCl_4$.[8] This forms the basis of the general procedure for making azidosilanes, involving the treatment of the analogous chlorosilane with excess metal azide. A wide range of organo(azido)silanes have subsequently been synthesised by applying this technique.[25, 26]

The most notable of these azidosilanes is trimethylsilyl azide (TMS(N_3)),[27] which itself has been used as an alternative to metal azides in the synthesis of other azidosilanes.[25]

Aside from azidosilanes, the other currently known class of azido-silicon compound are hypercoordinate complexes, which can be viewed as an adduct of an azidosilane with a Lewis-basic ligand. Previous work in this field has focused on adducts of Si(N_3)$_4$, where the introduction of ligands (2,2'-bipyridine or 1,10-phenanthroline) have been shown to render the highly explosive Si(N_3)$_4$ less sensitive, thus enabling structural characterisation.[6] The adduct of Si(N_3)$_4$ with two azide ions, [Si(N_3)$_6$]$^{2-}$, has also been found to exhibit remarkable stability and is structurally characterised as its PPN salt (PPN$^+$ = [N(PPh$_3$)$_2$]$^+$).[5]
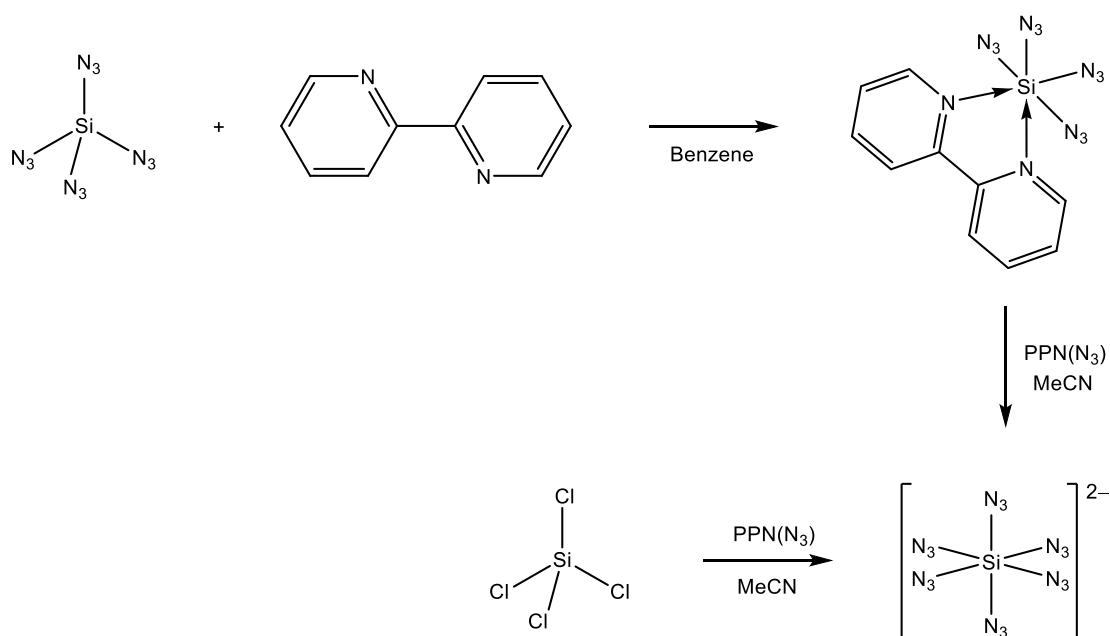
Figure 1.8. Synthesis of hexacoordinate silicon azide complexes.

1.2. Low-valent *p*-block chemistry

1.2.1. Electronic structure

The *p*-block elements typically form compounds in which *p*-block atoms are each surrounded by four pairs of electrons in their valence shell. This observation forms the basis of the historical "octet theory",[28] in which atoms with fewer than eight valence shell electrons form covalent bonds in order to reach this number. For elements in Groups 15, 16

and 17, this gives rise to a natural valence number of 3, 2 and 1, respectively, representing the number of unpaired electrons available to form covalent bonds, and the number of such bonds needed to form an octet.[29] Elements of Group 13 have a natural valence of 3 as they have a maximum of three unpaired electrons. However, the formation of three covalent bonds is not sufficient to complete an octet. Therefore, compounds of Group 13 typically form adducts with 2-electron donors in order to attain eight valence electrons.

The nature of Group 14 elements is somewhat more complicated. They have a total of four valence electrons which can, in theory, form a valence state of 4 allowing for the formation of four bonds and a complete octet. This situation is clearly very typical for carbon, and indeed all Group 14 elements are known to form tetravalent compounds. However, particularly for heavier Group 14 elements, these elements are also known to form compounds with lower valency. This behaviour stems from the fact that the tetravalent state does not match the electronic arrangement of atomic ground state for Group 14 elements. The atomic ground state contains only two unpaired electrons and can therefore only form a valence state with a valency of 2. The remaining two valence electrons form a pair occupying the outer *s*-orbital. These electrons are sometimes referred to as an "inert pair", as their pairing renders them unavailable for covalent bonding. As such, for a Group 14 element to form four bonds, a formal excitation energy must be provided to access the quintet atomic state, which is able to form a tetravalent valance state shown in Figure 1.9.[29] For carbon, this energy is readily provided by the formation of two additional bonds. However, for heavier Group 14 elements, the average strength of covalent bonds decreases due to weaker orbital overlap. This gives rise to stable "low-valent" compounds of Group 14, where fewer bonds are formed owing to the lack of excitation to a tetravalent state. This class of compound can be readily identified by the presence of a non-bonding electron pair corresponding to the "inert pair" of the atomic ground state. As with Group 13 compounds, these species typically form adducts with electron donors in order to complete their octet and are otherwise rarely stable.
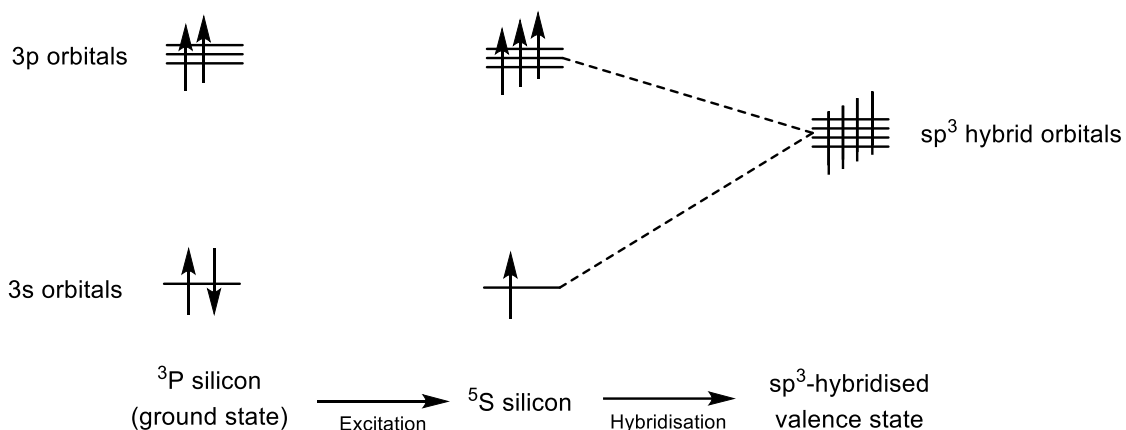
Figure 1.9. Comparison of the ground state, quintet excited state and tetrahedral valence state of silicon. Note that valence states do not have defined spin character,[29] so the electron occupancy has been indicated with a line rather than an arrow.

## 1.2.2. Stability of low-valent compounds

An indication of the readiness with which different Group 14 elements form low-valent compounds can be gleaned from the accessibility of their low-valent dichlorides compared to their tetrachlorides, as shown in Table 1.1.

	Dichloride	Tetrachloride
Carbon	Non-isolable reactive intermediate[30]	Stable (1820[31])
Silicon	Isolated (1953) only in high-temperature gas phase,[32] polymerises or disproportionates when condensed[33, 34]	Stable (1823[35])
Germanium	Stable under anoxic conditions (1928[36])	Stable (1886[37])
Tin	Stable (1792[38, 39])	Stable (1604[40] or earlier[39])
Lead	Stable (known since ancient times[41])	Isolated (1879), decomposes readily to the dichloride and chlorine gas[42]

Table 1.1. Stability and year of discovery of the group 14 di- and tetrachlorides. Note that all these compounds are sensitive to water except carbon tetrachloride and lead dichloride.

The instability of low-valent silicon dichloride when condensed exemplifies the difficulty in isolating low-valent silicon compounds. The cooling of $SiCl_2$ gas results in polymeric $(SiCl_2)_n$,[34] in which all silicon atoms are tetravalent due to the formation of Si–Si bonds.[43] Thus, the

isolation of low-valent silicon compounds requires the prevention of polymerisation. This is generally achieved by the introduction of a ligand, which can afford additional stabilisation depending on its nature: a π-donating ligand can reduce the electrophilicity of the low-valent silicon, a bulky ligand can provide steric hindrance to prevent reactions, and an anionic ligand can form a charged silanide which will have a coulombic barrier to oligomerisation. Several low valent silicon compounds are known utilising these strategies,[44] with some key examples shown in Figure 1.10.
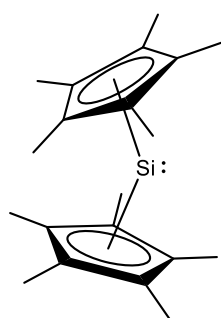
Stabilised by π-donation and steric bulk (Jutzi 1986)
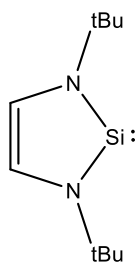
Stabilised by π-donation and some steric bulk (Denk 1994)
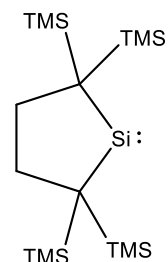
Stabilised only by steric bulk (Kira 1999)
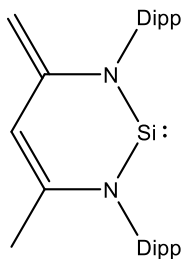
Stabilised by π-donation and steric bulk (Driess 2006)
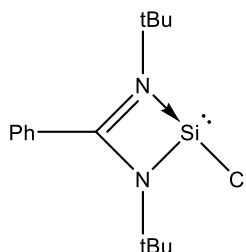
Stabilised by π-donation and some steric bulk (So, 2006)
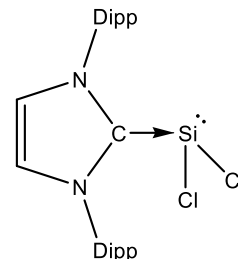
Stabilised by π-donation and steric bulk (Ghadwal 2009)
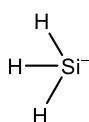
Stabilised by coulombic effects (Amberger 1968)
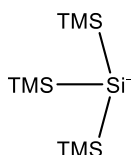
Stabilised by steric bulk and coulombic effects (Gilman 1968)
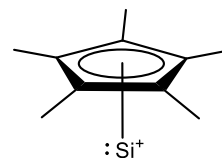
Stabilised by coulombic effects (Jutzi 2004)

Figure 1.10. Some examples of stable low-valent silicon compounds.[45-53]

(Dipp = 2,6-diisopropylphenyl-, TMS = trimethylsilyl-)

1.3. Characterisation of azido-silicon compounds

1.3.1. Single-crystal X-ray diffraction (SCXRD)

Single-crystal X-ray diffraction utilises the diffraction of X-rays to locate electron density within a crystal, enabling the construction of an accurate model of the material with precise inter-atomic distances and bond angles. SCXRD thus enables the identification of new compounds with a high degree of certainty, in addition to providing insights into the bonding within the compound. For azide-containing compounds, particular insight can be obtained from analysis of N−N bond lengths. The difference between the bond lengths of N_α−N_β and N_β−N_γ can indicate the degree of ionic character in an azido group, since a purely ionic azide has identical N−N bond lengths. Additionally, it is possible to identify the presence of π-interactions to an azido group based on comparison of the N−N bond lengths in relation to the formal resonance forms shown on Figure 1.6. For these reasons, SCXRD is often the most desirable form of characterisation, but can only be used if the material can be isolated as suitable single crystals. When suitable crystals are available, the next most significant issue with this technique is that it only analyses a single crystal from a sample, so it cannot assess the purity of bulk material. This is compounded by the issue that structurally similar compounds may crystallise together in the same crystal. This gives rise to solid solutions in which it may be difficult to distinguish the presence of a minor impurity due to the electron density of the structurally similar major compound being superimposed onto it. As such, other characterisation techniques are necessary for verifying the purity of a compound, monitoring reactions or analysing mixtures of products.

1.3.2. Infrared (IR) spectroscopy

Infrared spectroscopy utilises the property of chemical bonds to vibrationally excite by absorbing infrared light. The energy of this absorption correlates to the energy needed to excite the bond, which in turn is dependent on the bond force constant and reduced mass. For many organic molecules, most non-hydrogen bonds have very similar absorption wavenumbers (around $1500 - 500$ cm^{-1}), resulting in a difficult-to-interpret "fingerprint region" containing numerous overlapping absorption bands. The complexity of this region

can make it useful for identifying known pure substances by matching to the known "fingerprint", but for novel compounds it is desirable to have a functional group with a more distinct absorption range.

Azido groups typically have two strong IR absorption regions: one in the wavenumber range of 2200 – 2000 cm^{-1} corresponding to the asymmetric stretching vibration, and one in the range of 1300 – 1200 cm^{-1} corresponding to the symmetric stretching vibration.[54] Weaker absorptions may also be identified in the region of 3500 – 3200 cm^{-1} corresponding to the simultaneous excitation of both the asymmetric and symmetric vibrational modes, and the region of 800 – 600 cm^{-1} corresponding to the bending motions. In ionic azides, the symmetric vibration may not be IR-active due to the symmetry of the azide ion.

The asymmetric stretch absorbs in region where few other functional groups absorb, making it easily identified and interpreted. As the absorption wavenumber is dependent on the bond stretching force constant, IR spectroscopy provides insight into the bonding nature of the azido group. Weakly-coordinated ionic azides typically absorb around 2000 cm^{-1}, while covalent azides are typically higher, up to around 2200 cm^{-1}. This higher wavenumber (and thus greater force constant) may be attributed to the increased character of resonance forms containing an N≡N triple bond (see Figure 1.6).

While limited in the type of functional groups it can monitor, IR spectroscopy has a notable advantage that it can be used to study insoluble materials, something which many other analytical techniques struggle with. IR spectroscopy can also be conducted on solutions by using sealed solution cells, where the absorptions of the solvent can be compensated for by referencing the solution to a background of the pure solvent in the same cell. Solution-phase spectra typically contain sharper bands than solid-phase spectra due to the inherent homogeneity of solutions. Additionally, solution cells can be filled with reaction solutions, allowing for the monitoring of reactions by IR spectroscopy. Solution-phase IR spectroscopy does, however, have a major drawback that data cannot be obtained in wavenumber regions where the solvent completely absorbs all infrared light.

1.3.3. Nuclear magnetic resonance (NMR) spectroscopy

Nuclear magnetic resonance spectroscopy involves the induction and subsequent monitoring of precessing nuclear spins in a magnetic field.[55] The frequency of precession depends on the local magnetic field around a nucleus, which can vary according to the shielding effect of nearby electron pairs and the spin state of nearby magnetically-active nuclei. Hence, NMR spectroscopy provides a means of detecting different chemical environments and the relationship between magnetically active nuclei within a molecule.

For the study of azido-silicon compounds, there are typically three NMR-active nuclei of interest, with each offering different information about the identity of the compound(s) analysed.

- ^1H NMR: ^1H is the most studied NMR-active nucleus. Unfortunately, ^1H NMR can rarely offer much direct evidence on the nature of a silicon compound unless there is a hydrogen atom very close to the silicon coordination centre. The method does, however, allow for characterisation of ligands and can easily identify the difference between coordinated and uncoordinated ligands. ^1H NMR is a highly sensitive technique, and its spectra can usually be interpreted quantitatively, making it useful for determining the ratios of hydrogen-containing compounds. The high sensitivity also allows ^1H spectra to be recorded quickly, making it excellent for monitoring reactions.

- ^{14}N NMR: ^{14}N nuclei are quadrupolar, causing them to interact with electric field gradients. This interaction often results in extremely short relaxation times, resulting in broad signals due to a "lifetime broadening" phenomenon. This phenomenon arises from Heisenberg's uncertainty principle, where the short lifetime of a precession (and thus a small uncertainty in this lifetime) results in a higher uncertainty in the energy (and frequency) of the precession.[56] This phenomenon often renders ^{14}N NMR analysis unsuitable for most nitrogen-containing molecules, as the signals are too broad to discern from the baseline. In high symmetry environments, the local electric field around a nucleus is more uniform, so the nuclei exhibit longer relaxation times and the lifetime broadening effect is reduced. For the central (β) and terminal (γ) nitrogen nuclei of an azido group, this is often sufficient to render ^{14}N NMR an applicable technique. The α nitrogen nucleus of an azido

group is sometimes also detectable by ^{14}N NMR, but the signal is usually too broad to provide any distinction between compounds and is thus not useful for analysis. Figure 1.11 shows the ^{14}N NMR spectrum of a mixture of silicon tetraazide and acetonitrile (in toluene), showing the different extents of lifetime broadening for each nitrogen environment. For silicon azide complexes, ^{14}N NMR offers little additional information on the silicon centre over ^{29}Si NMR, since the latter probes the central silicon nucleus directly. However, as ^{29}Si NMR data is not readily interpreted quantitatively (*vide infra*), ^{14}N NMR offers a way of quantifying the ratio of different silicon azide species where ^{1}H NMR is not applicable. It should be noted that ^{15}N is also an NMR-active nucleus. ^{15}N is not a quadrupolar nucleus and thus does not suffer from lifetime broadening. However, ^{15}N NMR is not typically applicable for the study of nitrogen-containing molecules due to a combination of low sensitivity and low natural abundance. As such, ^{15}N NMR signals are often too weak to identify unless the analyte is ^{15}N-enriched, which can be prohibitively expensive.
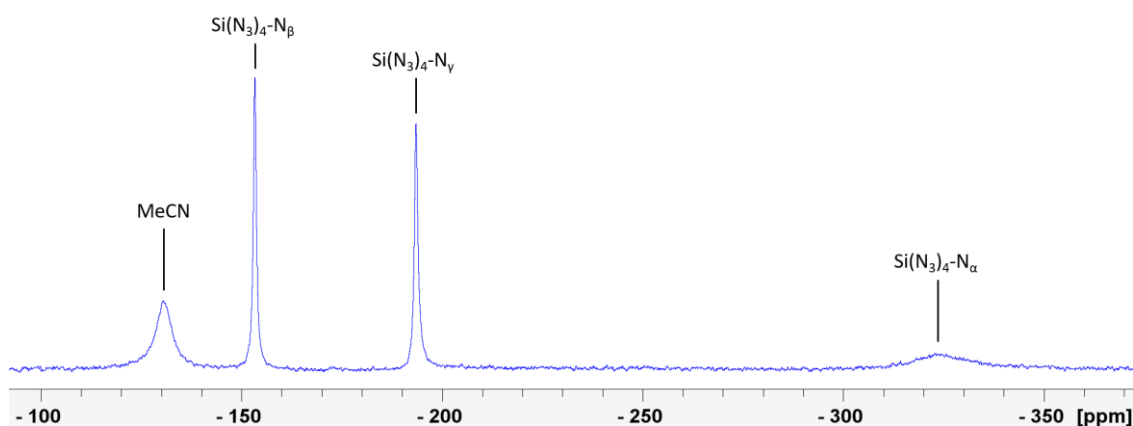
Figure 1.11. ^{14}N NMR spectrum of $Si(N_3)_4$ and MeCN in toluene (this work).

- ^{29}Si NMR: ^{29}Si NMR is useful for directly investigating the properties of a silicon environment. The technique can help identify the coordination number around the silicon atom, with tetracoordinate silanes typically occurring in the chemical shift range of +20 ppm to -120 ppm, while hexacoordinate silicon complexes occur at a more upfield range of -120 ppm to -200 ppm.[57] As with other nuclei, the electronic properties of substituents also affect the chemical shift of ^{29}Si nuclei, allowing for the distinction of species with different substituents. This is particularly useful for ligand-

17

bound silicon complexes, where the change in ligand environment may not be sufficient to distinguish similar complexes by ^{1}H NMR analysis. The low natural abundance and slow relaxation of [29]Si nuclei contribute to ^{29}Si NMR having low sensitivity, thus necessitating long experiment times and restricting quantitative analysis. All ^{29}Si NMR spectra contain an asymmetric broad signal with a maximum at around -110 ppm. This signal corresponds to the silicon resonance of the glass in the instrument probe and the NMR sample tube.[57] Typically, [29]Si signals are sufficiently sharp that even signals which overlap with the glass resonance are easily identified. For hydrido-silicon compounds, additional insight into the silicon environment can be gained from coupling between the [29]Si and ^{1}H nuclei. The resulting coupling pattern of a [29]Si signal can inform the number of protons which are one and two bonds away from the silicon atom. This coupling is also visible in ^{1}H spectra, in the form of a weak doublet equidistant from the main ^{1}H environment (satellite signals), separated by the same coupling constant value as observed in the [29]Si spectrum. These signals have approximately 2.3% of the intensity of the main signal (half the natural abundance of [29]Si), allowing them to be distinguished from any other weak signals nearby, and providing a clear indication of any proton environments that are closely associated with a silicon atom. The magnitude of the Si-H coupling value is dependent on the degree of *s*-character in the Si−H bond, with higher *s*-character affording a greater coupling constant.[58] This means that hydridosilicon compounds with higher coordination numbers will experience weaker Si-H coupling due to the silicon *s*-orbital being shared across more substituents. Similarly, changing the substituents on the silicon atom will also affect Si-H coupling due to the differing degrees to which these substituents interact with the silicon *s*-orbital.

2. Synthesis, reduction, and decomposition of hydrido(azido)silicon compounds

2.1. Introduction

2.1.1. Reactivity of hydrido(chloro)silicon complexes

The base-induced reductive elimination of HCl from hydrido(chloro)silicon compounds is currently one of the most effective methods of generating stable low-valent silicon chlorides. Trichlorosilane ($HSiCl_3$), upon being treated with the N-heterocyclic carbene 1,3-bis(2,6-diisopropylphenyl)imidazol-2-ylidene (IPr), forms the low-valent complex $IPrSiCl_2$ accompanied by elimination of [IPrH]Cl.[50] This is suspected to occur by reductive elimination from a hexacoordinate intermediate complex, IPr_2SiHCl_3, based on the isolation of the analogous dihydrido complex $IPr_2SiH_2Cl_2$.[59] Similarly, the treatment of $HSiCl_3$ with an amidinate reagent, lithium N,N'-di(tert-butyl)phenylamidinate (Li(^{tBu}NCN)), forms the hypercoordinate complex (^{tBu}NCN)SiHCl$_2$. Reaction of (^{tBu}NCN)SiHCl$_2$ with bases LiN(TMS)$_2$ or 1,3-di-tert-butylimidazol-2-ylidene (ItBu) forms the low-valent complex (^{tBu}NCN)SiCl (Figure 2.1).[60] Curiously, while amidinato complexes of the form (NCN)SiHCl$_2$ are isolable, the analogous N-heterocyclic carbene (NHC) complexes of the form (NHC)SiHCl$_3$ appear to be unstable with respect to disproportionation to (NHC)SiH$_2$Cl$_2$ and (NHC)SiCl$_4$.[61]
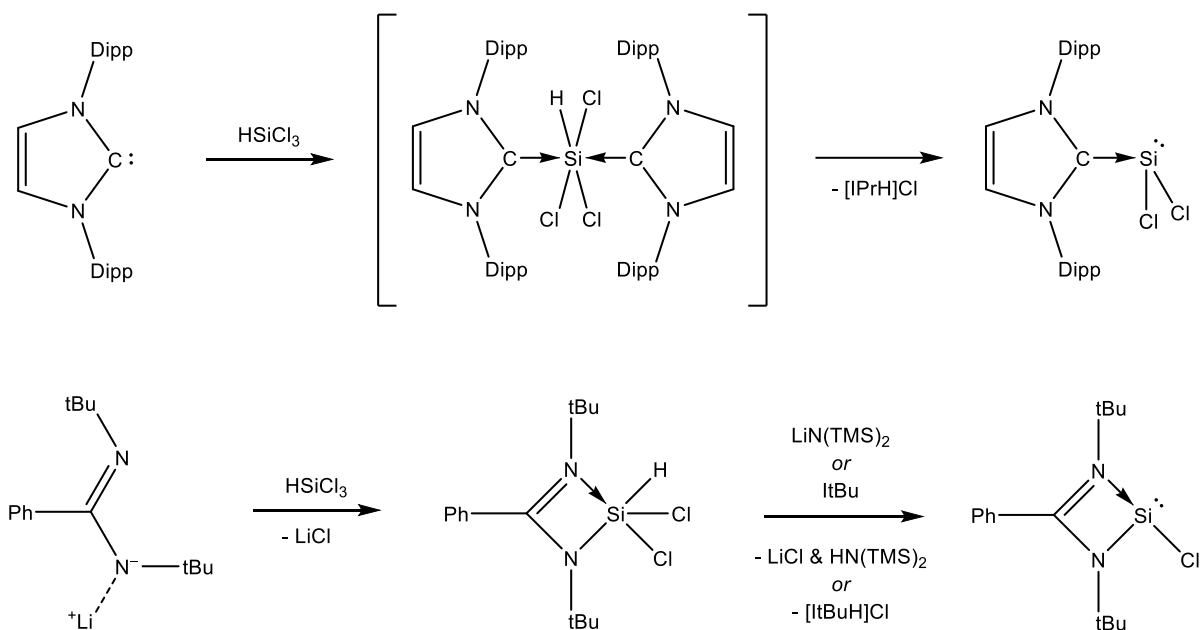
Figure 2.1. Synthesis of IPrSiCl$_2$ and (^{tBu}NCN)SiCl from HSiCl$_3$.

The syntheses of IPrSiCl$_2$ and (^{tBu}NCN)SiCl shown in Figure 2.1, afford high yields of 79% and 90% respectively. The same complexes can be made from direct reduction of the equivalent SiCl$_4$-derived complexes IPrSiCl$_4$ and (^{tBu}NCN)SiCl$_3$, using KC$_8$ and potassium metal respectively, producing yields of only 48% and 10%.[49, 50] The lower yields from direct reduction suggest that reductive elimination from hydrido complexes is a more selective method for the synthesis of low-valent silicon complexes.

2.1.2. Hydrido(azido)silicon complexes

For the reductive elimination method to be applicable to the synthesis of low-valent silicon azides, a suitable precursor hydrido(azido) silicon compound needs to be identified. Hydrido(azido) silicon compounds are extremely rare in the literature, many of which only contain a single azido group. By analogy to the elimination of HCl from hydrido(chloro) silicon complexes, a reductive elimination of hydrido(azido) silicon species would likely eliminate HN$_3$. For this process to form a low-valent silicon azide, the precursor would therefore need at least two azido groups and one hydrido group, further limiting the viable options. The known isolated hydrido(azido) silanes are shown in Figure 2.2.
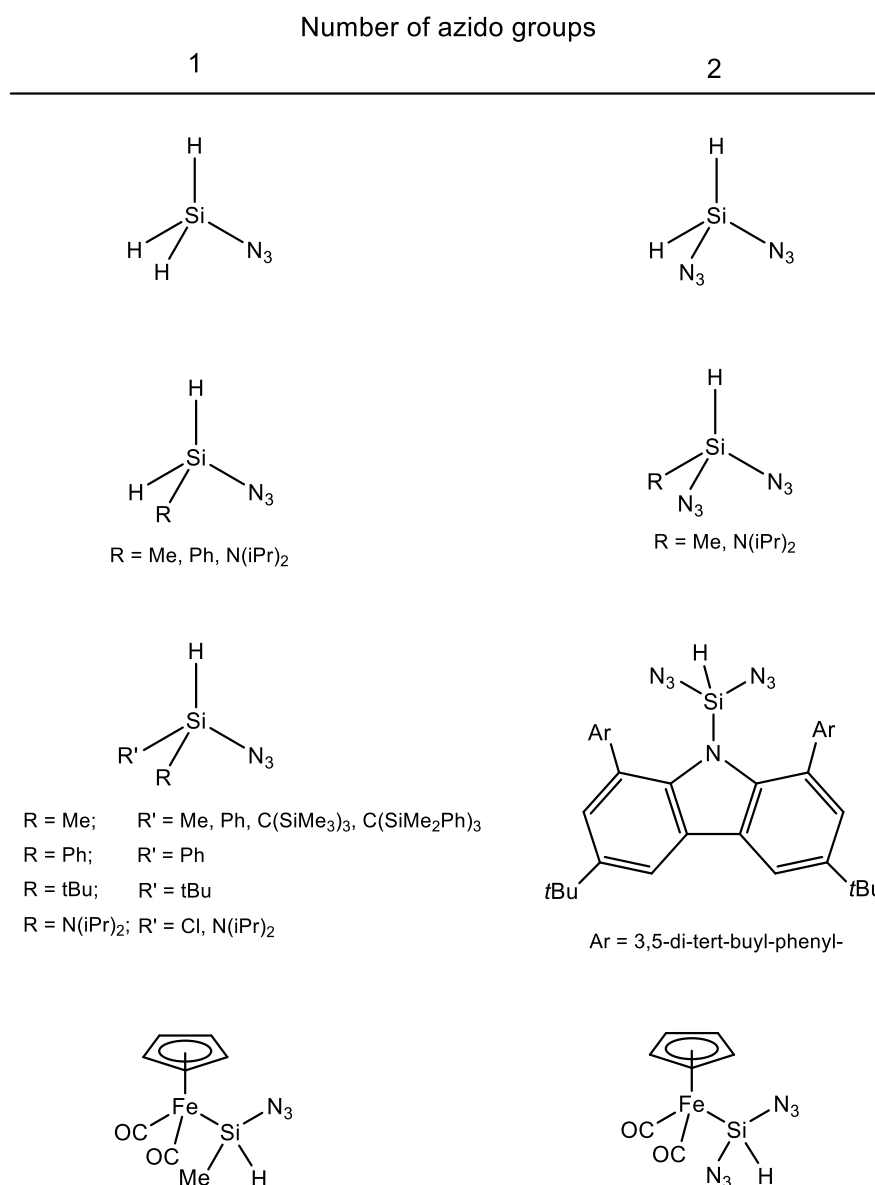
Figure 2.2. Isolated hydrido(azido)silane derivatives, sorted by number of azido substituents.[26, 62-71]

An important absence from Figure 2.2 is triazidosilane $(HSi(N_3)_3)$. $HSi(N_3)_3$ is the azide analogue of the $HSiCl_3$ used to make low-valent silicon chlorides (see Figure 2.1), so $HSi(N_3)_3$ could be a precursor to low-valent silicon azides by this analogy. Some attempts to synthesise $HSi(N_3)_3$ have been reported, but these have met with difficulty. The conventional synthesis of silicon azides by treating the chloride with metal azides has been shown to be ineffective. The reaction of $HSiCl_3$ with LiN_3 has been found to evolve monosilane (SiH_4),[72] and IR analysis of the reaction outcome of $HSiCl_3$ with NaN_3 revealed that silicon tetraazide $(Si(N_3)_4)$ is the sole azide-containing product.[73] The reasonable

conclusion from these results is that $HSi(N_3)_3$ undergoes disproportionation under these conditions according to the net reaction shown in Figure 2.3.

$$4\ HSi(N_3)_3 \longrightarrow SiH_4 + 3\ Si(N_3)_4$$

Figure 2.3. Disproportionation of triazidosilane.

The species azidosilane ($H_3Si(N_3)$)) and diazidosilane ($H_2Si(N_3)_2$) are presumably formed as intermediates in this process, but were not detected under these conditions. $H_3Si(N_3)$ and $H_2Si(N_3)_2$ are isolable compounds, but are notably synthesised using a covalent azide reagent, tributyltin azide, rather than ionic azides.[62, 63] This suggests that the presence of azide ions may catalyse the disproportionation of hydrido(azido)silanes, since these species have only been observed in the absence of ionic azides. An attempt to synthesise $HSi(N_3)_3$ using tributyltin azide is reported by Glatthaar in his dissertation, where the formation of $HSi(N_3)_3$ was confirmed by mass spectrometry, but it was contaminated with the disproportionation product $Si(N_3)_4$.[74] While it is thus shown that a covalent azide reagent can be used to synthesise $HSi(N_3)_3$, $HSi(N_3)_3$ appears to be too susceptible to disproportionation under the existing methods to isolate in decent purity.

As a synthetic alternative to $HSi(N_3)_3$, Peerless synthesised an amidinato complex ($^{Dipp}NCN)SiH(N_3)_2$ by reacting $HSiCl_3$ with lithium N,N'-bis(2,6-diisopropylphenyl)-(4-tert-butylphenyl)amidinate Li(^{Dipp}NCN), followed by treatment with excess NaN_3 (Figure 2.4).[73] The resulting complex was the first isolated hypercoordinate hydrido(azido)silicon compound, and is analogous to the complex (($^{tBu}NCN)SiHCl_2$) used to synthesise the low-valent compound ($^{tBu}NCN)SiCl$. ($^{Dipp}NCN)SiH(N_3)_2$ is therefore an ideal precursor for developing low-valent silicon azides and silicon nitrides.
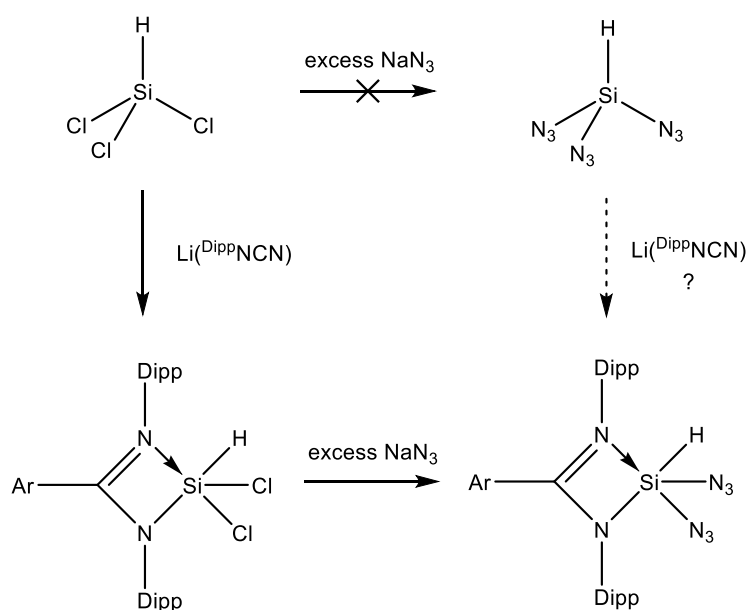
Figure 2.4. Reported synthesis of (^{Dipp}NCN)SiH(N$_3$)$_2$ via (^{Dipp}NCN)SiHCl$_2$, and the hypothetical synthesis via HSi(N$_3$)$_3$ rendered inaccessible by the lack of suitable conditions for synthesising HSi(N$_3$)$_3$. (Dipp = 2,6-diisopropylphenyl-, Ar = 4-tert-butylphenyl-)

Peerless found that (^{Dipp}NCN)SiH(N$_3$)$_2$ undergoes a range of reactions with various bases shown in Figure 2.5.[73] While each base displayed a different mode of reactivity towards the complex, no low-valent silicon complex was observed from any of these reactions, in contrast to the reported chemistry of (^{tBu}NCN)SiHCl$_2$.
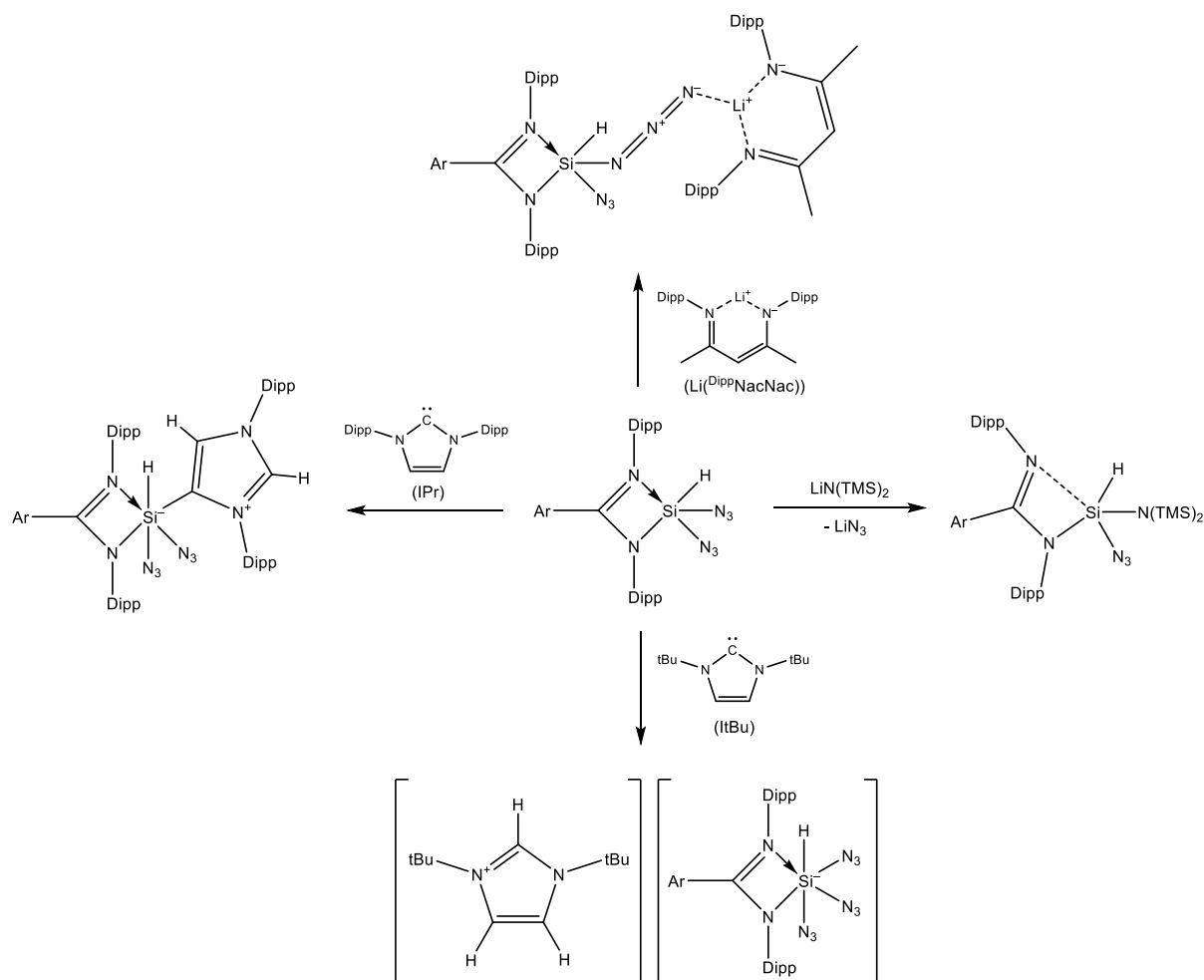
Figure 2.5. Peerless' reactions of (^{Dipp}NCN)SiH(N$_3$)$_2$ (Dipp = 2,6-diisopropylphenyl-, Ar = 4-tert-butylphenyl-, TMS = trimethylsilyl-).

Of these observations, the most important one is that with 1,3-bis(2,6-di-tert-butyl)imidazol-2-ylidene (ItBu). The observed reaction product, [ItBuH][(^{Dipp}NCN)SiH(N$_3$)$_3$], cannot be made from simple addition of ItBu to (^{Dipp}NCN)SiH(N$_3$)$_2$. Instead, this product is formally the combination of ItBu, (^{Dipp}NCN)SiH(N$_3$)$_2$ and HN$_3$. Thus, the observed formation of [ItBuH][(^{Dipp}NCN)SiH(N$_3$)$_3$] indicates a source of HN$_3$ in this reaction mixture. This implies that the intended reductive elimination of (^{Dipp}NCN)SiH(N$_3$)$_2$ with formal release of HN$_3$ may have occurred, but no resulting low-valent silicon complex was isolated. It remains to be seen whether this is because the expected product (^{Dipp}NCN)Si(N$_3$) is unstable, or if it is merely more difficult to isolate than [ItBuH][(^{Dipp}NCN)SiH(N$_3$)$_3$]. If the compound is unstable, the expected mechanism of decomposition would involve elimination of N$_2$, thus potentially forming a silicon nitride derivative that is also of interest.

2.2. Results and Discussion

2.2.1. Synthesis of triazidosilane

Considering the use of $HSiCl_3$ as a precursor to low-valent silicon chlorides, the synthesis of $HSi(N_3)_3$ was revisited. As the previously reported attempts to synthesise $HSi(N_3)_3$ have been conducted in pyridine[72] and benzene[73], the synthesis of $HSi(N_3)_3$ was attempted in MeCN to determine if the use of a more polar solvent has any effect. The solution-phase IR spectrum of the resulting reaction solution showed a characteristic absorption of the hexaazidosilicate ion ($Si(N_3)_6^{2-}$) at 2110 cm^{-1}. Considering that $Si(N_3)_6^{2-}$ is the known product of reaction between $SiCl_4$ and excess NaN_3 in MeCN,[5] it can be concluded that the disproportionation of $HSi(N_3)_3$ has occurred in MeCN, forming $Si(N_3)_4$ which subsequently reacts with the excess NaN_3 to form $Si(N_3)_6^{2-}$ (Figure 2.6).
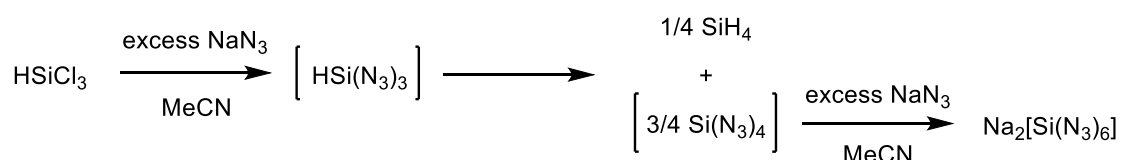
Figure 2.6. Reaction of $HSiCl_3$ with NaN_3 in MeCN, with likely intermediates.

Since changing the polarity of the solvent does not appear to prevent the disproportionation of $HSi(N_3)_3$, alternative azide transfer reagents are considered for enabling the synthesis of $HSi(N_3)_3$. Ionic azides are likely to react similarly to each other, so the use of alternative covalent azides was considered. Thus, the reaction of $HSiCl_3$ with trimethylsilyl azide ($TMS(N_3)$) was conducted in C_6D_6 and monitored by NMR spectroscopy (Figures 2.7, 2.8). There is likely little thermodynamic driving force for exchanging chlorides and azides between two different silanes, so the $TMS(N_3)$ was added in significant excess (approximately 10 equivalents) to ensure high conversion. It should therefore be noted that the $TMS(N_3)$ comprised approximately 0.2 mL of the 0.7 mL sample, making it a meaningful percentage of the solvent. ^1H, ^{14}N and ^{29}Si NMR spectra were then recorded of the sample at various time points.
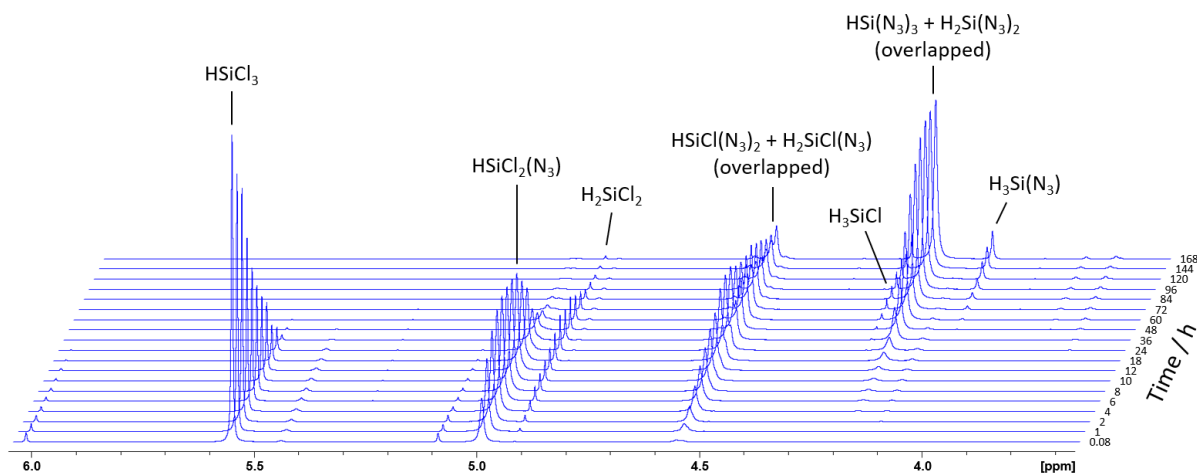
Figure 2.7. ^{1}H NMR spectra from the reaction mixture of trichlorosilane with trimethylsilyl azide, recorded at different times during the reaction. Note that the time axis is not linear.

At a glance, the series of ^{1}H NMR spectra of the reaction mixture show the conversion of $HSiCl_3$ into three other compounds in sequence, with each conversion changing the chemical shift of the associated hydride by approximately the same amount. This is the behaviour one would expect for the stepwise conversion of $HSiCl_3$ > $HSiCl_2(N_3)$ > $HSiCl(N_3)_2$ > $HSi(N_3)_3$. However, closer inspection shows there are two other major species are formed, with signals that overlap with the those of the expected signals for $HSiCl(N_3)_2$ and $HSi(N_3)_3$, as well as three minor species. The overlapped major signals can be distinguished by their [29]Si satellite signals, which do not overlap. Using this method, a total of nine distinct hydridosilanes can be identified from this series of spectra. A series of analytical techniques can be employed to identify these compounds. First, the proton-coupled [29]Si spectra (such as shown in Figure 2.8) can be analysed, which defines the number of protons on each major silane species based on the observed coupling pattern. These assignments can then be matched to the associated signal in the ^{1}H NMR spectrum by their $^1J_{Si-H}$ coupling constants. All major (non-trimethylsilyl) [29]Si signals observed throughout the experiment are either singlets, doublets, or triplets, corresponding to species with 0, 1 or 2 hydride substituents respectively. However, it should be noted that some species observed in the ^{1}H NMR spectra were of too low concentration to be detectable by the less sensitive ^{29}Si NMR analysis. There was only one detected product with no hydride substituents, which was identified as $Si(N_3)_4$ by comparison to its literature specta.[6] The remaining major species are therefore identified to be species of the form H_2SiX_2 and $HSiX_3$ (X = Cl, N_3), with H_3SiX species being plausible minor products.

26
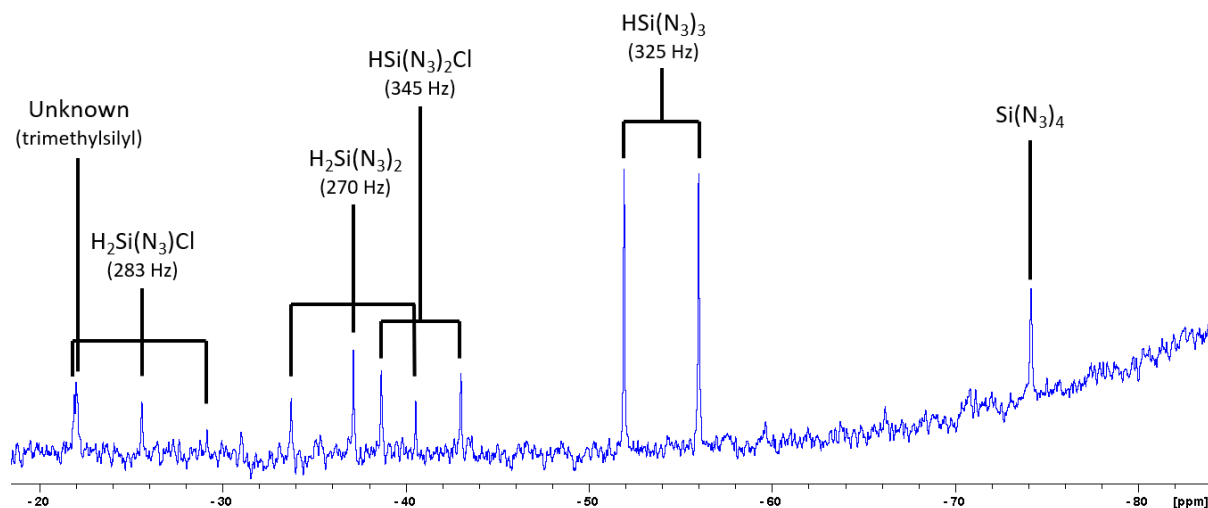
Figure 2.8. One of the proton-coupled ^{29}Si spectra recorded from the reaction mixture of trichlorosilane with trimethylsilyl azide. This spectrum was recorded between 86 – 96 hours after reaction start. The chemical shift of $Si(N_3)_4$ is known to the literature,[15] other assignments are made based on match to calculated chemical shifts and observed coupling patterns.

In order to distinguish the observed species, *ab initio* calculations were performed with assistance from Dr Thomas Speak in order to predict the chemical shift and Si-H coupling values of the series of compounds H_3SiX, H_2SiX_2 and $HSiX_3$ (X = Cl, N_3). Structures were determined at the MP2(FULL)/cc-pVTZ level, chemical shift values were calculated at the MP2(FULL)/aug-cc-pVTZ level, Si-H coupling constants were calculated at the MPW1K/aug-cc-pVTZ level. These functionals have previously been shown to be effective for the calculation of ^{29}Si chemical shift values in small silanes.[75] As the reaction progressed, the chemical shift values of the newly observed compounds closely match the calculated chemical shift trend for the substitution of a chloride for an azide in the series $HSiX_3$ and H_2SiX_2. Figures 2.9, 2.10 and 2.11 show the ^1H chemical shifts, ^{29}Si chemical shifts and Si-H coupling constants for the observed species (sorted by their substituents) and compared against the calculated values for these species. In the case of $H_3Si(N_3)$, the calculated ^{29}Si and $^1J_{Si-H}$ values closely match a very weak doublet in some of the ^{29}Si spectra, which is assumed to be the expected quartet pattern where the weaker two signals are undetectable.
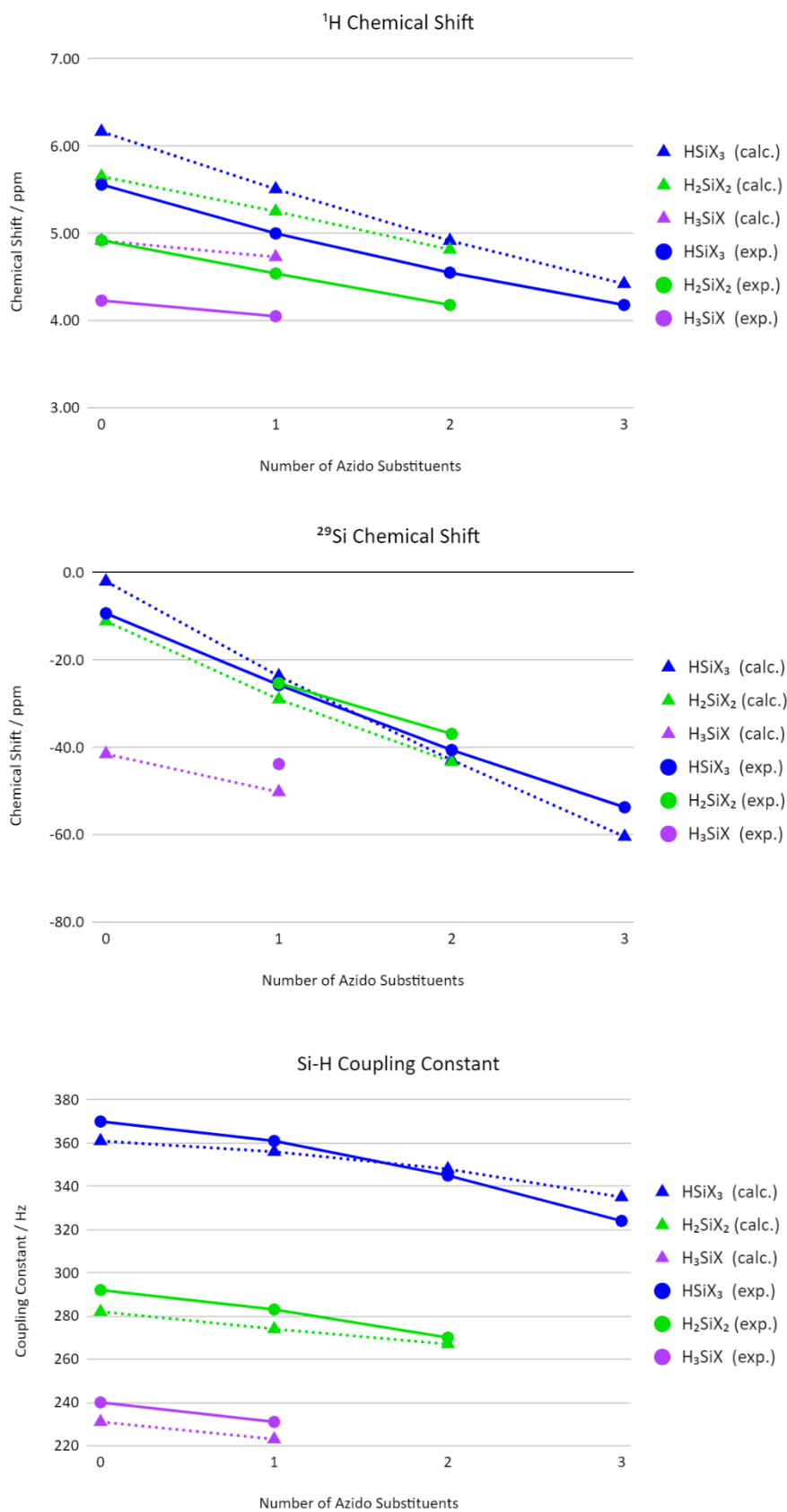
Figures 2.9, 2.10, 2.11. Comparisons of calculated (calc.) and experimental (exp.) NMR data for the series of compounds HSiX₃ (in blue), H₂SiX₂ (in green) and H₃SiX (in purple) (X = Cl, N₃).

As ^{1}H NMR spectra can be interpreted quantitatively, the integrals of the signals in the ^{1}H NMR spectra can be used to monitor the change in concentration of the observed species over the course of the reaction. Plotting these concentrations against time provides a clear overview of the changes occurring in the reaction mixture, shown in Figure 2.12.
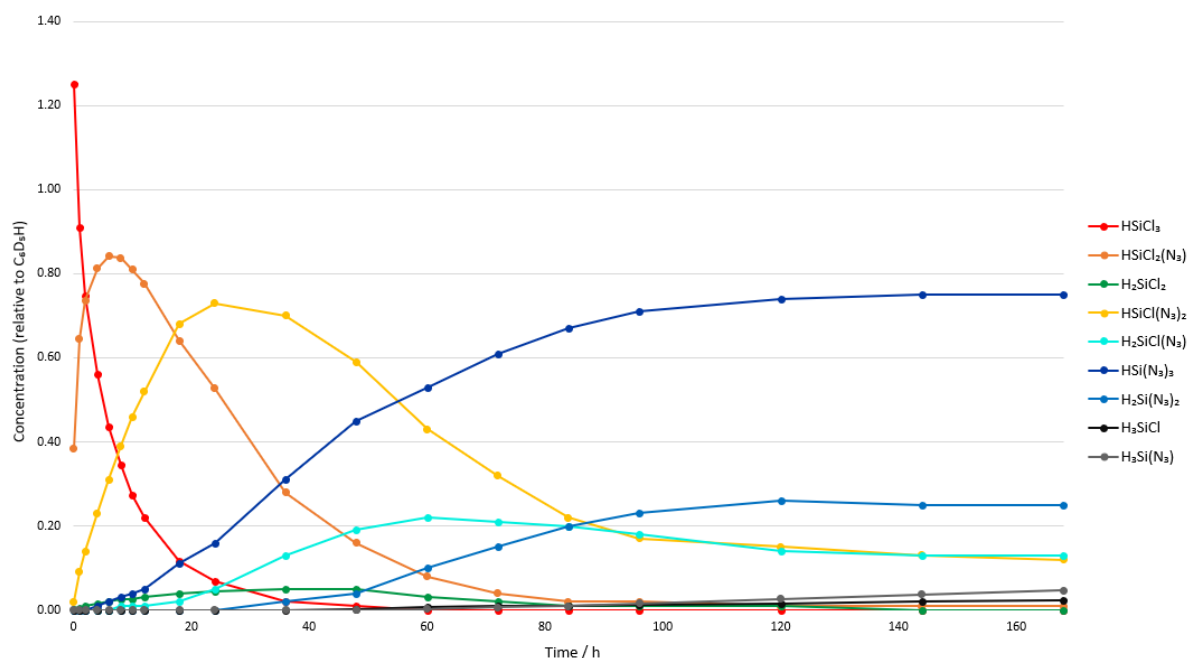
Figure 2.12. Concentration-over-time graph for the nine hydrido-silane species detected from reaction of TMS(N_3) with $HSiCl_3$. Concentrations are set relative to the residual solvent signal of C_6D_6.

From Figure 2.12, it can be seen that the dominant product of the reaction is indeed the desired compound $HSi(N_3)_3$, but its formation occurs concurrently with a disproportionation reaction which appears to slow down after a week, reaching a mixture containing about 0.33 molar equivalents of $H_2Si(N_3)_2$ per $HSi(N_3)_3$. [14]N NMR integrals confirm this ratio and indicate there is approximately 0.59 equivalents of $Si(N_3)_4$ per $HSi(N_3)_3$ at this point. After another week, the signals assigned to H_3SiCl and $H_3Si(N_3)$ grew in intensity at the expense of $HSi(N_3)_3$ and $H_2Si(N_3)_2$. A final series of spectra taken 76 days after reaction start show the presence of significant quantities of SiH_4, identified by comparison of the chemical shift and [1]J_{Si-H} values to literature.[76] Thus, the entire sequence of formation and disproportionation of $HSi(N_3)_3$ towards $Si(N_3)_4$ and SiH_4 has been verified spectroscopically.

Throughout the experiment, no evidence of any species of the form SiX_4 other than $Si(N_3)_4$ was obtained, suggesting the only major disproportionation processes are those that involve

the formation of $Si(N_3)_4$. It is thus assumed that the formation of $Si(N_3)_4$ represents a thermodynamic sink that ultimately drives the disproportionation. Since it is unlikely that any given reaction would involve the simultaneous exchange of more than one substituent at a time, the dominant disproportionation reactions must therefore involve $HSi(N_3)_3$, with the hydride being exchanged for an azide of another azidosilane to form $Si(N_3)_4$, according to the process shown in Figures 2.13 and 2.14.

$$HSiX_2(N_3) \quad + \quad HSi(N_3)_3 \quad \longrightarrow \quad H_2SiX_2 \quad + \quad Si(N_3)_4$$
$$X = Cl, N_3$$
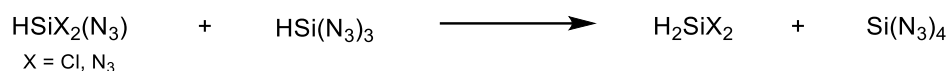
Figure 2.13. Hypothesised reaction scheme of $Si(N_3)_4$ formation in solutions containing $HSi(N_3)_3$.
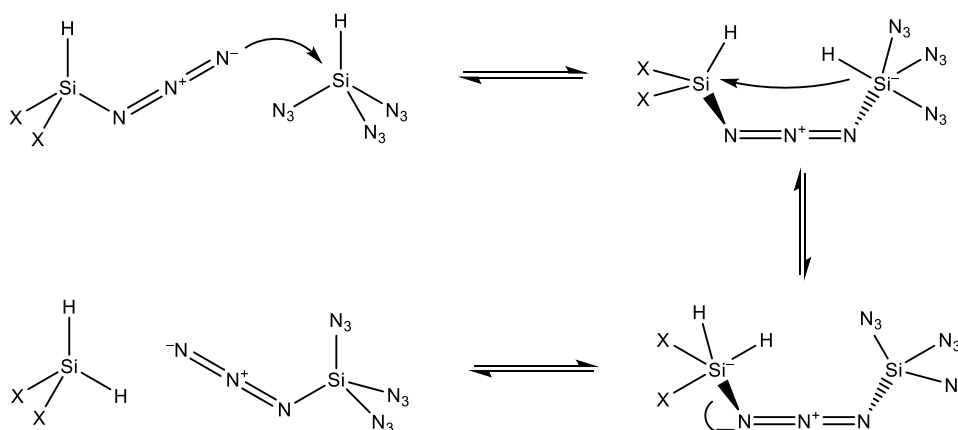
Figure 2.14. Hypothesised mechanism for reaction between a hydrido(azido)silane $HSiX_2(N_3)$ (X = Cl, N_3) and $HSi(N_3)_3$ to form H_2SiX_2 and $Si(N_3)_4$.

Further reactions to form H_3SiX and SiH_4 are observed to be much slower, which may explain why $H_2Si(N_3)_2$ and $H_3Si(N_3)$ are more readily isolated than $HSi(N_3)_3$. If disproportionation is only favourable in the event of $Si(N_3)_4$ formation, then it is also possible that $H_2Si(N_3)_2$ and $H_3Si(N_3)$ are stable due to their inability to disproportionate directly to $Si(N_3)_4$ (without simultaneous exchange of multiple substituents). The hypothesised mechanism shown in Figure 2.14 would explain why this disproportionation occurs to $HSi(N_3)_3$ but not $HSiCl_3$, as the latter would not readily form bridged dimeric intermediates due to the lower nucleophilicity of chloro groups compared to azido groups. It should be noted that, under certain catalytic conditions, $HSiCl_3$ can also undergo disproportionation.[77] This shows that $HSiCl_3$ is also unstable with respect to

disproportionation, and thus its relative stability compared to $HSi(N_3)_3$ may be predominantly a kinetic effect rather than a thermodynamic effect.

The observed formation of SiH_4 and $Si(N_3)_4$ from the reaction of $HSiCl_3$ with $TMS(N_3)$ is in agreement with prior attempts to synthesise $HSi(N_3)_3$. Unfortunately, the observed disproportionation in this reaction means $HSi(N_3)_3$ generated this way cannot be readily used for subsequent study. The considerable excess of $TMS(N_3)$ present in the solution also poses an issue for conducting experiments with $HSi(N_3)_3$, as removal of the solvent would likely leave behind explosive azidosilane residues in dangerous concentrations.

In combination with the $HSi(N_3)_3$ formation reported by Glatthaar using tributyltin azide,[74] the formation of $HSi(N_3)_3$ from $HSiCl_3$ using $TMS(N_3)$ reinforces the evidence that covalent azides may be used to synthesise $HSi(N_3)_3$. However, in both cases the disproportionation of $HSi(N_3)_3$ poses an issue. If disproportionation-free $HSi(N_3)_3$ is to be synthesised, it must therefore be formed much faster than the disproportionation process. To facilitate this, the reagent sodium tetraazidoaluminate tetrakis(THF) $(NaAl(N_3)_4(THF)_4)$[78] was selected, as the formation of $NaAlCl_4$ should provide a stronger driving force for azide-chloride exchange compared to the use of $TMS(N_3)$. $NaAl(N_3)_4(THF)_4$ is poorly soluble in benzene, so after addition of this reagent to a solution of $HSiCl_3$ in C_6D_6, reaction was enabled by sonication with intermittent vigorous shaking. The ^1H NMR spectrum of these reaction solutions typically show near full conversion after just a few minutes of sonication, with $HSi(N_3)_3$ being identified as the major product (based on the NMR data obtained from the prior reaction using $TMS(N_3)$). If left standing, filtered or unfiltered, $HSi(N_3)_3$ solutions made in this way will gradually disproportionate to a mixture of $H_2Si(N_3)_2$, $HSi(N_3)_3$ and $Si(N_3)_4$ over the course of 1–2 days. The ^{27}Al NMR spectrum of these solutions shows the presence of multiple aluminium species, believed to primarily be species of the form $(THF)AlX_3$ (X = Cl, N_3). As tetrachloroaluminate salts are poorly soluble in benzene, an attempt to scavenge these compounds by filtering through excess PPNCl was made with the intention of forming insoluble $[PPN][AlX_4]$. Unfortunately, exposure to PPNCl accelerated the disproportionation of $HSi(N_3)_3$. It is possible that the addition of chloride ions (or indeed any coordinating anionic species) may catalyse disproportionation by forming hypercoordinate silicates that more readily form bridged disproportionation intermediates, since the resulting negatively charged complex would be more nucleophilic (Figure 2.15). This apparent catalysis of

HSi(N$_3$)$_3$ disproportionation by anionic species may also explain why HSi(N$_3$)$_3$ cannot be made using ionic metal azides.
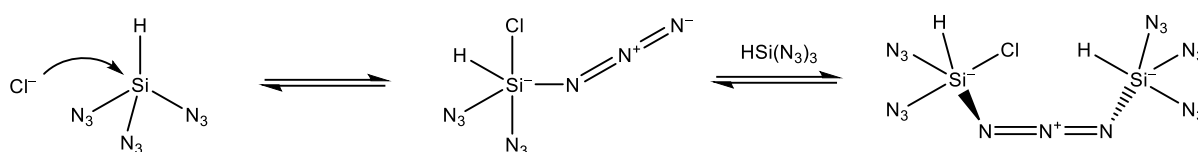
Figure 2.15. Addition of Cl$^-$ to HSi(N$_3$)$_3$, and subsequent formation of a dimeric complex analogous to the intermediate shown in Figure 2.14.

A suitable method of reducing the aluminium content of the solution was found by diluting the reaction solution with several times its volume in hexane. This induces precipitation of the aluminium species, removing most (but not all) aluminium content from solution, according to ^{27}Al NMR spectroscopy. This dilution with hexane also renders the disproportionation of HSi(N$_3$)$_3$ much slower, with only traces of H$_2$Si(N$_3$)$_2$ detectable even after two days. The slower disproportionation is likely to be caused by a combination of lower HSi(N$_3$)$_3$ concentration and reduced solubility of any residual ionic species.

While this method *can* produce disproportionation-free HSi(N$_3$)$_3$, it is unfortunately extremely unreliable. The method is frequently prone to incomplete conversion due to the limited available surface area of the poorly soluble aluminate reagent. Using a greater excess of this reagent or longer reaction times to compensate for this was found to risk inducing disproportionation of HSi(N$_3$)$_3$.

Using THF as the solvent allows Na[Al(N$_3$)$_4$](THF)$_4$ to be soluble, thus enabling a homogenous reaction with HSiCl$_3$. In this case, disproportionation was much faster than conversion, resulting in H$_2$Si(N$_3$)Cl and HSi(N$_3$)$_2$Cl as dominant products. Reaction of this solution with Na(^{Dipp}NCN)(THF) affords (^{Dipp}NCN)SiH$_2$(N$_3$) and (^{Dipp}NCN)SiH(N$_3$)$_2$, as would be expected for the reaction shown in Figure 2.16, helping to verify the identity of these products.
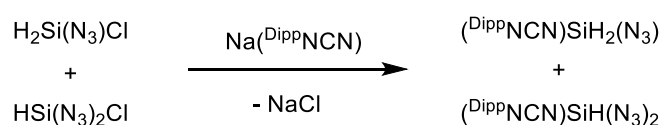
Figure 2.16. Expected outcome from treating a mixture H$_2$Si(N$_3$)Cl and HSi(N$_3$)$_2$Cl with Na(^{Dipp}NCN)(THF)$_x$.

Based on the previous observations from diluting benzene solutions with hexane, using hexane as the reaction solvent may limit the rate of disproportionation. However, here the issue of inconsistent conversion becomes even more significant. In an effort to improve the solubility of the $[Al(N_3)_4]^-$ ion in non-polar solutions, $Na[Al(N_3)_4](THF)_4$ was reacted with 15-crown-5 to make sodium(15-crown-5) tetraazidoaluminate (structure shown in Figure 2.17 as its THF solvate, formed by recrystallising from THF). While apparently more soluble in benzene solutions, this reagent is still insoluble in hexane, and is therefore only an alternative rather than an improvement to $Na[Al(N_3)_4](THF)_4$ for the synthesis of $HSi(N_3)_3$.
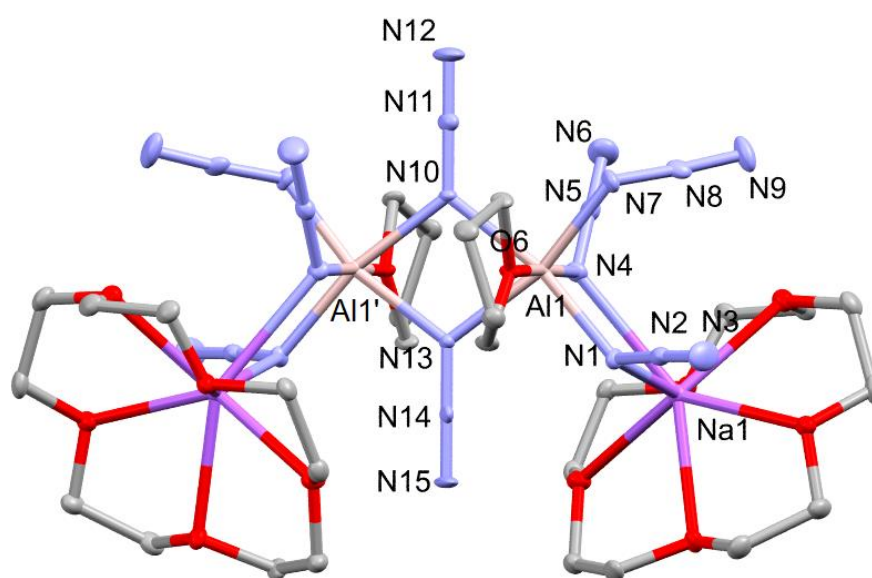
Figure 2.17. Thermal ellipsoid plot of $(Na(15c5)Al(N_3)_4(THF))_2$. Ellipsoids at the 50% probability level, hydrogen atoms are omitted for clarity. The structure has C_2 symmetry with two-fold rotational symmetry along the N10–N13 axis. Selected bond lengths (Å) and angles (°): Al1–O6 2.014(2), Al1–N1 1.955(3), Al1–N4 1.962(2), Al1–N7 1.938(3), Al1–N10 2.020(2), Al1–N13 2.012(2), Na1–N1 2.540(3), Na1–N4 2.648(3), N1–N2 1.220(3), N2–N3 1.147(4), N4–N5 1.204(3), N5–N6 1.153(4), N7–N8 1.198(3), N8–N9 1.157(4), N10–N11 1.233(5), N11–N12 1.125(5), N13–N14 1.214(5), N14–N15 1.133(5), O6–Al1–N1 88.64(10), O6–Al1–N4 176.94(10), O6–Al1–N7 85.46(10), O6–Al1–N10 88.52(6), O6–Al1–N13 87.57(6), N1–Al1–N5 99.39(11), N1–Al1–N4 88.37(10), Al1–N4–Na1 102.01(10), N4–Na1–N1 63.46(8), Na1–N1–Al1 106.09(10), N10–Al1–N13 74.12(10), Al1–N10–Al1' 105.54(15), Al1–N13–Al1' 106.21(15).

A fundamentally different approach to the synthesis of $HSi(N_3)_3$ was attempted by the reaction of $Si(N_3)_4$ with hydride reagents. The proposed reaction scheme is shown in Figure 2.18.

$$Si(N_3)_4 \quad + \quad "H^-" \quad \longrightarrow \quad HSi(N_3)_3 \quad + \quad N_3^-$$
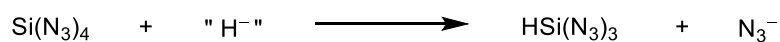
Figure 2.18. Hypothesised reaction outcome of $Si(N_3)_4$ with a hydride source.

The reaction of $Si(N_3)_4$ with sodium hydride (NaH) in toluene for 4 days produced no major products detectable by ^1H NMR. According to ^{14}N and ^{29}Si NMR spectra, most of the material remained as $Si(N_3)_4$. This slow reactivity is likely a result of the insolubility of NaH in toluene. An unknown compound was formed in small amounts, but it lacks Si-H coupling in the ^{29}Si spectrum, indicating this compound is not a hydridosilane.

As a more soluble hydride reagent, lithium tri(tert-butoxy)aluminium hydride ($LiAl(OtBu)_3H$) was thus reacted with $Si(N_3)_4$. Two products are observed by ^{29}Si NMR: a major product with no hydrido substituents and a minor product with one hydrido substituent (based on the Si-H coupling pattern). The chemical shifts of these products are slightly upfield of those expected for $Si(N_3)_4$ and $HSi(N_3)_3$ respectively. The most likely explanation for this is that $LiAl(OtBu)_3H$ transfers a tert-butoxide instead, or in addition to, the hydride. Therefore, these two products are likely $Si(N_3)_3(OtBu)$ and $HSi(N_3)_2(OtBu)$, respectively. The ^1H NMR spectrum supports this hypothesis, showing the presence of multiple different tert-butyl environments in solution. As with the ^{29}Si NMR spectrum, the ^{14}N NMR spectrum shows one major azido product and one minor azido product in solution. Assuming these are the same products observed in the ^{29}Si spectrum, this indicates that both products still retain at least one azido group.

To prevent the issue of tert-butoxide transfer, the reaction between $Si(N_3)_4$ and lithium aluminium hydride ($LiAlH_4$) was tested in toluene, with some DME added to assist in phase transfer. Upon addition of $LiAlH_4$, the reaction mixture bubbled, suggesting that the reagent had reduced azido groups instead of undergoing a hydride-azide exchange reaction. ^1H and ^{29}Si NMR show the presence of $HSi(N_3)_3$ in the solution, but ^1H NMR integration indicates the reaction only formed $HSi(N_3)_3$ in 6% spectroscopic yield. No other identifiable signal could be detected in the ^{29}Si NMR spectrum, indicating the remaining silicon-containing products were insoluble. The solution contains several additional signals in the ^1H NMR

spectrum. Additionally, a ^{7}Li NMR experiment shows the presence of lithium ions in solution. The identity of the compounds giving rise to these ^{1}H and ^{7}Li NMR signals is unclear. The insoluble residue was analysed by IR spectroscopy and found to contain four major absorption bands in the region of $2200 - 2000$ cm^{-1}: 2178 cm^{-1} (s, br), 2161 cm^{-1} (vs, br), 2126 cm^{-1} (m), 2105 cm^{-1} (s). Of these, the absorption at 2105 cm^{-1} is likely to be from $[Si(N_3)_6]^{2-}$ (lit. 2109 cm^{-1})[5], resulting from addition of azide ions to $Si(N_3)_4$. The compounds giving rise to the remaining absorptions may be the result of reduction of $Si(N_3)_4$. The broad signal at 2161 cm^{-1} somewhat resembles the absorption of the hypothesised compound $[Si(N)(N_3)]_n$ (see Chapter 2.2.4). The identity of the other signals remains unknown. While this reaction shows that $HSi(N_3)_3$ can be synthesised from treatment of $Si(N_3)_4$ with a hydride source, this method is not a viable preparative method unless a more selective reagent can be identified.

While the synthesis of pure $HSi(N_3)_3$ (in solution) has now been demonstrated, the methods developed thus far are inconsistent and the limited lifetime of $HSi(N_3)_3$ requires it to be made freshly prior to every study. Thus, despite its analogy to $HSiCl_3$, $HSi(N_3)_3$ was deemed less suitable for further study of hydrido(azido)silicon compounds than the much more stable $(NCN)SiH(N_3)_2$ complexes.

2.2.2. Synthesis of amidinato (NCN) complexes of silicon azides

The synthetic route to $(^{Dipp}NCN)SiH(N_3)_2$ reported by Peerless proceeds with a poor overall yield of 5.9% starting from commercially available reagents (Figure 2.19). While these reagents are not particularly expensive, their cost is certainly not negligible if converted in such poor yields.[79, 80] Thus, the synthesis of $(^{Dipp}NCN)SiH(N_3)_2$ has been investigated to improve the yields to more acceptable levels and facilitate further study.
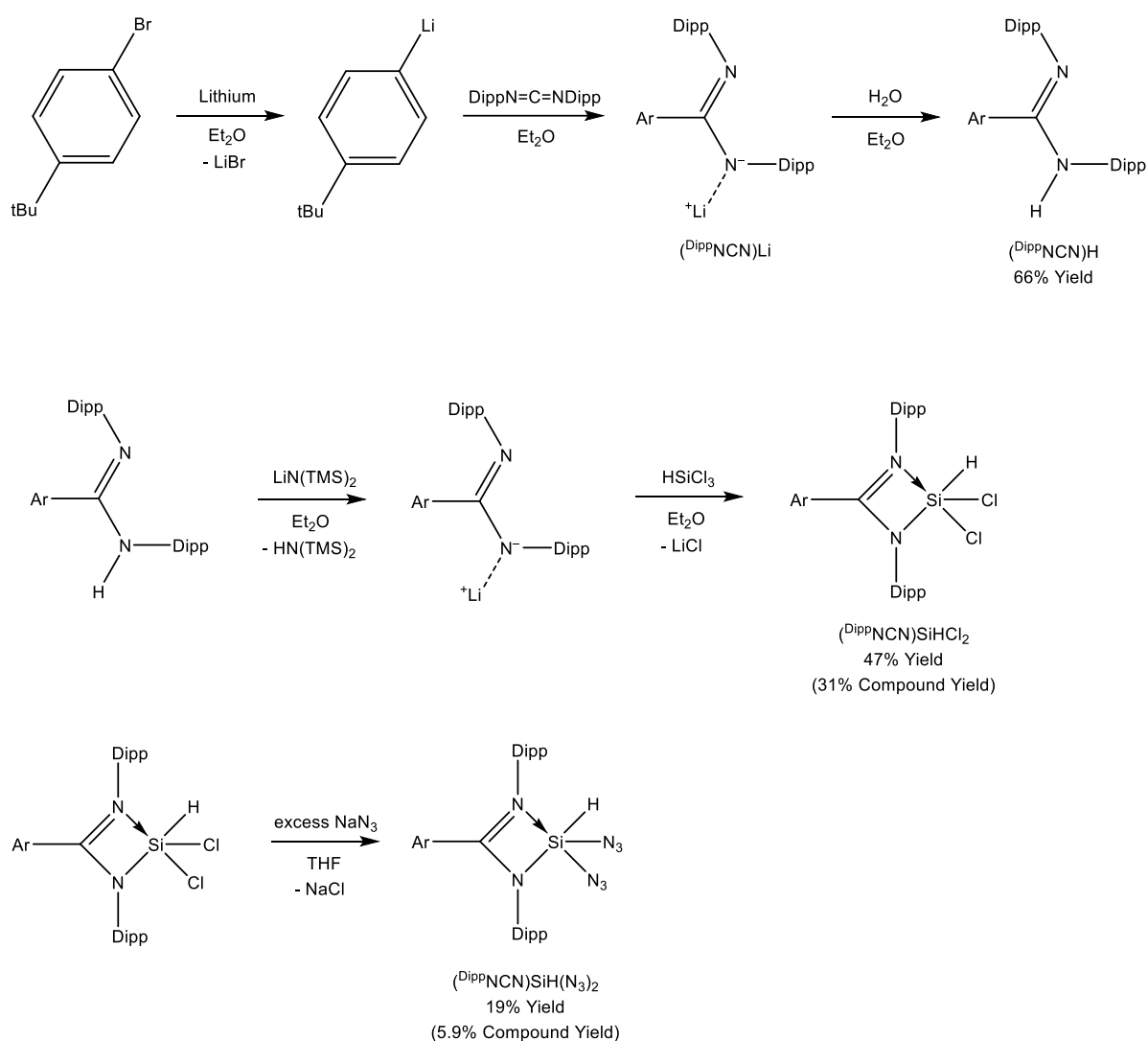
Figure 2.19. Overall reaction scheme for the synthesis of (^{Dipp}NCN)SiH(N$_3$)$_2$ starting from commercially available reagents, with isolated yields for each step and compound yields for the overall sequence.

In the process outlined in Figure 2.19, the protonation of crude Li(^{Dipp}NCN) to isolate (^{Dipp}NCN)H only to deprotonate it again was deemed potentially wasteful, so the crude Et$_2$O solution of Li(^{Dipp}NCN) formed by the reaction of 4-tert-butylphenyllithium with N,N'-bis-(2,6-diisopropylphenyl)carbodiimide was treated directly with HSiCl$_3$. While the primary product of this reaction is indeed found to be (^{Dipp}NCN)SiHCl$_2$ by ^{1}H NMR, it is rather impure. The subsequent solution forms an oily residue upon concentration, from which crystallisation of pure (^{Dipp}NCN)SiHCl$_2$ was difficult. An isolated yield of only 33% could be obtained after weeks of crystallisation, affording only a marginal improvement over the existing compound yield of 31%.

(^{Dipp}NCN)H can be converted to Na(^{Dipp}NCN) (as a THF solvate) instead of Li(^{Dipp}NCN) by reaction with excess NaH in THF. When HSiCl$_3$ is treated with Na(^{Dipp}NCN)(THF)$_x$ and the subsequent reaction mixture filtered and dried under vacuum, the resulting residue contains (^{Dipp}NCN)SiHCl$_2$ of suitably high purity to not require any additional loss-inducing purification steps, affording near quantitative yield (Figure 2.20).
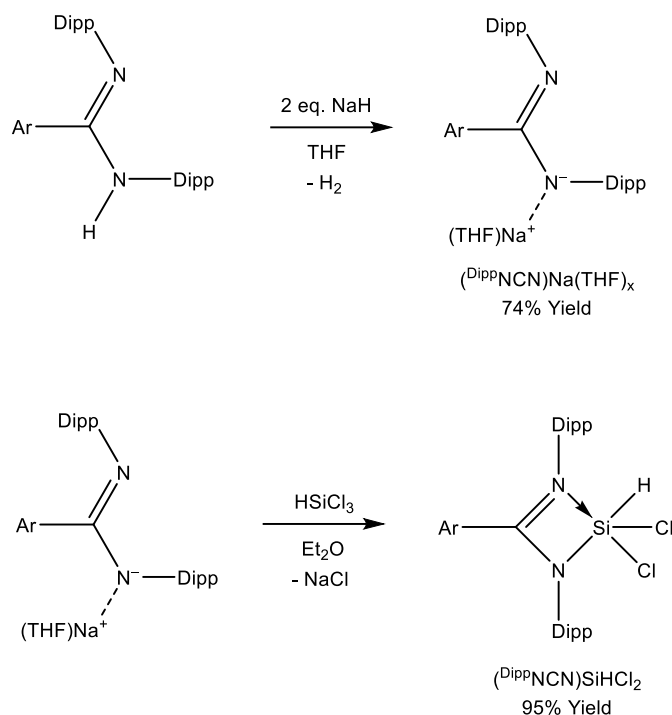
Figure 2.20. Synthesis of isolated (^{Dipp}NCN)Na(THF)$_x$ and subsequent conversion to (^{Dipp}NCN)SiHCl$_2$.

The biggest yield loss in the synthesis of (^{Dipp}NCN)SiH(N$_3$)$_2$ is the final conversion of (^{Dipp}NCN)SiHCl$_2$ to (^{Dipp}NCN)SiH(N$_3$)$_2$. When the products from the reaction of (^{Dipp}NCN)SiHCl$_2$ with NaN$_3$ in THF were analysed after initial extraction, one third of the ^{Dipp}NCN-containing product was found to be (^{Dipp}NCN)H instead of the desired (^{Dipp}NCN)SiH(N$_3$)$_2$. It was therefore investigated if (^{Dipp}NCN)SiH(N$_3$)$_2$ converts to (^{Dipp}NCN)H in the presence of azide ions. Thus, to a solution of (^{Dipp}NCN)SiH(N$_3$)$_2$ in C$_6$D$_6$, PPN(N$_3$) was added, and the mixture sonicated to break up the poorly soluble azide salt. After leaving standing overnight, the mixture was analysed by ^{1}H NMR and found to contain primarily (^{Dipp}NCN)H with no detectable (^{Dipp}NCN)SiH(N$_3$)$_2$ remaining. While the mechanism of this decomposition is unclear, it is likely that the poor yield reported by Peerless for the conversion of (^{Dipp}NCN)SiHCl$_2$ to (^{Dipp}NCN)SiH(N$_3$)$_2$ is due to reaction of the excess azide with the product.

Three different modifications to this synthesis were thus developed. These are outlined in Figure 2.21 with their associated (isolated) yields.
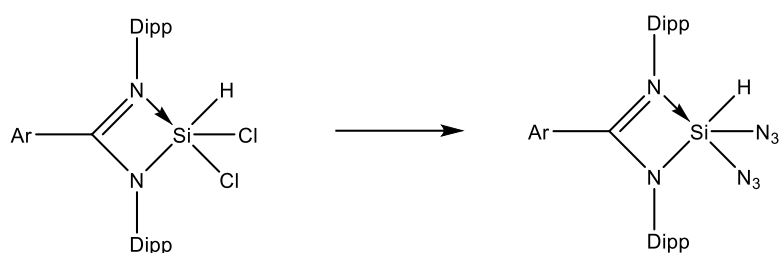
Method 1: 40 eq. TMSN$_3$; 50% yield
Method 2: 2.5 eq. NaN$_3$, 0.01 eq. AlCl$_3$(MeCN), THF; 71% yield
Method 3: 6 eq. NaN$_3$, 0.02 eq. AlCl$_3$, Et$_2$O; 70% yield

Figure 2.21. Conditions and associated yields for the conversion of (^{Dipp}NCN)SiHCl$_2$ to (^{Dipp}NCN)SiH(N$_3$)$_2$.

Taking inspiration from the syntheses of HSi(N$_3$)$_3$, (^{Dipp}NCN)SiHCl$_2$ was suspended in 40 equivalents of TMS(N$_3$) (using the TMS(N$_3$) itself as the solvent). After stirring for just 45 mins and cooling to -40 °C before filtering, a crude mixture of largely (^{Dipp}NCN)SiH(N$_3$)$_2$ and some (^{Dipp}NCN)H was obtained as the filter residue. Although this process also evidently suffers from formation of (^{Dipp}NCN)H, an isolated yield of 50% was obtained after purification – a considerable improvement over the NaN$_3$ in THF method. This method also has the advantage of much faster conversion. Unfortunately, TMS(N$_3$) is a much more expensive reagent than NaN$_3$, and while the leftover solution can be regenerated and recycled by treatment with NaN$_3$ followed by distillation, this adds significant complexity to the synthesis.

Na[Al(N$_3$)$_4$](THF)$_4$ may also be an effective azide transfer reagent for this process by analogy to the syntheses of HSi(N$_3$)$_3$. However, preparing Na[Al(N$_3$)$_4$](THF)$_4$ on sufficient scale for bulk synthesis of (^{Dipp}NCN)SiH(N$_3$)$_2$ is not particularly desirable as it has the potential to be explosive. Crude impact and friction testing on NaAl(N$_3$)$_4$(THF)$_4$ has not found it to be particularly sensitive to explosion in this form. However, it is likely that this stability is aided by the presence of the coordinating THF molecules. It is unclear how readily this material loses THF to evaporation, or the effect of this loss on its stability. Furthermore, storing the material as a THF solution to prevent this hazard results in an increasing yellow discolouration over time, indicating some degree of decomposition. As an alternative, the

reaction of (^{Dipp}NCN)SiHCl$_2$ was conducted with a slight excess of NaN$_3$ and catalytic amounts of AlCl$_3$(MeCN) in THF with the intention of forming Na[Al(N$_3$)$_4$] *in-situ*. The resulting conversion was monitored by taking aliquots for NMR study throughout the reaction and was found to be complete after 88 hours. During the reaction, AlCl$_4$$^-$ can be detected by ^{27}Al NMR, which remains present until the conversion is complete. After conversion has completed, no signals are detected in the ^{27}Al spectrum, believed to be due to the conversion of AlCl$_4$$^-$ to the less-soluble Al(N$_3$)$_4$$^-$. No (^{Dipp}NCN)H formation was detected, however trace disproportionation to (^{Dipp}NCN)Si(N$_3$)$_3$ and (^{Dipp}NCN)SiH$_2$(N$_3$) necessitated purification steps, ultimately resulting in an isolated yield of 71%. It is unclear if this major yield improvement is the result of using AlCl$_3$ as a catalyst, or if it is simply the result of using a lesser excess of NaN$_3$ and stopping the reaction as soon as conversion had finished, thus reducing the exposure of the (^{Dipp}NCN)SiH(N$_3$)$_2$ to azide ions. While it does offer a substantial yield improvement, this synthesis does still have a major drawback – the slow rate of reaction may be the result of passivation of the limited NaN$_3$. While a slow reaction is not intrinsically an issue, passivation may cause the rate of reaction and degree of conversion may vary greatly depending on available reactant surface area. Since (^{Dipp}NCN)SiH(N$_3$)$_2$ appears to decompose in the presence of excess azide, constant monitoring of this synthesis would need to be conducted each time in order to prevent over-reaction.

A more effective method of converting (^{Dipp}NCN)SiHCl$_2$ to (^{Dipp}NCN)SiH(N$_3$)$_2$ was found using excess NaN$_3$ and catalytic AlCl$_3$ in Et$_2$O (based on the synthesis of Si(N$_3$)$_4$ in Et$_2$O discussed in Chapter 3.2.1). The insolubility of NaN$_3$ in Et$_2$O should prevent much direct reaction with (^{Dipp}NCN)SiH(N$_3$)$_2$, while azide-chloride exchange can still occur via the *in-situ* formation of aluminium azides. After 16 hours of reaction, conversion is already completed with little decomposition. Product crystallisation was complicated by the poor solubility of (^{Dipp}NCN)SiH(N$_3$)$_2$ in Et$_2$O, but despite issues with workup an isolated yield of 70% was still obtained. It is likely a much higher yield can be obtained from this reaction if a better workup procedure can be developed, but no further syntheses of (^{Dipp}NCN)SiH(N$_3$)$_2$ were required for this project.

In addition to (^{Dipp}NCN)SiH(N$_3$)$_2$, the analogous complex (^{tBu}NCN)SiH(N$_3$)$_2$ (Figure 2.22) was synthesised according to Method 2 in Figure 2.21 with a yield of 72%. This complex should

serve as a direct comparison to the literature complex (^{tBu}NCN)SiHCl$_2$ used to make the low-valent silicon complex (^{tBu}NCN)SiCl. In contrast to the more stable (^{Dipp}NCN)SiH(N$_3$)$_2$, (^{tBu}NCN)SiH(N$_3$)$_2$ exhibits slow disproportionation in solution (according to ^{1}H NMR spectra), to what is assumed to be (^{tBu}NCN)SiH$_2$(N$_3$) and (^{tBu}NCN)Si(N$_3$)$_3$.
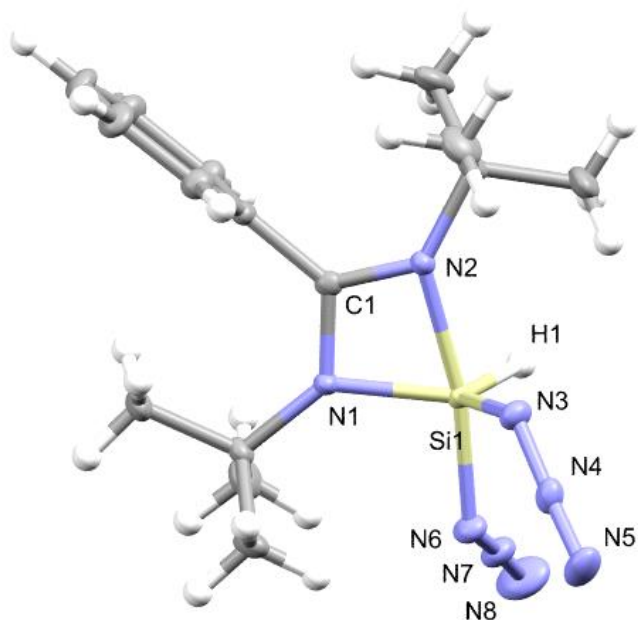
Figure 2.22. Thermal ellipsoid plot of (^{tBu}NCN)SiH(N$_3$)$_2$. Ellipsoids set at the 50% probability level, hydrogen atoms are shown as spheres of fixed radius (0.2 Å). Selected bond lengths (Å) and angles (°): Si1–H1 1.425(14), Si1–N1 1.802(1), Si1–N2 1.923(1), Si1–N3 1.764(1), Si1–N6 1.840(1), C1–N1 1.369(2), C1–N2 1.308(2), N3–N4 1.226(2), N4–N5 1.134(2), N6–N7 1.213(2), N7–N8 1.141(2), N1–Si1–N2 69.82(5), N1–Si1–H1 121.3(6), N1–Si1–N3 116.76(6), N1–Si1–N6 99.25(5), N3–Si1–N6 93.88(6), N6–Si1–N1–N2 dihedral 179.22(6).

A new (NCN)SiHCl$_2$ complex, (^{TMS}NCN)SiHCl$_2$, was also synthesised, and converted to the azido complex (^{TMS}NCN)SiH(N$_3$)$_2$ based on Method 3 from Figure 2.21. The overall synthesis is shown in Figure 2.23. Li(^{TMS}NCN) is synthesised using a different method to the ^{Dipp}NCN and ^{tBu}NCN analogues, using the readily-available reagents benzonitrile and LiN(TMS)$_2$. This makes the ^{TMS}NCN ligand much cheaper to synthesise compared to ^{Dipp}NCN and ^{tBu}NCN.
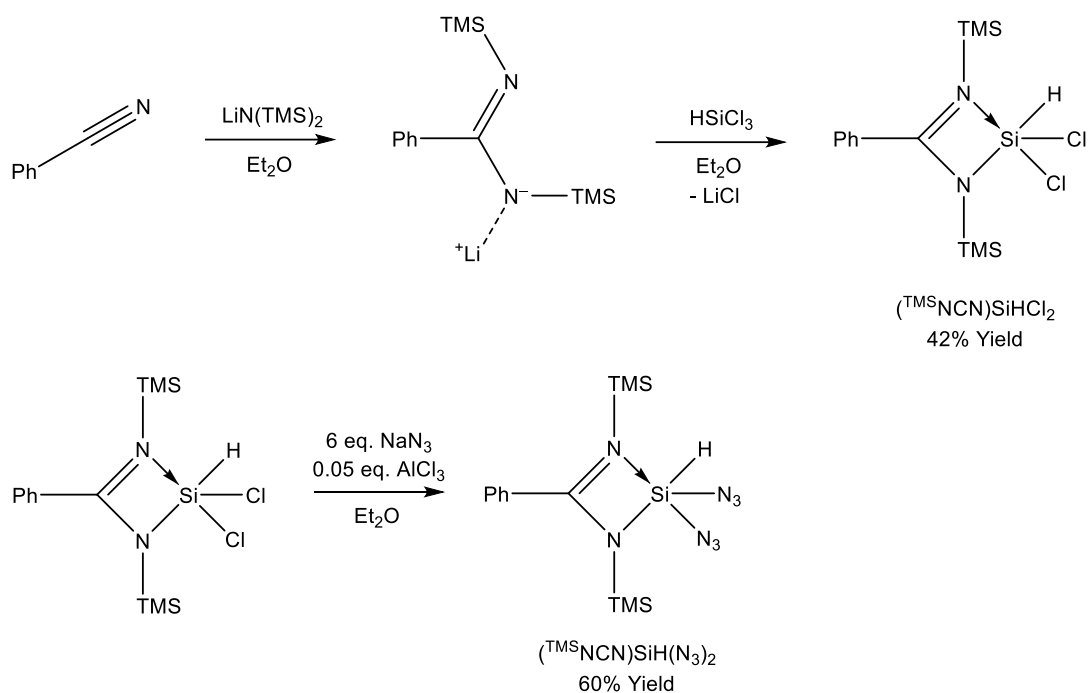
Figure 2.23. Synthesis of (^{TMS}NCN)SiH(N$_3$)$_2$ and its precursor complex (^{TMS}NCN)SiHCl$_2$.
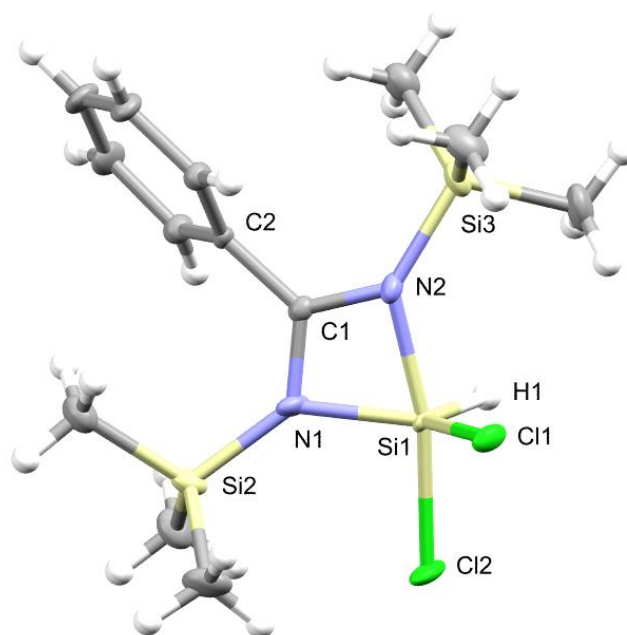
Figure 2.24. Thermal ellipsoid plot of the dominant (80% occupancy) disorder component within crystals of (^{TMS}NCN)SiHCl$_2$. Ellipsoids set at the 50% probability level, hydrogen atoms are shown as spheres of fixed radius (0.2 Å). The minor component is rotated 180 ° around the C1–C2 axis. Selected bond lengths (Å) and angles (°): Si1–H1 1.40(3), Si1–N1 1.832(2), Si1–N2 1.919(2), Si1–Cl1 2.083(1), Si1–Cl2 2.174(1), C1–N1 1.355(2), C1–N2 1.320(2), N1–Si2 1.784(2), N2–Si3 1.768(2), N1–Si1–N2 70.99(7), N1–Si1–H1 124.0(13), N1–Si1–Cl1 119.02(8), N1–Si1–Cl2 96.73(6), Cl1–Si1–Cl2 95.27(4), Cl2–Si1–N1–N2 dihedral -177.90(8).
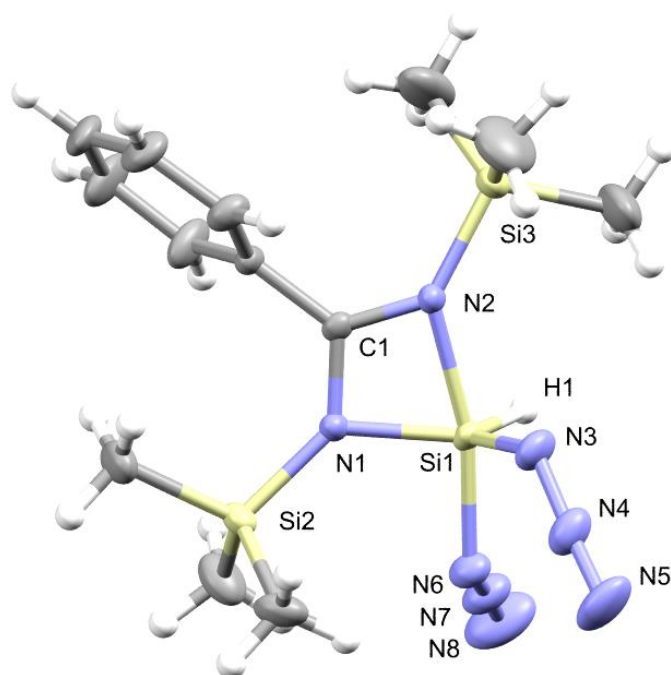
Figure 2.25. Thermal ellipsoid plot of (^{TMS}NCN)SiH(N$_3$)$_2$. Ellipsoids set at the 50% probability level, hydrogen atoms are shown as spheres of fixed radius (0.2 Å). Selected bond lengths (Å) and angles (°): Si1–H1 1.43(2), Si1–N1 1.797(2), Si1–N2 1.948(2), Si1–N3 1.748(2), Si1–N6 1.851(2), C1–N1 1.361(3), C1–N2 1.307(3), N1–Si2 1.768(2), N2–Si3 1.755(2), N3–N4 1.231(3), N4–N5 1.140(4), N6–N7 1.218(3), N7–N8 1.142(4), N1–Si1–N2 70.75(9), N1–Si1–H1 125.5(9), N1–Si1–N3 116.20(11), N1–Si1–N6 95.89(10), N3–Si1–N6 95.54(11), N6–Si1–N1–N2 dihedral -178.33(10).

(^{TMS}NCN)SiH(N$_3$)$_2$ adopts the same conformation as the (^{tBu}NCN)SiH(N$_3$)$_2$, which is unsurprising given their isostructural relationship. The bonding within the two structures is also nearly identical, with almost all bond lengths in (^{TMS}NCN)SiH(N$_3$)$_2$ being within 0.01 Å of the equivalent bonds in (^{tBu}NCN)SiH(N$_3$)$_2$ (with the trivial exception of bonds to Si2 and Si3). The most significant difference is in the Si1–N2 bond, which is longer in (^{TMS}NCN)SiH(N$_3$)$_2$ than in (^{tBu}NCN)SiH(N$_3$)$_2$ (1.948 Å and 1.923 Å respectively). This is surprising, as the strong σ-donating nature of trimethylsilyl groups is predicted to make ^{TMS}NCN a stronger donating ligand than ^{tBu}NCN. As such, it would be expected for (^{TMS}NCN)SiH(N$_3$)$_2$ to have the shorter Si–NCN bond lengths. The longer bond length may be due to silyl groups being weakly π-accepting, thus counteracting the σ-donation effect.

The close similarity of the Si1 coordination centre in (^{tBu}NCN)SiH(N$_3$)$_2$ and (^{TMS}NCN)SiH(N$_3$)$_2$ means these centres are likely to react in similar ways. Unfortunately, work conducted on

the complex (^{TMS}NCN)SiCl$_3$ by MChem student Michael Jones found that the ^{TMS}NCN ligand was prone to activation of the trimethylsilyl groups.[81] As such, no reactivity studies were conducted on (^{TMS}NCN)SiH(N$_3$)$_2$, in favour of (^{Dipp}NCN)SiH(N$_3$)$_2$ and (^{tBu}NCN)SiH(N$_3$)$_2$.

2.2.3. Reactivity and structures of amidinato complexes of silicon azides

(^{tBu}NCN)SiH(N$_3$)$_2$ was found to react with LiN(TMS)$_2$ by the substitution of an azido group for the bis(trimethylsilyl)amide (Figure 2.26), analogous to the reactivity of (^{Dipp}NCN)SiH(N$_3$)$_2$ and contrary to the reactivity of (^{tBu}NCN)SiHCl$_2$. This confirms that the previously observed difference in reactivities of (^{Dipp}NCN)SiH(N$_3$)$_2$ and (^{tBu}NCN)SiHCl$_2$ towards LiN(TMS)$_2$ is due to the difference between azido and chloro groups, rather than differences in the ligand.
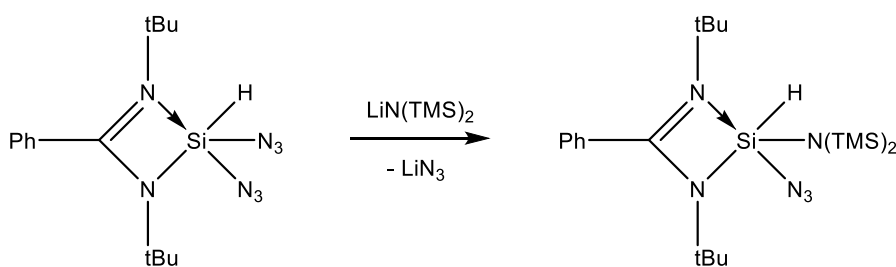
Figure 2.26. Reaction of (^{tBu}NCN)SiH(N$_3$)$_2$ with LiN(TMS)$_2$.
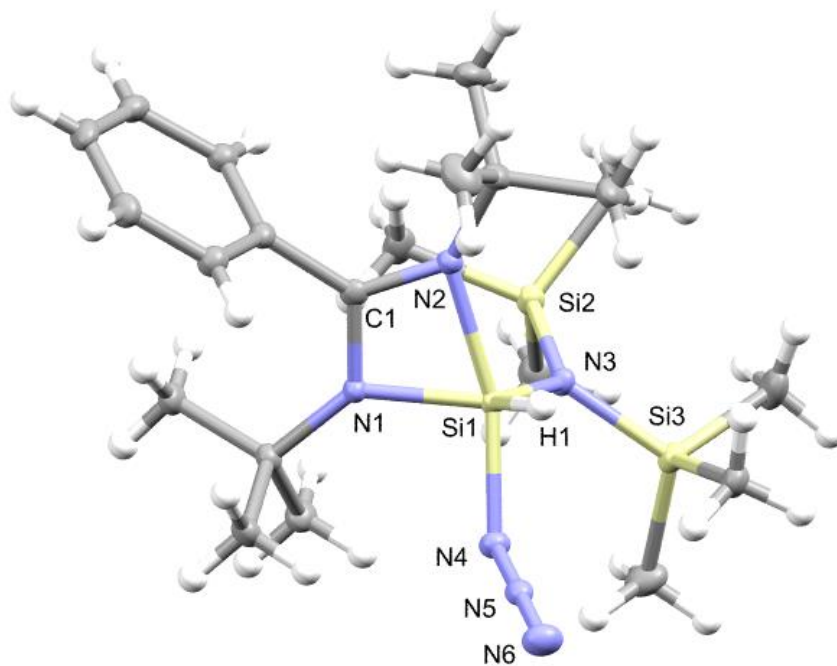
Figure 2.27. Thermal ellipsoid plot of (^{tBu}NCN)SiH(N$_3$)(N(TMS)$_2$). Ellipsoids set at the 50% probability level, hydrogen atoms are shown as spheres of fixed radius (0.2 Å). Selected bond lengths (Å) and angles (°): Si1–H1 1.421(15), Si1–N1 1.816(1), Si1–N2 1.974(1), Si1–N3 1.735(1), Si1–N4 1.881(1), C1–N1 1.360(2), C1–N2 1.317(2), N3–Si2 1.756(1), N3–Si3 1.766(1), N4–N5 1.216(2), N5–N6 1.143(2), N1–Si1–N2 68.88(5), N1–Si1–H1 118.1(6), N1–Si1–N3 119.73(5), N1–Si1–N4 95.90(5), N3–Si1–N4 96.56(5), N4–Si1–N1–N2 dihedral 167.81(5).

A comparison of the silicon coordination environment in the crystal structures of (^{tBu}NCN)SiH(N$_3$)$_2$, (^{tBu}NCN)SiH(N$_3$)(N(TMS)$_2$) and their ^{Dipp}NCN analogues is shown in Table 2.1, and the bonding of their azido groups in Table 2.2.

Compound	(NCN) bite-angle / °	Si–(NCN) (equatorial) length / Å	Si–(NCN) (axial) length / Å	Si–H (equatorial) length / Å	Si–N$_3$ (axial) length / Å	Si–N$_3$ (equatorial) length / Å	Si–N(TMS)$_2$ (equatorial) length / Å
(^{Dipp}NCN)SiH(N$_3$)$_2$	68.74(14)	1.786(3)	1.972(3)	1.31(4)	1.805(4)	1.751(4)	–
(^{Dipp}NCN)SiH(N$_3$)-(N(TMS)$_2$)†	57.51(8) 56.62(8)	1.780(2) 1.774(2)	2.649(2) 2.674(2)	1.37(2) 1.38(2)	1.762(2) 1.758(2)	–	1.704(2) 1.710(2)
(^{tBu}NCN)SiH(N$_3$)$_2$	69.82(5)	1.802(1)	1.923(1)	1.425(14)	1.840(1)	1.764(1)	–
(^{tBu}NCN)SiH(N$_3$)-(N(TMS)$_2$)	68.88(4)	1.816(1)	1.974(1)	1.421(15)	1.881(1)	–	1.735(1)

Table 2.1. Table of ligand bite-angles and bond lengths around the central silicon atom of (^{Dipp}NCN)SiH(N$_3$)$_2$,[73] (^{Dipp}NCN)SiH(N$_3$)(N(TMS)$_2$),[73] (^{tBu}NCN)SiH(N$_3$)$_2$ and (^{tBu}NCN)SiH(N$_3$)(N(TMS)$_2$). All complexes can be described as distorted trigonal bipyramidal, so ligands have been categorised into axial and equatorial substituents. † (^{Dipp}NCN)SiH(N$_3$)(N(TMS)$_2$) crystallises with two symmetrically distinct complexes with slightly different conformations.

Compound	Si–N$_3$ (axial) length / Å	N$_\alpha$–N$_\beta$ (axial) length / Å	N$_\beta$–N$_\gamma$ (axial) length / Å	Si–N$_3$ (equatorial) length / Å	N$_\alpha$–N$_\beta$ (equatorial) length / Å	N$_\beta$–N$_\gamma$ (equatorial) length / Å	Azide asym. absorption / cm^{-1}
(^{Dipp}NCN)SiH(N$_3$)$_2$	1.805(4)	1.211(5)	1.146(6)	1.751(4)	1.233(5)	1.133(6)	2159s 2148s 2119s
(^{Dipp}NCN)SiH(N$_3$)-(N(TMS)$_2$)†	1.762(2) 1.758(2)	1.224(3) 1.215(3)	1.132(3) 1.137(3)	–	–	–	2145s 2118m
(^{tBu}NCN)SiH(N$_3$)$_2$	1.840(1)	1.213(2)	1.141(2)	1.764(1)	1.226(2)	1.134(2)	2151s 2136s 2128s
(^{tBu}NCN)SiH(N$_3$)-(N(TMS)$_2$)	1.881(1)	1.216(2)	1.143(2)	–	–	–	2111s

Table 2.2. Table of Si–N$_3$ and N–N bond lengths in (^{Dipp}NCN)SiH(N$_3$)$_2$,[73] (^{Dipp}NCN)SiH(N$_3$)(N(TMS)$_2$),[73] (^{tBu}NCN)SiH(N$_3$)$_2$ and (^{tBu}NCN)SiH(N$_3$)(N(TMS)$_2$), and their respective azido group asymmetric stretching frequencies. All complexes can be described as distorted trigonal bipyramidal, so ligands have been categorised into axial and equatorial substituents. † (^{Dipp}NCN)SiH(N$_3$)(N(TMS)$_2$) crystallises with two symmetrically distinct complexes with slightly different conformations.

The complex (^{tBu}NCN)SiH(N$_3$)$_2$ has the same arrangement of substituents as (^{Dipp}NCN)SiH(N$_3$)$_2$. The ^{tBu}NCN binds in a slightly more symmetric fashion, with a smaller difference between the axial and equatorial Si–N bond lengths compared to (^{Dipp}NCN)SiH(N$_3$)$_2$. The average of the Si–(NCN) bonds is also slightly shorter for the ^{tBu}NCN

complex at 1.863 Å compared to 1.879 Å, implying it is slightly more strongly bound overall. This can be rationalised by the fact that tert-butyl groups are stronger electron donors than diisopropylphenyl groups, thus making the ligand an overall slightly stronger electron donor. The stronger binding of the ligand may also explain why all other bonds to the silicon atom are longer in (^{tBu}NCN)SiH(N$_3$)$_2$ compared to (^{Dipp}NCN)SiH(N$_3$)$_2$, as the bonding orbitals to the ^{tBu}NCN ligand would contain a greater silicon s-orbital character, thus reducing the s-orbital character of other bonds to the silicon, rendering them weaker. Curiously, this difference seems to have no effect on the bonding within each azido group, as all N–N bond lengths in (^{tBu}NCN)SiH(N$_3$)$_2$ are the same as the equivalent bonds in (^{Dipp}NCN)SiH(N$_3$)$_2$ (within standard deviation). This suggests that the N–N bonds are significantly less sensitive to the change of ligand than the Si–N$_3$ bonds, consistent with the diminishing effects of sigma donation with increasing substituent distance. The N–N bond lengths of the (axial) azido group of (^{tBu}NCN)SiH(N$_3$)(N(TMS)$_2$) are also the same as the equivalent bonds in the axial azido group of (^{tBu}NCN)SiH(N$_3$)$_2$, similarly indicating that the bonding within the azido group is not very sensitive to the change of a substituent on the silicon centre, provided the coordination geometry remains similar.

The complexes (^{tBu}NCN)SiH(N$_3$)(N(TMS)$_2$) and (^{Dipp}NCN)SiH(N$_3$)(N(TMS)$_2$) have a much more staggering difference between them. In (^{Dipp}NCN)SiH(N$_3$)(N(TMS)$_2$), the axial nitrogen atom of the ligand has been effectively de-coordinated, with a much greater Si–N bond length than any other (NCN)–Si complex. This nitrogen still appears to exert steric pressure on the silicon centre, so the complex still resembles a distorted trigonal bipyramidal structure rather than a tetrahedral one, but the length of the Si–N bond indicates there is only a very weak interaction. By contrast, (^{tBu}NCN)SiH(N$_3$)(N(TMS)$_2$) adopts a very similar conformation to (^{tBu}NCN)SiH(N$_3$)$_2$. The unusual de-coordination of the ^{Dipp}NCN axial nitrogen atom in (^{Dipp}NCN)SiH(N$_3$)(N(TMS)$_2$) is likely the result of steric pressure being exerted by the N(TMS)$_2$ group. It can therefore be explained that this phenomenon does not occur for (^{tBu}NCN)SiH(N$_3$)(N(TMS)$_2$) because the tert-butyl groups are less sterically demanding than diisopropylphenyl groups. The coordination of the axial ^{tBu}NCN nitrogen atom significantly increases the Si–N bond length of the azide *trans* to it, as it is donating electron density into the antibonding orbital of the Si–N$_3$ bond. The equatorial Si–(NCN) bond length also increases due to rearrangement of electrons in the ligand to adopt a more symmetric

coordination geometry. The significantly longer Si–N3 interaction in (^{tBu}NCN)SiH(N$_3$)(N(TMS)$_2$) can be seen to also have an effect on the N–N bonding within the azido group. The N4–N5 bond length is essentially equal to the (average) corresponding length in (^{Dipp}NCN)SiH(N$_3$)(N(TMS)$_2$) (1.216 Å and 1.219 Å respectively), however the N5–N6 bond is slightly longer than its equivalent in (^{Dipp}NCN)SiH(N$_3$)(N(TMS)$_2$) (1.142 Å and 1.135 Å respectively). The difference between the N$_\alpha$–N$_\beta$ and N$_\beta$–N$_\gamma$ bond lengths is thus lesser in (^{tBu}NCN)SiH(N$_3$)(N(TMS)$_2$) than (^{Dipp}NCN)SiH(N$_3$)(N(TMS)$_2$) (0.074 Å and 0.084 Å respectively), indicating a slightly more ionic azido group, which can also be seen in the slightly lower IR absorption frequency.

With exception of the Si–H bond length, all other bonds to the silicon atom are longer in (^{tBu}NCN)SiH(N$_3$)(N(TMS)$_2$) compared to the analogous bond in (^{tBu}NCN)SiH(N$_3$)$_2$. This effect likely arises from a combination of the stronger donating character and higher steric demand of the N(TMS)$_2$ group compared to the azido group it replaced. Since the Si–H bond length appears to be unaffected, it is likely that the steric effect is more significant, however there is inherent difficulty in accurately determining bond lengths to hydrogen using SCXRD, so the effect on the hydrogen is less certain.

The known reaction of (^{tBu}NCN)SiHCl$_2$ with LiN(TMS)$_2$ to form (^{tBu}NCN)SiCl has also been conducted and the reaction of (^{tBu}NCN)SiCl with Na[Al(N$_3$)$_4$](THF)$_4$ was conducted with intention of forming the low-valent (^{tBu}NCN)Si(N$_3$). However, on addition of the tetraazidoaluminate reagent bubbling was observed, suggesting the decomposition of azido groups. The reaction was monitored by NMR spectroscopy, from which the (^{tBu}NCN)SiCl was observed to have been completely consumed. No new products were identified by ^{1}H or ^{29}Si NMR, indicative of the reaction products precipitating from solution. No identifiable product could be isolated from the precipitate, however it seems the intended complex (^{tBu}NCN)Si(N$_3$) did not form, as this complex would likely be soluble in C$_6$D$_6$. Considering the visible effervescence, it is hypothesised that (^{tBu}NCN)Si(N$_3$) is unstable with respect to a polymerisation process involving the elimination of N$_2$. The product of such a process may be a form of polymeric nitrido-silicon compound, however this is purely speculative given the inability to isolate any product from this reaction (Figure 2.28).
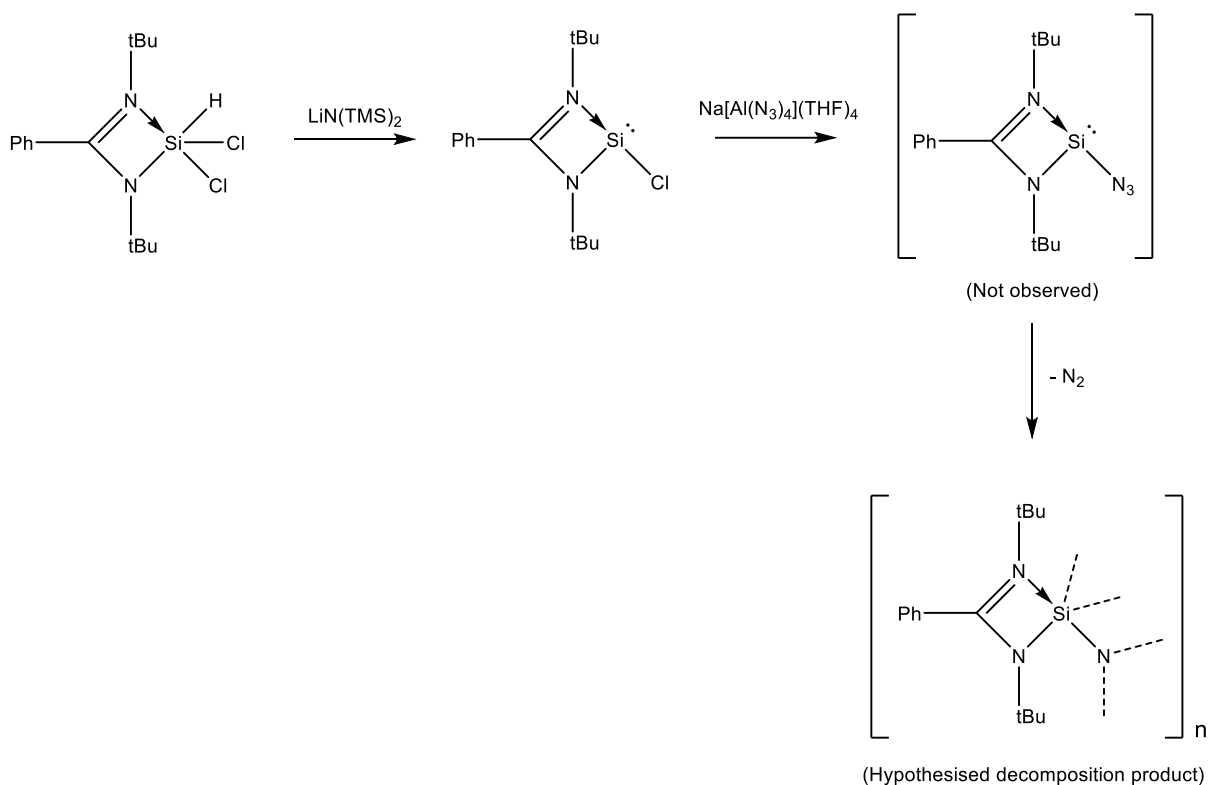
Figure 2.28. Formation of (^{tBu}NCN)SiCl and subsequent reaction with Na[Al(N$_3$)$_4$](THF)$_4$, with hypothesised products.

The reaction of (^{Dipp}NCN)SiH(N$_3$)$_2$ and ItBu has been previously observed to form [ItBuH][(^{Dipp}NCN)SiH(N$_3$)$_3$].[73] The formation of this product hints at the possible formation of a low-valent azidosilicon complex (^{Dipp}NCN)Si(N$_3$) based on reaction stoichiometry (see Chapter 2.1.2). To better understand this reaction, the addition of 1 equivalent of ItBu to a C$_6$D$_6$ solution of (^{Dipp}NCN)SiH(N$_3$)$_2$ was monitored by NMR spectroscopy over several days. Over the first 2 hours, some initial conversion to a new product is observed by ^{1}H NMR spectroscopy. The new signals contain evidence of both ^{Dipp}NCN and ItBu ligands in new environments, as well as a new Si–H environment. All of these new signals remain at the same ratio throughout the experiment, indicating they either belong to the same compound or are different products formed by the same reaction. Curiously, the tert-butyl signals of the ItBu-containing product are split when the spectrum is recorded at 293 K, but merge to a single signal at 298 K. The split signal shows that these two tert-butyl groups are in slightly different environments, indicating the presence of coordinated ItBu rather than an [ItBuH]$^+$ ion, since these groups would be equivalent in the latter. There is only one clearly identifiable new signal that can be attributed to imidazolyl protons, based on the criteria

48

that such a signal should be a singlet in aromatic region of the ^1H spectrum and should have ^{13}C satellite signals. This signal appears at 7.99 ppm, a significantly higher chemical shift than the imidazolyl proton of ItBu (6.79 ppm), and curiously only has a relative integral of 1H (compared to 18H for the merged tert-butyl group signal). This suggests that the ItBu in the product is coordinated in an abnormal fashion (coordinating through the 4-position of the imidazole ring rather than the normal 2-position), as ItBu in its normal coordination mode should have two equivalent imidazolyl protons. This abnormal coordination is not surprising, considering the existence of the known compound ($^{Dipp}NCN)SiH(N_3)_2(ab$-IPr),[73] which involves a different N-heterocyclic carbene, IPr, coordinated to the same silicon complex in the same abnormal fashion. The Si−H environment of the product has a $^1J_{Si-H}$ coupling value of 290 Hz. This is down from the 311 Hz of the starting complex ($^{Dipp}NCN)SiH(N_3)_2$. Reduction of the Si-H coupling value is expected for the conversion of a pentacoordinate silicon complex to a hexacoordinate complex. Since the Si-H coupling value is dependent on the degree of s-character in the Si−H bond, it can be estimated that this conversion would reduce the $^1J_{Si-H}$ value to approximately 5/6 of its original value (since the Si s-orbital is shared between 6 substituents instead of 5). As such, the $^1J_{Si-H}$ value of ($^{Dipp}NCN)SiH(N_3)_2$ would be expected to be reduced to approximately 259 Hz if converted to a hexacoordinate complex by addition of another ligand. The observed product's $^1J_{Si-H}$ value of 290 Hz is not consistent with this predicted change, but is nonetheless lower than the value for ($^{Dipp}NCN)SiH(N_3)_2$. This lesser reduction in the $^1J_{Si-H}$ coupling value might instead arise from the substitution of an azido group for a more strongly donating ItBu group.

Despite the starting complex, ($^{Dipp}NCN)SiH(N_3)_2$, remaining clearly detectable in all ^1H NMR spectra recorded over the first 4 days of reaction, it was not detected by ^{29}Si NMR analysis. The absence of ($^{Dipp}NCN)SiH(N_3)_2$ signals by ^{29}Si NMR may be indicative of rapid chemical exchange, broadening the ^{29}Si signals of ($^{Dipp}NCN)SiH(N_3)_2$, while the ^1H spectrum may remain unaffected due to the different frequency ranges of ^1H NMR and ^{29}Si NMR. On the other hand, the reaction product is observed in both ^1H and ^{29}Si spectra (identified as the same compound in each by the $^1J_{Si-H}$ coupling constant). As such, if ($^{Dipp}NCN)SiH(N_3)_2$ is undergoing rapid chemical exchange, the product observed in the ^1H and ^{29}Si spectra must not be part of this rapid exchange process.

The ratio of product : $(^{Dipp}NCN)SiH(N_3)_2$ was monitored by the ratio of the ^1H integrals of the product's imidazolyl proton (7.99 ppm) and the $(^{Dipp}NCN)SiH(N_3)_2$ Si–H proton (6.09 ppm). These signals were chosen as they are not convoluted by overlap with other signals. The ratios observed during the first 4 days of reaction are listed in Table 2.3.

Time after reaction start	Product : $(^{Dipp}NCN)SiH(N_3)_2$ ratio
5 minutes	0.12 : 1
45 minutes	0.25 : 1
1 hour	0.26 : 1
2 hours	0.37 : 1
16 hours	0.45 : 1
4 days	0.69 : 1

Table 2.3. The ratio of observed product (from reaction of ItBu with $(^{Dipp}NCN)SiH(N_3)_2$) to the starting complex $(^{Dipp}NCN)SiH(N_3)_2$. Ratios are determined by integration of ^1H NMR spectra.

From Table 2.3, the reaction appears to slow down significantly after the first few hours, despite both $(^{Dipp}NCN)SiH(N_3)_2$ and free ItBu remaining in higher concentrations than the product. This is indicative of an equilibrium reaction, where the product concentration is tending towards an equilibrium value rather than complete conversion. During the first few days, a few large crystals grew in the solution which were found to be $[ItBuH][(^{Dipp}NCN)SiH(N_3)_3]$ by SCXRD. This is a curious result, as it implies that the crystallisation of $[ItBuH][(^{Dipp}NCN)SiH(N_3)_3]$ out of solution does not disrupt the equilibrium in the solution phase. If this crystallisation is not highly thermodynamically favoured, it may also be in equilibrium with the solution phase reactants, thus failing to drive the reaction to completion. To confirm the equilibrium hypothesis, 2 more equivalents of ItBu were added shortly after the "4-days" spectrum was recorded, bringing the total ItBu content added to the reaction to 3 equivalents. Just 5 minutes after this addition, the ratio of product : $(^{Dipp}NCN)SiH(N_3)_2$ had increased to 1.00 : 1. Again, rapid conversion was observed over the first few hours, with a ratio of 1.47 : 1 after 2 hours, but with very little subsequent conversion (ratio after 15 hours = 1.56 : 1). The temperature dependence of the equilibrium was then tested by cooling the sample down to 10 °C for the next 22 hours, resulting in a significant increase in conversion, with a product : $(^{Dipp}NCN)SiH(N_3)_2$ ratio of 4.07 : 1.

Subsequently the sample was returned to room temperature. After just 1 hour at room temperature, the intensity of the signal for (^{Dipp}NCN)SiH(N$_3$)$_2$ had mostly returned to the level it was at before cooling (Figure 2.29), with a product : (^{Dipp}NCN)SiH(N$_3$)$_2$ ratio of 1.89 : 1.
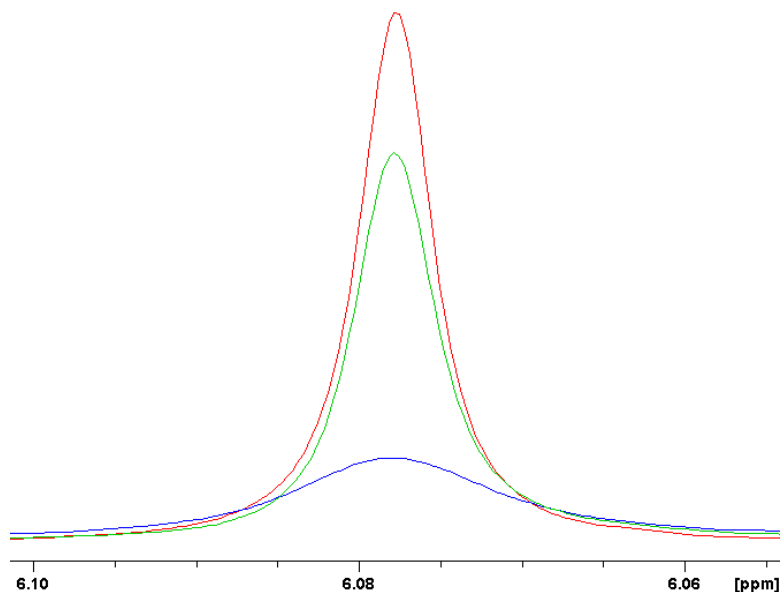
Figure 2.29. Stacked ^{1}H NMR spectra, showing the Si-H resonance of (^{Dipp}NCN)SiH(N$_3$)$_2$ 15 hours after addition of extra ItBu (red), after standing at 10 °C for 22 hours (blue), and 1 hour after subsequently returning to room temperature (green). All spectra are normalised such that the solvent signal has the same profile and intensity. The signals have been adjusted to the same chemical shift for the sake of comparison; the chemical shift of the Si-H resonance was observed to vary by up to 0.02 ppm with changes in temperature.

The low concentration of (^{Dipp}NCN)SiH(N$_3$)$_2$ in the ^{1}H spectrum recorded at 10 °C allows the aromatic proton environments of the product to be more easily identified. The peak at 7.99 ppm remains the only signal readily attributable to an imidazolyl proton. This suggests that the ItBu in the product is not only coordinated, but also deprotonated, thus only has one imidazolyl proton. This can explain the source of the proton needed to form the [ItBuH]$^+$ ion of [ItBuH][(^{Dipp}NCN)SiH(N$_3$)$_3$]. The origin of this proton had previously been elusive, as both reagents and the solvent had been verified spectroscopically to be free of acidic impurities, and the reaction conducted under a sealed inert atmosphere. Based on these observations, the full reaction scheme for the addition of ItBu to (^{Dipp}NCN)SiH(N$_3$)$_2$ is proposed in Figure 2.30.
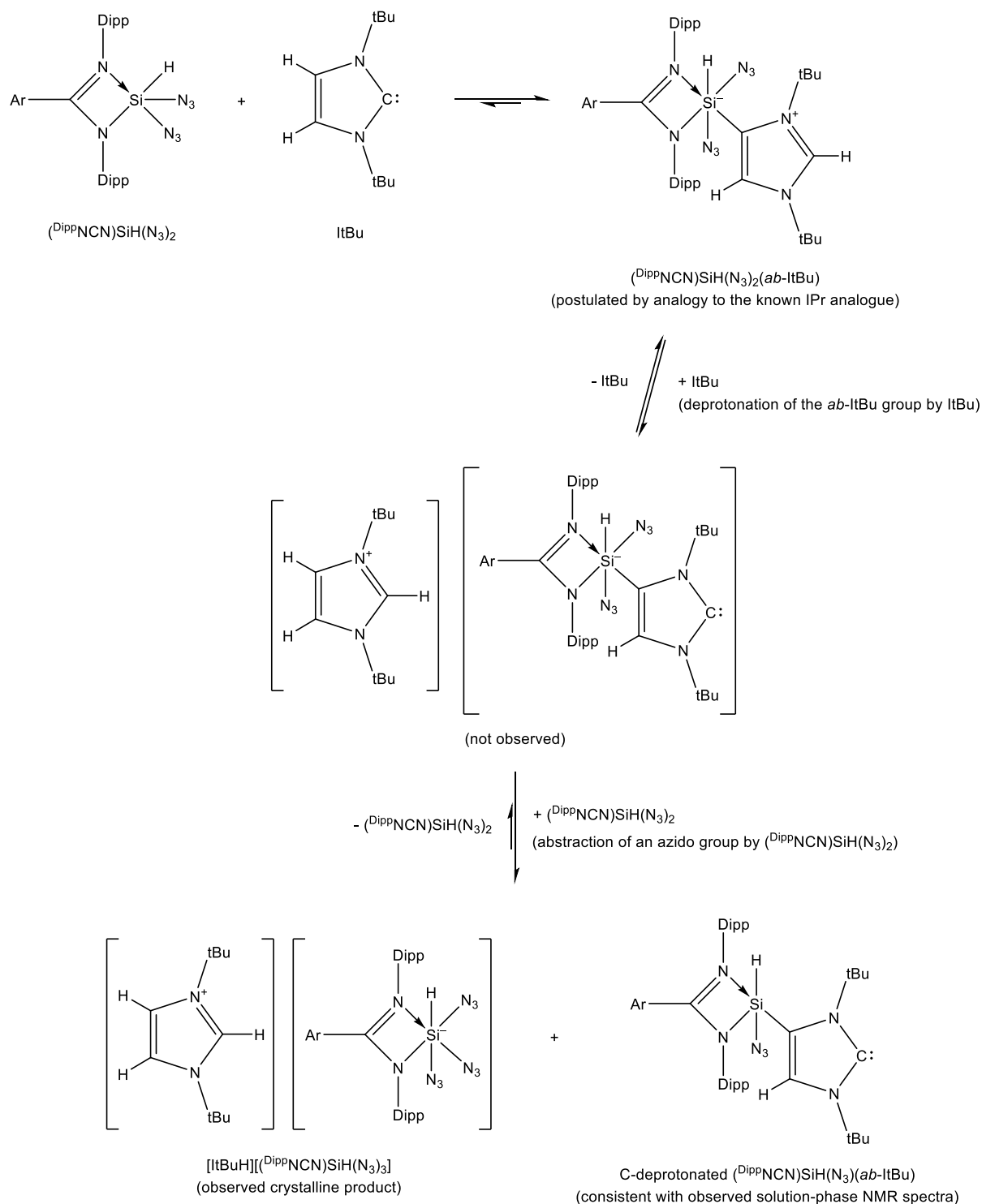
Figure 2.30. Proposed reaction scheme for ItBu with (^{Dipp}NCN)SiH(N$_3$)$_2$ based on the observed product and solution-phase spectra.

The reaction scheme in Figure 2.30 satisfies the stoichiometry needed to produce the known insoluble product [ItBuH][(^{Dipp}NCN)SiH(N$_3$)$_3$] while the proposed product in solution matches the solution-phase NMR observations. The overall reaction from (^{Dipp}NCN)SiH(N$_3$)$_2$(*ab*-ItBu) to the products involves transfer of a proton from a silicon-

52

substituted ItBu molecule to an unsubstituted ItBu molecule, and transfer of an azide ion from one hexacoordinate ^{Dipp}NCN-silicon complex to form another hexacoordinate ^{Dipp}NCN-silicon complex. As such, it is reasonable that this reaction has minimal driving force and thus settles as an equilibrium rather than going to completion. It should be noted that the "C-deprotonated (^{Dipp}NCN)SiH(N$_3$)(*ab*-ItBu)" shown in Figure 2.30 is deprotonated in the 2-position of the imidazole ring, however deprotonation on the 5-position of the ring would also be consistent with the observed NMR spectra. Regardless of structure, the NMR spectra clearly show that the solution-phase product still retains a silicon-bound hydrogen. As such, no reductive elimination of HN$_3$ from the silicon centre has occurred in this reaction, so the low-valent complex (^{Dipp}NCN)Si(N$_3$) is not formed, contrary to the prior hypothesis. As such, the reaction of (^{Dipp}NCN)SiH(N$_3$)$_2$ with ItBu (and perhaps N-heterocyclic carbenes as a whole) is not effective for the synthesis of low-valent silicon azides.

Na(^{Dipp}NCN)(THF)$_x$ was found to not react with (^{Dipp}NCN)SiH(N$_3$)$_2$ in C$_6$D$_6$ under ambient conditions, but when heated at 100 °C in the presence of 15-crown-5, conversion to a new product over 46 hours was observed by NMR spectroscopy and accompanied by precipitate formation. The solution was filtered and dried, and crystals of the hexacoordinate complex (^{Dipp}NCN)$_2$SiH(N$_3$) were obtained as a toluene solvate after recrystallisation of the dried residue from toluene. The reaction is as shown in Figure 2.31.
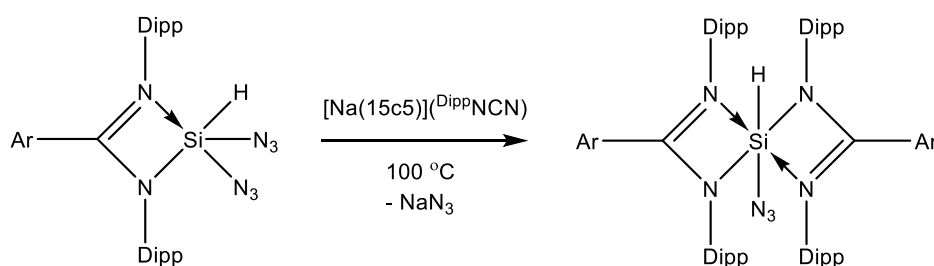
Figure 2.31. Synthesis of (^{Dipp}NCN)$_2$SiH(N$_3$).
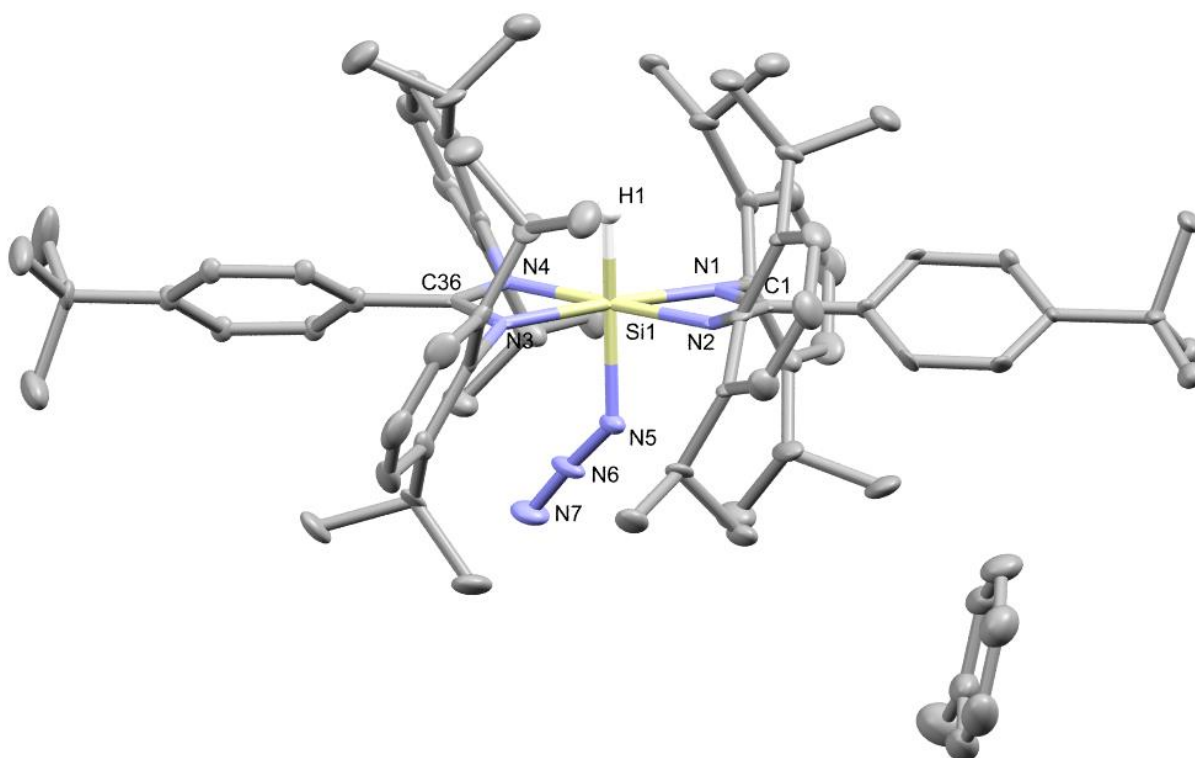
Figure 2.32. Thermal ellipsoid plot of (^{Dipp}NCN)$_2$SiH(N$_3$)·(toluene). Ellipsoids set at the 50% probability level. The hydride is shown as a sphere of fixed radius (0.2 Å), other hydrogen atoms are omitted for clarity. Selected bond lengths (Å) and angles (°): Si1–H1 1.46(13), Si1–N1 1.933(5), Si1–N2 1.906(5), Si1–N3 1.940(5), Si1–N4 1.905(5), Si1–N5 1.863(6), C1–N1 1.338(8), C1–N2 1.338(8), C36–N3 1.334(8), C36–N4 1.351(8), N5–N6 1.223(9), N6–N7 1.138(9), N1–Si1–N2 68.8(2), N3–Si1–N4 69.1(2), N5–Si–N1 88.1(2), N5–Si–N2 87.1(2), N5–Si–N3 88.6(2), N5–Si–N4 93.3(2) N4–Si1–N5–N6 dihedral 6.6(7).

The two ^{Dipp}NCN ligands in (^{Dipp}NCN)$_2$SiH(N$_3$) bind *trans* to each other, as this is the only way to avoid steric clash between the ligands. Both ligands bind in a slightly asymmetric fashion, with one nitrogen of each ^{Dipp}NCN ligand bonding slightly closer to the silicon than the other. Interestingly, the bonding is such that the short (^{Dipp}NCN)–Si bonds are *trans* to each other (Si1–N2, Si1–N4). The ^{Dipp}NCN ligands adopt a conformation that gives the overall complex near-C$_2$ symmetry, with the azido group breaking this symmetry. As viewed down the N5–Si1 bond axis, the azido group eclipses N4 with a dihedral angle N6–N5–Si1–N4 of only 6.6 °. As such, the azido group exerts steric pressure on N4, causing the N5–Si1–N4 angle to be the widest N5–Si1–N angle (93.3 °) and twisting the N3/N4 ^{Dipp}NCN ligand to be slightly out of plane with the N1/N2 ligand (N1–N2–N3–N4 dihedral angle = -3.2(2) °).

In sharp contrast to the substitution reactions of LiN(TMS)$_2$ and Na(^{Dipp}NCN), addition of the silanide reagent (THF)$_3$LiSi(TMS)$_3$ to a C$_6$D$_6$ solution of (^{Dipp}NCN)SiH(N$_3$)$_2$ results in immediate vigorous bubbling, implying the decomposition of an azido group with loss of N$_2$. The precipitate was filtered off and found to contain LiN$_3$ by IR spectroscopy. The solvent was removed under vacuum and replaced with hexane. Slow evaporation of the hexane solution afforded crystals of a hydridosilaimine complex (^{Dipp}NCN)Si(H)=NSi(TMS)$_3$ (Figure 2.33). The mechanism of this process is not certain, with two plausible routes outlined in Figure 2.34.
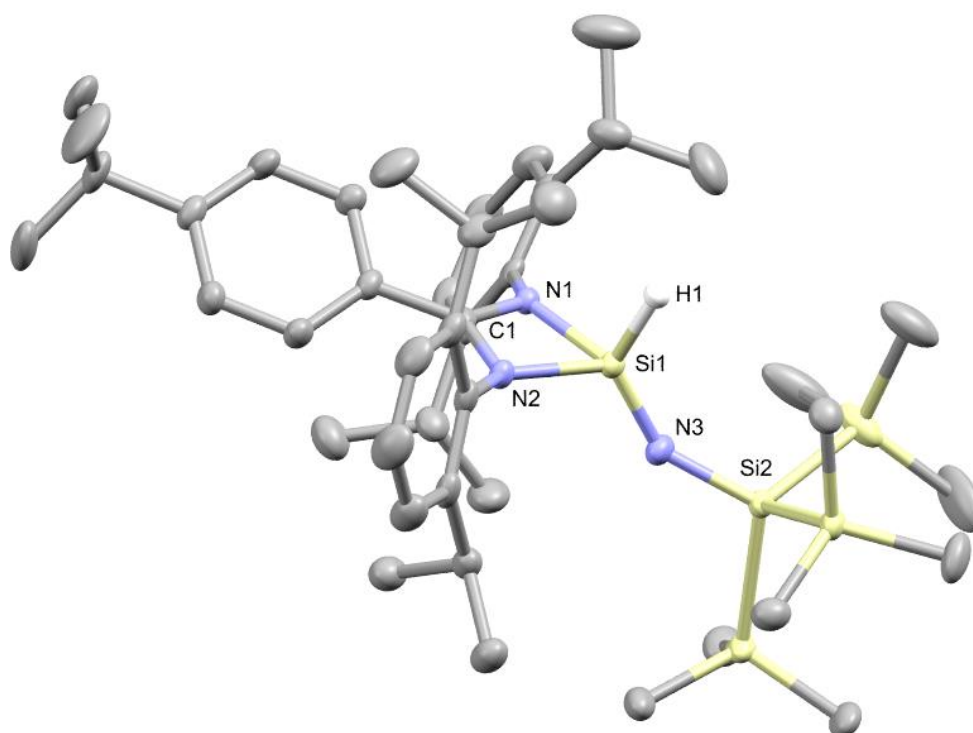
Figure 2.33. Thermal ellipsoid plot of (^{Dipp}NCN)Si(H)=NSi(TMS)$_3$. Ellipsoids set at the 50% probability level. The hydride is shown as a sphere of fixed radius (0.2 Å), other hydrogen atoms are omitted for clarity. Selected bond lengths (Å) and angles (°): Si1–H1 1.42(3), Si1–N1 1.832(2), Si1–N2 1.854(2), Si1–N3 1.582(2), C1–N1 1.342(3), C1–N2 1.339(3), N3–Si2 1.703(2), N1–Si1–N2 71.29(10), N3–Si1–N1 119.64(11), N3–Si1–N2 121.50(11), N3–Si1–H1 125.7(11), Si1–N3–Si2 144.47(13).
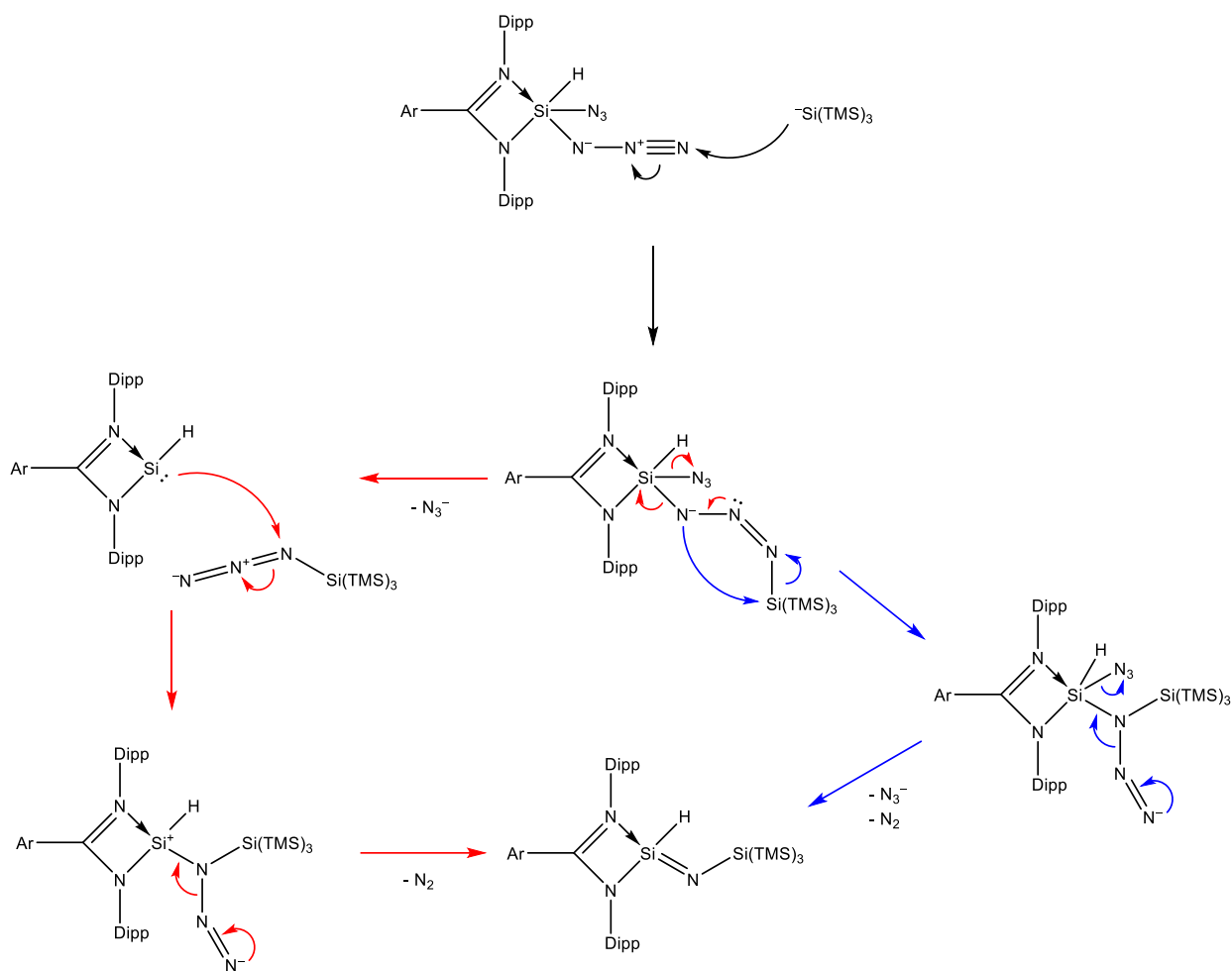
Figure 2.34. Two proposed mechanisms for the formation of (^{Dipp}NCN)Si(H)=NSi(TMS)$_3$.

It is assumed that the reaction proceeds by attack on an azido γ-nitrogen by $^-$Si(TMS)$_3$ to form a triazenate intermediate, as direct attack on the silicon centre or an α-nitrogen would be highly sterically restricted. This assumption is reinforced by literature, where triazenates are known to form as products from the reaction of bulky silicon azides with silanions.[82] For the triazenate to convert to the observed silaimine complex, one equivalent of azide and one equivalent of dinitrogen must be lost, with the uncertainty in the mechanism corresponding to the order in which these are eliminated. If the azide is eliminated first, then a low-valent silicon complex, (^{Dipp}NCN)SiH, may exist as an intermediate in this reaction.

The analogous reaction of (THF)$_3$LiSi(TMS)$_3$ with (^{Dipp}NCN)Si(N$_3$)$_3$ would produce an azido silaimine, so the synthesis of (^{Dipp}NCN)Si(N$_3$)$_3$ was conducted for the purposes of this reaction.

An initial attempt to synthesise (^{Dipp}NCN)Si(N$_3$)$_3$ from the reaction of Si(N$_3$)$_4$ with Li(^{Dipp}NCN) in toluene afforded crystals of [(^{Dipp}NCN)H$_2$][Si(N$_3$)$_5$] (Figure 2.35) after slow evaporation of the solvent over the course of a week. This compound contains the previously unknown anion Si(N$_3$)$_5$$^-$, representing a new homoleptic azido-silicon compound.

Figure 2.35. Thermal ellipsoid plot of [(^{Dipp}NCN)H$_2$][Si(N$_3$)$_5$], showing hydrogen bonds to adjacent formula units. Ellipsoids set at the 50% probability level. Carbon-bound hydrogen atoms are omitted for clarity, nitrogen-bound hydrogen atoms are shown as spheres of fixed radius (0.2 Å). Bond lengths within the Si(N$_3$)$_5$$^-$ ion are summarised in Table 2.4. Other selected bond lengths (Å) and angles (°): C1–N16 1.323(2), C1–N17 1.325(2), N16–N4 2.909(3), N17–N3 3.074(2), N1–Si1–N4 177.08(7), N1–Si1–N7 88.57(8), N1–Si1–N10 90.59(8), N1–Si1–N13 93.45(8), N7–Si1–N10 121.28(9), N10–Si1–N13 119.99(8), N13–Si1–N7 118.66(8), N2–N1–N4–N5 dihedral 122.10(19), N8–N7–Si1–N4 dihedral 6.80(18), N11–N10–Si1–N1 dihedral -17.92(18), N14–N13–Si1–N1 dihedral 9.37(16).
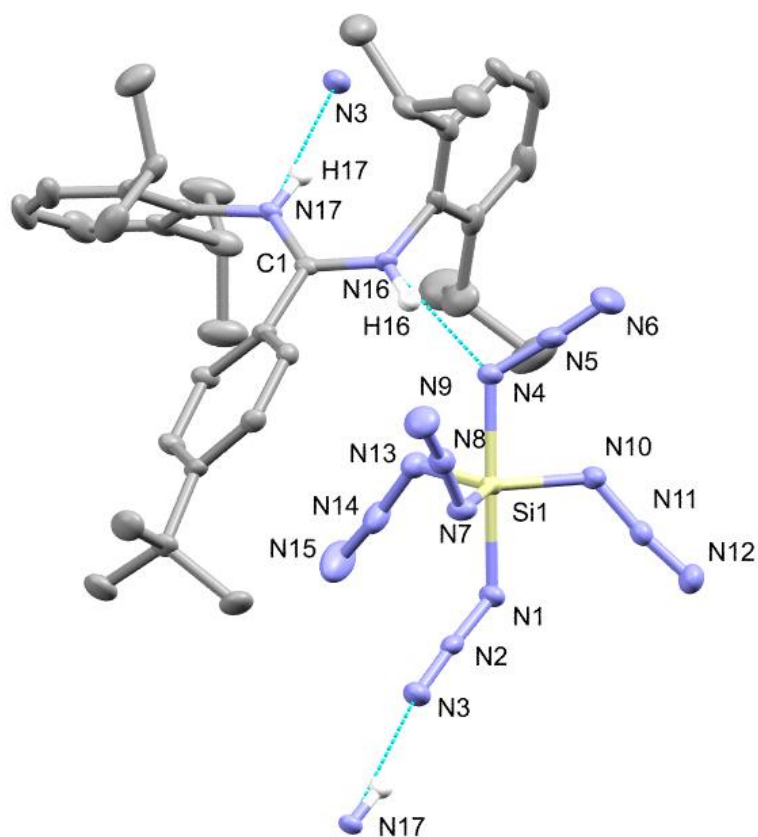
	Azido group	Si–N_α	N_α–N_β	N_β–N_γ	(N_α–N_β) - (N_β–N_γ)
Axial azides	**N1–N2–N3**	1.870(2)	1.215(2)	1.145(2)	0.070
	N4–N5–N6	1.872(2)	1.224(2)	1.139(2)	0.085
Equatorial azides	**N7–N8–N9**	1.762(2)	1.229(2)	1.132(2)	0.097
	N10–N11–N12	1.767(2)	1.225(2)	1.128(2)	0.097
	N13–N14–N15	1.768(2)	1.226(2)	1.133(3)	0.093

Table 2.4. Bond lengths (Å) (and associated estimated standard deviations) within the $Si(N_3)_5^-$ anion of $[(^{Dipp}NCN)H_2][Si(N_3)_5]$, sorted by azido group.

The coordination environment around the silicon atom in $[(^{Dipp}NCN)H_2][Si(N_3)_5]$ is trigonal bipyramidal, with longer Si–N bond lengths for the axial azides than the equatorial azides, as is typical for trigonal bipyramidal complexes. In addition to the longer Si–N bond lengths, the axial azido groups have shorter N_α–N_β bonds and longer N_β–N_γ bonds, consistent with the group having electronic character closer to that of a free azide ion. The effect is significantly more pronounced for the N1–N2–N3 azido group than the N4–N5–N6 azido group. This difference is likely due to the different hydrogen bonding arrangements of the two azido groups – N1–N2–N3 engages in hydrogen bonding to $[(^{Dipp}NCN)H_2]^+$ from N_γ (N3), whilst N4–N5–N6 engages in hydrogen bonding from N_α (N4). The hydrogen bonding interaction is expected to favour the accumulation of negative charge on the hydrogen-bonded nitrogen, as the interaction will help stabilise this charge. As such, the observed differences in bond lengths between the axial azido groups can be rationalised according to the resonance forms of the azido groups shown in Figure 2.36. It should also be noted that the N16–H16–N4 hydrogen bond is significantly shorter than the N17–H17–N3 hydrogen bond, with N–N distances of 2.909 Å and 3.074 Å respectively.
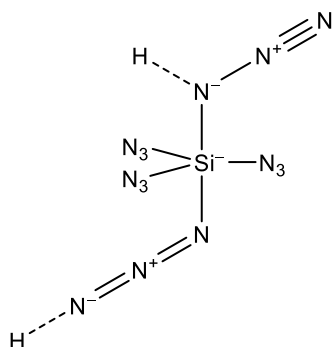
Figure 2.36. Partial structure of $Si(N_3)_5^-$, showing different resonance forms for the two axial azido groups, and their respective hydrogen bonding interactions.

The bonding of the N1–N2–N3 azido group is extremely similar to the bonding of the azido groups in $[PPN]_2[Si(N_3)_6]$, which have mean values of Si–N_α 1.871(5), N_α–N_β 1.202(3), N_β–N_γ 1.145(1).[5] This similarity is unsurprising, as in both cases the azido group is bound to an anionic silicon centre with another azido group oriented *trans* to it. The N_α–N_β bond in the N1–N2–N3 azido group is slightly longer (at 1.215 Å), indicating a slightly lower ionic character, which can be attributed to it being part of a singly-anionic complex $Si(N_3)_5^-$, as opposed to the doubly-anionic $Si(N_3)_6^{2-}$.

Based on the spectra of $(^{Dipp}NCN)Si(N_3)_3$ that was synthesised in a subsequent reaction, the reaction of $Li(^{Dipp}NCN)$ with $Si(N_3)_4$ did initially afford $(^{Dipp}NCN)Si(N_3)_3$ as the dominant product. The formation of $[(^{Dipp}NCN)H_2][Si(N_3)_5]$ is thus believed to be a result of trace moisture exposure accumulating over the week-long evaporation. The hydrolysis of silicon azides is expected to afford HN_3 and oxo-silicon compounds. The formation of $[(^{Dipp}NCN)H_2][Si(N_3)_5]$ can then be rationalised from the addition of two equivalents of HN_3 to $(^{Dipp}NCN)Si(N_3)_3$, according to the reaction scheme shown in Figure 2.37.
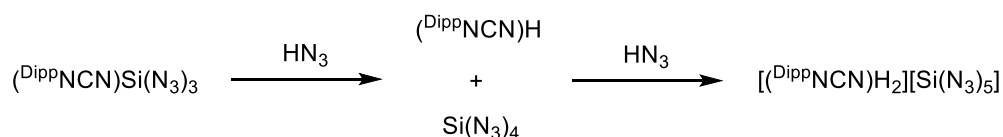
Figure 2.37. Hypothesised reaction scheme for the formation of $[(^{Dipp}NCN)H_2][Si(N_3)_5]$ from reaction of $(^{Dipp}NCN)Si(N_3)_3$ with HN_3

Based on the proposed reaction scheme in Figure 2.37, a rational synthesis of $[(^{Dipp}NCN)H_2][Si(N_3)_5]$ was achieved by the one-pot combination of $(^{Dipp}NCN)H$, HN_3 and

$Si(N_3)_4$. Further investigation on the synthesis and properties of the $Si(N_3)_5^-$ ion was conducted by MChem student Michael Jones[81] and is outside of the scope of this thesis.

(^{Dipp}NCN)Si(N$_3$)$_3$ was subsequently synthesised by the reaction of Na(^{Dipp}NCN)(THF)$_x$ with Si(N$_3$)$_4$. (^{Dipp}NCN)Si(N$_3$)$_3$ was found to react with (THF)$_3$LiSi(TMS)$_3$ in the same manner as (^{Dipp}NCN)SiH(N$_3$)$_2$, thus affording the azido-substituted silaimine complex (^{Dipp}NCN)Si(N$_3$)=NSi(TMS)$_3$ (Figure 2.38).
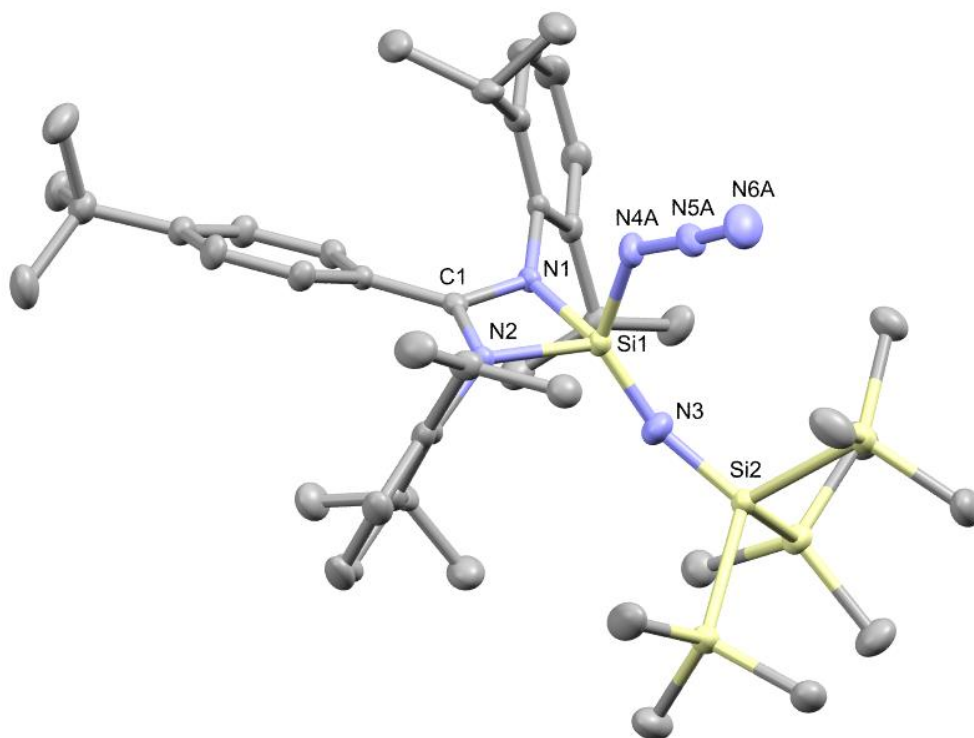
Figure 2.38. Thermal ellipsoid plot of the dominant (85% occupancy) disorder component within the crystal structure of (^{Dipp}NCN)Si(N$_3$)=NSi(TMS)$_3$. Ellipsoids set at the 50% probability level. Hydrogen atoms are omitted for clarity. As viewed down the N4A−Si1 bond axis, the azido group in this major component is approximately eclipsing the Si1−N3 bond. In the minor component the azido group instead eclipses the Si1−N2 bond. Selected bond lengths (Å) and angles (°): Si1−N1 1.842(2), Si1−N2 1.821(2), Si1−N3 1.570(2), Si1−N4A 1.745(2), C1−N1 1.341(2), C1−N2 1.351(2), N3−Si2 1.697(2), N4A−N5A 1.217(3), N5A−N6A 1.136(3), N1−Si1−N2 71.81(7), N3−Si1−N1 126.58(9), N3−Si1−N2 118.32(9), N3−Si1−N4A 126.79(11), Si1−N3−Si2 157.54(13).

(^{Dipp}NCN)Si(H)=NSi(TMS)$_3$ and (^{Dipp}NCN)Si(N$_3$)=NSi(TMS)$_3$ both adopt a similarly distorted tetrahedral geometry around the central silicon atom. The ^{Dipp}NCN ligand bite-angle is nearly identical in the two complexes, at 71.29 ° and 71.81 °, which is significantly larger than the 68.74 ° of (^{Dipp}NCN)SiH(N$_3$)$_2$. The widening of the bond angles around the silicon is

expected for a tetracoordinate complex compared to a pentacoordinate one. Within each complex, the two (^{Dipp}NCN)–Si bond lengths are almost the same. These lengths are also very similar between the two complexes, indicating the replacement of a hydride for an azide has little effect on the bonding of the ligand. The Si1–N3 and N3–Si2 bond lengths are also similar between the two complexes, however the Si1–N3–Si2 bond angle changes dramatically, with values of 144.47 ° and 157.54 ° for (^{Dipp}NCN)Si(H)=NSi(TMS)$_3$ and (^{Dipp}NCN)Si(N$_3$)=NSi(TMS)$_3$ respectively. Given that this is not accompanied by a change in bond lengths to N3, this is likely not an electronic effect and probably the result of steric pressure from the azido group, which is close to eclipsing the Si1–N3 bond as viewed down the N4A–Si1 bond axis (N5A–N4A–Si1–N3 dihedral angle = -19.3(4) °). There are no previously known silaimines with an N-bound Si(TMS)$_3$ group, however there are a handful of examples with the smaller SiMe$_3$ group, including some with NCN-type ligands.[83-86] These compounds possess Si=N bond lengths ranging from 1.581 Å – 1.595 Å. The Si=N bond of (^{Dipp}NCN)Si(H)=NSi(TMS)$_3$ is on the shortest end of this range at 1.582 Å, while (^{Dipp}NCN)Si(N$_3$)=NSi(TMS)$_3$ has an even shorter bond at 1.570 Å. These short Si=N bonds can be rationalised as an effect of Si(TMS)$_3$ being a stronger electron-donating group than SiMe$_3$, thus also rendering the imine nitrogen a stronger donating group. This effect can also be seen from an example of an NCN-bound silaimine with the much less donating SiI$_3$ group, which has a significantly longer Si=N bond at 1.618 Å.[87] Similarly, the shorter Si=N bond in (^{Dipp}NCN)Si(N$_3$)=NSi(TMS)$_3$ compared to (^{Dipp}NCN)Si(H)=NSi(TMS)$_3$ can be attributed to the central silicon being a better electron acceptor due to the presence of the electron-withdrawing azido group in place of the hydride. Published silaimines also show this correlation between the Si=N bond length and the electron-withdrawing ability of the silicon's substituents.[84]

The reagent (THF)$_3$LiSi(TMS)$_3$ was found to act as a chlorine abstractor from (^{tBu}NCN)SiCl$_3$, reducing the complex to form the known low-valent silicon chloride (^{tBu}NCN)SiCl. This observation adds plausibility to the hypothesis that the reactions of (THF)$_3$LiSi(TMS)$_3$ with (^{Dipp}NCN)SiH(N$_3$)$_2$ and (^{Dipp}NCN)Si(N$_3$)$_3$ may proceed via low-valent silicon hydride and low-valent silicon azide intermediates respectively. This observed reduction of (^{tBu}NCN)SiCl$_3$ also shows that (THF)$_3$LiSi(TMS)$_3$ has potential to be a useful reductant for other silicon chlorides, since it is highly soluble in non-polar solvents.

2.2.4. Thermal decomposition of $(^{Dipp}NCN)SiH(N_3)_2$

When attempting to measure the melting point of $(^{Dipp}NCN)SiH(N_3)_2$ in a thin capillary with a slow heating rate, the sample appeared to melt around 178 °C accompanied by bubbling, indicating decomposition with loss of gas (likely N_2). An experiment on a larger sample (14 mg) was found to observe no melting after heating to 195 °C for 3 hours, however NMR analysis of the resulting material found a significant amount of it had converted to $(^{Dipp}NCN)H$. The melting point of $(^{Dipp}NCN)H$ was measured to be 177 – 178 °C, thus it is concluded that $(^{Dipp}NCN)SiH(N_3)_2$ decomposes slowly without melting at temperatures in the range of 170 – 200 °C, forming $(^{Dipp}NCN)H$ which will melt above 177 °C once sufficient concentrations of it have formed.

According to stoichiometry, if $(^{Dipp}NCN)SiH(N_3)_2$ decomposes to $(^{Dipp}NCN)H$, then it must also produce products with a combined empirical formula "SiN_6". This could potentially be the yet unreported low-valent compound diazidosilylene $Si(N_3)_2$, so further studies were conducted on this decomposition. $Si(N_3)_2$ is not expected to be stable at the temperatures of $(^{Dipp}NCN)SiH(N_3)_2$ decomposition. However, its expected decomposition with elimination of N_2 may lead to interesting nitrido-silicon compounds (Figure 2.39).

$$(^{Dipp}NCN)SiH(N_3)_2 \xrightarrow{\Delta} (^{Dipp}NCN)H \ + \ SiN_{(6-2x)} \ + \ xN_2$$
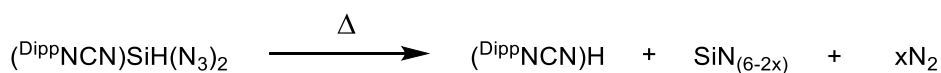
Figure 2.39. Expected products from thermal decomposition of $(^{Dipp}NCN)SiH(N_3)_2$.

The result of heating $(^{Dipp}NCN)SiH(N_3)_2$ was found to vary considerably depending on the conditions, making the study of this decomposition difficult. Table 2.5 summarises the list of heating experiments conducted on $(^{Dipp}NCN)SiH(N_3)_2$, with observations and identified products (by ^1H NMR in C_6D_6 solution).

Table 2.5 (see next page). Table of experiments involving heating of $(^{Dipp}NCN)SiH(N_3)_2$. †Except where otherwise stated, experiments were conducted under active vacuum where the residual pressure is from leaks from the ambient air. Atmospheric pressure (1000 mbar) experiments were conducted in sealed vessels, so gas generated by decomposition will have increased the pressure over the course of decomposition. Experiments 7 and 8 were conducted under evacuation by a gas phase mass-spectrometer – the pressure in the reaction vessel is only approximately known based on the pressure change at the mass spectrometer relative to ambient. ††In cases where the amount of product was measured, the mass is stated. In some cases, the sublimed material and soluble residue were combined by extraction of all soluble products.

Experiment	Material heated	Temp. /°C	Pressure† /mbar	Duration /h	Sample melted?	Sublimed material††	Soluble residue††	Insoluble residue††
1	14 mg $(NCN)SiH(N_3)_2$, 4% $(NCN)H$ contamination	183-188	6×10^{-2}	3	no	94% $(NCN)SiH(N_3)_2$ 6% $(NCN)H$	94% $(NCN)SiH(N_3)_2$ 6% $(NCN)H$	none
2	~100 mg 40% $(NCN)H$ 60% $(NCN)SiH(N_3)_2$	150	6×10^{-2}	48	no	14% $(NCN)SiH(N_3)_2$ 86% $(NCN)H$	97% $(NCN)SiH(N_3)_2$ 3% $(NCN)H$	none
3	14mg $(NCN)SiH(N_3)_2$	195	1000 (argon)	3	no	none	20% $(NCN)SiH(N_3)_2$ 60% $(NCN)H$ 20% Unknown*	white powder + brown specks
4	14 mg $(NCN)SiH(N_3)_2$ 127mg naphthalene	200	1000 (argon)	3	yes	none	8% $(NCN)SiH(N_3)_2$ 55% $(NCN)H$ 37% Unknown*	traces of colourless glass-like shards
5	450 mg $(NCN)SiH(N_3)_2$	150	$3 \times 10^{-4} - 3 \times 10^{-3}$	168	no	367 mg 77% $(NCN)SiH(N_3)_2$ 21% $(NCN)H$	none	11 mg porous white solid
6	333 mg 80% $(NCN)SiH(N_3)_2$ 20% $(NCN)H$	160	5×10^{-2}	96	no	60% $(NCN)SiH(N_3)_2$ 40% $(NCN)H$	none	6 mg porous white solid
7	61mg $(NCN)SiH(N_3)_2$	200	~10 – 100	5	no	49 mg 9% $(NCN)SiH(N_3)_2$ 86% $(NCN)H$ 4% $(NCN)Si(N_3)_3$	3 mg 60% $(NCN)H$ 36% $(NCN)Si(N_3)_3$	8 mg porous pale-yellow solid
8	122 mg $(NCN)SiH(N_3)_2$	200	~10 – 100	16	no	112mg 3% $(NCN)SiH(N_3)_2$ 75% $(NCN)H$ 22% Unknown*		2 mg porous white solid
9	1218 mg $(NCN)SiH(N_3)_2$	200	2×10^{-4}	3	no	1149 mg (isolated) 99% $(NCN)SiH(N_3)_2$	none	negligible
10	30 mg $(NCN)SiH(N_3)_2$	200	1000 (argon)	4	yes	negligible	10% $(NCN)SiH(N_3)_2$ 60% $(NCN)H$ 30% Unknown*	traces of colourless glass-like shards
11	30 mg $(NCN)SiH(N_3)_2$	200	1000 (argon)	22	yes	55% $(NCN)H$ 45% Unknown*		white powder + brown specks
12	15 mg $(NCN)SiH(N_3)_2$	200	10 – 24 (static vacuum)	6	?	90% $(NCN)H$ 10% Unknown*		sticky brown film
13	15 mg $(NCN)SiH(N_3)_2$	200	0.8 – 1.0	5	no	80% $(NCN)SiH(N_3)_2$ 20% $(NCN)H$		porous white solid
14	609 mg $(NCN)SiH(N_3)_2$	200	3.0 – 3.3 (argon flow)	4	yes	191 mg 20% $(NCN)SiH(N_3)_2$ 80% $(NCN)H$	9% $(NCN)SiH(N_3)_2$ 57% $(NCN)H$ 34% Unknown*	13 mg white powder + 13 mg black specks
15	304 mg $(NCN)SiH(N_3)_2$	165	0.9 – 1.0 (argon flow)	87	no	240 mg 5% $(NCN)SiH(N_3)_2$ 92% $(NCN)H$ 3% Unknown	8 mg 5% $(NCN)SiH(N_3)_2$ 90% $(NCN)H$ 5% Unknown	26 mg porous white solid
16	30 mg $(NCN)SiH(N_3)_2$	165	1000 (argon)	2	no	none	$(NCN)SiH(N_3)_2$ (undecomposed)	none
17	30 mg $(NCN)SiH(N_3)_2$	165	1000 (argon)	165	no	73% $(NCN)SiH(N_3)_2$ 18% $(NCN)H$ 9% Unknown*		colourless powder

The results in Table 2.5 show that (^{Dipp}NCN)H is the major (C_6D_6-soluble) product in all cases where decomposition has occurred. However, in many cases unknown products are also formed. This appears to be predominantly the same product(s) in all cases marked with an asterisk. The "Unknown" compound is soluble in C_6D_6 and is identified in ^{1}H NMR spectra by extremely broad, poorly resolved bands in chemical shift regions where ^{Dipp}NCN protons are typically observed. When a significant quantity of this product is formed, it is also accompanied by the formation of brown or black insoluble residues in addition to the white/colourless residues formed in most experiments. These additional products are far more prevalent in cases where the sample melted, thus sample melting is considered undesirable. Broad signals for non-labile proton environments in NMR spectra are typically indicative of paramagnetic species and amorphous species. Paramagnetic molecules are often intensely coloured, so the latter option is more likely as these solutions are either colourless or pale yellow. Experiments 10 and 11, conducted on a 0.050 mmol scale, both generated considerable quantities of the unknown product. These reactions were conducted in sealed tubes, so the quantity of gas generated could be measured volumetrically by allowing the gas to expand to atmospheric pressure after reaction. In Experiment 10, 90% of the added (^{Dipp}NCN)SiH(N$_3$)$_2$ decomposed after 4 hours. 30% of the ^{Dipp}NCN-containing product was the unknown material with the remainder being (^{Dipp}NCN)H and undecomposed (^{Dipp}NCN)SiH(N$_3$)$_2$. This decomposition generated 1.0 (± 0.1) mL of gas, corresponding to 0.045 (± 0.004) mmol. Experiment 11 was conducted for a longer duration (22 hours), after which all (^{Dipp}NCN)SiH(N$_3$)$_2$ decomposed. 45% of the ^{Dipp}NCN-containing product is the "Unknown" material with the remainder being (^{Dipp}NCN)H. This decomposition generated 1.1 (± 0.1) mL of gas, corresponding to 0.049 (± 0.004) mmol. In both reactions, the molar quantity of gas generated is equal to the number of moles of (^{Dipp}NCN)SiH(N$_3$)$_2$ decomposed, and irrespective of how much of the unknown material is formed. Hence, the initial decomposition is assumed to occur with elimination of one equivalent of N$_2$, in addition to (^{Dipp}NCN)H. The unknown product then likely forms from a slow subsequent reaction of the generated (^{Dipp}NCN)H with the residual silicon-containing product, without the generation of additional gaseous products. The hypothesised reaction sequence is thus shown in Figure 2.40, with the suggested identity of the "Unknown" material being a polymer of (^{Dipp}NCN)SiN.

$$(^{Dipp}NCN)SiH(N_3)_2 \xrightarrow[- N_2]{\Delta} (^{Dipp}NCN)H \quad + \quad [Si(N)(N_3)]_n$$

$$HN_3 \quad + \quad [(^{Dipp}NCN)Si(N)]_n$$
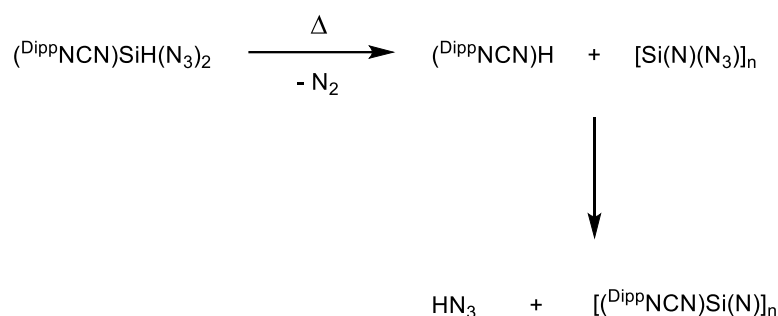
Figure 2.40. Proposed reaction pathway for the formation of a polymeric material containing ^{Dipp}NCN ligands.

Experiments conducted under reduced pressure were found to be highly inconsistent. In some cases, the reduced pressure allows for the decomposition of $(^{Dipp}NCN)SiH(N_3)_2$ above the melting point of $(^{Dipp}NCN)H$ without the latter melting, as it instead sublimes. However, as observed in Experiments 1 and 9, low pressure may also result in $(^{Dipp}NCN)SiH(N_3)_2$ sublimation with negligible decomposition. The decomposition at atmospheric pressure and below the melting point of $(^{Dipp}NCN)H$ (Experiments 16 and 17) was extremely slow, and still resulted in the "Unknown" product forming. As such, it may be that this product can only be avoided if $(^{Dipp}NCN)SiH(N_3)_2$ is decomposed under sublimation conditions of $(^{Dipp}NCN)H$, where subsequent reactions of $(^{Dipp}NCN)H$ are prevented due to its physical separation from the other products. Experiments 7 and 15 were the only cases where near complete decomposition occurred without the formation of the "Unknown" product, with Experiments 5, 6 and 13 affording partial decomposition without the "Unknown" product. In all five of these experiments, the remaining insoluble residue is a soft white solid with extremely low density, which turns into a gel upon wetting with solvents. IR analysis was conducted on the insoluble residues of Experiments 5-8, 12, 14 and 15. The black residue of Experiment 14 was analysed separately to the white residue, but found to have no significant IR absorptions. IR analysis of the other residues show the presence of the same two compounds, in varying ratios.
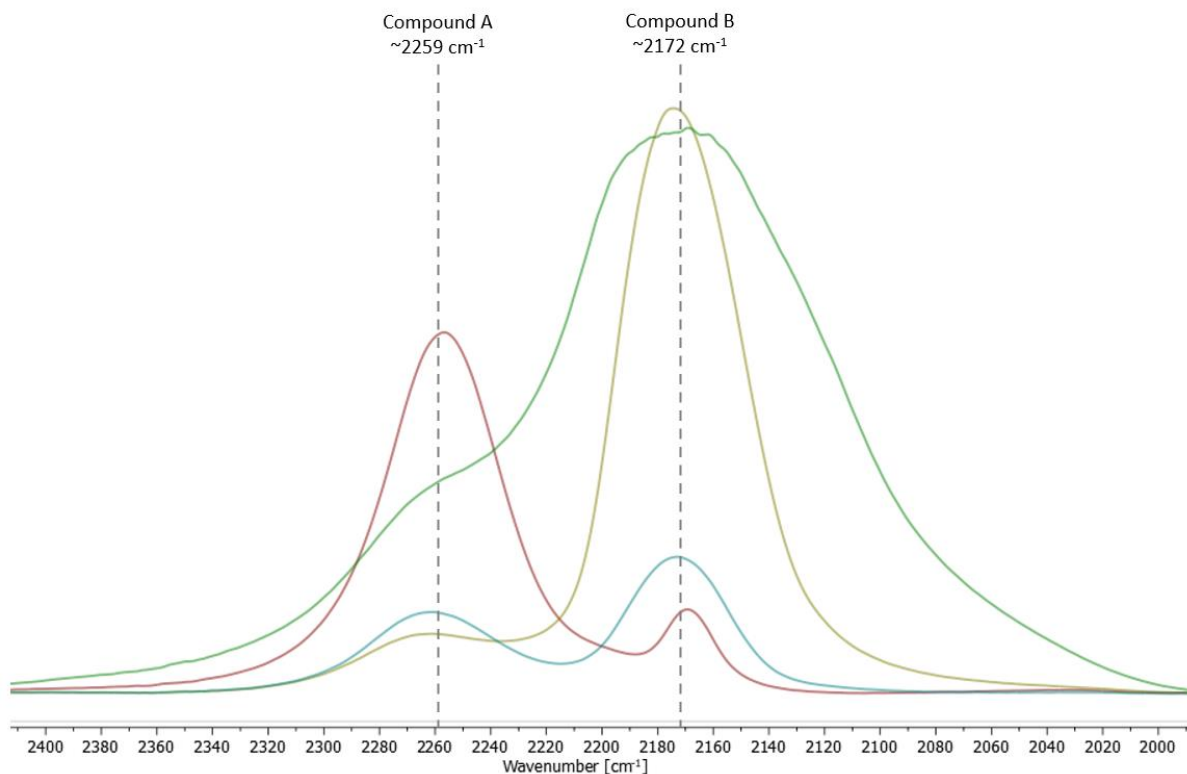
Figure 2.41. Stacked IR absorption spectra of the residues from Experiments 5 (blue), 7 (green), 8 (yellow) and 15 (red). Intensity is in arbitrary units.

Both of the observed compounds each have one IR absorption band near the asymmetric azide stretching region: one at around 2259 cm^{-1} and the other around 2172 cm^{-1}, with slight variation between experiments. These two compounds will henceforth be referred to as Compound A and Compound B respectively.

The IR absorption of Compound A (2259 cm^{-1}) is at abnormally high wavenumbers for a standard azido group. It is less intense than the other absorptions of Compound A, which appear in the 1200-800 cm^{-1} range. While absorptions in this wavenumber range can be attributed to other vibrational modes of azido groups, it is highly unusual for these modes to provide more intense absorptions than the asymmetric stretch. Additionally, Compound A does not have any absorption band attributable to the combination of azide asymmetric and symmetric stretching, which typically appear in the region of 3500 cm^{-1} – 3300 cm^{-1}.[88] While not all azide-containing species exhibit this absorption mode, this does add further weight to the possibility that Compound A does not contain an azido group. The absorption at 2259 cm^{-1} may instead be the result of diazo groups, which are known to absorb in the wavenumber region 2300 – 2100 cm^{-1}.[89] The residue from Experiment 15 contained the

highest proportion of Compound A among those analysed by IR spectroscopy, with an absorption at 2257 cm^{-1} approximately 10 times more intense than an absorption at 2169 cm^{-1}. This experiment involved 0.50 mmol of (^{Dipp}NCN)SiH(N$_3$)$_2$. Based on the NMR data, 0.46 mmol of the (^{Dipp}NCN)SiH(N$_3$)$_2$ decomposed to form (^{Dipp}NCN)H with almost no other proton-containing products. Based on this observation and mass of soluble and sublimed material, all ^{Dipp}NCN ligand is accounted for in the soluble and sublimed products. Therefore, the solid residue must contain no atoms other than silicon and nitrogen (unless atmospheric contamination occurred, which may introduce traces of oxygen). Since the unknown products in the soluble residue are only in trace quantities, the silicon atoms from the 0.46 mmol of decomposed (^{Dipp}NCN)SiH(N$_3$)$_2$ are assumed to be all in the insoluble residue, thus accounting for 13 mg of the 26 mg residue. If the remaining 13 mg is assumed to be all nitrogen, then the sample would contain 0.93 ($\pm$ 0.04) mmol nitrogen atoms (1.9 – 2.1 equivalents per silicon), so the empirical formula of Compound A is taken to be SiN$_2$. The total mass lost in the experiment is 30 ($\pm$ 2) mg, corresponding to an N$_2$ loss of 1.07 ($\pm$ 0.07) mmol. This then indicates a decomposition process per the reaction scheme in Figure 2.42.

$$(^{Dipp}NCN)SiH(N_3)_2 \xrightarrow{\quad -2\ N_2 \quad} (^{Dipp}NCN)H \ + \ SiN_2$$
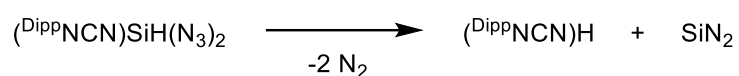
Figure 2.42. Deduced decomposition reaction of (^{Dipp}NCN)SiH(N$_3$)$_2$ to form SiN$_2$ (Compound A).

Experiments 7, 8, 12 and 14 produced high proportions of Compound B relative to Compound A, all four of which were conducted under low vacuum levels (1 – 100 mbar), so it may be that pressure has a role in the selectivity of decomposition. The IR absorption band around 2172 cm^{-1} of Compound B varies greatly in width, with the material from Experiment 12 producing a band with a full width at half-maximum (FWHM) of 124 cm^{-1}, while the material from Experiment 8 had an FWHM of just 51 cm^{-1} at comparable intensity. As the bands are quite symmetric, it is likely that the broadness of the signal results from the material being amorphous. It is worth noting that in all residues containing a significant proportion of Compound A (Experiments 5, 6, 15), the bands corresponding to Compound B were on the narrow end of the range.

The residue from Experiment 12 contained almost exclusively Compound B, but was on too small of a scale for gravimetric analysis of the products. Experiment 7 resulted in decomposition to largely Compound B without forming any of the unknown soluble product.

Experiment 7 was conducted on a 0.10 mmol scale, of which 0.086mmol decomposed to (^{Dipp}NCN)H along with some sublimed and disproportionated material. As there is no significant unidentified product in solution, the 8 mg of insoluble residue is therefore assumed to contain 0.086 mmol silicon (2.4 mg of silicon). As with Experiment 15, the remaining mass is then assumed to be nitrogen, so the residue is expected to contain 5.6 mg (0.40 ± 0.04 mmol) of nitrogen atoms (4.2 – 5.1 equivalents per silicon). This is close to the expected product for one equivalent of N_2 elimination (SiN_4). It should be noted that the small scale of this experiment means a mistake in weighing of even 1 mg would change the calculated moles of nitrogen atoms to be as low as 0.33 mmol (3.8 equivalents) or as high as 0.47 mmol (0.55 equivalents). Likewise, the total mass loss from this experiment (1 ± 2 mg) has too high an uncertainty to provide much additional verification, as this could indicate anywhere between 0 and 0.1 mmol of N_2 lost (0 – 1 equivalents). Both values do, however, indicate that fewer than two equivalents of N_2 have been eliminated. This experiment was conducted while connected to a gas-phase spectrometer (Hiden Analytical QGA). The resulting gas analysis shows the evolution of N_2, and indicates no other gaseous products are formed in significant quantity. Assuming the decomposition occurs via a stoichiometric process, it is therefore likely that Compound B has the empirical formula SiN_4, resulting from the elimination of (^{Dipp}NCN)H and one equivalent of N_2 from (^{Dipp}NCN)SiH(N_3)$_2$. The presence of the strong absorption around 2172 cm^{-1} clearly indicates that Compound B still retains an azido group, thus Compound B is assumed to be a mixed azido(nitrido)silicon compound, with a hypothesised structure shown in Figure 2.43.

$$($^{Dipp}NCN)SiH(N_3)_2 \xrightarrow{-N_2} ($^{Dipp}NCN)H + [Si(N)(N_3)]_n$$
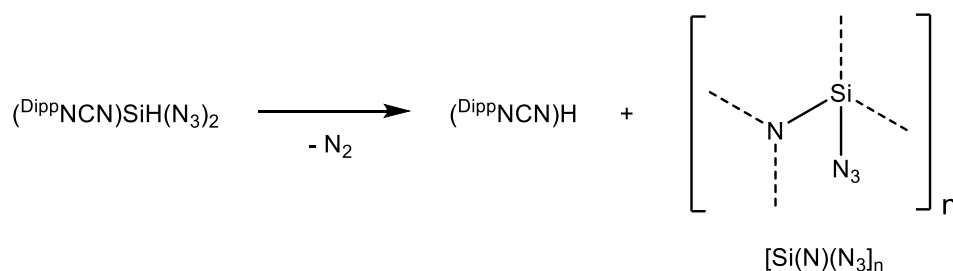
Figure 2.43. Deduced decomposition reaction of (^{Dipp}NCN)SiH(N_3)$_2$ to form [Si(N)(N_3)]$_n$ (Compound B).

When another experiment, under identical conditions to Experiment 7, was conducted with twice the material and a longer duration (Experiment 8), the formation of small amounts of the "Unknown" product was observed. It may be that the larger sample size makes the

escape of (^{Dipp}NCN)H more difficult, thus resulting in the side reaction proposed in Figure 2.40. Experiment 8 produced Compound A and Compound B in approximately the same ratio as Experiment 7, but curiously, the Compound B from Experiment 8 produced much sharper IR absorption bands than from Experiment 7. This may indicate that some form of annealing process occurs to Compound B when heated under vacuum for longer periods of time, reducing the amorphicity of the sample. The quantity of insoluble residue produced by Experiment 8 is abnormally low − a quarter of the amount from Experiment 7 despite being double the reaction scale. As with Experiment 7, gas analysis indicates N_2 as the only major gaseous product. A bright yellow material was found to sublime in this experiment (in addition to (^{Dipp}NCN)H), the only time such a material was observed. It is therefore assumed that the formation of this yellow material is related to the abnormally low quantity of residue observed. Considering that the conditions of Experiment 8 were identical to Experiment 7, aside from the scale and duration, it is reasonable to assume that the same reaction initially proceeds. Thus Experiment 8 likely initially produced Compound B in the same manner as Experiment 7, which was subsequently converted to a volatile (at 200 °C) material. In combination with the annealing observation, it may be that on prolonged heating under vacuum, polymeric Compound B converts to smaller oligomers, which are then more readily sublimed. Unfortunately, difficulty in reproducing this material on a larger scale prevented further study of it.

2.3. Conclusions

NMR spectroscopic data for the species $HSiX_3$, H_2SiX_2 and H_3SiX (X = Cl, N_3) have been obtained from the reaction of $HSiCl_3$ with $TMS(N_3)$ in C_6D_6, marking the first NMR data on most of these compounds. Triazidosilane $HSi(N_3)_3$, the azide analogue of $HSiCl_3$, has been synthesised free of disproportionation by using the reagent $Na[Al(N_3)_4](THF)_4$ in benzene. The instability of $HSi(N_3)_3$ with respect to disproportionation makes the synthesis developed here inconsistent, however it does demonstrate that the synthesis of $HSi(N_3)_3$ as a pure solution is possible, in contrast to previous reports.

The synthesis of the hydrido(azido)silicon complex (^{Dipp}NCN)SiH(N_3)$_2$ has been optimised, allowing it to be synthesised in suitable quantities for further study. Reaction of this

compound with the base ItBu has been revisited, and no evidence of a low-valent silicon product has been observed, in contrast to the observed reactivity of $(^{tBu}NCN)SiHCl_2$.[60] The previously observed difference in reactivity of $LiN(TMS)_2$ towards $(^{tBu}NCN)SiCl_2$ and $(^{Dipp}NCN)SiH(N_3)_2$ was confirmed to be an effect of the azido groups rather than the difference in ligand, as the complex $(^{tBu}NCN)SiH(N_3)_2$ was found to react with $LiN(TMS)_2$ by substitution of an azide analogous to $(^{Dipp}NCN)SiH(N_3)_2$. A hexacoordinate hydrido(azido)silicon complex, $(^{Dipp}NCN)_2SiH(N_3)$ has been synthesised by the high-temperature (100 °C) reaction of $(^{Dipp}NCN)SiH(N_3)_2$ with $Na(^{Dipp}NCN)(THF)_x$ in the presence of 15-crown-5. The reaction of complexes $(^{Dipp}NCN)SiH(N_3)_2$ and $(^{Dipp}NCN)Si(N_3)_3$ with $(THF)_3LiSi(TMS)_3$ were found to result in reduction of an azido group, thus forming stable silaimines $(^{Dipp}NCN)(H)Si=NSi(TMS)_3$ and $(^{Dipp}NCN)(N_3)Si=NSi(TMS)_3$. The reaction of $(THF)_3LiSi(TMS)_3$ with $(^{tBu}NCN)SiCl_3$ forms $(^{tBu}NCN)SiCl$, suggesting the reactions of $(THF)_3LiSi(TMS)_3$ with $(^{Dipp}NCN)SiH(N_3)_2$ and $(^{Dipp}NCN)Si(N_3)_3$ may form via the low-valent silicon intermediates $(^{Dipp}NCN)SiH$ and $(^{Dipp}NCN)Si(N_3)$. However, a plausible alternative mechanism is also proposed.

$(^{Dipp}NCN)SiH(N_3)_2$ has been found to be a highly promising silicon nitride precursor by thermal decomposition. This decomposition produces $(^{Dipp}NCN)H$, thus leaving behind residues that contain only silicon and nitrogen. IR analysis shows these residues contain two different materials which can be identified by broad absorption bands at approximately 2259 cm^{-1} and 2172 cm^{-1} respectively. Gravimetric analysis suggests these materials have the empirical formulae SiN_2 and SiN_4 respectively, and the selectivity of formation appears to be pressure dependent. Consistently synthesising these materials remains a challenge, as build-up of the $(^{Dipp}NCN)H$ decomposition product can cause side reactions resulting in polymeric ^{Dipp}NCN-containing products. It is likely that many amidinato complexes of the form $(NCN)SiH(N_3)_2$ would undergo the same decomposition process, so reliable syntheses of SiN_2 and SiN_4 may be possible with an alternative complex where the protonated ligand is more easily separated from the complex by sublimation. If $HSi(N_3)_3$ can be synthesised as a pure solution in an inert, high boiling point solvent, then $HSi(N_3)_3$ may undergo comparable decomposition with release of HN_3 instead of $(NCN)H$, providing an alternative solution to this problem.

3. Reduction of silicon azides

3.1. Introduction

Although the reduction of hydridosilicon complexes has proven to be a favourable method of producing low-valent silicon chlorides, low-valent silicon compounds can also be synthesised by direct reduction of tetravalent chlorides using alkali metal reducing agents (Figure 3.1).
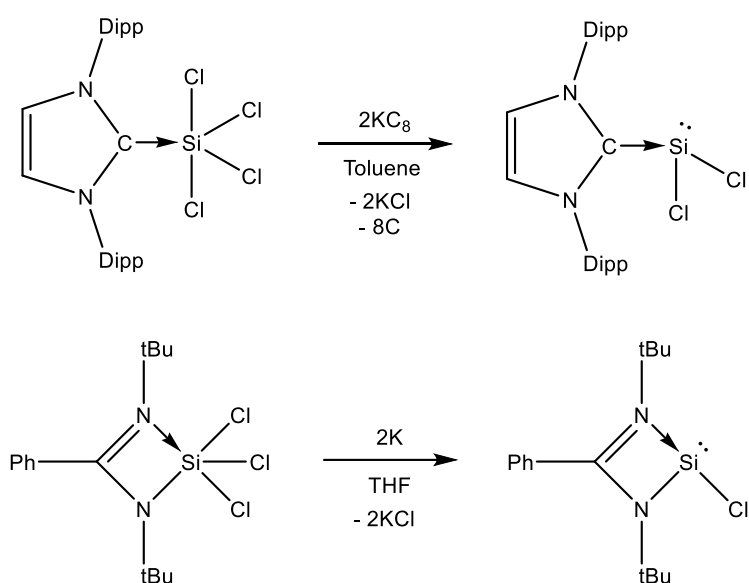
Figure 3.1. Reported synthesis of the low-valent silicon chlorides $IPrSiCl_2$ and $(^{tBu}NCN)SiCl$ using alkali metal reagents.[49, 50]

By analogy to these reactions, Peerless attempted the reduction of $Si(N_3)_4$, $IPrSi(N_3)_4$ and $(^{Dipp}NCN)Si(N_3)_3$ in benzene or toluene, summarised in Table 3.1.[73]

Silicon compound	Reductant	Azide IR absorption of product(s) / cm^{-1}	Reported assignments of IR absorptions
IPrSi(N$_3$)$_4$	3 eq. KC$_8$	2150 (solution) 2014 (solution)	IPrSi(N$_3$)(μ^2-N)$_2$Si(N$_3$)IPr (speculative) [IPrH](N$_3$)
(^{Dipp}NCN)Si(N$_3$)$_3$	2.2 eq. KC$_8$	2044 (solution)	Unknown
Si(N$_3$)$_4$	1 eq. [(^{Mes}NacNac)Mg]$_2$	2156 (solution) 2108 (solution) 2160 (solid) 2116 (solid)	(^{Mes}NacNac)Mg(N$_3$) [Si(N$_3$)$_6$]$^{2-}$ (^{Mes}NacNac)Mg(N$_3$) [Si(N$_3$)$_6$]$^{2-}$
IPrSi(N$_3$)$_4$	1 eq. [(^{Dipp}NacNac)Mg]$_2$	2195 (solid)	(^{Dipp}NacNac)Mg(N$_3$)
(^{Dipp}NCN)Si(N$_3$)$_3$	1 eq. [(^{Dipp}NacNac)Mg]$_2$	2198 (solution)	(^{Dipp}NacNac)Mg(N$_3$)

Table 3.1. Peerless' reduction reactions of silicon azides: IR observations and product assignments. While not listed in the table, IR absorptions corresponding to the starting silicon compound were detected in all reactions.

When using [(NacNac)Mg]$_2$ as a reducing agent, Peerless found no detectable azido-silicon products, but did detect unreacted starting material despite evidence of magnesium azide species. This suggests the silicon azides are selectively reduced in a manner that removes or decomposes all azido groups, suggesting that partially reduced silicon azides are more prone to subsequent reduction than the starting silicon azides.

With KC$_8$ as the reducing agent, new covalent azide species were detected by IR, indicating the possible presence of a reduced silicon azide, but no product could be isolated. It should be noted that Peerless was attempting to synthesise a low-valent silicon azide in these reactions by reducing the silicon centre, however no such compound was ever identified from these reactions (and indeed no low-valent silicon azide is currently known in the literature). Peerless speculates that the low-valent silicon azide IPrSi(N$_3$)$_2$ may form from the reduction of IPrSi(N$_3$)$_4$, but this subsequently reacts with another equivalent of IPrSi(N$_3$)$_2$ with elimination of N$_2$, ultimately resulting in the compound proposed in Figure 3.2. It is also possible that reduction of azido groups occurs directly instead of reduction of the silicon centre, in which case a silicon amide would form rather than a low-valent silicon azide.
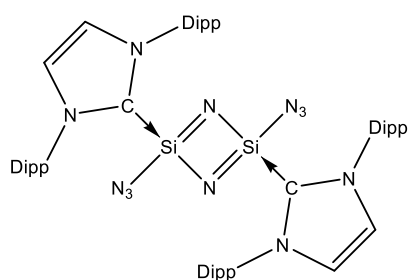
Figure 3.2. Product predicted by Peerless from reduction of IPrSi(N_3)$_4$.

There is only one published structure in the literature containing a disiladiazacyclobutadiene ring like the one shown in Figure 3.2,[90] so there is limited precedence for the decomposition product of IPrSi(N_3)$_2$ to adopt this structure. However, regardless of the structure of the product, reduction of azido groups is highly likely, either from direct reduction by the added reducing agent, or *via* a reduced silicon complex. Reduction of organo-azides is commonly used as a method of synthesising amines,[91] and as such a wide range of methods are known to facilitate azido group reduction, including: palladium-catalysed hydrogenation,[92] sodium bisulphite reduction,[93] tin-acid reduction,[94] and treatment with reducing agents such as LiAlH$_4$,[23] NaBH$_4$,[95] (NH$_4$)$_2$S,[96] K$_3$AsO$_3$,[97] TiCl$_3$.[98] Typically the reduction and/or workup is conducted with water as the source of protons for the resulting amine. This would not occur in the anhydrous conditions which Peerless was working in, thus a nitride might be expected instead of an amine.

Carbenes and silylenes are also known to reduce azides, forming imines[99] and silaimines respectively (Figure 3.3).[100] This poses an issue for both the synthesis of low-valent silicon azides and the stabilisation of silicon azides (of any valency) using carbene-type ligands. While the addition of the N-heterocyclic carbene IPr to Si(N_3)$_4$ does afford the intended adduct IPrSi(N_3)$_4$, the addition of ItBu to Si(N_3)$_4$ instead reduces two of the azido groups to form the iminosilane (ItBu=N)$_2$Si(N_3)$_2$.[73]
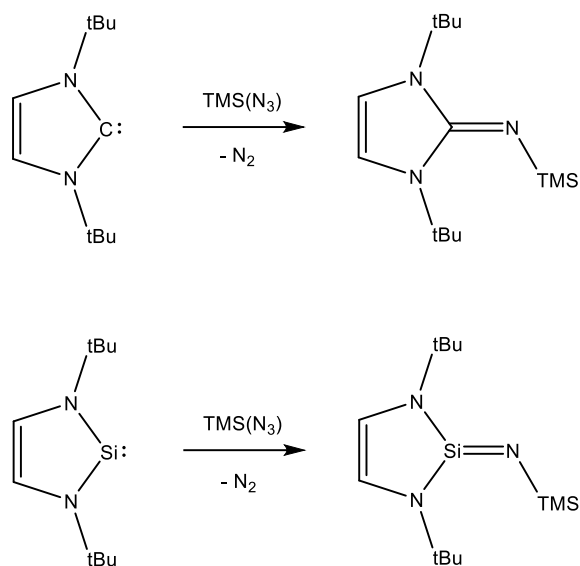
Figure 3.3. Reduction of the azido group of TMS(N₃) by both the N-heterocyclic carbene ItBu and the N-heterocyclic silylene SItBu.

While the reduction of azido groups is problematic for the isolation of low-valent silicon azides, the possibility of amido/nitrido compound formation warrants further investigation, thus additional experiments on the reduction of silicon azides were conducted.

3.2. Results and Discussion

3.2.1. Reduction of silicon tetraazide

Several attempts to reduce silicon tetraazide (as a solution in toluene) by alkali metals under various conditions have been attempted, summarised in Table 3.2.

Experiment	Reductant	Solvent	Observations / (method of detection)
1	2 eq. Na	Toluene	No reaction
2	0.5 eq. NaK	Toluene	$Si(N_3)_4$ (solution IR) NaN_3 (solid IR) KN_3 (solid IR) dark grey precipitate
3a	1 eq. NaK	Toluene	Significant unreacted $Si(N_3)_4$ (^{14}N NMR)
3b	Experiment 3a + 1 eq. NaK	Toluene	Only trace $Si(N_3)_4$ in solution (^{14}N NMR) NaN_3 (solid IR) KN_3 (solid IR) Unknown (solid IR: 2175 cm^{-1})
4	2 eq. NaK	5:1 HMPA : toluene ($Si(N_3)_4$ in toluene added to a solution of NaK in HMPA)	Deep red solution, faded to orange over time MN_3 (solution IR) trace white precipitate
5	2 eq. NaK	5:1 HMPA : toluene (HMPA added to a mixture of NaK, toluene and $Si(N_3)_4$)	Deep red solution, intensified over time MN_3 (solution IR) trace white precipitate
6	4 eq. Na	5:1 HMPA : toluene (HMPA added to a mixture of Na, toluene and $Si(N_3)_4$)	Clear deep pink solution NaN_3 (solution IR)
7	1 eq. K, 1.4 eq. anthracene	Et$_2$O	Grey precipitate, visually similar to Experiment 2

Table 3.2. Experiments and observations on the reduction of $Si(N_3)_4$ with alkali metals.

In Experiment 1, it is likely that no reaction occurred due to passivation of sodium in toluene, since the liquid alloy NaK did not suffer this issue. In Experiment 2, the reaction of $Si(N_3)_4$ with 0.5 equivalents of NaK (1 equivalent of alkali metal) did not consume all $Si(N_3)_4$, indicating that the initial reduction product is more prone to engaging in further reduction than the starting $Si(N_3)_4$. This observation indicates that $Si(N_3)_4$ is selectively reduced until all

azido groups are removed. This is the same result as was observed by Peerless using [(NacNac)Mg]$_2$ reducing agents. Additional evidence that the reduction occurs with removal of all azido groups is provided by the lack of any detectable azide-containing product other than sodium/potassium azides and hexaazidosilicates (the latter being the addition product of azide ions with unreacted silicon tetraazide). Given these observations, it is likely that the grey solid produced by the reaction contains elemental silicon. Thus, the reaction in Experiment 2 follows as per Figure 3.4.

$$Si(N_3)_4 \quad + \quad 2\ NaK \quad \longrightarrow \quad Si \quad + \quad 2\ NaN_3 \quad + \quad 2\ KN_3$$

Figure 3.4. Equation for the reaction of Si(N$_3$)$_4$ with NaK.

The observations of Experiment 3 indicate that four equivalents of alkali metal are required to consume all Si(N$_3$)$_4$. There is a small amount of residual Si(N$_3$)$_4$, attributed to a slight mismatch in stoichiometry due to the small scale these reactions were conducted on. Also of note is the presence of a solid material with a broad IR absorption at 2175 cm^{-1}. While this is close to the absorption wavenumber of Si(N$_3$)$_4$ (IR in toluene: 2171 cm^{-1}), this is unlikely to be Si(N$_3$)$_4$, since Si(N$_3$)$_4$ is readily soluble in toluene and thus should not be in the filter residue and typically gives rise to a sharp IR signal rather than a broad one. An alternative explanation for this absorption band is that it may arise from the mixed azido-nitrido compound [Si(N)(N$_3$)]$_n$ ("Compound B" in Chapter 2.2.4, IR absorption: ~2172 cm^{-1}). Much like Compound B this material was found to decompose on exposure to air, which is typical of silicon azides due to their susceptibility to hydrolysis. The formation of [Si(N)(N$_3$)]$_n$ here is reasonable, particularly given the apparent deficit of reductant, with a proposed reaction scheme shown in Figure 3.5.

$$Si(N_3)_4 \quad + \quad NaK \quad \longrightarrow \quad [Si(N)(N_3)]_n \quad + \quad NaN_3 \quad + \quad KN_3 \quad + \quad N_2$$
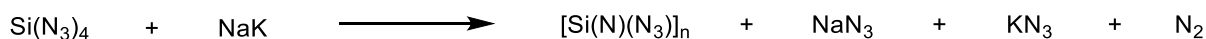
Figure 3.5. Hypothesised formation of the polymeric azido-nitrido silicon compound [Si(N)(N$_3$)]$_n$, from Si(N$_3$)$_4$ and NaK.

Given that 4 equivalents of alkali metal are required for (almost) all Si(N$_3$)$_4$ to be consumed, it is likely that the proposed scheme in Figure 3.5 is a minor side-reaction since it only consumes two equivalents of alkali metal, with the reaction in Figure 3.4 being more dominant. It may also be that the resulting [Si(N)(N$_3$)]$_n$ reacts further with NaK, the products

of which would not be readily identified by IR spectroscopy if they no longer contain an azido group.

Experiments 4-6 were conducted in hexamethylphosphoramide (HMPA), as this solvent is able to dissolve alkali metals, thus allowing for homogenous reaction. In all cases, four equivalents of alkali metal were added, all of which was consumed, and metal azide was the only azide-containing product detectable in agreement with the equation in Figure 3.4. Curiously, these reactions produced little or no precipitate, and formed brightly coloured orange/red solutions. This may indicate silicon nanoparticle formation instead of elemental silicon precipitate. The reduction of $SiCl_4$ with KC_8 is known to produce silicon nanoparticles, derivatives of which are reported to be orange.[101] Since the photoluminescent properties of silicon nanoparticles are reported to change with particle size,[102] particle size variation may also explain the slight variations in colour seen between Experiments 4-6.

An attempt to conduct a reduction of $Si(N_3)_4$ in Et_2O was enabled by the development of a synthesis of $Si(N_3)_4$ in Et_2O. The reaction of $SiCl_4$ and NaN_3 does not readily occur in Et_2O at room temperature, likely due to the insolubility of NaN_3 in Et_2O. However, addition of 0.02 equivalents of $AlCl_3(MeCN)$ was found to have a significant catalytic effect, affording full conversion to $Si(N_3)_4$ overnight. The resulting aluminium by-products are insoluble in Et_2O (determined by ^{27}Al NMR spectroscopy), so the solution only needs to be filtered without further purification being required. This then represents a rapid facile method of generating $Si(N_3)_4$, which alternatively requires several days of reaction time in hot benzene/toluene. Unfortunately, the volatility of Et_2O makes solutions of $Si(N_3)_4$ in Et_2O potentially dangerous, as evaporation of the solvent may leave explosive $Si(N_3)_4$ residues. In Experiment 7, the reaction mixture dried out, presumably due to inadequate sealing of the reaction vessel. While the products visually seemed to match the observations of Experiment 2 (suggesting the presence of KN_3 and elemental silicon), the products were carefully disposed of without analysis due to the explosion risk of unreacted $Si(N_3)_4$. Other work with $Si(N_3)_4$ in Et_2O has in one case resulted in a (contained) explosion due to the unintended evaporation of the solvent, so Experiment 7 was not deemed sufficiently promising to be worth repeating in light of the hazards associated with Et_2O solutions of $Si(N_3)_4$.

Considering the reductive properties of $(THF)_3LiSi(TMS)_3$ discussed in Chapter 2.2.3, the reaction of $Si(N_3)_4$ with this reagent was conducted in toluene. Based on the NMR signals of

the TMS groups, this reaction initially forms one major and two minor products, with one of the minor products gradually converting to the other. The products were found to be too soluble in the toluene reaction solvent for effective crystallisation. Replacing the solvent with hexane and allowing it to slowly evaporate afforded crystals of a previously unknown compound, 2,2,4,4-tetraazido-1,3-bis(tris(trimethylsilyl)silyl)cyclodisilazane (TABTC). This product is formally a dimer of a silaimine, $(TMS)_3Si-N=Si(N_3)_2$, thus the initial reaction can be considered analogous to that of $(THF)_3LiSi(TMS)_3$ with $(^{Dipp}NCN)Si(N_3)_3$. The lack steric protection then allows for subsequent dimerisation of the reactive Si=N double bond (Figure 3.6).
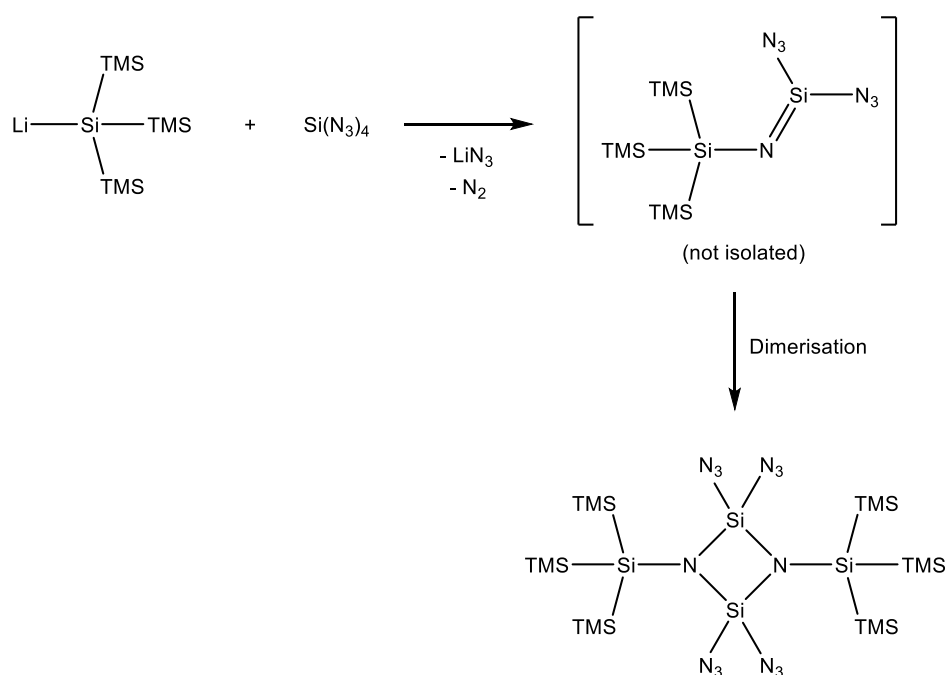
Figure 3.6. Reaction sequence to form 2,2,4,4-tetraazido-1,3-bis(tris(trimethylsilyl)silyl)cyclodisilazane (TABTC).
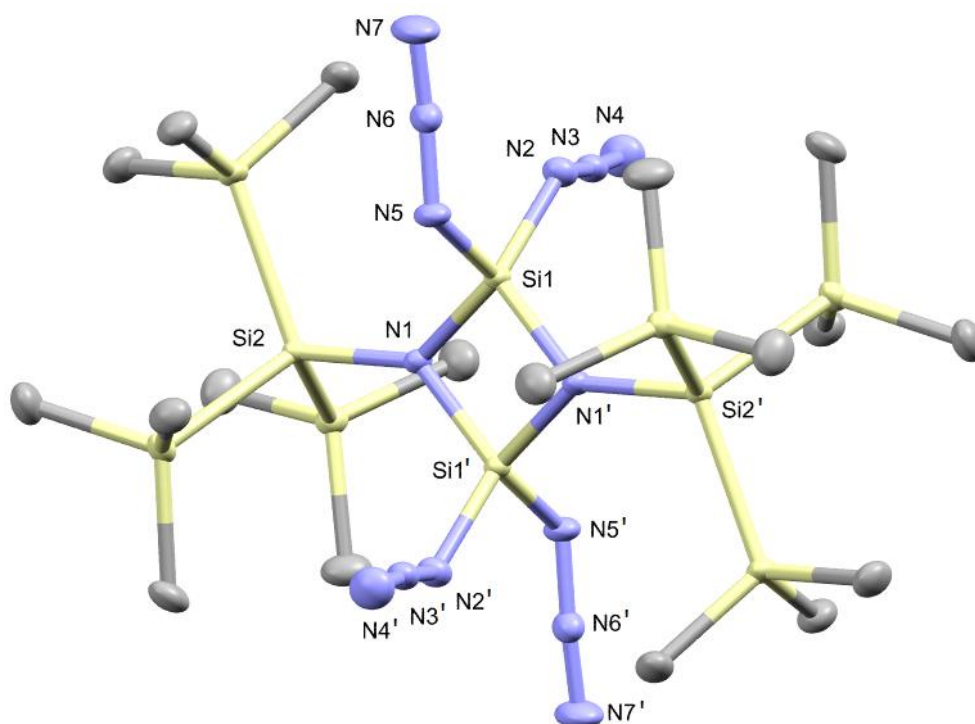
Figure 3.7. Thermal ellipsoid plot of TABTC. Ellipsoids set at the 50% probability level, hydrogen atoms are omitted for clarity. Selected bond lengths (Å) and angles (°): Si1–N1 1.727(2), Si1–N1' 1.716(2), Si1–N2 1.721(2), Si1–N5 1.724(2), Si1–Si1' 2.414(1), N1–Si2 1.784(2), N2–N3 1.228(2), N3–N4 1.130(2), N5–N6 1.232(2), N6–N7 1.126(2), N1–Si1–N1' 90.93(8), Si1–N1–Si1' 89.07(8), Si2–N1–Si1 136.91(10), Si2–N1–Si1' 133.56(9), N2–Si1–N5 102.18(8), N1–Si1–N1'–Si1' dihedral 0.00(3), Si2–N1–Si1–N1' dihedral 172.52(18).

Several compounds containing the cyclodisilazane structure are known to the literature.[103] Of those that have been structurally characterised by SCXRD, there is only one other azido-substituted cyclodisilazane to compare azido groups with: 2,4-diazido-2,4-di-tert-butyl-1,3-bis(azido(DippNacNac)aluminyl)-cyclodisilazane (ATAC, Figure 3.8).[104]
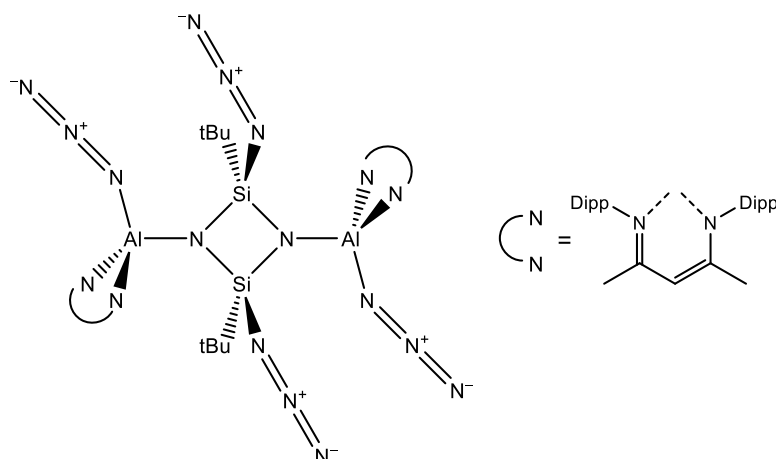
Figure 3.8. Structural diagram of the known compound 2,4-diazido-2,4-di-tert-butyl-1,3-bis(azido([Dipp]NacNac)aluminyl)cyclodisilazane (ATAC).

The bonding of the azido groups in TABTC are essentially identical to each other, despite arranging two different orientations. This suggests that there are no significant π-interactions from Si1 affecting these azido groups, as such an interaction would affect the azido groups differently depending on orientation. All azido groups orient themselves in a plane perpendicular to the N1–Si2 bond axis to avoid the steric pressure of the $Si(TMS)_3$ groups. The azido of ATAC are oriented with their N–N bonds near-parallel to the plane of cyclodisilazane ring, and thus have a similar geometry to the N5–N6–N7 azido group of TABTC. The Si1–N5 bond length of TABTC is somewhat shorter than the average $Si–N_3$ length in ATAC, at 1.724 Å and 1.760 Å respectively. The longer $Si–N_3$ bond in ATAC may be a result of significant steric clash between the azido and tert-butyl groups, as these groups are forced into a near-eclipsing conformation by the steric pressure of the [Dipp]NacNac ligand (average N–N–Si–tBu dihedral angle in ATAC = 41.0 °). As is expected, the longer $Si–N_3$ bond in ATAC makes the N–N bonding character closer to that of a free azide ion, resulting in a shorter $N_\alpha–N_\beta$ bond compared to TABTC (1.225 Å and 1.232 Å respectively) and a longer $N_\beta–N_\gamma$ bond compared to TABTC (1.140 Å and 1.126 Å respectively).

There are no previously known cyclodisilazanes with a tris(trimethylsilyl)silyl substituent, however there is an example containing the structurally analogous tris(tert-butyl)silyl group.[105] Several structures are also known for cyclodisilazanes with the smaller trimethylsilyl group,[106-108] including some with spiro-fused ring systems.[109-113]

Molecules of TABTC crystallise with inversion symmetry, so comparison is made to other silyl-substituted disilazanes with inversion symmetry in Table 3.3, with the atom labels as defined in Figure 3.9.
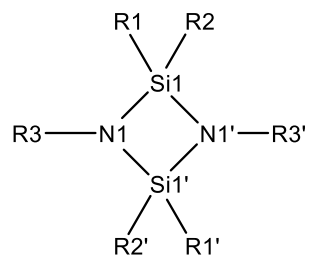
Figure 3.9. Atom labels used to define centrosymmetric cyclodisilazanes in Table 3.3.

R1	R2	R3	Si1–N1	Si1–N1'	N1–R3	N1–Si1–N1'	Si1–N1–Si1'	R1–Si1–R2	N1–Si1–N1'–Si1'	R3–N1–Si1–N1'
TABTC (R1, R2 = N$_3$, R3 = Si(TMS)$_3$)			1.727	1.716	1.784	90.9	89.1	102.2	0.0	172.5
Me	Me	Si(tBu)$_3$	1.778	1.774	1.774	91.1	88.4	102.8	0.5	176.9
Me	Me	Si(Me)$_3$	1.741	1.747	1.715	89.6	90.4	108.1	0.0	169.4
N(iPr)(TMS)	Ph	Si(Me)$_3$	1.758	1.745	1.732	88.3	90.9	110.2	4.4	178.3
(μ-NPh)$_2$Si(Me)$_2$		Si(Me)$_3$	1.722	1.736	1.734	88.8	91.2	85.8	0.0	170.7
H	H	Si(tBu)$_2$Me	1.728	1.740	1.733	90.3	89.7	93.8	0.0	171.7
F	F	Si(tBu)$_2$Me	1.713	1.701	1.768	91.7	88.3	102.6	0.0	174.3
F	F	Si(tBu)$_2$Ph	1.701	1.707	1.783	91.6	88.4	102.1	0.0	171.9

Table 3.3. Selected bond lengths (Å), angles (°) and dihedrals (°) of literature cyclodisilazanes[105, 108, 113-117] in comparison to TABTC. ESD values have been omitted, distances and angles have been universally rounded to three and one decimal places respectively for ease of viewing. R1, R2, R3 refer to the substituents of the cyclodisilazane as per Figure 3.9. Note that for some of these compounds, the reported structure is not modelled as perfectly centrosymmetric, so values differ very slightly for the inversion-equivalent bonds and angles.

The Si–N bonds in the cyclodisilazane ring of TABTC are shorter than in those where R1/R2 are organic groups, but longer than in those where R1, R2 = F. This indicates that the Si1–N1 bond lengths are dependent on the electron-withdrawing capability of the substituents on the silicon, with stronger withdrawing substituents correlating to a shorter bond. This may be a result of electron-withdrawing substituents facilitating π-donation from the ring nitrogen atoms to the ring silicon atoms. Curiously, this change does not appear to have any effect on the R1–Si1–R2 bond angle for the compounds where R1 = R2 = N_3, Me, F. Instead, this angle appears to be dependent primarily on the steric bulk of R3, with larger R3 groups forcing the R1 and R2 substituents closer together. The involvement of π-interactions is likely to contribute to the bonding of TABTC, as the Si_2N_2 ring is perfectly planar in TABTC as is the case for most cyclodisilazanes. The R3 substituent of TABTC is directed only 7.5 ° away from this plane, which seems quite average among the compared species. The N–Si bond to the R3 substituent is however slightly longer in TABTC than most other cyclodisilazanes. This is likely a steric effect of the Si(TMS)$_3$ group, as a similar N1–R3 bond length is observed in a cyclodisilazane with comparably bulky Si(tBu)$_2$Ph R3 groups. It is also of interest that the Si1–Si1' distance is remarkably short, at only 2.415 Å, comparable to the length of Si–Si single bonds (for comparison, the average Si–Si bond length in the Si(TMS)$_3$ groups of TABTC is 2.363 Å). Although the proximity of Si1 and Si1' is likely forced by the ring geometry rather than a direct result of Si–Si bonding, some Si–Si interactions must inevitably occur due to this proximity. These interactions may explain why the intermediate silaimine proposed in Figure 3.6 favours the formation of a dimeric product with a four-membered cycle rather than, for example, a trimeric product with a less-strained six-membered cycle.

The ring nitrogen atoms in TABTC are each bound to three silicon atoms and no other atoms, so TABTC can be defined as a substituted silicon nitride. Furthermore, uniquely among cyclodisilazanes, the ring silicon atoms are each bound to four nitrogen atoms – two azides and two nitrides. As such, the central ring structure of TABTC may represent a structural motif in amorphous azido-nitrido silicon materials such as those seen in Chapter 2.2.4.

Only a few crystals of TABTC were obtained and no other products were successfully isolated, so spectroscopic verification of whether this was the major or minor product could not be conducted due to lack of sample. Another likely product of this reaction is (TMS)$_3$Si-

Si(N$_3$)$_3$ resulting from the substitution of azide with (TMS)$_3$Si$^-$, but no crystallographic evidence for this was obtained.

3.2.2. Reaction of silicon tetraazide with alkali metal amides

While attempting to synthesise HSi(N$_3$)$_3$, it was found that LiAlH$_4$ appeared to reduce Si(N$_3$)$_4$ with little hydride-azide exchange (Chapter 2.2.1). Given that LiAlH$_4$ is known to reduce azides to amines, a likely intermediate in this reaction would be HN$^-$–Si(N$_3$)$_3$. Such an intermediate material could theoretically be synthesised from Si(N$_3$)$_4$ and NaNH$_2$ without the possibility of hydride exchange producing hydride-containing products. *In-situ* deprotonation with NH$_2$$^-$, followed by elimination of N$_3$$^-$, may then afford [Si(N)(N$_3$)]$_n$ as shown in Figure 3.10. The proposed reaction is analogous to the known synthesis of alkynes by elimination of H$^+$ and X$^-$ (X = Cl, Br) from haloalkanes using NaNH$_2$.[118]
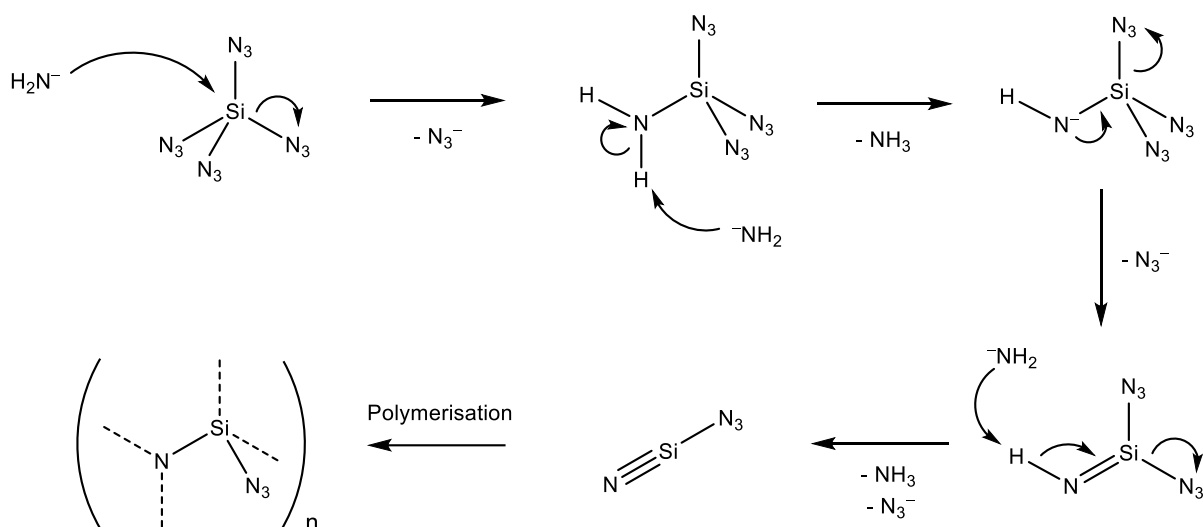
Figure 3.10. Hypothetical reaction scheme for the addition of $^-$NH$_2$ to Si(N$_3$)$_4$ to form an azido(nitrido)silicon compound. For simplicity, the possibility of polymerisation beginning at the silicon amide or silaimine intermediates has been neglected.

The reaction of Si(N$_3$)$_4$ with one equivalent of NaNH$_2$ in toluene for 10 days resulted in considerable quantities of Si(N$_3$)$_4$ remaining unreacted in solution. IR analysis of the residue shows a large, structured band between 2200 cm^{-1} – 2040 cm^{-1}, which can largely be

attributed to solid sodium azide. Due to the broadness and intensity of this signal, it is difficult to determine if any other minor azide species are present.

The reaction of $Si(N_3)_4$ with three equivalents of $NaNH_2$ at higher concentrations in toluene for 64 hours resulted in the same observations, but also formed small white beads in addition to powdered residue. These beads are amorphous and slightly porous by microscope analysis. When crushed and analysed by IR spectroscopy, the spectrum shows the presence of almost pure $NaNH_2$ with no significant azide absorptions, implying that they are either composed of $NaNH_2$, or a mixture of $NaNH_2$ and compounds with no characteristic IR absorption bands in the region of 4000 cm^{-1} – 500 cm^{-1}.

The observed formation of NaN_3 clearly indicates a reaction between $NaNH_2$ and $Si(N_3)_4$ occurs. However, it is currently unclear what the silicon-containing product of this reaction is. Given this formation of NaN_3, it is likely that the intended initial substitution process shown in Figure 3.10 does occur. However, this process may ultimately substitute all azido groups from the silicon atom, which would explain the lack of any obvious silicon-bound azide absorption by IR. In this event, the product may still be a form of silicon nitride, but this could not be verified. In addition to possible over-substitution, repeats of this reaction suffer from inconsistent conversion due to the low solubility of $NaNH_2$. As such, an alternative reagent was sought.

$LiN(TMS)_2$ has similar reactive properties to $NaNH_2$ while being highly soluble in low-polarity solvents. The addition of a C_6D_6 solution of $LiN(TMS)_2$ to a toluene solution of $Si(N_3)_4$ in equimolar quantities results in almost instant precipitation. After filtering, ^1H and ^{29}Si NMR analysis of the solution indicates only one trimethylsilyl environment in the products, and one other silicon environment which is not coupled to a proton. This is consistent with selective conversion to the species $(TMS)_2N–Si(N_3)_3$ shown in Figure 3.11. Due to the possible explosion hazard of silicon azides with high nitrogen content, this product was not isolated, and the filtered solution was used directly for subsequent reaction.
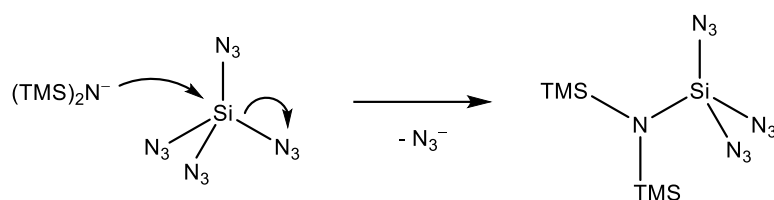
Figure 3.11. Reaction of $^-$N(TMS)$_2$ with Si(N$_3$)$_4$ to form (TMS)$_2$N–Si(N$_3$)$_3$.

The reaction shown in Figure 3.11 is analogous to the first step proposed in Figure 3.10. By continued analogy to Figure 3.10, the formal elimination of TMS(N$_3$) from (TMS)$_2$N–Si(N$_3$)$_3$ could afford the proposed azido(nitrido)silicon material [Si(N)(N$_3$)]$_n$. However, most bases and nucleophiles that would attack trimethylsilyl groups would also attack the triazidosilyl group, resulting in substitution of the azido groups. By using azide ions as the nucleophile, substitution of azido groups is no longer a concern, and the elimination process would be catalytic as it would release azide ions back into solution (Figure 3.12).
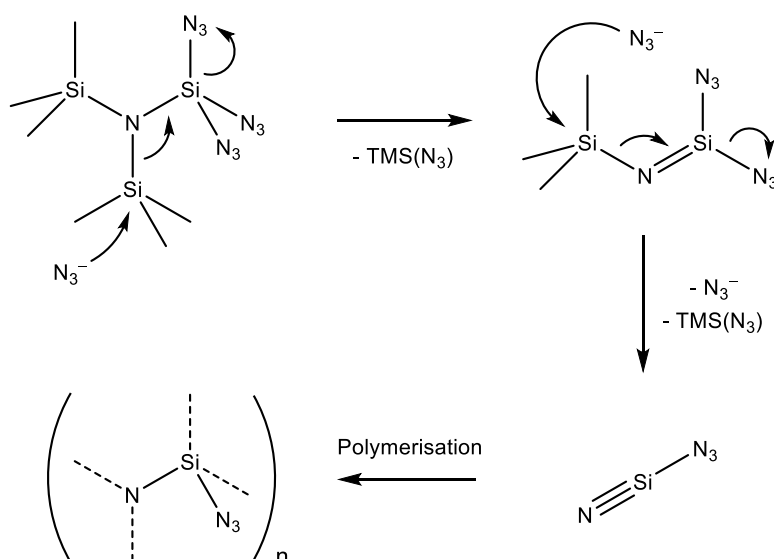
Figure 3.12. Proposed azide-catalysed decomposition of (TMS)$_2$N–Si(N$_3$)$_3$ to afford TMS(N$_3$) and [Si(N)(N$_3$)]$_n$.

(TMS)$_2$N–Si(N$_3$)$_3$ is formed with elimination of LiN$_3$, so it is evident that this process does not occur with LiN$_3$. This can be rationalised by the high lattice enthalpy of LiN$_3$, which renders it insoluble in benzene/toluene, and makes the azide ion less reactive than in weakly coordinated azide salts. Thus, to test the decomposition of (TMS)$_2$N–Si(N$_3$)$_3$, PPN(N$_3$) was chosen as an azide source, as it possesses lower lattice enthalpy and trace solubility in benzene/toluene. 0.1 equivalents of PPN(N$_3$) were added to the previously described NMR

sample of $(TMS)_2N{-}Si(N_3)_3$, and the resulting changes monitored by NMR spectroscopy. Over the following 22 days, ^1H and ^{29}Si NMR show $(TMS)_2N{-}Si(N_3)_3$ gradually converted to a single product (in solution). After a few days, it was noticed that the previously insoluble solid $(PPN(N_3))$ had largely dissolved, and the solution had separated into two layers. The lower layer had a very small volume (~0.05 mL) and was thus below the detection area of the NMR probe during analysis. For reference, the volume of the upper layer is ~1.0 mL. PPN^+ salts are poorly soluble in toluene/C_6D_6, so the apparent solvation of all $PPN(N_3)$ is likely due to it dissolving in a polar reaction product (expected to be $TMS(N_3)$). The resulting mixture would be highly ionic, explaining why it does not mix with toluene/C_6D_6, despite pure $TMS(N_3)$ being miscible with both toluene and C_6D_6. After 22 days, ^1H NMR analysis (of the upper layer) indicates 89% of the $(TMS)_2N{-}Si(N_3)_3$ had reacted, based on its ^1H NMR integral compared to that of the toluene methyl signal. Addition of small amounts of $TMS(N_3)$ to this sample increased the intensity of the product signals, rather than adding new signals to the spectra, thus confirming the product's identity as $TMS(N_3)$. Based on the integral values, The quantity of $TMS(N_3)$ dissolved in the upper layer has 60% of the integral that $(TMS)_2N{-}Si(N_3)_3$ had prior to reaction. Taking into account the fact that each molecule of $TMS(N_3)$ has half the number of protons as $(TMS)_2N{-}Si(N_3)_3$, and the observation that only 89% of $(TMS)_2N{-}Si(N_3)_3$ has decomposed, the integral values indicate 1.35 equivalents of $TMS(N_3)$ formed per $(TMS)_2N{-}Si(N_3)_3$. As the lower layer is predicted to be a mixture of $PPN(N_3)$ and $TMS(N_3)$, however, this number is a minimum estimate, and the actual value is likely greater than 1.35 equivalents. As such, the observed decomposition is consistent with the hypothesised decomposition process shown on Figure 3.12, involving release of 2 equivalents of $TMS(N_3)$. Small quantities of amorphous white residues formed on the walls of the NMR tube during the reaction, which may be the $[Si(N)(N_3)]_n$ predicted by the reaction scheme in Figure 3.12. Unfortunately, this material was not able to be analysed, as it was in too small a quantity, and stuck to the walls of the NMR tube.

In order to analyse the residues of this reaction, a larger scale reaction of $(TMS)_2N{-}Si(N_3)_3$ with 0.1 equivalents of $PPN(N_3)$ in toluene was conducted. After 11 days, an aliquot taken for ^1H NMR analysis shows the integral of $TMS(N_3)$ to be slightly over twice that of $(TMS)_2N{-}Si(N_3)_3$. Curiously, the residue from this experiment is brown rather than white of the smaller NMR scale experiment. The reason for this difference is unknown. IR analysis of

this residue (as a Nujol mull) shows a broad band consisting of multiple overlapped absorptions in the wavenumber range of 2300 – 2000 cm^{-1}. The most intense of these absorptions appear at v/cm^{-1} = ~2168 s br, 2148 s, ~2098 m br (Figure 3.13). The strong absorption at 2148 cm^{-1} likely results from residual TMS(N$_3$) (lit. 2146 cm^{-1} as a thin film).[119] The broad absorption around 2168 cm^{-1} is consistent with [Si(N)(N$_3$)]$_n$ from Chapter 2.2.4. The absorption at 2098 cm^{-1} cannot be readily assigned to any known compound. The broad nature of this absorption, as well as the insolubility of the residue in toluene, suggests that this absorption may also correspond to an amorphous polymeric material like [Si(N)(N$_3$)]$_n$. Since the decomposition of (TMS)$_2$N−Si(N$_3$)$_3$ had not completed at the time of analysis, this material may perhaps result from polymerisation of the reaction intermediate, (TMS)N=Si(N$_3$)$_2$, proposed in Figure 3.12.
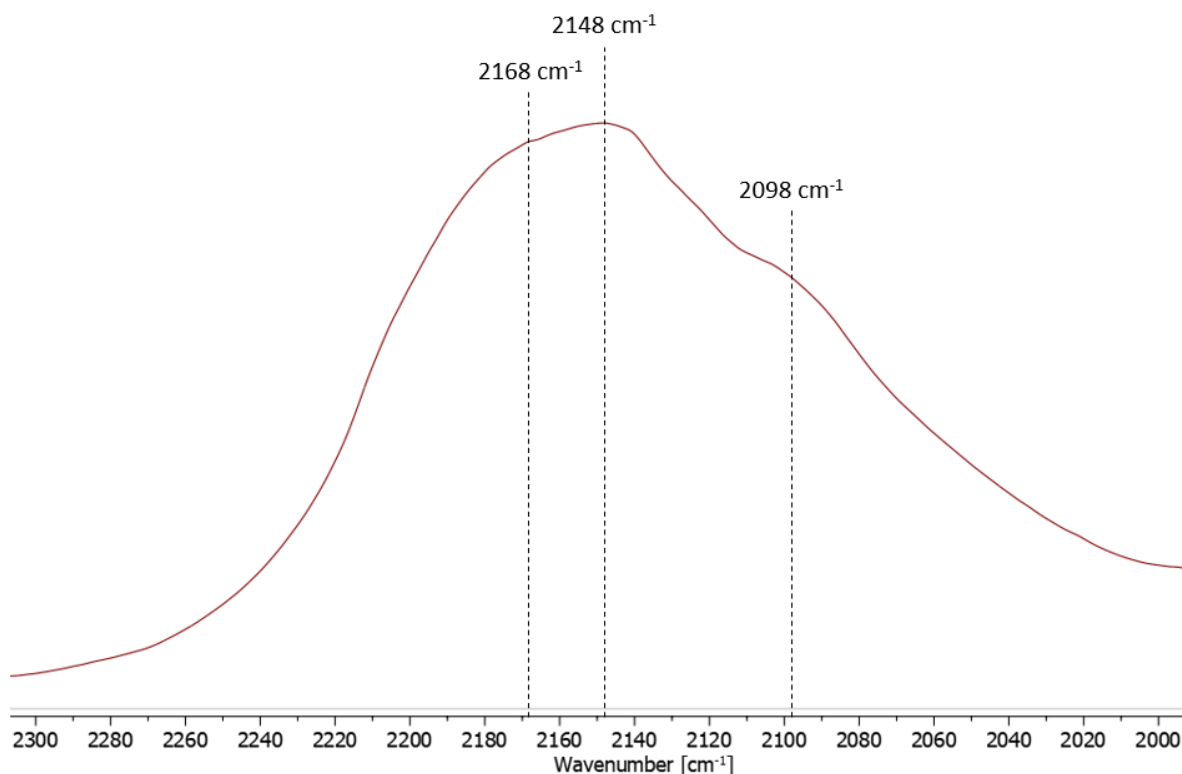
Figure 3.13. IR absorption spectrum of the insoluble residue from reaction of (TMS)$_2$N−Si(N$_3$)$_3$ with catalytic PPN(N$_3$), in the wavenumber range of 2300 – 2000 cm^{-1}. Assigned peak positions are shown with dashed lines.

The identification of a product with an IR absorption consistent with [Si(N)(N$_3$)]$_n$ is in agreement with the proposed reaction scheme in Figure 3.12. If the reaction conditions are optimised, the decomposition of (TMS)$_2$N−Si(N$_3$)$_3$ may be a more consistent route towards

synthesising $[Si(N)(N_3)]_n$ than the thermal decomposition of $(^{Dipp}NCN)SiH(N_3)_2$. Unfortunately, due to time limitations, these optimisations and further study of $[Si(N)(N_3)]_n$ were not able to be conducted.

3.4. Conclusions

The reduction of $Si(N_3)_4$ with alkali metal reducing mixtures seems to predominantly form elemental silicon and metal azides, thus making it an unsuitable method of synthesising low-valent silicon azides or silicon nitrides. The detection of material with an IR absorption matching "Compound B" ($[Si(N)(N_3)]_n$) from Chapter 2.2.4 suggests that some mixed azido(nitrido)silicon compounds may form during this reaction, but they are only minor products. Alternatively, the reduction of $Si(N_3)_4$ with $(THF)_3LiSi(TMS)_3$ appears to proceed with reduction of an azido group analogous to the reduction of $(^{Dipp}NCN)Si(N_3)_3$ with the same reagent. Unlike the silaimine formed from the reduction of $(^{Dipp}NCN)Si(N_3)_3$, this reduction of $Si(N_3)_4$ forms a four-membered cyclic disilazane, which can be seen as the dimerisation product of a silaimine. This product can be described as a substituted azido(nitrido)silicon compound and may represent part of the structural nature of $[Si(N)(N_3)]_n$.

The reaction of $Si(N_3)_4$ with alkali metal amides was conducted as an alternative pathway towards $[Si(N)(N_3)]_n$. $NaNH_2$ was found to react with $Si(N_3)_4$ to afford NaN_3, but no azido-silicon compound could be identified from the products. The poor solubility of $NaNH_2$ in suitable solvents also poses an issue for this reaction. By contrast, $LiN(TMS)_2$ reacts selectively with $Si(N_3)_4$ to afford $(TMS)_2N-Si(N_3)_3$. This compound can be decomposed catalytically by azide ions to afford a material with an IR spectrum consistent with $[Si(N)(N_3)]_n$. The observed byproduct, $TMS(N_3)$, also indicates the formation of $[Si(N)(N_3)]_n$ based on the reaction stoichiometry. This method is proposed as a potentially more consistent route towards $[Si(N)(N_3)]_n$ than the thermal decomposition of $(^{Dipp}NCN)SiH(N_3)_2$ shown in Chapter 2.2.4.

4. Synthesis of low-valent silicon chloride complexes

4.1. Introduction

While low-valent silicon azides are currently an unknown class of compound, low-valent silicon chloride complexes have been known for some time, as exemplified in Chapter 1.2.2. A conceivable route towards low-valent silicon azides would be to exchange the chloro groups for azido groups on low-valent silicon chloride complexes by means of an azide transfer reagent. Peerless recognised this possibility and investigated the reaction of NaN_3 with the low-valent complexes $IPrSiI_2$ and $IPrSiCl_2$ with the goal of synthesising $IPrSi(N_3)_2$.[73] The reaction with $IPrSiI_2$ produced a solution in which only a single asymmetric azide stretch was detected by IR, at 2152 cm^{-1}. This is a higher wavenumber than the azide absorption bands for $IPrSi(N_3)_4$ (v / cm^{-1} = 2150, 2136, 2117, 2102).[73] For the analogous germanium compounds, the azide absorption of $IPrGe(N_3)_2$ (v / cm^{-1} = 2075)[120] is at a lower wavenumber than the absorptions of $IPrGe(N_3)_4$ (v / cm^{-1} = 2128, 2108, 2088, 2077).[73] Based on this analogy, the target compound, $IPrSi(N_3)_2$, is expected to have a lower absorption wavenumber than $IPrSi(N_3)_4$, so the product giving rise to absorption at 2152 cm^{-1} is assumed to be a decomposition product of $IPrSi(N_3)_2$ (such as proposed in Chapter 3.1). This absorption band was also observed in the reaction of NaN_3 with $IPrSiCl_2$, in addition to two weak absorption bands at 2102 cm^{-1} and 2086 cm^{-1}. Peerless suggests these weak absorptions may belong to the desired product, $IPrSi(N_3)_2$, but no compound associated with these bands was successfully isolated.

If $IPrSi(N_3)_2$ is unstable, then alternative ligand systems will be needed to isolate low-valent silicon azides. Peerless proposes the decomposition involves the attack of an azido group by the silicon lone pair of $IPrSi(N_3)_2$, forming a silaimine. A desirable ligand would thus be one which can prevent this attack, either by steric hindrance or electronic stabilisation of the silicon lone pair.

Based on this requirement, the bis(imino)pyridine ligand 2,6-bis(N-(2,6-diisopropylphenyl)acetimino)pyridine (BIP) (Figure 4.1) was selected as a candidate for stabilising low-valent silicon azides. Its large steric bulk and tridentate nature is expected to provide a barrier towards reactions of the silicon centre. Additionally, bis(imino)pyridine ligands are known to act as electron acceptors in metal complexes.[121, 122] This electron

accepting nature of the BIP ligand should reduce the reactivity of the silicon lone pair in a low-valent silicon complex. However, this may have an oxidising effect on the silicon atom, leading to some ambiguity in its oxidation state (and thus valence state), as exemplified in Figure 4.1.

(uncoordinated)

(tridentate coordination)

(resonance form with oxidised metal)
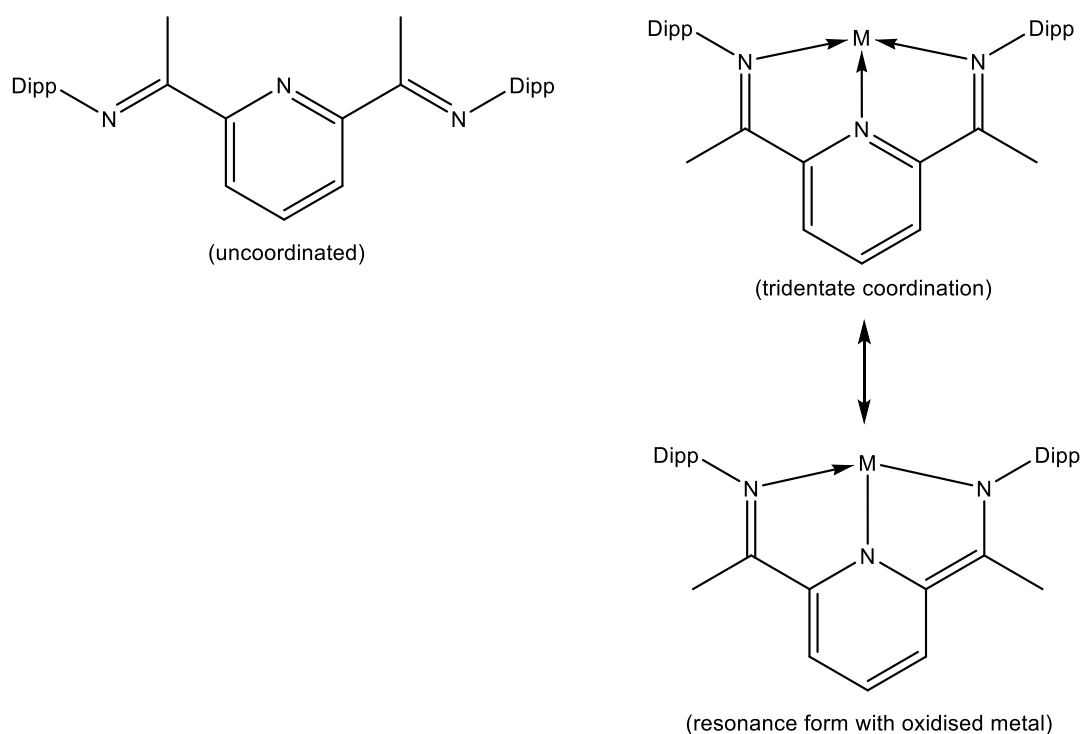
Figure 4.1. Structure of 2,6-bis(N-(2,6-diisopropylphenyl)acetimino)pyridine (BIP) as a free molecule and as a tridentate ligand to an unspecified metal centre "M". A resonance form of the BIP–M complex showing the formal oxidation of the metal and reduction of the ligand is also drawn.

There are no previously known bis(imino)pyridine complexes of silicon. This is perhaps unsurprising, as any tetravalent silane would struggle to accommodate a neutral tridentate ligand due to overcrowding of the coordination sphere. Germanium and tin complexes of BIP are known, but are formed from the divalent reagents germanium dichloride and tin dichloride respectively, as shown in Figure 4.2.[123]
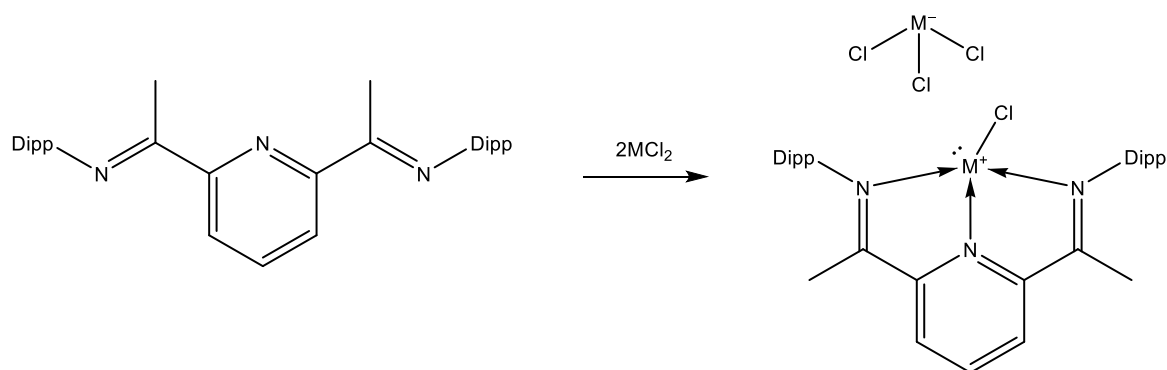
Figure 4.2. Synthesis of [(BIP)MCl][MCl$_3$]. M = Ge, Sn.

In the germanium and tin complexes in Figure 4.2, the steric demand of the BIP ligand is evident, forcing the de-coordination of a chloride from the Group 14 centre and resulting in a cationic complex. The charged nature of such complexes would limit dimerisation reactions, so the analogous silicon azide complex [(BIP)Si(N$_3$)]$^+$ would be a promising target for a stable low-valent silicon complex. The most obvious precursors to such a complex would be the yet-unknown complexes [(BIP)SiCl]$^+$ or (BIP)SiCl$_2$.

4.2. Results and discussion

4.2.1. Alternative attempts to synthesise IPrSi(N$_3$)$_2$

Before investigating the synthesis of BIP complexes of silicon, alternative routes to synthesise IPrSi(N$_3$)$_2$ were considered based on reagents used in Chapters 2 and 3.

The reaction of IPrSiCl$_2$ with Na[Al(N$_3$)$_4$](THF)$_4$ in C$_6$D$_6$ results in precipitate formation, and bubbling indicating the loss of dinitrogen has occurred. After the reaction had stopped, the solution was filtered and allowed to slowly evaporate under an inert atmosphere, affording disordered crystals of the previously unknown complex IPrAl(N$_3$)$_3$ (Figure 4.4), along with a pale brown residue. No silicon-containing product was successfully identified. It is assumed that silicon-containing product(s) was either insoluble or composes part of the amorphous brown residue. Based on the observations of this reaction, the reaction scheme in Figure 4.3 is proposed.
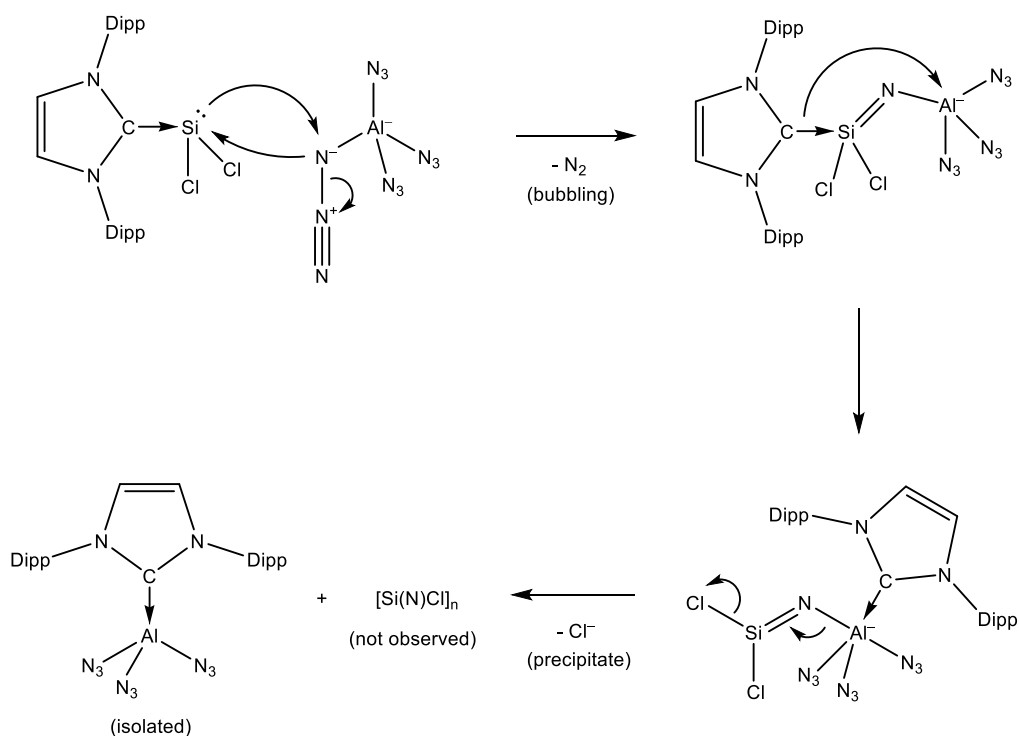
Figure 4.3. Proposed mechanism for reaction of $IPrSiCl_2$ with $Al(N_3)_4^-$.
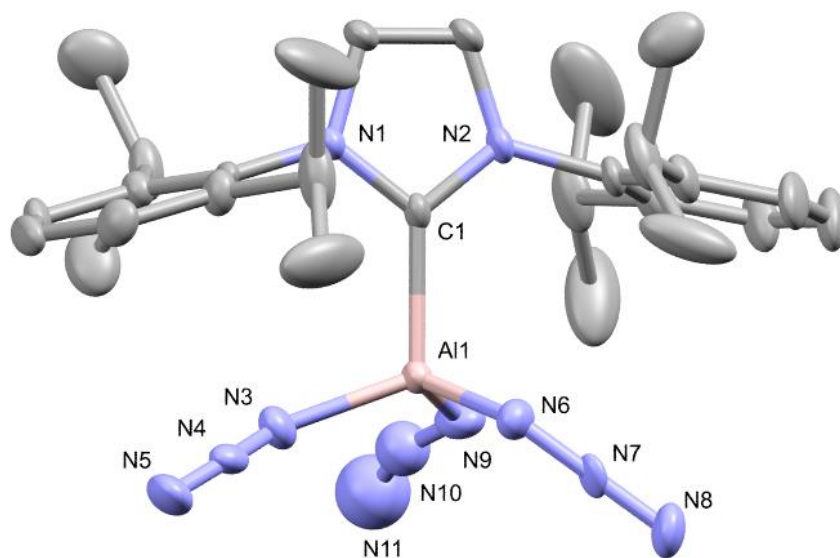
Figure 4.4. Thermal ellipsoid plot of one disorder component from crystals of $IPrAl(N_3)_3$. The disorder prevented anisotropic modelling of N10, N11. Ellipsoids set at the 50% probability level, hydrogen atoms are omitted for clarity. Selected bond lengths (Å) and angles (°): C1–Al1 2.005(5), Al1–N3 1.849(5), Al1–N6 1.858(5), Al1–N9 1.848(5), N3–N4 1.120(10), N4–N5 1.119(10), N6–N7 1.169(9), N7–N8 1.138(8), C1–Al1–N3 109.5(3), C1–Al1–N6 105.6(3), C1–Al1–N9 106.6(3). Bonding within the N9–N10–N11 azido group could not be reliably determined due to disorder.

The disordered nature of the crystals of $IPrAl(N_3)_3$ preclude detailed structure comparisons. It does however appear that the bonding within the azido groups is quite close to that of azide ions, with the N3–N4 bond being the same length as N4–N5, and the N6–N7 bond being only 0.03 Å longer than N7–N8. While these values have high uncertainty due to the poor structure, this small difference between the N_α–N_β and N_β–N_γ bond lengths is significantly contrasting to $IPrSi(N_3)_4$, where the average difference between N_α–N_β and N_β–N_γ is 0.07 Å for the axial azides, and 0.11 Å for the equatorial azides.[73] This highly ionic azide character may help explain why aluminium azides (e.g. $NaAl(N_3)_4$) are able to act as effective azide transfer reagents, although $IPrAl(N_3)_3$ itself has not been used for such a purpose.

The formation of $IPrAl(N_3)_3$ from $IPrSiCl_2$ and $Na[Al(N_3)_4](THF)_4$ indicates that aluminium azide reagents may not be suitable for azide transfer to carbene-stabilised low-valent silicon complexes, since the carbenes may transfer to the aluminium centre thus leaving the silicon without its ancillary ligand. Additionally, the isolation of $IPrAl(N_3)_3$ as the apparent major product (see note in Chapter 8.4.1) indicates that very little chloride-azide exchange has occurred.

Further verification for the lability of the IPr ligand in $IPrSiCl_2$ was obtained from NMR monitoring of the reaction of $IPrSiCl_2$ with 2 equivalents of $PPN(N_3)$ in d8-THF. After 2 days of reaction, free IPr is formed in near-quantitative yield. No signals were detected by ^{14}N or ^{29}Si NMR analysis of the solution, so if any azidosilicon products are formed, they are insoluble. IR analysis of the insoluble residue shows multiple intense bands in the range 2010–1990 cm^{-1}, indicating that the dominant azide-containing species are ionic azide salts. Several much weaker bands are also observed at v/cm^{-1} = 2234, 2220, 2168, 2115, 2106. Of these, the most intense band is the one at 2168 cm^{-1}. This band is broad and degrades on exposure to air, and is thus consistent with $[Si(N)(N_3)]_n$ (Compound B from Chapter 2.2.4). The formation of this material is predicted to occur from the decomposition of $Si(N_3)_2$. A plausible overall reaction scheme is presented in Figure 4.5.
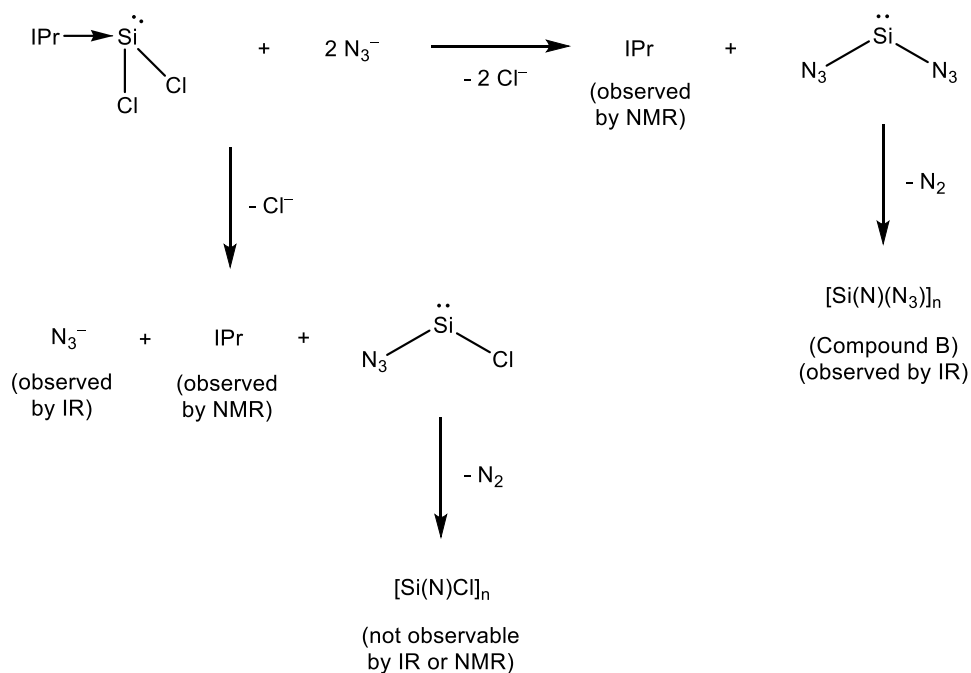
Figure 4.5. Proposed reaction sequence of $IPrSiCl_2$ with 2 eq. N_3^-, to match the observation of IPr, $[Si(N)(N_3)]_n$ and unreacted N_3^-.

The reduction of $IPrSi(N_3)_4$ with $(THF)_3LiSi(TMS)_3$ was found to occur with vigorous bubbling, consistent with the other reactions of $(THF)_3LiSi(TMS)_3$ with silicon azides. Based on this, and the known reactivity of $(THF)_3LiSi(TMS)_3$ towards $(^{Dipp}NCN)Si(N_3)_3$ and $Si(N_3)_4$ (Chapters 2.2.3 and 3.2.1 respectively), a likely sequence of this reaction involves the formation of an imine which may or may not be stable (Figure 4.6). No crystalline product could be isolated from the reaction mixture, so the structure of the product remains speculative. The visible loss of gas does however offer evidence that at least some azido groups are reduced, so the outcome is unlikely to be $IPrSi(N_3)_2$.
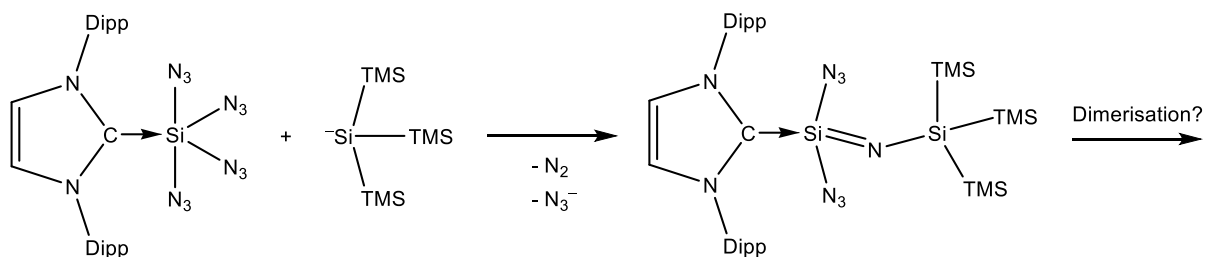
Figure 4.6. Proposed initial reaction of $IPrSi(N_3)_4$ with $(THF)_3LiSi(TMS)_3$.

4.2.2. Synthesis of silicon complexes bearing tridentate ligands

For the synthesis of [(BIP)SiCl]$^+$ or (BIP)SiCl$_2$, the BIP ligand would need to react with an *in-situ* source of SiCl$_2$, as SiCl$_2$ is not an available reagent. The synthesis and reactions of BIP with silicon compounds were conducted alongside MSc student Zekun Han, who helped carry out ideas I have put forward based on this requirement.

As was expected, BIP does not react with SiCl$_4$ or HSiCl$_3$ under ambient conditions in C$_6$D$_6$. More surprisingly, Si$_2$Cl$_6$ was similarly unreactive under these conditions, despite being a known source of SiCl$_2$ for ligand-stabilised complexes[124] (see Chapter 5.1).

SiCl$_4$ remained unreactive towards BIP even at 100 °C. As SiCl$_4$ is not known to be a source of SiCl$_2$ without the presence of reducing agents, this is unsurprising. However even after the addition of lithium granules and catalytic naphthalene to reduce the SiCl$_4$, still no reaction was observed.

Upon heating to 100 °C, HSiCl$_3$ was observed to react with BIP, identified by a visible darkening of the yellow solution and changes to the ^{1}H NMR spectrum. After 4 days of heating, all HSiCl$_3$ was consumed. The dominant signals in the ^{1}H NMR spectrum can be attributed to free BIP ligand, but many weaker signals are observed near the ligand signals. Heating for a further 9 days resulted in no further change. Additional signals near to those of the ligand suggest the formation of ligand complexes, but the number of signals is too great to be interpretable, with approximately forty peak maxima in the region of 1.75 ppm – 0.85 ppm (the spectral region associated with the isopropyl-CH$_3$ group of BIP). This large number of signals implies highly unselective reactivity, and no isolated compound was successfully obtained from this mixture. There is a report of HSiCl$_3$ reacting with a different bis(imino)pyridine ligand, where it was found that HSiCl$_3$ can reduce the imino groups to amino groups by hydrosilylation.[125] The numerous products may therefore be complexes containing modified BIP ligands, including those resulting from hydrosilylation. Additional signals may arise if HSiCl$_3$ disproportionates, affording a variety of possible silicon environments for each type of ligand present.

When Si$_2$Cl$_6$ was heated with BIP in C$_6$D$_6$ at 100 °C, the solution turned dark brown after 16 hours. After heating for a further 48 hours, the ^{1}H NMR spectrum still shows free BIP ligand as the dominant signal, but with many other major signals surrounding the BIP ligand. The

number of signals is significantly less than for the $HSiCl_3$ reaction, with fourteen prominent signals in the vicinity of the BIP isopropyl CH_3 signal. Removal of the solvent did not afford any crystalline product. Redissolving the residue in hexane and allowing the hexane to slowly evaporate afforded a few blue-black crystals among a predominantly dark-orange residue. These blue-black crystals were found to consist of a compound related to the targeted complex (BIP)SiCl₂, where a hydrogen atom of an acetimino group has been substituted for a trichlorosilyl group (Figure 4.7). The resulting compound is referred to as (^{SiCl3}BIP)SiCl₂.
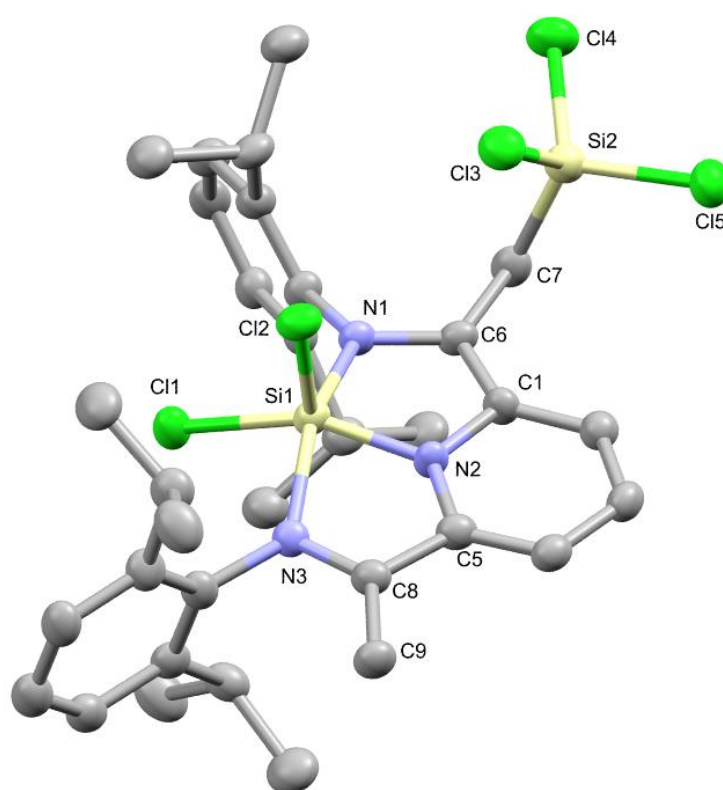
Figure 4.7. Thermal ellipsoid plot of (^{SiCl3}BIP)SiCl₂. Ellipsoids at the 50% probability level, hydrogen atoms and a hexane solvate molecule are omitted for clarity. Selected bond lengths (Å) and angles (°): Si1–N1 1.821(4), Si1–N2 1.743(4), Si1–N3 1.980(4), Si1–Cl1 2.081(2), Si1–Cl2 2.114(2), N1–C6 1.395(6), N3–C8 1.323(6), C7–C6 1.498(6), C6–C1 1.372(6), C1–N2 1.408(6), N2–C5 1.387(6), C5–C8 1.437(6), C8–C9 1.484(6), Si2–C7 1.854(5), Si2–Cl3 2.026(2), Si2–Cl4 2.035(2), Si2–Cl5 2.042(2), N1–Si1–N2 84.75(16), N2–Si1–N3 80.52(16), N1–Si1–N3 158.5(2), N3–Si1–Cl1 90.01(11), Cl1–Si1–N1 95.00(11), Cl2–Si1–N1 102.82(16), Cl2–Si1–N2 104.52(16), Cl2–Si1–N3 96.03(14), Cl2–Si1–Cl1 104.94(8).

(^{SiCl3}BIP)SiCl$_2$ curiously adopts a square pyramidal geometry. The BIP backbone is almost perfectly planar (dihedral angles: N1–C6–C1–N2 1.3 °, N2–C5–C8–N3 -0.7 °). Si1 is offset from this plane slightly, dihedral angle N1–N3–N2–Si1 = 12.1 °, while Cl1 is offset from this plane in the other direction (N1–N3–N2–Cl1 = -8.4 °) The Si1–Cl2 bond is then approximately equiangular with the other bonds to Si1, with angles of 95 ° – 105 °. This unusual geometry may in part be due to steric pressure from the silicon lone pair, which could occupy some of the void opposite Cl2. From the bonding within the ligand, it is clear that the resonance form involving the formal reduction of the ligand (Figure 4.4) contributes to the electronic structure of (^{SiCl3}BIP)SiCl$_2$. The Si1–N1 bond length (1.821 Å) is significantly shorter than the Si1–N3 bond length (1.980 Å), consistent with the asymmetric coordination shown in Figure 4.4. As would be expected from the bond orders in the reduced ligand form, N1–C6 is longer than N3–C8 (1.395 Å and 1.323 Å respectively, C1–N2 is longer than N2–C5 (1.408 Å and 1.387 Å respectively) and C6–C1 is shorter than C5–C8 (1.372 Å and 1.437 Å respectively). The imine and pyridine C–N bonds are all longer than in free BIP ligand, which has an average imine C–N bond length of 1.270 Å and an average pyridine C–N bond length of 1.351 Å.[126] Furthermore, both the C1–C6 and C5–C8 bonds are shorter than the respective bonds in BIP which average to 1.487 Å. Thus, it seems the reducing effect of the SiCl$_2$ group is affecting the entire ^{SiCl3}BIP ligand, but with the effect most pronounced on the bonding in the N1–C6–C1–N2 section. The SiCl$_3$ group does not appear to have much significant effect on the bonding in the complex, as the C7–C6 bond length is comparable to C8–C9 at 1.498 Å and 1.484 Å respectively. The long bond length in both cases indicates a lack of π-interactions in these bonds. The σ-donating capability of the SiCl$_3$ group may however explain why the asymmetric coordination of Si1 preferentially binds closer to N1 rather than N3.

Although the target complex (BIP)SiCl$_2$ was not successfully isolated, (^{SiCl3}BIP)SiCl$_2$ represents the only known example of an isolable bis(imino)pyridine silicon complex. Unfortunately, the extremely low yield of this material renders it impractical for future study. Additionally, the trichlorosilyl group on the ligand is undesirable for reaction of the complex with azide transfer reagents, as this group would also undergo substitution reactions with azide. The resulting triazidosilyl group would be far less protected than the central silicon atom of the

complex, which may result in the azido groups being prone to attack by reduced silicon species.

Et$_2$O extraction of the remaining dark orange residue from the dried reaction solution, followed by evaporation this extract afforded orange crystals. These crystals consist of a disordered mixture of different (BIP)SiCl$_2$-derived complexes. This mixture was best modelled as a two-component system (both components shown separately in Figure 4.8). In one component, the BIP ligand has been formally dehydrogenated, affording methylene groups in place of the backbone methyl groups. This complex is referred to as ($^{-H2}$BIP)SiCl$_2$. In the other component, the BIP ligand has been formally hydrogenated, reducing the imino groups to amido ($^-$NR$_2$) groups. This complex is referred to as ($^{+H2}$BIP)SiCl$_2$. The ratio $^{-H2}$BIP : $^{+H2}$BIP in these crystals is best modelled as 0.73 : 0.27. It should be noted that the ligands of these complexes are referred to here as $^{-H2}$BIP and $^{+H2}$BIP to emphasise their relationship with BIP. They are not strictly bis(imino)pyridine ligands, as they no longer contain imino groups and are instead best described as deprotonated bis(amino)pyridine ligands.
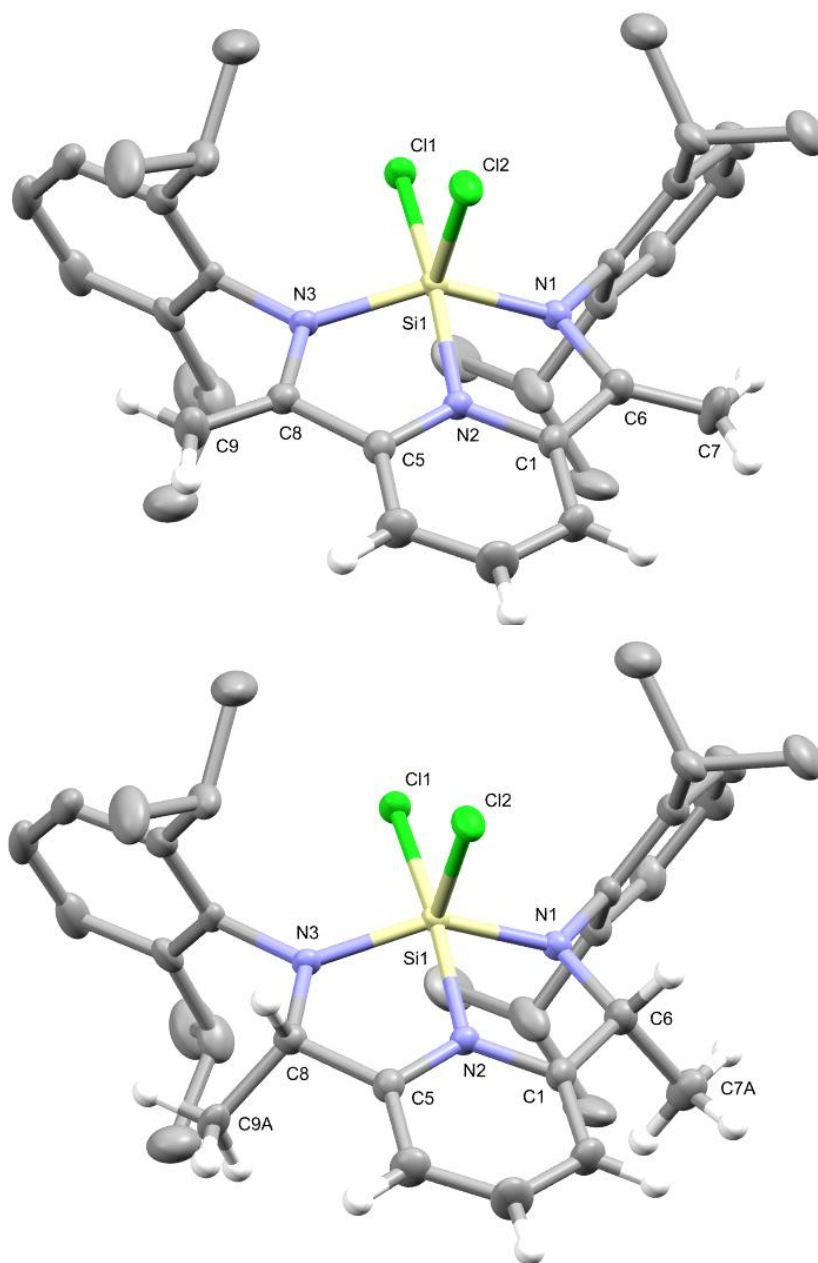
Figure 4.8. Thermal ellipsoid plots of ($^{-H2}$BIP)SiCl$_2$ (top) and ($^{+H2}$BIP)SiCl$_2$ (bottom), which are superimposed on each other within the same crystal. Ellipsoids at the 50% probability level, Dipp-group hydrogen atoms are omitted for clarity, other hydrogen atoms are displayed as spheres of fixed radius (0.2 Å). Two of the isopropyl groups have slight conformational disorder – the major component is shown here. Selected bond lengths (Å) and angles (°): Si1–N1 1.790(2), Si1–N2 1.880(2), Si1–N3 1.789(2), Si1–Cl1 2.119(1), Si1–Cl2 2.118(1), N1–C6 1.423(4), N3–C8 1.430(3), C7–C6 1.329(5), C7A–C6 1.492(14), C6–C1 1.476(4), C1–N2 1.341(3), N2–C5 1.335(3), C5–C8 1.474(4), C8–C9 1.332(5), C8–C9A 1.494(13), N1–Si1–N2 82.01(10), N2–Si1–N3 81.88(10), N1–Si1–N3 145.74(11), N3–Si1–Cl1 94.15(8), Cl1–Si1–N1 94.06(8), Cl2–Si1–N1 105.05(8), Cl2–Si1–N2 93.74(8), Cl2–Si1–N3 106.00(8), Cl2–Si1–Cl1 100.60(4).
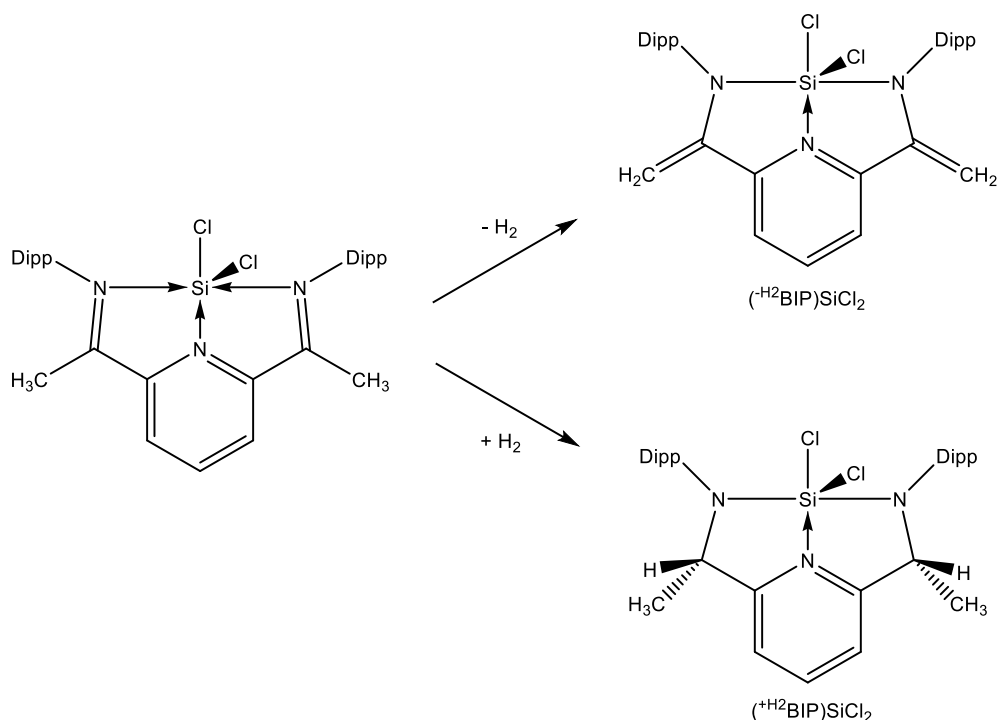
Figure 4.9. Disproportionation of (BIP)SiCl$_2$ to ($^{-H2}$BIP)SiCl$_2$ and ($^{+H2}$BIP)SiCl$_2$.

As ($^{-H2}$BIP)SiCl$_2$ and ($^{+H2}$BIP)SiCl$_2$ are superimposed in the crystal structure, structure analysis is limited to the weighted average of the two structures. Nonetheless, the ellipsoids in the structure have reasonable size and shape, and the structure refines to an acceptable quality (R_1 = 5.81%). Thus, with exception of C7/C7A and C9/C9A which are treated separately, the two structures appear to be sufficiently similar that the averaged structure is a good representation of both. This averaged structure will be referred to as ($^{\pm H2}$BIP)SiCl$_2$. In contrast to the asymmetric binding in (^{SiCl3}BIP)SiCl$_2$, ($^{\pm H2}$BIP)SiCl$_2$ is almost perfectly mirror symmetric, with the diisopropylphenyl groups being the only part of the molecule that does not obey C$_s$ symmetry. Also in contrast to (^{SiCl3}BIP)SiCl$_2$, the Si1–N2 bond is the longest Si–N bond in ($^{\pm H2}$BIP)SiCl$_2$, at 1.880 Å (compared to 1.790 Å for Si1–N1). This can be readily interpreted from the formal electronic structures shown in Figure 4.9, where the Si1–N2 bond is a dative bond, whereas the bonds to N1 and N3 are formal covalent bonds. Unsurprisingly, this also means that the Si1–N1 and Si1–N3 bonds are shorter than their equivalent bonds in (^{SiCl3}BIP)SiCl$_2$. Consistent with the bis(amino)pyridine structure drawn in Figure 4.9, the N1–C6 bond is significantly longer than the imine C=N bond in free BIP ligand[126] (1.423 Å and 1.27 Å respectively), indicating that this bond now only has a bond order of 1. The bis(amino)pyridine backbone is approximately planar, as with the bis(imino)pyridine backbone of (^{SiCl3}BIP)SiCl$_2$, and again Si1 sits slightly above (perspective

shown in Figure 4.8) this plane, with a dihedral angle N1–N3–N2–Si1 of 21.82 ° (compared to 12.1 ° for (^{SiCl3}BIP)SiCl$_2$). Unlike with (^{SiCl3}BIP)SiCl$_2$ however, Cl1 is also above this plane, with a dihedral angle N1–N3–N2–Cl1 of 11.58 ° (compared to -8.4 ° for (^{SiCl3}BIP)SiCl$_2$). This represents a distortion of the complex away from the square pyramidal arrangement in (^{SiCl3}BIP)SiCl$_2$ towards a more trigonal bipyramidal structure (with trigonal plane defined by N1, N3, Cl2), which can also be seen in the narrowing of the N1–Si1–N3 angle towards the ideal 120 ° for a trigonal bipyramidal complex (N1–Si1–N3 = 145.7 ° and 158.5 ° for ($^{±H2}$BIP)SiCl$_2$ and (^{SiCl3}BIP)SiCl$_2$ respectively). This distortion is likely being driven by the strengthening of the Si1–N1 and Si1–N3 bonds, as the stronger bond disfavours the placement of another substituent directly opposed to it due to the *trans*-influence.

$^{-H2}$BIP and $^{+H2}$BIP are formally the disproportionation products of BIP involving the transfer of two atoms of hydrogen (Figure 4.9). If this is process is occurring to (BIP)SiCl$_2$ in the reaction solution, it implies that (BIP)SiCl$_2$ is unstable under these conditions and may not be a readily isolable compound. In the case of (^{SiCl3}BIP)SiCl$_2$, it is possible that the presence of the SiCl$_3$ group disfavours the hydrogen elimination process, as the resulting sp^2 hybridisation of C7 would force the SiCl$_3$ group to move planar with the N1–C6–C1 plane, causing significant steric clash with either the pyridine ring or the adjacent Dipp group.

An alternative tridentate ligand 4,5-bis(diphenylphosphino)-9,9-dimethylxanthene (Xantphos) was found to not coordinate Si$_2$Cl$_6$ at room temperature. Instead, Si$_2$Cl$_6$ in the presence of Xantphos slowly decomposes it into SiCl$_4$ and an off-white precipitate presumed to be polymeric (SiCl$_2$)$_n$, with the Xantphos remaining unreacted (based on ^{1}H, ^{29}Si, ^{31}P NMR reaction monitoring). It was thus attempted to utilise this reactivity to catalyse the reaction of BIP with Si$_2$Cl$_6$ by using catalytic quantities (0.1 equivalents) of Xantphos to generate SiCl$_2$ *in-situ*, with the goal of removing the need to heat the reaction and thus improving its selectivity. Unfortunately, when BIP, Si$_2$Cl$_6$ and Xantphos were combined in C$_6$D$_6$ and monitored by NMR, no reaction of the BIP ligand was observed, and only the catalytic decomposition of Si$_2$Cl$_6$ occurred. Tertiary amines are known to catalytically induce the disproportionation of Si$_2$Cl$_6$,[127, 128] so the reaction of BIP with Si$_2$Cl$_6$ in the presence of diisopropylethylamine was also attempted, but similarly resulted in only Si$_2$Cl$_6$ decomposition with no significant reaction of BIP. Mixtures of tertiary amines and HSiCl$_3$ are

also known to be a method of generating *in-situ* $SiCl_2$,[44] however the combination of BIP, $HSiCl_3$ and diisopropylethylamine resulted in no significant reaction.

Given the apparent issue of isolating $(BIP)SiCl_2$, reaction of BIP directly with silicon azides was also investigated. BIP was found not to undergo any significant reaction with $Si(N_3)_4$ in a mixture of toluene and C_6D_6, even after heating at 100 °C for 6 days, analogous to the observation with $SiCl_4$. Curiously, after the sample was left in a sealed tube in the light for 2 days, it turned grey-green. The colour intensified after deliberate exposure to sunlight for 2 weeks, however no change was measured by NMR spectroscopy, so it is assumed the colour results from trace $Si(N_3)_4$ photolysis products reacting with BIP, with the bulk material remaining unreacted.

An attempt to react BIP with $HSi(N_3)_3$ was also conducted by addition of BIP to a hexane/C_6D_6 solution containing $HSi(N_3)_3$ and some residual aluminium chlorides. Unlike with $HSiCl_3$, reaction was observed without the need for heating. A ^{29}Si NMR spectrum recorded 1 hour after addition already shows significant disproportionation of $HSi(N_3)_3$ to $H_2Si(N_3)_2$ and $Si(N_3)_4$. After 1 day, the reaction solution was allowed to slowly evaporate, affording crystals that were identified by SCXRD to consist of a cationic silicon complex with a dimerised BIP ligand joined at the 4-position of the pyridine ring, with $AlCl_4^-$ as the counterion (Figure 4.10). This compound is referred to as $(H_2SiBIP)_2[AlCl_4]_2 \cdot 2(C_6D_6)$. It should be noted that the structure model for this compound could not be well refined (R_1 value = 17.55%). It is suspected that this poor structure refinement is due to unresolvable twinning in the crystals that were obtained.
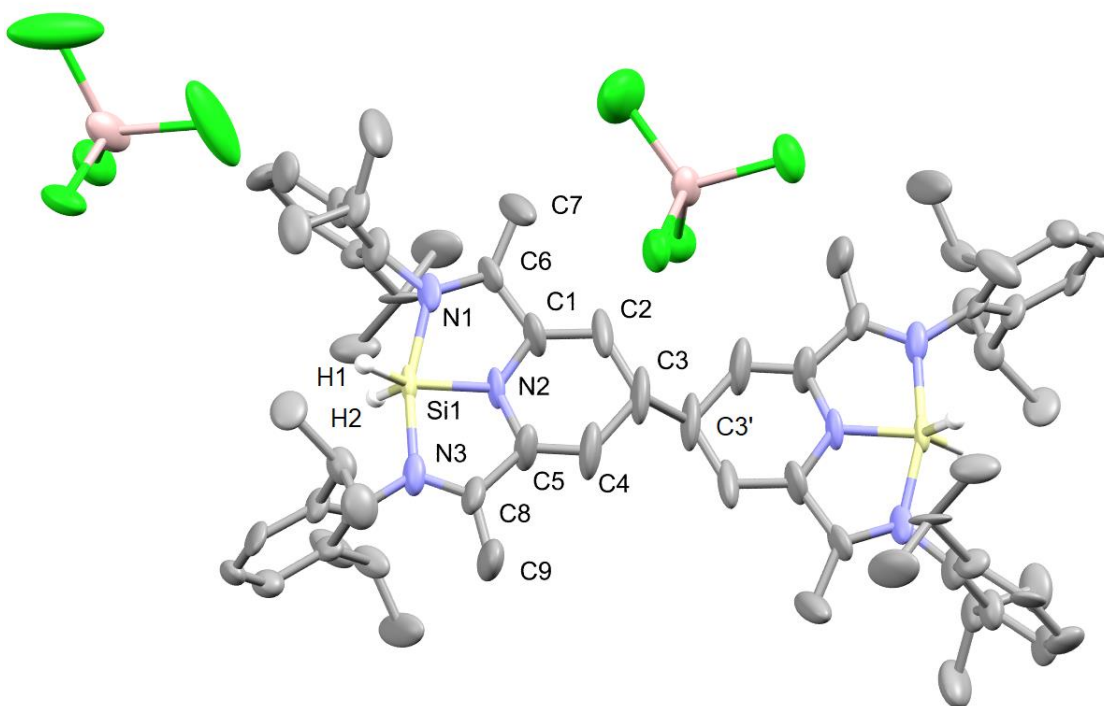
Figure 4.10. Thermal ellipsoid plot of $(H_2SiBIP)_2[AlCl_4]_2$. Ellipsoids at the 50% probability level. For clarity, C_6D_6 solvate molecules and hydrogen atoms have been omitted, except for hydrides bound to silicon. Hydrides are shown as spheres of fixed radius (0.2 Å). The $[(H_2SiBIP)_2]^{2+}$ ion has a centre of inversion at the midpoint of the C3–C3' bond. Selected bond lengths (Å) and angles (°): Si1–N1 1.933(15), Si1–N2 1.748(11), Si1–N3 1.959(15), Si1–H1 1.37(10), Si1–H2 1.38(10), N1–C6 1.27(2), N2–C1 1.32(2), N2–C5 1.45(2), N3–C8 1.29(2), C1–C2 1.36(2), C2–C3 1.49(3), C3–C4 1.53(3), C4–C5 1.30(2), C1–C6 1.56(2), C6–C7 1.41(2), C5–C8 1.44(2), C8–C9 1.47(3), C3–C3' 1.61(3), N1–Si1–N2 82.8(6), N2–Si1–N3 81.3(6), N1–Si1–N3 163.7(5).

The poor quality of the structure model for $(H_2SiBIP)_2[AlCl_4]_2$ prevents detailed structure analysis, as there is significant uncertainty in the bond lengths. There are, however, some noteworthy bond comparisons with statistically significant differences in length. The Si1–N2 bond is significantly shorter than the Si1–N1 and Si1–N3 bonds (1.748 Å, 1.933 Å, 1.959 Å respectively). This is the opposite arrangement to the structure of $(^{\pm H2}BIP)SiCl_2$, and indicates the Si1–N2 bond is a formal covalent bond while the Si1–N1 and Si1–N3 bonds are dative. This is reinforced by the short N1–C6 and N3–C8 bonds at 1.27 Å and 1.29 Å respectively, indicating they still retain the double bond character of free BIP ligand. Also of note is that the C1–C2 and C4–C5 bonds are significantly shorter than the C2–C3 and C3–C4 bonds (1.36 Å, 1.30 Å, 1.49 Å, 1.53 Å respectively). In addition to the tetrahedral geometry

around C3, this indicates that the "pyridine" ring is no longer aromatic and is instead an azacyclohexadiene ring.

The presence of two hydrido substituents on $[(H_2SiBIP)_2]^{2+}$ suggests that this product formed from reaction with $H_2Si(N_3)_2$ rather than $HSi(N_3)_3$. The mechanism of the oxidative dimerisation of the ligand unclear, but is presumably facilitated by decomposition of an azido group, thus the proposed formation and electronic structure of $[(H_2SiBIP)_2]^{2+}$ as shown in Figure 4.11. The $AlCl_4^-$ counterion is believed to be from the residual by-products left over after the synthesis of $HSi(N_3)_3$.
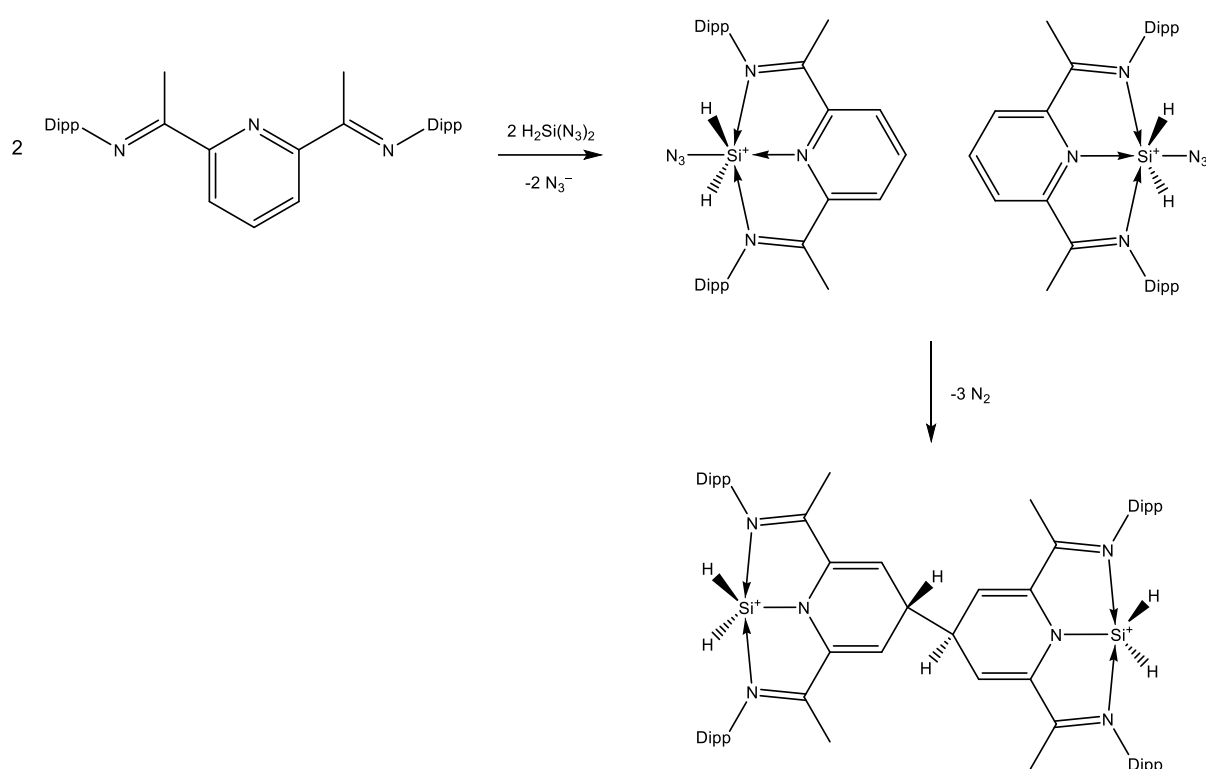
Figure 4.11. Proposed reaction to form $[(H_2SiBIP)_2]^{2+}$ from $H_2Si(N_3)_2$ and BIP.

Although the reactions of BIP with chloro/azido silanes have been shown to produce some interesting complexes, it is clear that BIP complexes of low-valent silicon suffer from chemical activation of the ligand. As an alternative, the commercially available ligand 2,2':6,2''-terpyridine was also tested for reaction with Si_2Cl_6, as it has a similar arrangement of coordinating nitrogen atoms. While this ligand may still suffer from activation of pyridine rings, it does at least lack the labile methyl hydrogens of BIP.

In sharp contrast to the chemistry of BIP, the addition of Si_2Cl_6 to a C_6D_6 solution of 2,2';6,2''-terpyridine (Terpy) results in a spontaneous reaction without the need for heating,

causing the solution to turn darken to near black immediately on addition. Over time, a black residue forms on the walls of the reaction vessel, which eventually grows into black crystals. These crystals were identified by SCXRD to contain a complex of $SiCl_2$ bound to a modified terpyridine ligand in which a hydrogen atom has been substituted by an $SiCl_3$ group, referred to as (^{SiCl3}Terpy)$SiCl_2$, shown in Figure 4.12.
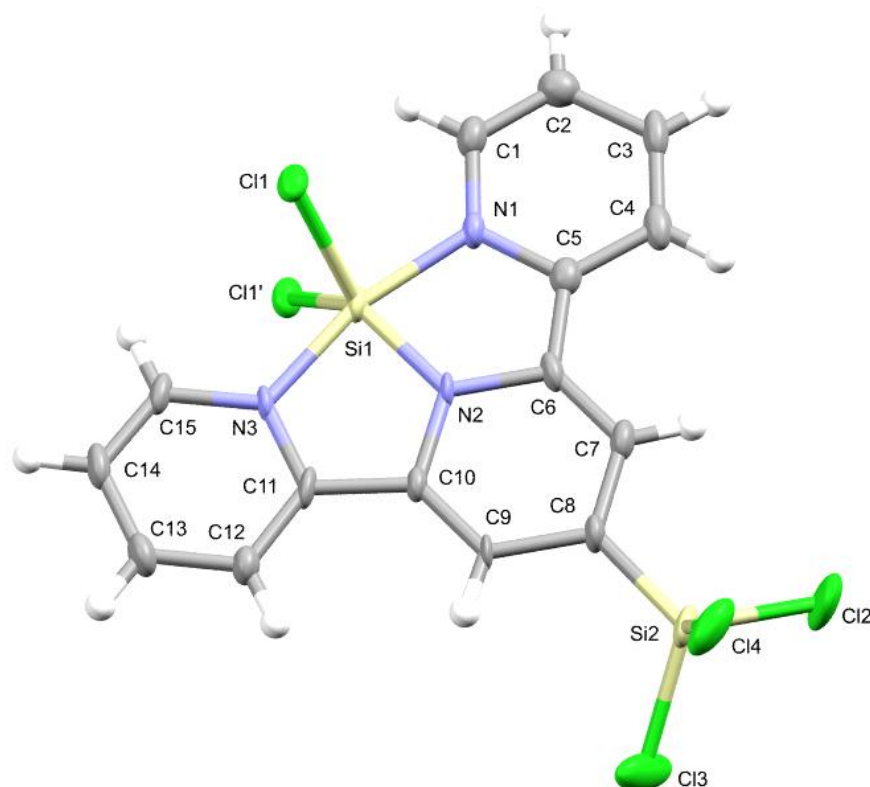
Figure 4.12. Thermal ellipsoid plot of one of the disorder components of (^{SiCl3}Terpy)$SiCl_2$. All H, C, N and Si atoms are in a symmetry plane. The disorder mirrors Cl2, Cl3, Cl4 in this plane. Ellipsoids at the 50% probability level, hydrogen atoms are shown as spheres of fixed radius (0.2 Å). Selected bond lengths (Å) and angles (°): Si1–N1 1.884(9), Si1–N2 1.707(9), Si1–N3 1.900(9), Si1–Cl1 2.099(2), Si2–C8 1.800(11), Si2–Cl2 2.038(5), Si2–Cl3 2.025(6), Si2–Cl4 2.033(5), **[Ring 1**: N1–C1 1.371(15), C1–C2 1.350(16), C2–C3 1.433(16), C3–C4 1.362(18), C4–C5 1.417(15), C5–N1 1.378(13), C5–C6 1.414(15)**]**, **[Ring 2**: N2–C6 1.412(12), C6–C7 1.355(15), C7–C8 1.425(15), C8–C9 1.450(12), C9–C10 1.345(15), C10–N2 1.443(13), C10–C11 1.440(13)**]**, **[Ring 3**: N3–C11 1.354(14), C11–C12 1.401(16), C12–C13 1.367(14), C13–C14 1.417(17), C14–C15 1.344(16), C15–N3 1.378(12)**]**, N1–Si1–N2 82.9(4), N2–Si1–N3 83.0(4), Cl1–Si1–Cl1' 104.24(15).

The coordination bond lengths around Si1 in (^{SiCl3}Terpy)SiCl$_2$ clearly indicates the presence of strong covalent bonds to N2 and Cl1. The Si1–N2 bond is the shortest Si–N bond of the compounds studied in this chapter, while the Si1–Cl1 bond is the second shortest Si–Cl bond of a pentacoordinate silicon centre in this chapter. By contrast, the Si1–N1 and Si1–N3 bonds are quite long, at 1.884 Å and 1.900 Å respectively, indicating that they are dative bonds rather than full covalent bonds. Despite this, they are shorter than other formally dative bonds of the BIP complexes described, aside from the Si1–N2 bond in ($^{±H2}$BIP)SiCl$_2$. The short bonds (for their type) to Si1 may indicate partial positive charge on the silicon atom, thus rendering it a stronger electron acceptor. The terpyridine framework shows clear localisation of π-bonds, with distinct bond length differences between formal single bonds (C–C > 1.41 Å) and formal double bonds (C–C < 1.38 Å). Curiously, C8 appears to only form single bonds, leaving it with only three formal covalent bonds. These observations thus point to (^{SiCl3}Terpy)SiCl$_2$ being best described by the formal zwitterionic structure shown in Figure 4.13, where the SiCl$_3$ group helps to stabilise the negative charge on C8, while the dative Si–N bonds stabilise the positive charge on Si1.
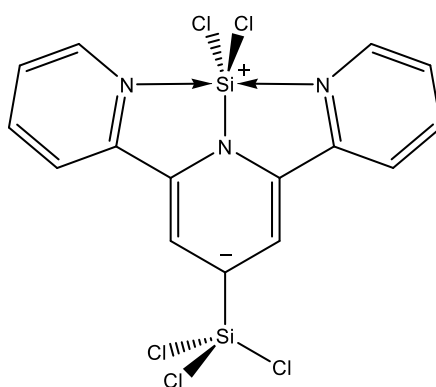
Figure 4.13. Formal structure best describing (^{SiCl3}Terpy)SiCl$_2$, based on the bond length data obtained from SCXRD.

It is likely that Terpy reacts with Si$_2$Cl$_6$ to initially form SiCl$_4$ and the intended complex (Terpy)SiCl$_2$. However, if this complex exhibits a similar electronic structure to (^{SiCl3}Terpy)SiCl$_2$, the resulting negative charge on the ligand pyridine rings would activate these rings towards an electrophilic substitution, which thus explains the observed substitution of a hydrogen atom for an SiCl$_3$ group on C8 based on the proposed reaction scheme in Figure 4.14.
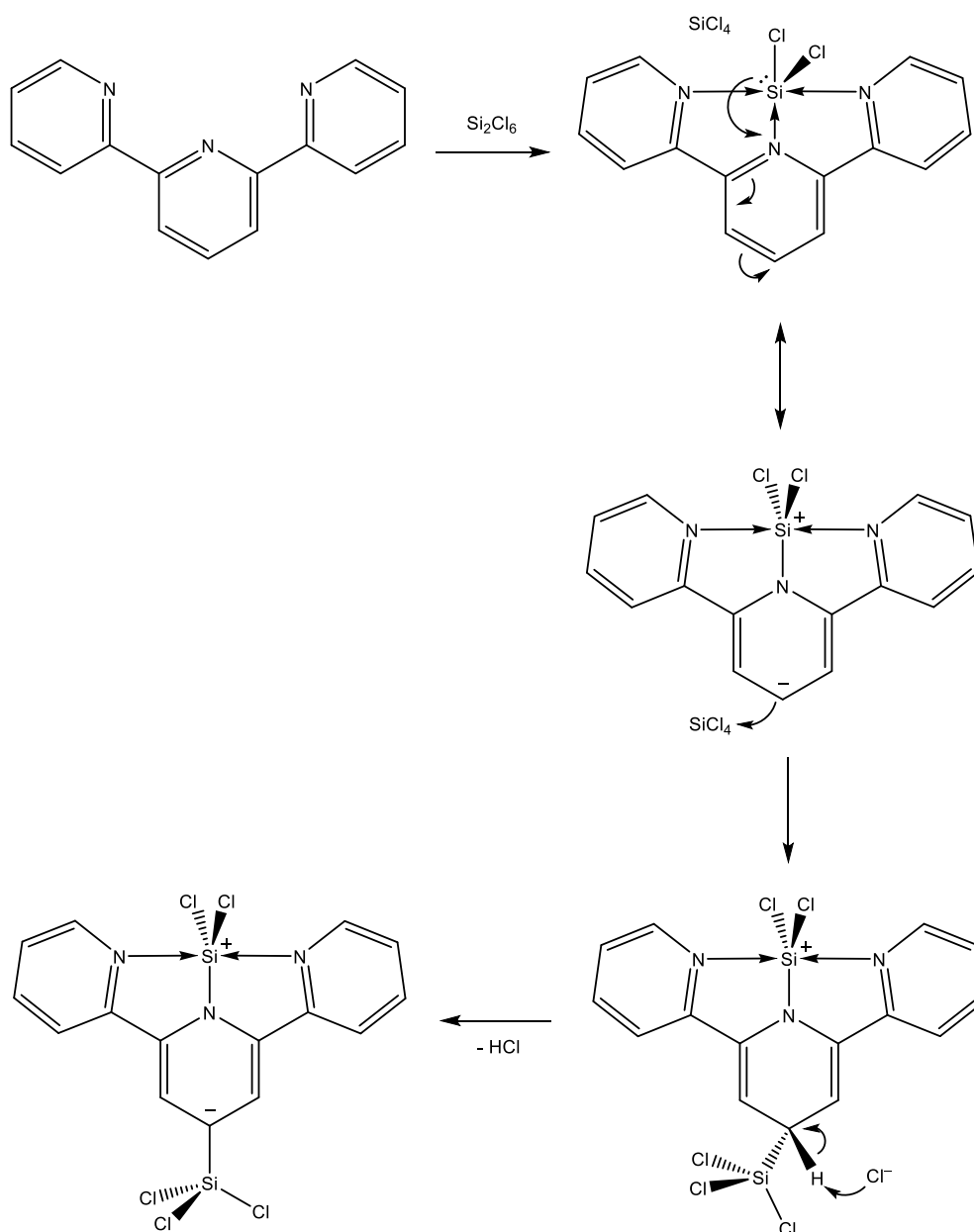
Figure 4.14. Proposed mechanism of formation of (^{SiCl3}Terpy)SiCl$_2$ from reaction of Terpy with Si$_2$Cl$_6$.

The proposed structure indicates Si1 is best described as a silicon(IV) cation. As such, it is not electronically analogous to silicon(II) compounds such as IPrSiCl$_2$. Importantly, it appears to lack the "inert pair" on the silicon atom, which would be expected to exert some degree of steric pressure on the coordination centre if it were present. Hence, (^{SiCl3}Terpy)SiCl$_2$ is not a suitable precursor for the synthesis of low-valent silicon(II) azides.

4.3. Conclusions

Attempting to use $NaAl(N_3)_4$ to convert $IPrSiCl_2$ to $IPrSi(N_3)_2$ results in the transfer of the IPr ligand, forming $IPrAl(N_3)_3$. This indicates that aluminium azides may be unsuitable azide transfer reagents for low-valent silicon chlorides due to the abstraction of ancillary ligands from the silicon. NMR analysis of the reaction between $IPrSiCl_2$ and $PPN(N_3)$ show that free IPr is the only major THF-soluble product of the reaction, further indicating that $IPrSiCl_2$ readily suffers from loss of IPr, thus destabilising any resulting low-valent product. Reaction of $IPrSi(N_3)_4$ with $(THF)_3LiSi(TMS)_3$ results in azido group decomposition as observed for other silicon azides in Chapters 2 and 3. Considering the numerous attempts to synthesise $IPrSi(N_3)_2$ to date, it seems likely that $IPrSi(N_3)_2$ is not a stable compound and is thus not a suitable target for a low-valent silicon azide.

The bis(imino)pyridine complex $(BIP)SiCl_2$ has been considered as a target compound as a more suitable precursor to a low-valent silicon azide than $IPrSiCl_2$. Attempts to synthesise $(BIP)SiCl_2$ resulted in numerous structures containing BIP structural elements bound to silicon, however in all cases modifications to the BIP ligand occurred. In two cases, this occurred with oxidation of the BIP ligand to either a bis(amino)pyridine ligand or a bis(imino)amine ligand, resulting in a complex that no longer contains low-valent silicon. In one case, the modification of the ligand involved the substitution of a methyl hydrogen atom for a trichlorosilyl group, with the remainder of the ligand being unchanged, thus this complex, $(^{SiCl3}BIP)SiCl_2$ represents the first complex of a bis(imino)pyridine ligand with silicon. Although this complex is a low-valent silicon chloride, it was not produced in sufficient quantities for investigating its reaction with azide. Thus, while the formation of bis(imino)pyridine adducts of $SiCl_2$ is demonstrated, a more selective synthesis will need to be identified in order to use these complexes as precursors to low-valent silicon azides. The reaction of an alternative ligand with similar electronic structure, 2,2':6,2''-terpyridine, was also tested with Si_2Cl_6 as this ligand lacks the active methyl groups. Unlike with the reaction between Si_2Cl_6 and BIP, this reaction occurs at room temperature. Unfortunately, the terpyridine ligand also suffers from ligand modification during reaction with Si_2Cl_6, affording the complex $(^{SiCl3}Terpy)SiCl_2$, which adopts a structure that indicates the transfer of an electron from the silicon to the ligand. This electron transfer means the silicon atom is formally a silicon(IV) cation, so $(^{SiCl3}Terpy)SiCl_2$ is not a silicon(II) complex. For the isolation of

bis(imino)pyridine or terpyridine complexes of divalent silicon, a ligand would need to be synthesised where the activation-prone hydrogen atoms are replaced with inert alkyl groups, with an example shown in Figure 4.15.
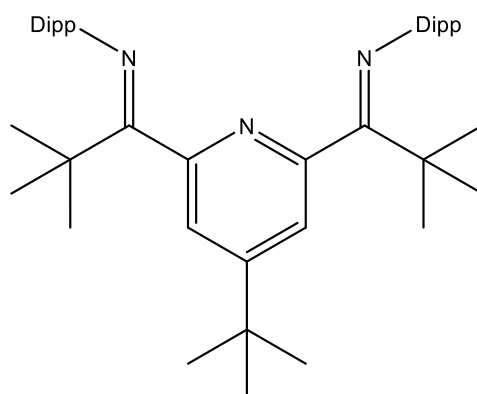
Figure 4.15. A bis(imino)pyridine ligand with tert-butyl substituents in the locations where activation has been observed.

5. Reactivity of hexachlorodisilane (Si$_2$Cl$_6$) and the formation trichlorosilanide (SiCl$_3^-$)

5.1. Introduction

Si$_2$Cl$_6$ has been known since the 1870s, formed from reaction of SiCl$_4$ with elemental silicon and as a by-product of the synthesis of SiCl$_4$ from the reaction of silicides with chlorine.[129-131] Although originally of academic interest only, it has since found potential application as a reducing agent[132] and as a feedstock in chemical vapour deposition of silicon-containing materials,[133] including a synthesis of Si$_3$N$_4$ from NH$_3$ and Si$_2$Cl$_6$.[134] In recent decades, Si$_2$Cl$_6$ has gained considerable interest as a precursor to low-valent and reduced chloro-silicon compounds.[33, 44] Si$_2$Cl$_6$ serves as an alternative precursor to HSiCl$_3$ in the synthesis of IPrSiCl$_2$ and (^{tBu}NCN)SiCl,[124] and can also be used to synthesise various other perchlorosilanes. These include oligomers of SiCl$_2$,[135] which have themselves been shown to act as an SiCl$_2$ source for the synthesis of IPrSiCl$_2$ (Figure 5.1).[136]
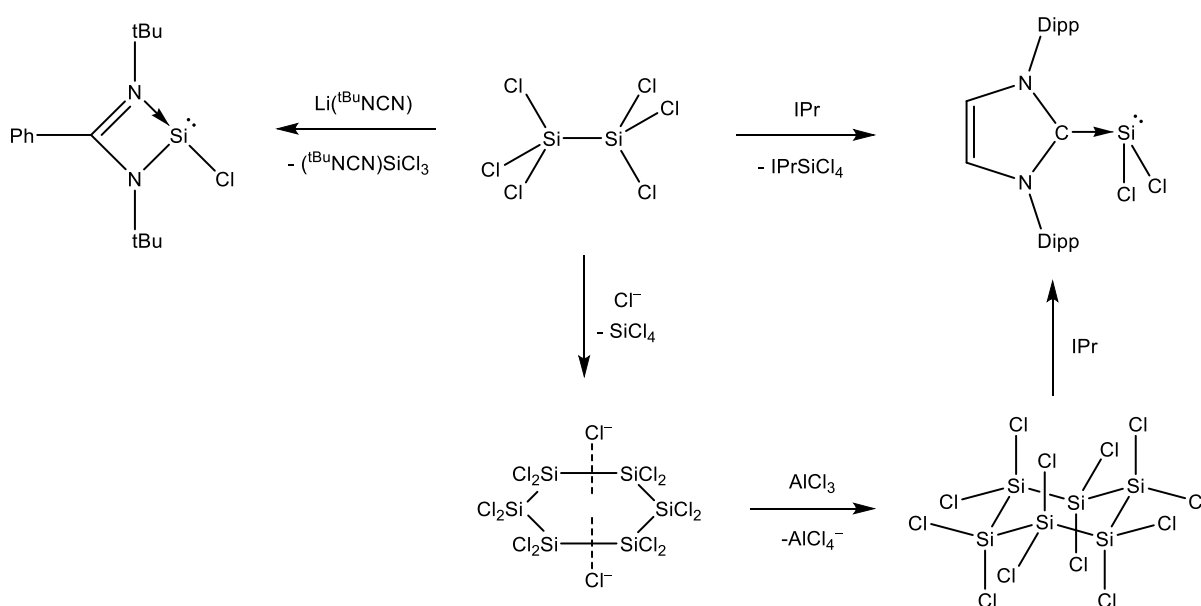
Figure 5.1. Conversion of Si$_2$Cl$_6$ to low-valent silicon chloride complexes, both directly and *via* (SiCl$_2$)$_6$.

The conversion of Si_2Cl_6 to other chlorosilane species, including $[Si_6Cl_{14}]^{2-}$ shown on Figure 5.1, is predicted to proceed via the trichlorosilanide ion ($SiCl_3^-$) as an intermediate.[135] No salt of $SiCl_3^-$ has ever been isolated, but its existence in solution from the deprotonation of $HSiCl_3$ has been inferred by both NMR exchange experiments[137] and chemical tests[138] (Figure 5.2).
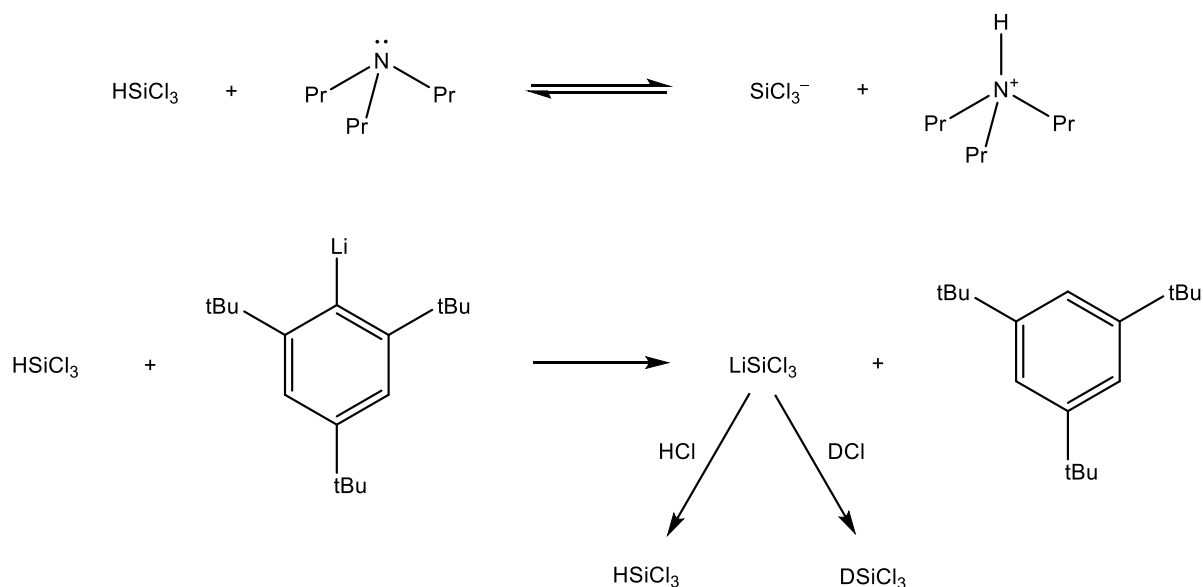
Figure 5.2. Deprotonation of $HSiCl_3$ by NPr_3 and 2,4,6-tri(tert-butyl)phenyllithium (Mes*Li).

The analogous anions $GeCl_3^-$ and $SnCl_3^-$ are isolable, formed by addition of Cl^- to MCl_2(dioxane) (M = Ge, Sn). These can then be readily converted to the low-valent anions $M(N_3)_3^-$ on treatment with NaN_3.[139, 140] Salts of both of these ions are readily isolated, and are stable without the need for large coordinating ligands. This stabilisation is likely due to coulombic repulsion disfavouring dimerisation reactions. For the same reason, the analogous $Si(N_3)_3^-$ ion may also have isolable salts. Neither $SiCl_2$(dioxane) nor $SiCl_3^-$ are available as isolated materials, so a suitable synthesis of $SiCl_3^-$ needs to be identified, ideally with isolation. If $SiCl_3^-$ is to be used *in-situ*, it must be free of any neutral silicon chlorides, as treatment of these with NaN_3 would form neutral silicon azides that would be attacked by $Si(N_3)_3^-$, based on the chemistry of $Si(TMS)_3^-$ observed in Chapters 2 and 3. Other species that would likely react with silanides must also be absent from the solution if $Si(N_3)_3^-$ is to be synthesised.

5.2. Results and discussion

Since Si_2Cl_6 is a useful source of *in-situ* $SiCl_2$ for base-stabilised complexes, the unknown compound $Si_2(N_3)_6$ would theoretically be a source of *in-situ* $Si(N_3)_2$. The reaction of Si_2Cl_6 with Na(15-crown-5)N_3 in THF resulted in bubbling, and after stirring for 3 days, no signals were detected in ^{14}N or ^{29}Si NMR spectra of the solution. This indicates that $Si_2(N_3)_6$ was not formed. Si_2Cl_6 undergoes disproportionation reactions in the presence of chloride ions as well as nucleophilic amines.[44] It is likely that this also occurs in the presence of azide ions due to their nucleophilicity, posing an issue for the formation of $Si_2(N_3)_6$. When Si_2Cl_6 is instead reacted with NaAl$(N_3)_4$(THF)$_4$ in C_6D_6, based on the synthesis of $HSi(N_3)_3$, even more vigorous bubbling is observed, clearly indicating the decomposition of azido groups. The ^{29}Si NMR spectrum of this solution shows $Si(N_3)_4$ as a major product in solution, providing evidence for the disproportionation of Si_2Cl_6 to release $SiCl_4$, which then converts to $Si(N_3)_4$ by reaction with NaAl$(N_3)_4$(THF)$_4$. A strong broad signal (-31 to -96 ppm), distinct from the glass background, is also observed in this spectrum, which may indicate the formation of a polymeric silicon product in solution. $Si(N_3)_4$ is again the dominant product observed by ^{29}Si NMR when the reaction is conducted in THF, where the NaAl$(N_3)_4$ is more soluble. Two broad ^{29}Si NMR signals are also observed from this reaction mixture (-51 to -52 ppm and -57 to -60 ppm), however they are much weaker and narrower than the signal observed from the reaction in C_6D_6. The detection of signals attributable to $Si(N_3)_3Cl$ and $Si(N_3)_2Cl_2$ in the C_6D_6 reaction suggest that disproportionation of Si_2Cl_6 occurs before the transfer of azido groups is complete. Figure 5.3 illustrates the expected course of reaction if disproportionation occurs completely before azide transfer.

$$Si_2Cl_6 \xrightarrow[\text{disproportionation}]{\text{catalytic}} SiCl_2 \quad + \quad SiCl_4$$

(with $SiCl_2 \xrightarrow{NaAl(N_3)_4} Si(N_3)_2$ and $SiCl_4 \xrightarrow{NaAl(N_3)_4} Si(N_3)_4$; $Si(N_3)_2 \xrightarrow{\text{decomposition}} N_2 + \text{unknown}$)
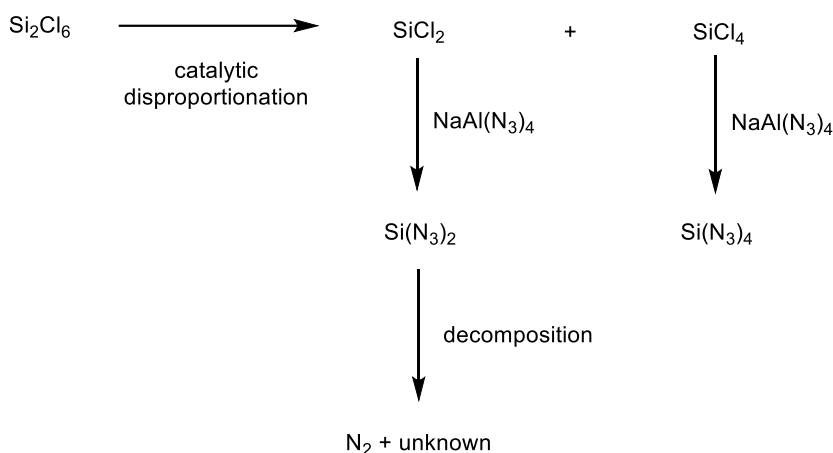
Figure 5.3. Hypothesised reaction of Si_2Cl_6 based on the observed formation of $Si(N_3)_4$ and N_2.

The ^{14}N and ^{29}Si NMR spectra show additional minor signals in the proximity of those of $Si(N_3)_4$. Given the similar chemical shift to $Si(N_3)_4$, these are likely to result from tetravalent silicon species rather than low-valent species and may perhaps be the result of reaction between low-valent silicon products and $Si(N_3)_4$.

As a less nucleophilic azide transfer reagent, the reaction of $TMS(N_3)$ with Si_2Cl_6 was also tested. This reaction was found to be extremely slow, as even after 3 months at room temperature the majority of the Si_2Cl_6 remained unreacted. Similar to the reaction with $NaAl(N_3)_4(THF)_4$, the dominant product detected by ^{29}Si NMR was $Si(N_3)_4$ indicating that disproportionation reactions still occur even with $TMS(N_3)$. An early [29]Si spectrum recorded 3 days into the reaction shows the presence of $SiCl_4$, confirming that disproportionation of Si_2Cl_6 begins before exchange of chloride for azide. As such, it does not appear to be possible to synthesise $Si_2(N_3)_6$ by treating Si_2Cl_6 with known azide transfer reagents.

$SiCl_3^-$ was thus targeted as a precursor for the azidosilanide $Si(N_3)_3^-$. The reported synthesis of $SiCl_3^-$ from $HSiCl_3$ and 2,4,6-tri(tert-butyl)phenyllithium (Mes*Li) in THF[138] was repeated to obtain ^{29}Si NMR data with a more modern spectrometer. Thus, to a slightly impure sample of Mes*Li, a slight excess of $HSiCl_3$ was added. The resulting solution gave rise to three major environments in the ^{29}Si NMR spectrum (in THF, with d6-DMSO capillary for locking) δ/ppm = +29.6 (s), -9.9 (d, $^1J_{Si-H}$ = 381 Hz, $HSiCl_3$), -18.1 (t, $^1J_{Si-H}$ = 312 Hz, H_2SiCl_2). Minor singlet signals are also observed at -39.3 ppm and -138.6 ppm. The signal at +29.6 is most likely $LiSiCl_3$ (lit. +30.9 in THF/Et$_2$O).[138] It is unclear why this reaction produces H_2SiCl_2; this may be due to unknown impurities in the Mes*Li, but it is also possible for this to be a

side product of the reaction. The previous report claims only approximately 50% conversion of $HSiCl_3$ to $LiSiCl_3$ (based on the quantity of $DSiCl_3$ formed by treating the product with DCl), so it is evident that this reaction is not suitable for preparing high purity solutions containing $SiCl_3^-$.

In an attempt to synthesise $Si(N_3)_3^-$ directly, Mes*Li was added at -40 °C to a hexane solution containing a 1:1 mixture of $HSi(N_3)_2Cl$ and $HSi(N_3)_3$. Based on the literature reaction of Mes*Li with $HSiCl_3$, reaction with these species is expected to afford $LiSi(N_3)_2Cl$ and $LiSi(N_3)_3$ respectively. After warming up to room temperature, NMR analysis of the reaction solution shows no evidence of these two species. The only two species detectable by ^{29}Si NMR are both proton-containing: δ/ppm = -37.9 (d, $^1J_{Si-H}$ = 263 Hz), -40.8 (t, $^1J_{Si-H}$ = 228 Hz). Both environments can be matched to proton environments with the same $^1J_{Si-H}$ coupling constants at 5.54 ppm and 5.20 ppm respectively, and a respective ^1H integral ratio of 1 : 0.74. Neither ^{29}Si environment is in the range expected for hypercoordinate complexes, so it is clear from the Si-H coupling pattern that these two major products of this reaction are compounds of the form $HSiX_3$ and H_2SiX_2 (where X is unknown). Neither compound matches the observed coupling constant values for the azidosilanes in Chapter 2.2.1, meaning at least one substituent on the silicon must not be H, N_3 or Cl. Relative to the silanes from Chapter 2.2.1, both observed products have low Si-H coupling constant values for their respective series ($HSiX_3$ and H_2SiX_2), indicating a weaker Si-H interaction, which would be caused by the presence of a strongly donating substituent. It is interesting to note that there is only one product of each of the series $HSiX_3$ and H_2SiX_2 despite the reaction starting with a mixture of $HSi(N_3)_2Cl$ and $HSi(N_3)_3$. These observations are all consistent with the dominant product in solution being $HSi(N_3)_2Mes*$, which can form according to the reaction shown in Figure 5.4.
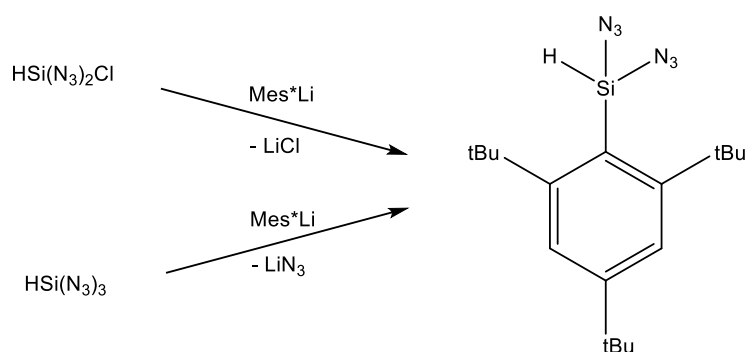
Figure 5.4. Formation of HSi(N$_3$)$_2$Mes* from both HSi(N$_3$)$_2$Cl and HSi(N$_3$)$_3$.

By extension, the compound of the form H$_2$SiX$_2$ is likely to be H$_2$Si(N$_3$)Mes*. The ^{1}H integral values for the two dominant aromatic environments is also consistent with this hypothesis, with both the aromatic and Si−H signals agreeing on an HSi(N$_3$)$_2$Mes* : H$_2$Si(N$_3$)Mes* ratio of 1 : 0.4. Considering the observed tendency of HSi(N$_3$)$_3$ to undergo disproportionation to H$_2$Si(N$_3$)$_2$ and Si(N$_3$)$_4$ (Chapter 2.2.1), the formation of H$_2$Si(N$_3$)Mes* can be readily attributed to the disproportionation of HSi(N$_3$)$_3$ prior to reaction with Mes*Li, or reaction of HSi(N$_3$)$_3$ with HSi(N$_3$)$_2$Mes*. In both cases, however, Si(N$_3$)$_4$ must be formed, which is not observed. When the filtered reaction solution was allowed to slowly evaporate over the course of a week, crystals of (Mes*)N=N(Mes*) were observed (Figure 5.5). The mechanism of (Mes*)N=N(Mes*) formation is unclear, but since the only source of nitrogen atoms in the reaction solution are azido groups, it is reasonable to assume that the initial step towards (Mes*)N=N(Mes*) formation involves the attack of an azido group by Mes*Li. This could explain the apparent absence of Si(N$_3$)$_4$. The silicon atom of Si(N$_3$)$_4$ is more sterically protected than in hydridosilanes, so it may be that Si(N$_3$)$_4$ preferentially undergoes attack of an azide by Mes*Li, rather than substitution at the silicon centre. A hypothesised overall reaction scheme that satisfies these observations is thus shown in Figure 5.6.

116
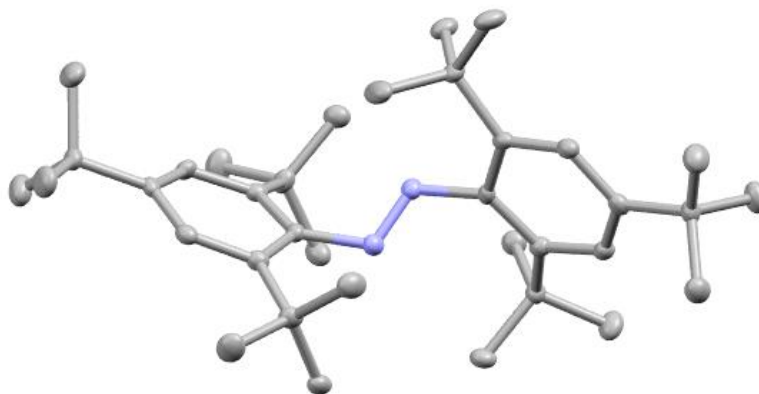
Figure 5.5. Thermal ellipsoid plot of (Mes*)N=N(Mes*) obtained in this work. Ellipsoids at the 50% probability level, hydrogen atoms are omitted for clarity. Note that this structure has already been reported prior to this work.[141]
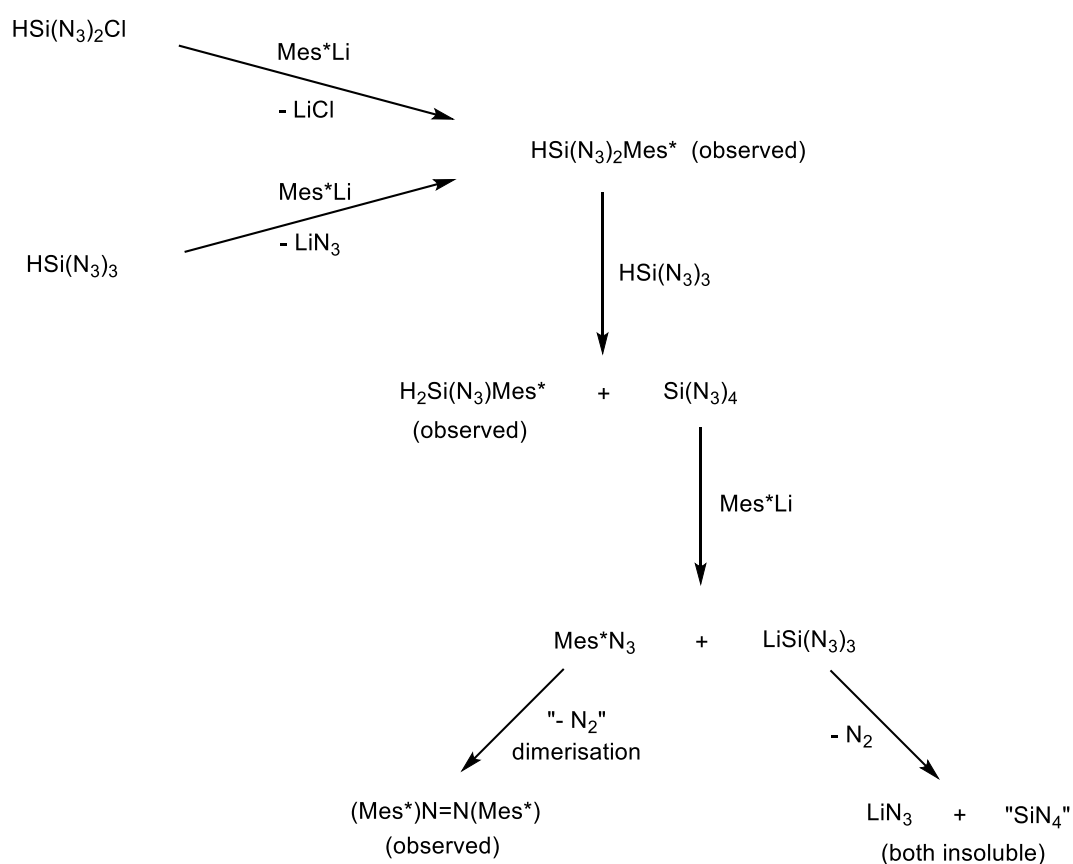
Figure 5.6. Hypothesised reaction scheme, based on observed products, from addition of Mes*Li to a mixture of $HSi(N_3)_2Cl$ and $HSi(N_3)_3$.

The proposed scheme in Figure 5.6 also explains the previously observed formation of H_2SiCl_2 from the addition of Mes*Li to $HSiCl_3$. Disproportionation of $HSiCl_3$ to H_2SiCl_2 and $SiCl_4$ was previously ruled out due to the absence of $SiCl_4$, however if $SiCl_4$ undergoes an analogous reaction to the one proposed for $Si(N_3)_4$ in Figure 5.6, then the observed product would instead be $LiSiCl_3$, which is present regardless due to the intended reaction of $HSiCl_3$ with Mes*Li. For the reaction with $HSi(N_3)_3$, the absence of the analogous $LiSi(N_3)_3$ may be attributed to decomposition with loss of LiN_3 and N_2. This decomposition may be facilitated by the solvent, as hexane does not effectively stabilise charged species in solution. Unfortunately, hexane is the only solvent in which $HSi(N_3)_3$ can be isolated without significant disproportionation, so an alternative method to synthesise $Si(N_3)_3{}^-$ needs to be considered.

The generation of $SiCl_3{}^-$ *in-situ* from Si_2Cl_6 and nucleophiles is proposed in the literature,[44] so the reaction of Si_2Cl_6 with various nucleophiles was tested and monitored by ^{29}Si NMR spectroscopy to determine suitable conditions for isolating $SiCl_3{}^-$, as summarised in Table 5.1.

Reagent	Solvent	Time of analysis (after reaction start) / h	SiCl$_3^-$ (+29.6 ppm)	Si$_2$Cl$_6$ (-5.9 ppm)	SiCl$_4$ (-18.9 ppm)	Nu–SiCl$_3$	Unknown (-138.7 ppm)	Other unknown(s)
tBuLi (1.7 M in hexane)	THF	0 – 15	1	–	0.99	0.06 (-96.1 ppm)	0.16	none
PPh$_4$Cl	CD$_2$Cl$_2$	2 – 3	1	–	1.50	[SiCl$_4$]	0.16	0.18 (+0.3 ppm) 0.04 (-125.6 ppm)
KTp*	THF	0 – 2	1	–	1.25	0.33 (-186.7 ppm)	0.19	0.30 (-65.8 ppm)
(THF)$_3$LiSi(TMS)$_3$	C$_6$D$_6$	0 – 15	1	–	2.08	?	–	see discussion
LiN(TMS)$_2$	THF	2 – 17	1	–	–	1.19 (-27.9 ppm)	0.19	0.13 (+1.5 ppm)
LiN(TMS)$_2$	THF (-15 °C)	1 – 8	1	–	–	1.08 (-28.4 ppm)	0.14	–
LiN(TMS)$_2$	DME	0 – 2	1	–	–	0.69 (-27.5 ppm)	0.11	0.20 (+2.8 ppm) 0.24 (+2.1 ppm)
K(18c6)OtBu	Toluene	7 – 18	1	–	6.76	3.40 (-49.4 ppm)	–	–
K(18c6)OtBu	DME	9 – 16	1	–	1.34	0.48 (-49.8 ppm)	0.15	0.09 (-72.9 ppm) 0.13 (-74.2 ppm) 0.13 (-77.7 ppm)

Table 5.1. Relative ^{29}Si NMR integrals of Si$_2$Cl$_6$, SiCl$_4$, Nu–SiCl$_3$ (Nu = nucleophile) and unidentified species, compared against the signal of SiCl$_3^-$, after addition of nucleophiles to Si$_2$Cl$_6$. All spectra were recorded using an interval of 10 seconds between scans (note that this scan frequency is too high for absolute quantitative analysis; these integrals are only used to compare these reactions with respect to each other). KTp* = potassium tris-(3,5-dimethylpyrazolyl)borate.

In all reactions tested, Si_2Cl_6 was consumed by the time of analysis. The low sensitivity of ^{29}Si prevents the acquisition of rapid spectra to observe the decay of Si_2Cl_6, however $SiCl_3^-$ exhibits sufficient stability in these solvents for this to not pose an issue for observing the products of reaction. Figure 5.7 outlines some plausible routes of reaction and their expected products.

$$Nu^- + Cl_3Si\!-\!SiCl_3 \longrightarrow Nu\!-\!SiCl_3 + SiCl_3^-$$

$$SiCl_3^- \longrightarrow \overset{..}{S}iCl_2 + Cl^-$$

$$\overset{..}{S}iCl_2 \longrightarrow polymerises$$

$$\underset{Nu}{\overset{Cl_2}{\underset{\diagdown}{\overset{Si}{\diagup}}}}\!SiCl_3 + Cl^- \longrightarrow Nu\!-\!\overset{-}{S}iCl_2 + SiCl_4$$

$$Nu\!-\!\overset{..}{S}iCl + Cl^-$$

$$polymerises$$
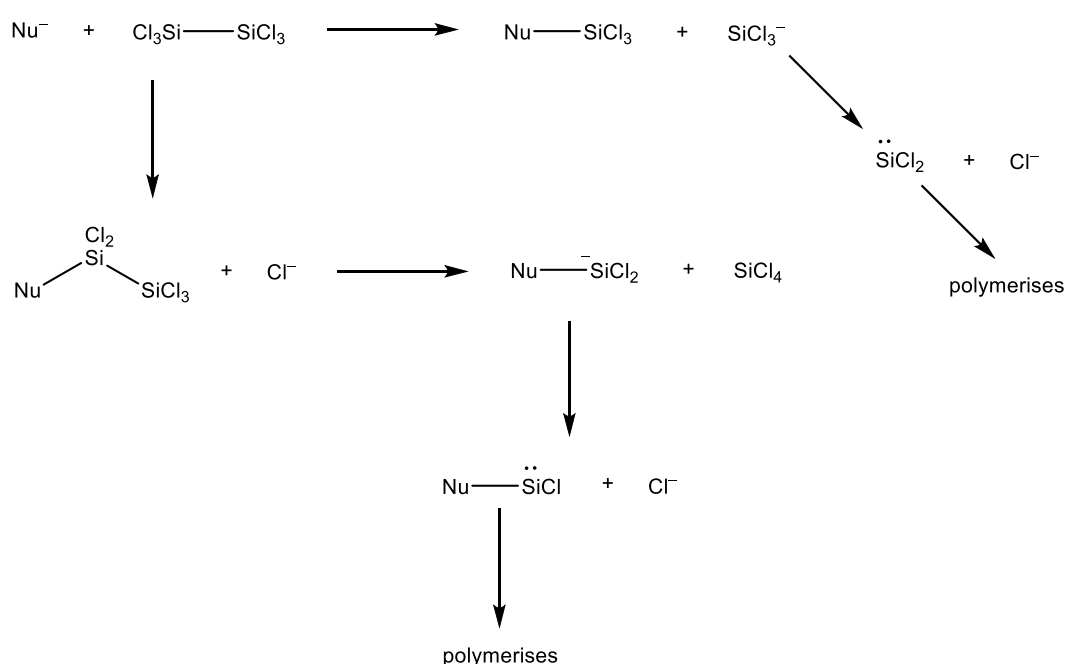
Figure 5.7. Possible products and intermediates from reaction of Si_2Cl_6 with an anionic nucleophile Nu^-.

Regardless of the Nu-containing product formed, the formation of $SiCl_4$ is an indication of an undesired reaction pathway (with exception of $Nu^- = Cl^-$). Hence, some insight into reaction selectivity can be gained from comparing the relative ratio of $SiCl_3^-$: $SiCl_4$ formed in each reaction. The reaction of Si_2Cl_6 with K(18c6)OtBu in toluene produced very little $SiCl_3^-$, while the same reaction in DME produced comparable quantities of $SiCl_3^-$ and $SiCl_4$. It is likely that the more polar ethereal solvent helps stabilise the $SiCl_3^-$ ion. $SiCl_3^-$ has been found to have negligible decomposition in dilute THF or DME over multiple days. This is in contrast to a previously reported half-life for $SiCl_3^-$ in THF of 62 hours.[138] This discrepancy may be due to the effect of other compounds present in solution, as the previously-reported value is from a crude reaction mixture where $LiSiCl_3$ was synthesised from $SiCl_3Br$ and 2,4,6-tri(tert-butyl)phenyllithium, as opposed to the reaction of Si_2Cl_6 with nucleophiles used in this work.

The reaction of Si_2Cl_6 with $(THF)_3LiSi(TMS)_3$ in C_6D_6 was found to deviate from the behaviour of other reactions tested. In this reaction, both $SiCl_3^-$ and $SiCl_4$ were formed in only trace quantities. This suggests the reaction only underwent substitution reactions, with elimination of chloride ions and no significant formation of low-valent silicon species. This reaction solution was dried and the solid recrystallised in hexane, affording crystals of the previously-unknown compound 1,1,1,4,4,4-hexakis(trimethylsilyl)-2,2,3,3-tetrachlorotetrasilane (HTTCT, Figure 5.8).
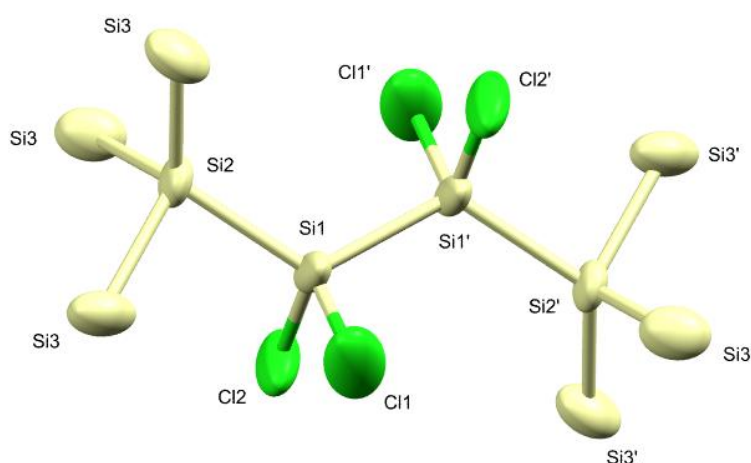
Figure 5.8. Thermal ellipsoid plot of hexakis(trimethylsilyl)tetrachlorotetrasilane (HTTCT). Ellipsoids at the 50% probability level, hydrogen and carbon atoms are omitted for clarity. Note that due to three-fold rotational disorder, all trimethylsilyl groups (Si3) are equivalent. Selected bond lengths (Å) and angles (°): Si1–Si1' 2.353(11), Si1–Si2 2.392(6), Si2–Si3 2.362(3), Si1–Cl1 2.025(11), Si1–Cl2 2.191(11), Si1'–Si1–Si2 119.8(4), Cl1–Si1–Cl2 104.6(5).

An analogous structure to HTTCT with methyl groups in place of chlorines, 1,1,1,4,4,4-hexakis(trimethylsilyl)-2,2,3,3-tetramethyltetrasilane (HTTMT) is known to the literature.[142] In HTTMT, the bond analogous to Si1–Si1' is the longest Si–Si bond, at 2.374 Å. By contrast, Si1–Si1' is the shortest Si–Si bond in HTTCT. This may be a result of the more labile chloro substituents producing longer bonds to Si1 than the analogous methyl groups, thus allowing for greater *s*-orbital character in the Si–Si bonds, resulting in a stronger Si1–Si1' bond. However, the Si1–Si2 bond is the longest of any Si–Si bond in either molecule, at 2.392 Å. This elongated bond may be the result of steric repulsion between the chloro groups of Si1 and the trimethylsilyl groups of Si2. The structure of HTTMT does not experience the three-fold rotational disorder in HTTCT, and thus has distinct trimethylsilyl groups which bond to the tetrasilane motif with Si–Si bonds ranging from 2.347 Å to 2.360 Å. The Si2–Si3 bond in

HTTCT is on the longer end of this range at 2.362 Å, but is sufficiently similar that the bonding of the trimethylsilyl groups can be considered the same between the two species.

In DME and THF, the reaction of Si_2Cl_6 with $LiN(TMS)_2$ proceeds with remarkable selectivity, resulting in no detectable $SiCl_4$. The only signals detected in ^{29}Si NMR other than $SiCl_3^-$ correspond to $(TMS)_2N–SiCl_3$ (by comparison to a genuine sample) and an unknown compound with a signal at -138.7 ppm. This compound is detected in every solution containing $SiCl_3^-$ except in cases where the signal of $SiCl_3^-$ is extremely weak. The product appears to have a fixed ratio of approximately 0.15 times the integral of $SiCl_3^-$, thus it is likely that this is a compound in equilibrium with $SiCl_3^-$. Given that it appears at the same chemical shift in both DME and THF, the nature of the compound is independent of solvent. It also appears in the solution of $SiCl_3^-$ generated from $HSiCl_3$ with Mes*Li, indicating its formation does not require the presence of Si_2Cl_6. The highly negative chemical shift may be indicative of hypercoordinate silicon species, or silyl-silanides. A possible candidate for the identity of this compound is $[Si_2Cl_5]^-$, where both silicon atoms appear at the same chemical shift due to rapid exchange of substituents (Figure 5.9).
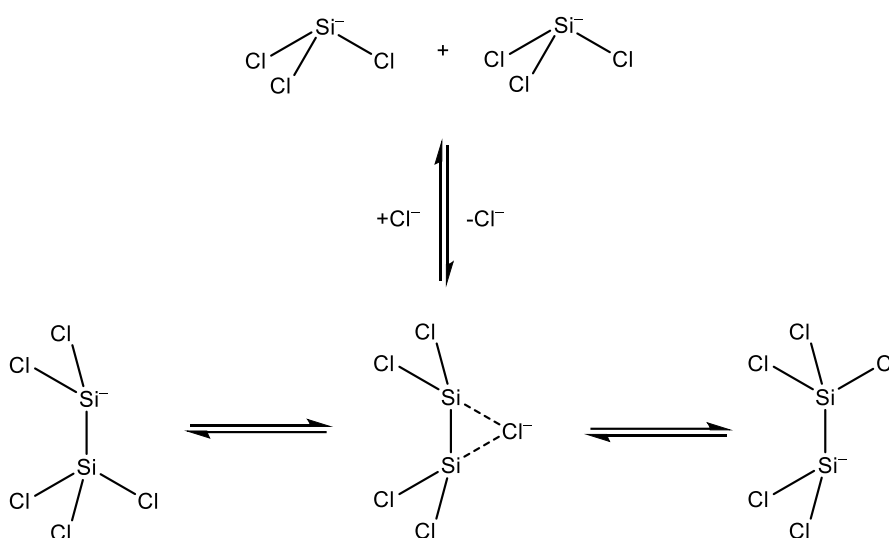
Figure 5.9. Proposed structures of $[Si_2Cl_5]^-$ and equilibrium with $SiCl_3^-$.

If the signal at -138.7 ppm is assumed to be an equilibrium species with $SiCl_3^-$, then the reaction of Si_2Cl_6 with $LiN(TMS)_2$ in ethereal solvents provides a facile route to selective formation of $SiCl_3^-$. Unfortunately, the presence of $(TMS)_2N–SiCl_3$ formed in this reaction is problematic for azide exchange reactions as described in Chapter 5.1 – addition of an azide reagent would convert $(TMS)_2N–SiCl_3$ into $(TMS)_2N–Si(N_3)_3$, which would likely react with any silanides formed from $SiCl_3^-$. Concentration of the solutions results in decomposition of the $SiCl_3^-$ to release LiCl and amorphous residues (presumed to be polymeric $SiCl_2$). In the case where the solvent used was DME, the LiCl crystallised as a previously unreported solvate $Li_2Cl_2(DME)$, exhibiting an unusual ladder polymer structure (Figure 5.10).
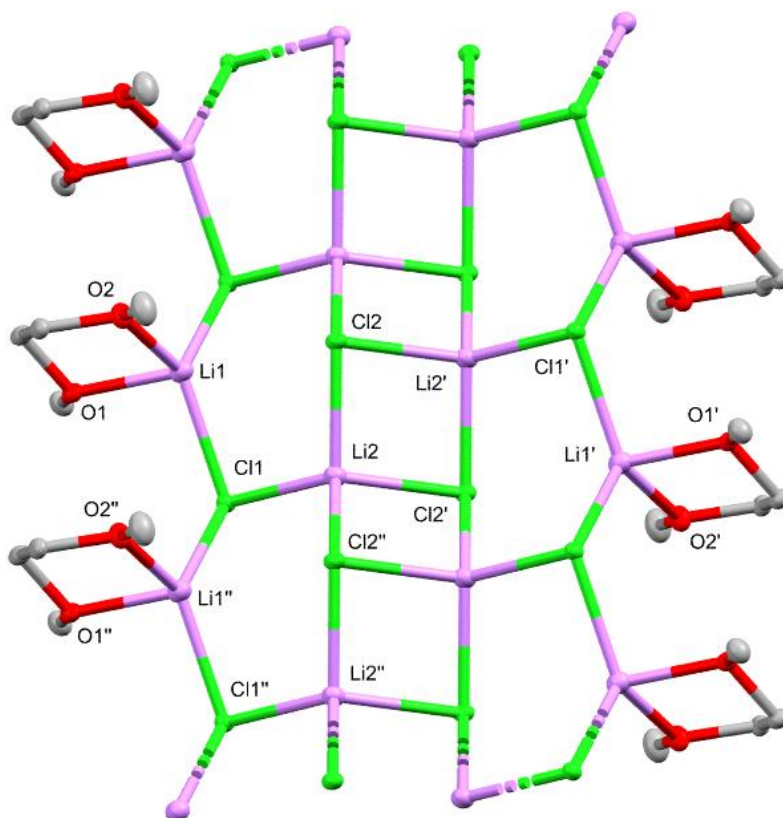
Figure 5.10. Thermal ellipsoid plot of a section of $Li_2Cl_2(DME)$ polymer, displaying six asymmetric units. Ellipsoids at the 50% probability level, hydrogen atoms are omitted for clarity. Selected bond lengths (Å) and angles (°): Li1–Cl1 2.406(3), Li1–Cl1'' 2.391(3), Li2–Cl1: 2.302(3), Li2–Cl2 2.361(3), Li2–Cl2'' 2.362(3), Li2–Cl2' 2.391(3), Li1–O1 2.022(3), Li1–O2 2.025(3), Li1–Cl1–Li2 91.48(11), Cl1–Li2–Cl2 107.15(12), Li2–Cl2–Li2' 80.22(11), Cl2–Li2'–Cl2' 99.78(11), Li2–Cl2–Li2'' 118.60(13), Cl2–Li2–Cl2'' 118.60(13), O1–Li1–O2 81.71(13).

In addition to the reaction of Si_2Cl_6 with nucleophiles, the synthesis of $SiCl_3^-$ could be envisioned by the direct reduction of Si_2Cl_6 with an alkali metal, as per the equation in Figure 5.11.

$$Si_2Cl_6 \quad + \quad 2\,M \quad \longrightarrow \quad 2\,MSiCl_3$$
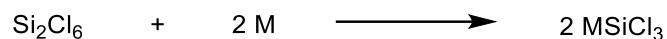
Figure 5.11. Hypothetical reaction of two equivalents of a metal (M) with Si_2Cl_6.

To test this hypothesis, the reaction of Si_2Cl_6 with 2 equivalents of potassium metal was conducted in DME, with 18-crown-6 added to aid in the dissolution of the potassium. After reacting for 30 minutes at -30 °C, then 1 hour at room temperature, the potassium appeared to passivate, becoming dull and no longer visibly decreasing in quantity. The amount of remaining potassium was found to be approximately 1.3 equivalents (relative to the quantity of Si_2Cl_6 added). After filtering and concentrating, the reaction solution slowly grew crystals over the course of a few months, identified to be $[K(18c6)]_2[Si_6Cl_{14}]$ (Figure 5.12).
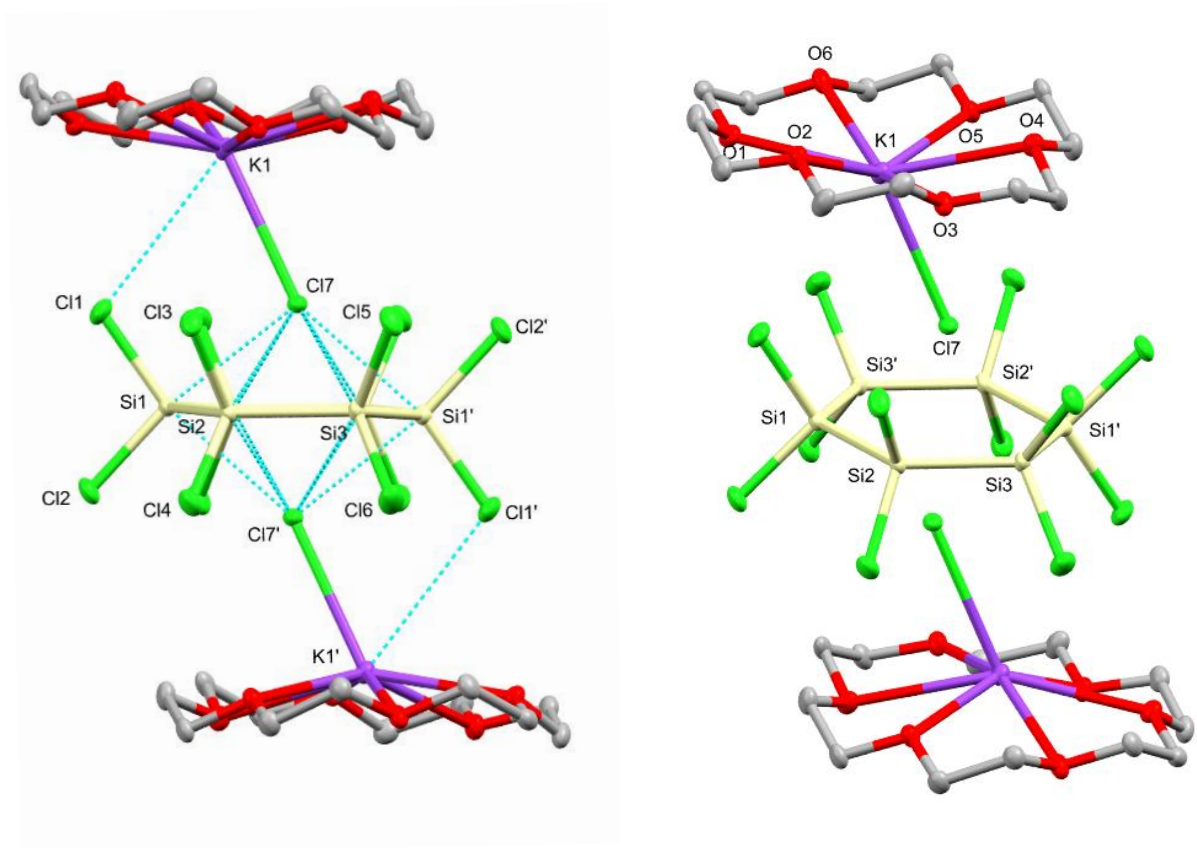
Figure 5.12. Thermal ellipsoid plots of [K(18c6)]$_2$[Si$_6$Cl$_{14}$], shown from two different perspectives. Ellipsoids at the 50% probability level, hydrogen atoms are omitted for clarity. Short contacts are shown in the left structure as dashed blue lines. Selected bond lengths (Å) and angles (°): Si1–Si2 2.338(1), Si2–Si3 2.330(1), Si3–Si1' 2.342(1), Si1–Cl1 2.089(1), Si1–Cl2 2.089(1), Si2–Cl3 2.078(1), Si2–Cl4 2.068(1), Si3–Cl5 2.079(1), Si3–Cl6 2.064(1), Cl7–Si1 2.992(1), Cl7–Si2 3.075(1), Cl7–Si3 3.041(1), Cl7–Si1' 3.035(1), Cl7–Si2' 2.989(1), Cl7–Si3' 3.047(1), K1–Cl7 3.149(1), K1–Cl1 3.741(1), K1–O1 2.869(2), K1–O2 2.848(2), K1–O3 2.862(2), K1–O4 2.907(2), K1–O5 2.790(2), K1–O6 2.949(2), Si3'–Si1–Si2 121.02(4), Si1–Si2–Si3 119.82(4), Si2–Si3–Si1' 118.88(4), Si1–Si2–Si3–Si1' dihedral -5.95(4), Cl1–Si1–Cl2 102.24(4), Cl3–Si2–Cl4 103.30(4), Cl5–Si3–Cl6 102.26(5), Cl7–Si1–Cl2 170.93(4), Cl7–Si2–Cl4 167.65(4), Cl7–Si3–Cl6 168.76(5), Cl7–Si1'–Cl1' 166.44(4), Cl7–Si2'–Cl3' 168.11(4), Cl7–Si3'–Cl5' 167.62(4).

The Si$_6$Cl$_{14}^{2-}$ ion is known to form by reaction of Si$_2$Cl$_6$ with either R$_4$NCl or R$_4$PCl (R = alkyl or phenyl groups) to afford [R$_4$N]$_2$[Si$_6$Cl$_{14}$] and [R$_4$P]$_2$[Si$_6$Cl$_{14}$] respectively.[135] [K(18c6)]$_2$[Si$_6$Cl$_{14}$] represents the first reported structure containing Si$_6$Cl$_{14}^{2-}$ associated with a metal-based cation.[143] The lack known metal salts of Si$_6$Cl$_{14}^{2-}$ hints at the possibility that this species is only stable in the presence of weakly coordinating cations. Hence, the formation of Si$_6$Cl$_{14}^{2-}$ in this reaction is likely enabled by the presence of 18-crown-6, which converts K$^+$ ions into

less-coordinating K(18c6)$^+$ ions. The potassium still exhibits some degree of coordination, representing the most significant difference in structure between [K(18c6)]$_2$[Si$_6$Cl$_{14}$] and known salts with non-coordinating cations (e.g. [PPh$_4$]$_2$[Si$_6$Cl$_{14}$]). Cl7 strongly coordinates to K1, causing the average Cl7–Si distance to be slightly longer than in [PPh$_4$]$_2$[Si$_6$Cl$_{14}$] (3.030 Å compared to 2.997 Å). There is also a weak interaction between K1 and Cl1, resulting in ring buckling due to Cl1 (and thus also Si1) being drawn towards K1, with an Si1–Si2–Si3–Si1' dihedral angle of -5.95 °. By comparison, the Si$_6$ ring of [PPh$_4$]$_2$[Si$_6$Cl$_{14}$] is perfectly planar (ring dihedral angles < 0.5 °). The average Si–Si bond length in the K(18c6)$^+$ salt is longer than in the PPh$_4$$^+$ salt, at 2.337 Å and 2.314 Å respectively. It may be that the stronger interaction with the central chlorides in the PPh$_4$$^+$ salt cause the Si$_6$ ring to contract slightly. Despite this change, the average Si–Cl bond length in the Si$_6$Cl$_{12}$ ring structure remains unaffected, with an average Si–Cl bond length of 2.078 Å for the K(18c6)$^+$ salt, and 2.082 Å for the PPh$_4$$^+$ salt.

The formation of [K(18c6)]$_2$[Si$_6$Cl$_{14}$] from the reaction of potassium, 18-crown-6 and Si$_2$Cl$_6$ only requires 0.67 equivalents of potassium per Si$_2$Cl$_6$. This is consistent with the observation of 1.3 equivalents of potassium remaining unreacted when 2 equivalents were added to the reaction, however the mechanism of this reaction is unclear. It is likely that the reaction of K(18c6)Cl with Si$_2$Cl$_6$ would result in the formation of [K(18c6)]$_2$[Si$_6$Cl$_{14}$] by analogy to the known synthesis of [PPh$_4$]$_2$[Si$_6$Cl$_{14}$]. If this reaction is the source of [K(18c6)]$_2$[Si$_6$Cl$_{14}$], however, then the K(18c6)Cl must be formed from a separate reaction. The known reaction of Si$_2$Cl$_6$ with Cl$^-$ is predicted to proceed via SiCl$_3$$^-$ as an intermediate.[135] Thus, an alternative mechanism is that the reaction of potassium, 18-crown-6 and Si$_2$Cl$_6$ forms the intended product, K(18c6)SiCl$_3$, which subsequently reacts further with Si$_2$Cl$_6$ to ultimately produce [K(18c6)]$_2$[Si$_6$Cl$_{14}$] without the need for K(18c6)Cl to initially be present. In either mechanism, it is likely that SiCl$_3$$^-$ does form to some degree during this reaction. However, it is evidently unsuitable as a method for producing solutions of SiCl$_3$$^-$ in high purity.

5.3. Conclusions

It does not appear to be possible to synthesise $Si_2(N_3)_6$ from Si_2Cl_6 by means of a simple azide-chloride exchange reaction. Attempts to do so result in considerable gas evolution, indicating decomposition of azido groups. $Si_2(N_3)_6$ would not be a low-valent species, and is thus likely to be stable. However, in the presence of nucleophiles, Si_2Cl_6 readily disproportionates into $SiCl_2/SiCl_3^-$ and $SiCl_4$, which may explain the issues in synthesising $Si_2(N_3)_6$. As such, a synthesis of $Si_2(N_3)_6$ would have to avoid strongly nucleophilic compounds. Due to the inherent nucleophilicity of azides, this may prove difficult.

$SiCl_3^-$ is found to exhibit considerable stability in THF solutions, more so than Si_2Cl_6. This makes $Si(N_3)_3^-$ a much more promising target for the isolation of a reduced silicon azide compound than $Si_2(N_3)_6$. A highly selective synthesis for $SiCl_3^-$ in solution has been identified from reaction of Si_2Cl_6 with $LiN(TMS)_2$. Unfortunately, the other product of this synthesis, $(TMS)_2N–SiCl_3$, would be incompatible with $Si(N_3)_3^-$, so these reaction solutions cannot be used directly. Pure solutions of $SiCl_3^-$ salts may be obtained if a selective reaction of nucleophile Nu^- with Si_2Cl_6 can be identified in which the byproduct, $Nu–SiCl_3$, is more volatile than the solvent, thus allowing this byproduct to be removed by vacuum. Attempts to isolate $SiCl_3^-$ as a pure lithium salt from these reaction solutions result in decomposition with elimination of LiCl. If a selective synthesis of $SiCl_3^-$ can be identified using a large weakly coordinating cation, then the driving force for elimination of a chloride salt may be low enough to allow for the isolation of $SiCl_3^-$. A possible means of achieving this would be to replace $LiN(TMS)_2$ with $KN(TMS)_2$, and conduct the reaction in the presence of 18-crown-6 to afford $[K(18\text{-crown-}6)]SiCl_3$. Such a salt would potentially be suitable for the synthesis of $Si(N_3)_3^-$ by analogy to the known syntheses of $Ge(N_3)_3^-$ and $Sn(N_3)_3^-$.

6. Investigation into the synthesis of pentazoles

6.1. Introduction

For the synthesis of novel silicon-nitrogen materials, there is interest in studying nitrogen-rich functional groups beyond the well-studied azido group. One such group which has seen major recent developments is the pentazolyl group – a cyclic aromatic group consisting of five nitrogen atoms (Figure 6.1). As with azido groups, the pure-nitrogen composition of pentazolyl groups make them potential precursors to nitrido groups by elimination of N_2.
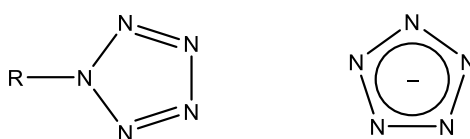
Figure 6.1. Structure of the pentazolyl group (left) and pentazolate ion (right).

6.1.1. Aryl-pentazoles (Ar–N_5)

The possibility of a pentazolyl group has been speculated for over one hundred years, with reports of pentazolyl compounds appearing in the early 1900s.[144, 145] These early reports were lacking in evidence and in some cases outright disproven.[146] The existence of a pentazolyl group was only adequately proven in 1956 with the synthesis of phenylpentazole from reaction of benzenediazonium chloride with azide ions.[147, 148] This method was quickly found to be suitable for the synthesis of a range of substituted aryl-pentazoles from their respective benzenediazonium derivatives.[149, 150] These aryl-pentazoles were found to readily decompose at room temperature to afford the corresponding aryl-azide and N_2, thus explaining the prior difficulty in isolating pentazole derivatives. Among the known aryl-pentazoles, it has been observed that π-donating substituents on the aryl ring help to stabilise the pentazolyl group, while π-withdrawing substituents destabilise it. These observations are backed up by more recent computational predictions of pentazole stability.[151] The stability of aryl pentazoles is also calculated to be dependent on the coplanarity of the aryl and pentazole rings. Methyl or oxido substituents *ortho* to the pentazolyl group prevent coplanarity due to steric effects and thus reduce the calculated barrier to decomposition. However, *ortho*-hydroxy groups were calculated to have a

stabilising effect attributed to intramolecular hydrogen bonding maintaining the coplanarity of the rings. The predicted destabilising effect of *ortho*-methyl substituents has subsequently been proven experimentally, where 4-pentazolyl-3,5-dimethylphenol was found to be considerably less stable than 4-pentazolylphenol, whereas 4-pentazolyl-2,6-dimethylphenol was slightly more stable than 4-pentazolylphenol (Figure 6.2).[152]
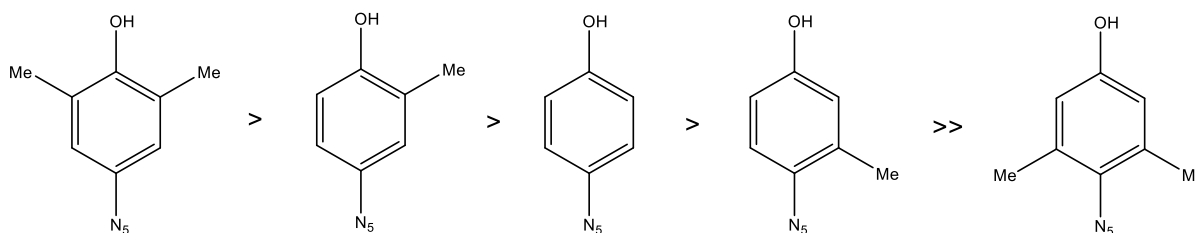
Figure 6.2. Relative stabilities of methyl-substituted derivatives of 4-pentazolylphenol, from left (most stable) to right (least stable).

The mechanism of formation of aryl-pentazoles has been investigated with a combination of ^{15}N labelling reactions and computational study. The conclusion of these investigations state that the formation of aryl-pentazoles does not proceed via a concerted cyclisation reaction, but instead via a pentazene chain intermediate, which can either undergo cyclisation to form the aryl-pentazole or elimination of N_2 to form the aryl-azide (Figure 6.3).[153]
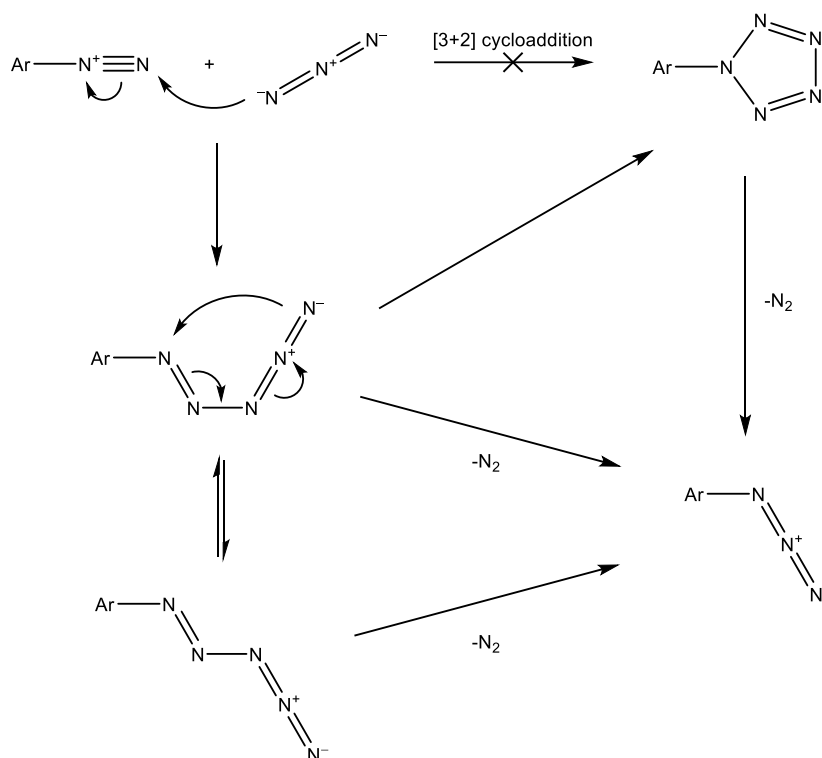
Figure 6.3. Butler's deduced mechanistic scheme for the formation of Ar–N$_5$ and Ar–N$_3$ from the corresponding aryl diazonium salt and azide ions.

The competition between pentazene cyclisation and pentazene N$_2$ elimination shown in Figure 6.3 is known to be a significant issue in the synthesis of aryl-pentazoles and is attributed as a major source of yield loss during their synthesis. For known aryl-pentazoles, the current synthetic method does not appear to be capable of achieving yields higher than ~60% due to concurrent formation of the respective aryl-azide.[154]

6.1.2. Other substituted pentazoles

While known aryl-pentazoles include numerous substituted derivatives of phenylpentazole, there is a lack of literature on the formation of pentazoles bound to 5-membered aromatic systems. A*b-initio* calculations suggest that all anionic azolates with a single pentazolyl substituent should be more stable than 4-(dimethylamino)phenylpentazole (one of the most stable known aryl-pentazoles), with pentazolyl cyclopentadienide calculated to be even more stable than the azolates.[155] Despite this, there is only one example of an isolated pentazole with a 5-membered aromatic substituent – 2-pentazolyl-4,5-dicyanoimidazolate (Figure 6.4).[154] Considering that electron-withdrawing substituents are known to destabilise

130

aryl-pentazoles, the cyano groups are likely to have a destabilising effect on this compound. No comment on the stability of 2-pentazolyl-4,5-dicyanoimidazolate is reported, but the lack of a published isolated yield may suggest difficulty in bulk isolation. Tetrazolylpentazole has also been detected by NMR spectroscopy as an unstable intermediate in the formation of azidotetrazole from reaction of tetrazolediazonium chloride and lithium azide.[156]
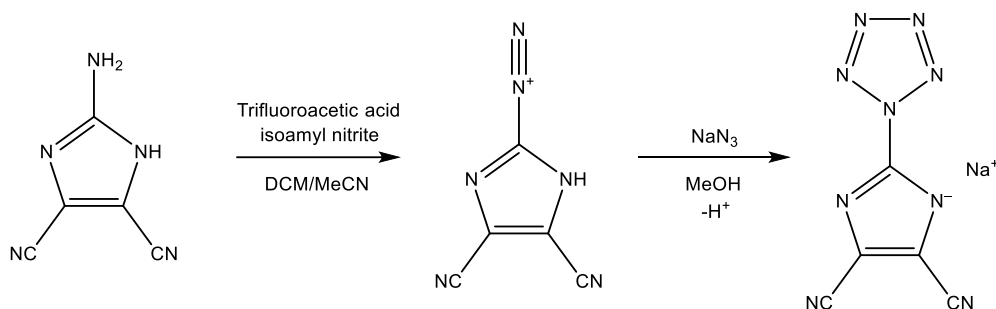
Figure 6.4. Synthesis of sodium 2-pentazolyl-4,5-dicyanoimidazolate.

There are only two known examples of substituted pentazoles with non-aromatic substituents. Aminopentazole has been identified as a ligand in a pair of cobalt complexes formed from reaction of cobalt(II) acetate, excess sodium azide, and a *p*-tert-butylthiacalix[4]arene ligand at 130 °C (Figure 6.5).[157] The formation of aminopentazole in this reaction is proposed as a cobalt-catalysed dimerisation of azide to form N_5–N^{2-}, followed by protonation. The evident stability of this aminopentazole ligand in the 130 °C synthesis conditions is remarkable and is presumably stabilised by its coordinating interactions to cobalt. Free aminopentazole has not yet been reported, so it may not be stable outside of this coordination environment.
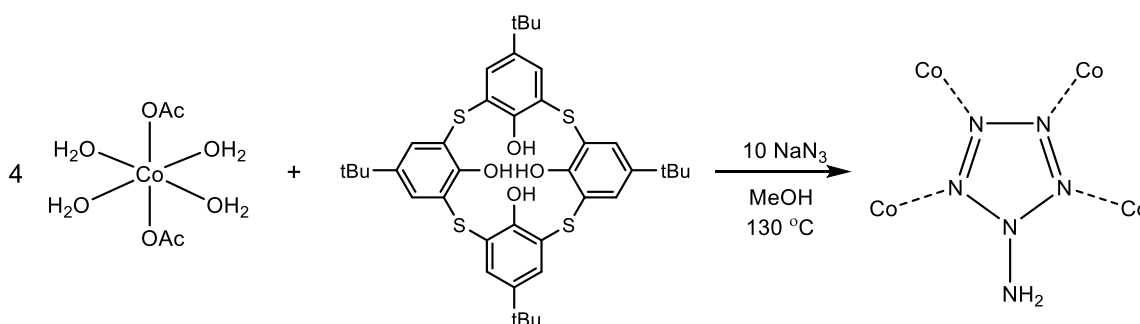
Figure 6.5. Reaction of cobalt(II) acetate hydrate, *p*-tert-butylthiacalix[4]arene and NaN₃. Note that the cobalt atoms in the product also have *p*-tert-butylthiacalix[4]arene and azido substituents.

Recently, the reaction of azide with the Vilsmeier reagent (chloro-N,N-dimethylmethaniminium chloride) has been shown to form an unusual imine-bound pentazole, shown in Figure 6.6.[158]

(not observed)
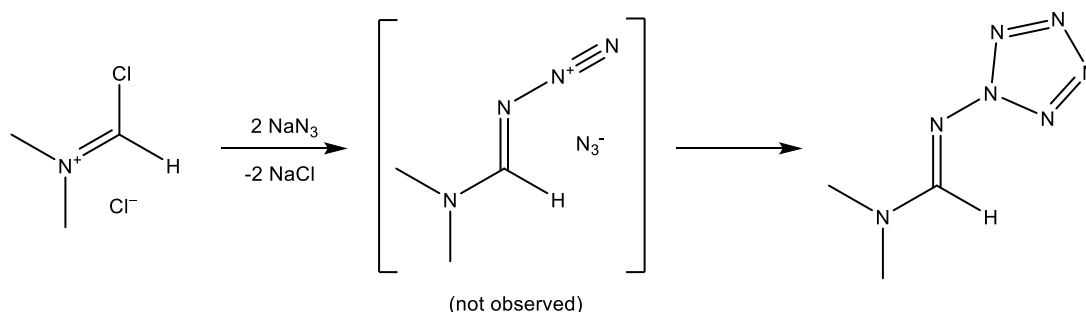
Figure 6.6. Reaction of the Vilsmeier reagent with NaN$_3$.

The resulting pentazole derivative is not characterised structurally, and its identity was deduced from ^{15}N NMR labelling experiments. As with aryl-pentazoles, this compound is not stable at room temperature, with an estimated half-life of 11 minutes at 21 °C.

6.1.3. The pentazolate ion (N$_5^-$)

The pentazolate ion has been subject to numerous computational investigations over the past 40 years.[159-163] Throughout the improvements in computational methods in the past decades, these studies consistently highlight that N$_5^-$ is thermodynamically unstable with respect to N$_3^-$ + N$_2$, but also note that the activation barrier of this decomposition is sufficiently high for N$_5^-$ to be an isolable species. There have been reports on the detection of N$_5^-$ by mass spectrometry dating back as far as 2002, achieved by subjecting aryl-pentazoles to various ionising conditions until a fragment with an m/z value of -70 could be detected.[164, 165] These claims were backed up by a theoretical report outlining the feasibility of N$_5^-$ being produced by high energy ionisation of aryl-pentazoles.[166]

The formation of N$_5^-$ was subsequently also detected by mass spectrometry from the alkali metal reduction of phenyl-pentazole in THF, but this method was found to be inadequate for the isolation of N$_5^-$ salts.[167] Subsequent work determined this method to be inconsistent, where the degree of N$_5^-$ detected was found to be dependent on the presence of a passivation layer on the reducing sodium.[168] The authors attribute this phenomenon to pure sodium being "too strong a reducer", however this seems a rather poor explanation since

passivated sodium is still formally the same chemical species, and thus has the same reduction potential. It is perhaps more likely that the compounds present in the passivation layer itself are responsible for enabling the formation of N_5^-. Regardless of how N_5^- is formed, this reaction is poorly understood, further limiting its viability as a synthetic procedure for the synthesis of bulk N_5^-.

Only very recently (2017) has the synthesis of bulk pentazolate salt been achieved.[169] This was done via the oxidative cleavage of N_5^- from 4-pentazolyl-2,6-dimethylphenol, affording a mixed pentazolate salt, $(NH_4)_4(H_3O)_3Cl(N_5)_6$, according to the overall reaction scheme outlined in Figure 6.7. Unlike known aryl-pentazoles which are unstable at room temperature, this salt decomposes at a remarkably high temperature of 117 °C. This stability was originally attributed to hydrogen bonding effects, however the simple salts NaN_5 and LiN_5 have since been found to have even higher decomposition temperatures of 139 °C and 133 °C respectively.[170, 171] These simple salts evidently lack hydrogen bonds, however they do still exhibit coordination of the nitrogen lone pairs to the metal cations. This coordination of the nitrogen lone pair, either to a hydrogen bond donor or a metal, is predicted to be important to the stability of N_5^- ions.[172]
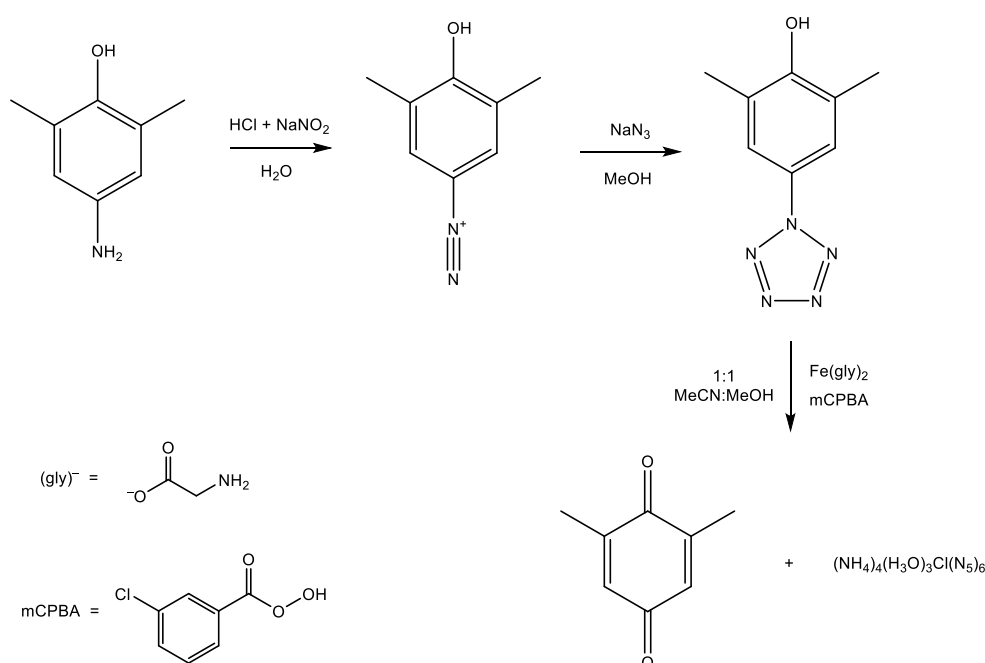
Figure 6.7. Reported procedure for the formation of the pentazolate-containing salt $(NH_4)_4(H_3O)_3Cl(N_5)_6$.

Although crystallographic data provides strong evidence for the formation of N_5^-, the reaction scheme shown in Figure 6.7 is not without fault. A computational report discussing the mechanism of this process is published,[173] but offers no insight into the origin of the chloride or ammonium ions present in the product. When the sodium 4-pentazolyl-2,6-dimethylphenoxide is used instead of the parent phenol, the formation of NaN_5 is reported without the presence of chloride or ammonium.[170] In addition to low yields (19% for the final step, 3% – 7% for the overall process shown in Figure 6.7),[152, 169] the synthesis has been found to be inconsistent by subsequent work.[140, 174] Nonetheless, evidence for the existence of isolated pentazolate is reinforced by the crystallographic characterisation of numerous salts of pentazolate in recent years, formed via salt metathesis reactions from $(NH_4)_4(H_3O)_3Cl(N_5)$ or NaN_5, typically *via* AgN_5 as an intermediate salt.[171, 175-177]

6.1.4. Oxides of Pentazolate ($N_5O_x^-$)

Although not yet experimentally characterised, pentazole oxide N_5O^- (also known as oxo-pentazolate) has been of significant interest in computational study. Much like N_5^-, N_5O^- is predicted to be unstable with respect to loss of N_2, but with a sufficiently high barrier to decomposition that it may be an isolable compound.[163, 178-180] These calculations predict a comparable stability to N_5^-, with some computational methods predicting even higher stability for N_5O^-. Considering the observed high stability of N_5^- salts, it is likely that salts of N_5O^- are isolable.

The most obvious route towards N_5O^- would be the oxidation of N_5^-. *N*-oxidation of heterocyclic azoles is a well-documented procedure using oxygen atom transfer reagents, including organic peroxyacids, $NaBO_3$ and $KHSO_5$.[181, 182] There is only one *ab-initio* study on the oxidation of N_5^- specifically, which suggests the oxidation of N_5^- to N_5O^- with ozone is feasible (Figure 6.8).[183] There has very recently been an attempt to oxidise NaN_5 using $KHSO_5$ in aqueous solution with AcOK as a pH buffer, which was reported as unsuccessful.[184] It should however be noted that the use of AcOK as a buffer would result in a pH value for the reaction solution in the range of the pKa value of AcOH (4.8). Existing work on oxidation of azoles suggests oxidation proceeds most effectively when the pH of the solution is

comparable to the pKa of the azole,[182] reasoning that at higher pH the oxidising agent is less active, while at lower pH the resulting protonated azole is not susceptible to oxidation. Since N_5^- has been known to crystallise as a mixed salt containing H_3O^+ cations, it can be reasonably assumed that the pKa of HN_5 is < 0, hence a pH of 4.8 would have been unsuitable for oxidation of N_5^-.

Existing *ab-initio* work also highlights a fundamentally different approach towards N_5O^-. While N_5O^- is thermodynamically unstable with respect to loss of N_2, it has been calculated to be thermodynamically favoured over a mixture of N_2O and N_3^-.[163] Thus, it could be conceivable that simply passing N_2O though an azide-containing solution may generate N_5O^- (Figure 6.8). Unfortunately, the barrier to this reaction is calculated to be slightly higher than the barrier to N_5O^- decomposition. The absence of experimental reports of N_5O^- in the 13 years since these calculations were published similarly suggest that this simple approach does not work.
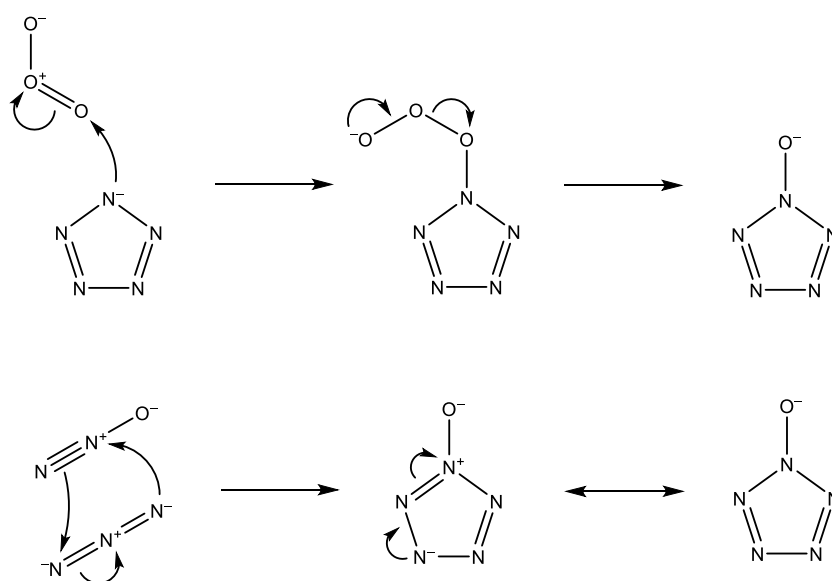
Figure 6.8. Possible routes for the formation of N_5O^-, determined by *ab-initio* calculations.

6.2. Results and Discussion

6.2.1. Attempted synthesis of pentazolyl cyclopentadienides

By analogy to the synthesis of phenylpentazole derivatives, the synthesis of pentazolylcyclopentadienide would require an analogous precursor to benzenediazonium salts. Aminocyclopentadiene is not a known compound, thus typical diazotisation reactions to form diazonium salts are not accessible. However, diazocyclopentadiene (CpN$_2$) can instead be made from the reaction of lithium cyclopentadienide with tosyl azide in Et$_2$O.[185] As diazocyclopentadiene is reported to be potentially explosive,[186] no attempt was made to isolate this compound pure, and it was instead synthesised as a solution in Et$_2$O. Solutions in solvents other than Et$_2$O can be obtained by diluting ethereal solutions with a different solvent, followed by concentration under vacuum to remove the Et$_2$O.

Addition of PPN(N$_3$) to an MeCN solution of CpN$_2$ resulted in bubbling and a darkening of the solution, however monitoring of the reaction solution by ^{1}H NMR spectroscopy showed no significant change in CpN$_2$ concentration even after 17 hours. ^{14}N NMR spectroscopy confirms the presence of unreacted CpN$_2$ and N$_3^-$. It is likely that the observed bubbling and colour change were from reaction of impurities present in the CpN$_2$, rather than the CpN$_2$ itself. Similarly, no reaction with CpN$_2$ in MeCN was observed for HN$_3$ or NaAl(N$_3$)$_4$(THF)$_4$. Considering the previously observed effectiveness of aluminium azides for azide exchange in Et$_2$O, the reaction of NaAl(N$_3$)$_4$(THF)$_4$ with CpN$_2$ was also tested in Et$_2$O, but likewise no reaction was observed. Curiously the aluminate reagent visually appears to decompose in these solutions, assumed to be the effect of unknown impurities left over from the CpN$_2$ synthesis, as no consumption of the CpN$_2$ is observed spectroscopically.

Due to the possible issues of handling isolated CpN$_2$, a slightly larger analogue was sought, which would have lower energy density and thus not pose an explosion hazard. The reaction of lithium tetramethylcyclopentadienide with tosyl azide was found to proceed analogous to that of lithium cyclopentadienide, affording a new diazocyclopentadiene derivative tetramethyldiazocyclopentadiene (Cp^{x}N$_2$) (Figure 6.9).
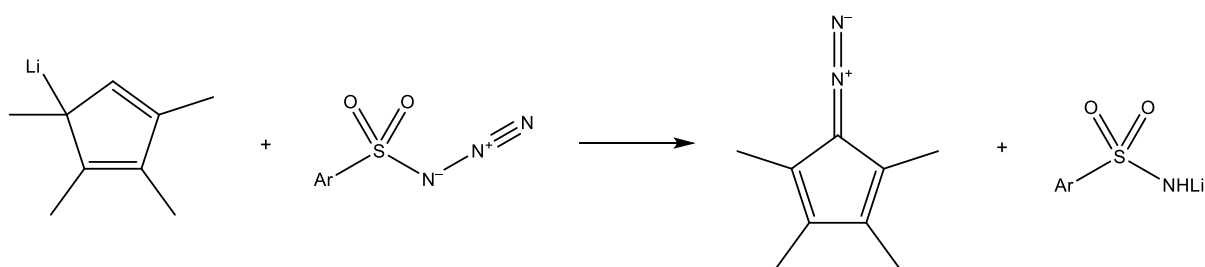
Figure 6.9. Synthesis of tetramethyldiazocyclopentadiene (Cp^{x}N$_2$), analogous to the synthesis of CpN$_2$.

As with CpN$_2$, Cp^{x}N$_2$ did not react with azide (as either a PPN or PPh$_4$ salt), in C$_6$D$_6$, acetone, MeOH or CDCl$_3$. There was also no reaction observed between Cp^{x}N$_2$ and HN$_3$ in Et$_2$O. For the reaction in C$_6$D$_6$, heating the reaction mixture to 60 °C was observed to have no effect. Heating to higher temperatures was avoided, as the desired pentazolylcyclopentadienide derivative is not likely to be stable at elevated temperatures. For the reaction attempt in acetone, after no reaction had been observed for 5 days, half an equivalent of FeCl$_2$ and 10 equivalents of pyridine were added to see if iron(II) complexes can catalyse the reaction. No significant reaction occurred at room temperature, so the mixture was heated to 60 °C for 4.5 hours, resulting in a darkening of the solution. On returning to room temperature, crystals of [PPh$_4$]$_2$[FeCl$_3$(N$_3$)] formed (Figure 6.10). The Cp^{x}N$_2$ remained unreacted according to NMR analysis, indicating that FeCl$_3$(N$_3$)$^-$ does not react with Cp^{x}N$_2$.
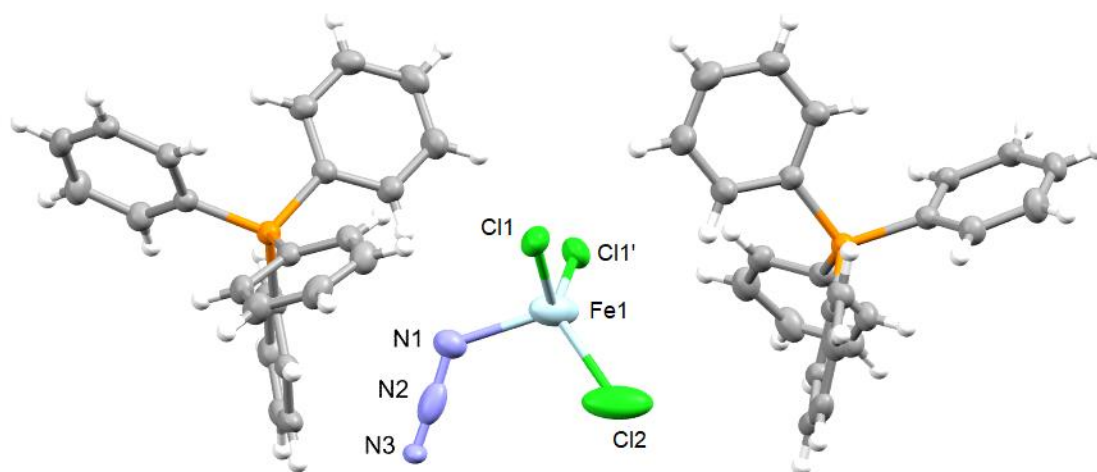
Figure 6.10. Thermal ellipsoid plot of one disorder component of [PPh$_4$]$_2$[FeCl$_3$(N$_3$)]. Ellipsoids at the 50% probability level, hydrogen atoms are shown as spheres of fixed radius (0.2 Å). The other disorder component is of equal occupancy, in which the FeCl$_3$(N$_3$)$^{2-}$ ion is mirrored in the Cl1−Fe1−Cl1' plane relative to the image shown here. This disorder results in unusual ellipsoids for N2 and Cl2, as they are superimposed and are thus difficult to refine separately.

137

The lack of reactivity of CpN_2 and Cp^xN_2 towards azide sources is in contrast to that of aryl diazonium salts. This is evidently due to the significant difference in electrophilicity of the diazo group. While aryl diazonium salts possess a formal positive charge on the diazo group, calculations have shown that the diazo group of CpN_2 is approximately neutral.[187] This observation indicates a dilemma in the synthesis of aryl-pentazoles – electron donating substituents stabilise aryl-pentazoles, but the same electron donation renders the diazonium group of the precursor less reactive towards azide. If one were to consider CpN_2 as its zwitterionic diazonium resonance form (i.e. $Cp^--N_2^+$), then the lack of reactivity of CpN_2 can be rationalised as an effect of the cyclopentadienido group being too strong of an electron donor due to its negative charge.

Ruthenium(II) halocyclopentadienide complexes have been show to readily undergo substitution of the halogen for azide on the cyclopentadiene ring.[188] It may therefore be possible that coordination to similar transition metal complexes can catalyse the reaction of CpN_2 with azide. Small quantities of a rhodium(III) azide complex, $RhCp^*(N_3)_2(PPh_3)$ was found available, so its reaction with CpN_2 in MeCN was tested. Over the next three days, crystals formed from the reaction solution, which were identified as $RhCp^*(N_3)_2(PPh_3) \cdot MeCN$ by SCXRD, indicating a lack of reaction with CpN_2. When heated to 60 °C for 4 hours, the solution darkened indicating some reaction occurs at this temperature. No product could be isolated from this reaction. ^{1}H NMR spectra of the solution shows some unreacted CpN_2, despite all $RhCp^*(N_3)_2(PPh_3)$ being consumed. The main product (in solution) appears to lack any Rh–Cp* coupling, indicating the Cp* ring has been dissociated from the rhodium. There is a new Cp-containing product which has a similar proton-proton coupling pattern as CpN_2. The ^{31}P spectrum shows only one product, which no longer exhibits coupling to the rhodium, but is also not consistent with free PPh_3. It is therefore likely that the known reaction of CpN_2 with PPh_3 to form $Cp=N-N=PPh_3$ has occurred.[189] Hence PPh_3-containing complexes appear to be unsuitable for catalysing reactions of CpN_2. An alternative rhodium(III) azide complex, $Rh(N_3)_6^{3-}$ (made *in-situ* from NaN_3 and $RhCl_3(H_2O)_3$), was also tested for reaction with CpN_2, but no reaction occurred.

The addition of $((C_6H_6)RuCl_2)_2$ to an unreacted mixture of Cp^xN_2 and PPh_4N_3 in d_4-methanol results in immediate bubbling. ^{1}H NMR analysis of the solution shows the formation of one dominant Cp^x-containing product, along with numerous minor products. Attempts to

crystallise the product(s) of reaction were unsuccessful, so it was not possible to prove its identity. If this reaction is conducted in the absence of PPh_4N_3, bubbling is still observed and numerous products are detected in the ^1H NMR spectrum, none of which match the previously observed major product. It is therefore reasonable to assume that this major product from reaction of Cp^xN_2, PPh_4N_3 and $((C_6H_6)RuCl_2)_2$ does involve a reaction of the azide. However, it is also clear from the reaction in the absence of azide that $((C_6H_6)RuCl_2)_2$ causes the decomposition of Cp^xN_2 with elimination of N_2. It is reported that diazofluorenes can react with Ru(II) complexes to form ruthenium-carbene complexes with elimination of N_2,[190] thus a likely course of reaction is as shown in Figure 6.11.
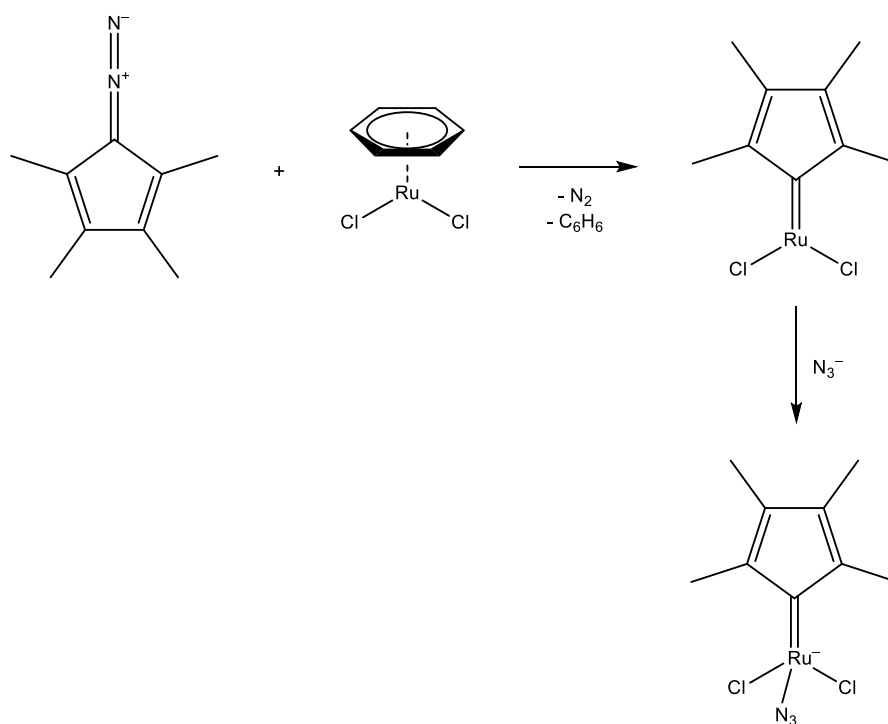
Figure 6.11. Proposed reaction scheme for the reaction of $(C_6H_6)RuCl_2$ with a mixture of Cp^xN_2 and PPh_4N_3.

Bubbling was also observed on addition of $RhCl_3(H_2O)_3$ to MeOH or MeCN solutions of Cp^xN_2, suggesting a similar decomposition. The decomposition of the diazo compound thus significantly complicates the use of transition metal catalysis to encourage the reaction of diazocyclopentadienes with azide.

Since the diazo group of diazocyclopentadienes appears to be too electron-rich for reaction with azide, the reaction of 2-diazoimidazole was also considered, as the imidazolyl group

should be more electron withdrawing than the cyclopentadienyl group. The reaction between protonated species imidazole-2-diazonium with azide ions is a known method for producing 2-azidoimidazole,[191] which is likely to occur via pentazene and/or pentazole intermediates that subsequently decompose to the azide. While the protonation of the imidazole will likely aid the reaction with azide, the resulting imidazolylpentazole is predicted to be much less stable than anionic 2-pentazolylimidazolate.[155] Thus, if possible, it is desirable to synthesise 2-pentazolylimidazolate without protonation, according to the reaction scheme shown in Figure 6.12.
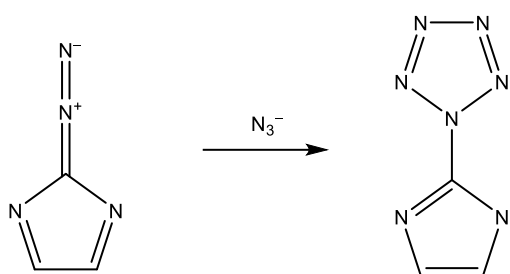
Figure 6.12. Proposed reaction of 2-diazoimidazole with azide.

The deprotonation of imidazole-2-diazonium chloride resulted in a dark brown suspension. The addition of azide to this suspension caused considerable bubbling, ultimately resulting in an inextricable black precipitate. The brown precipitate that formed upon deprotonation suggests that 2-diazoimidazole is not adequately stable under the reaction conditions used. The observation of significant bubbling on addition of azide indicates that some reaction does occur between 2-diazoimidazole and azide ions, in contrast to the lack of reactivity with diazocyclopentadiene. However, the formation of bubbles indicates at least some decomposition occurs, either of a pentazole product or a pentazene intermediate. With optimisation of conditions, it may still be possible to isolate a pentazole-containing product from this reaction mixture. Due to time limitations, however, this possibility was not pursued further.

6.2.2. Reaction of other neutral diazo compounds with azide

The synthesis of diazocyclopentadienes using tosyl azide highlights the tendency of sulphonyl azides to act as diazo transfer reagents rather than azide transfer reagents. Based on this reactivity, sulphonyl azides could be considered as diazonium-substituted sulphonamides, which may exhibit some analogous reactivity to diazonium salts. Sulphuryl diazide ($SO_2(N_3)_2$) can be synthesised from treatment of SO_2Cl_2 with excess NaN_3 in MeCN.[192] The excess of NaN_3 used makes it evident that no further reaction between azide and $SO_2(N_3)_2$ occurs under these conditions.

As an alternative azide source, $TMS(N_3)$ was considered. SO_2Cl_2 was added to a suspension of NaN_3 in a 1 : 1 (by volume) mixture of toluene : $TMS(N_3)$, with the intention of forming $SO_2(N_3)_2$ and reacting it *in-situ* with the NaN_3 and $TMS(N_3)$ mixture. However, this mixture afforded negligible conversion of SO_2Cl_2 to $SO_2(N_3)_2$, so it appears that $TMS(N_3)$ does not act as an effective azide transfer reagent or catalyst the purposes of synthesising $SO_2(N_3)_2$. $TMS(N_3)$ was separately found to have no reaction with TsN_3, thus also indicating a lack of reactivity towards sulphuryl azides.

In contrast to both NaN_3 and $TMS(N_3)$, if SO_2Cl_2 is added to a solution of 4 equivalents of $PPN(N_3)$ in MeCN, vigorous bubbling is observed. No precipitate is formed, and IR analysis of the solution shows the presence of some unreacted $PPN(N_3)$ (v = 2005 cm^{-1}) and only one other azide-containing species (v = 2017 cm^{-1}). If SO_2Cl_2 is first converted to $SO_2(N_3)_2$ by NaN_3 in MeCN, addition of one equivalent of $PPN(N_3)$ again results in bubbling, along with trace precipitate formation. The IR spectrum of the solution contains the same two bands at 2017 cm^{-1} and 2005 cm^{-1}, with the 2005 cm^{-1} band of the $PPN(N_3)$ being significantly weaker than in the previous reaction. The band at 2017 cm^{-1} matches the reported asymmetric azide stretching frequency of solution-phase $SO_2(N_3)^-$ (2016 cm^{-1}, Raman in liquid SO_2).[193] Based on this assignment, in combination with the observed gas evolution, the hypothesised reaction of $SO_2(N_3)_2$ with $PPN(N_3)$ is as shown in Figure 6.13.
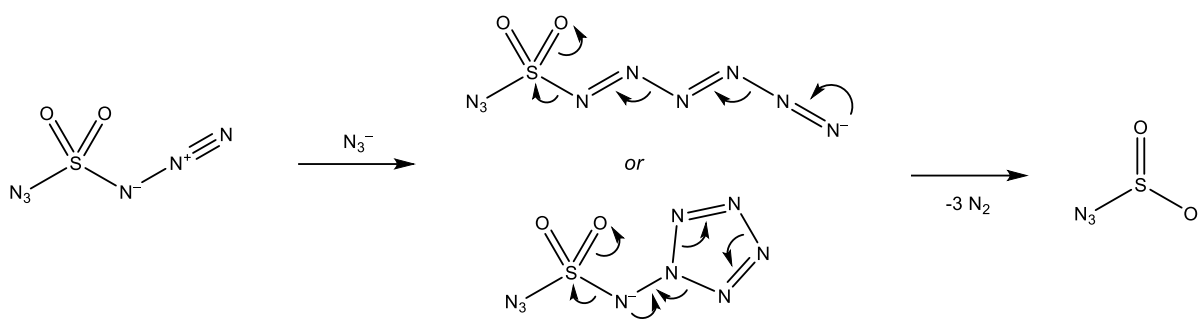
Figure 6.13. Two proposed mechanisms for the formation of $SO_2(N_3)^-$ from the addition of PPN(N_3) to $SO_2(N_3)_2$.

This reaction only occurs with PPN(N_3) and not NaN$_3$, which is likely due to the weakly-coordinating nature of the PPN$^+$ cation allowing the azide ion to be more reactive. It has been reported that a more electron-deficient sulphonyl azide, $(CF_3)SO_2(N_3)$, reacts with sodium or potassium azide to produce the analogous product, $SO_2(CF_3)^-$.[194, 195]

The reaction of NaN$_3$ with the Vilsmeier reagent (Figure 6.6)[158] is believed to proceed via an intermediate containing an electron-deficient azido group which is then attacked by azide ions. Considering the dominant product from this reported reaction is an N-bound pentazole, it is likely that an N-bound pentazole intermediate is also formed in the reaction between $SO_2(N_3)_2$ and PPN(N_3), as this also involves attack of azide on an electron-deficient azido group. However, this intermediate is clearly not isolable at room temperature, as the reaction mixture rapidly evolves gas to form the observed $SO_2(N_3)^-$.

To see if *in-situ* generation of azide ions affects the reaction with sulphonyl azides, the reaction of $SO_2(N_3)_2$ with amines was investigated, with the intention of generating azide ions by substitution of one of the two azido groups of $SO_2(N_3)_2$. When $SO_2(N_3)_2$ is treated with two equivalents of diisopropylamine, the formation of $SO_2(N_3)^-$ is again observed, along with a new azide-containing product which absorbs at 2109 cm^{-1}. It is assumed that HN(iPr)$_2$ eliminates N_3^- from $SO_2(N_3)_2$ and is subsequently deprotonated by another equivalent of HN(iPr)$_2$, resulting in the elimination of diisopropylammonium azide which then reacts with $SO_2(N_3)_2$ in the same manner as PPN(N_3). If the formation of alkylammonium salts is prevented by using an aprotic amine (triethylamine), $SO_2(N_3)_2$ is still consumed and bubbling is observed, however no formation of $SO_2(N_3)^-$ occurs, and no other

azide-containing products are generated. These observations can be rationalised according to the scheme in Figure 6.14.
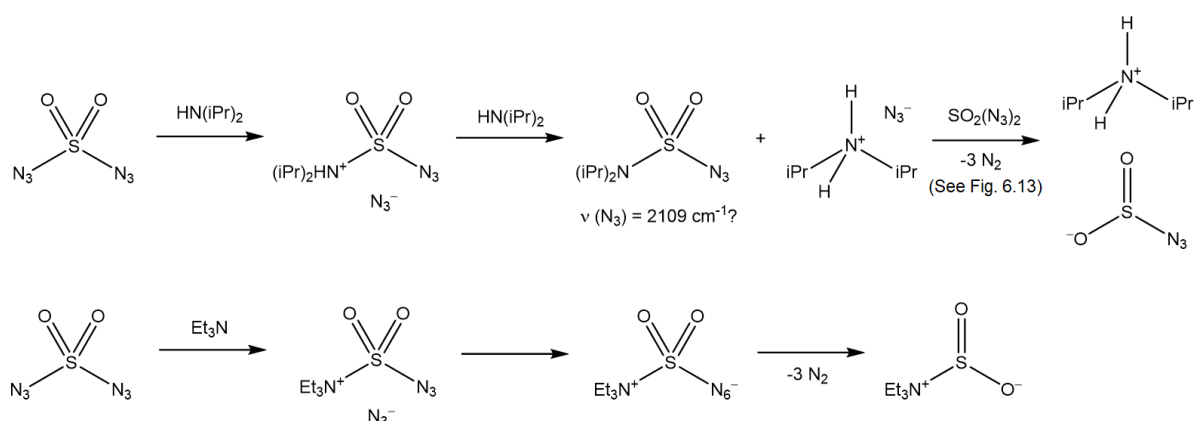
Figure 6.14. Hypothesised reaction sequence for reaction of $SO_2(N_3)_2$ with $HN(iPr)_2$ (top) and Et_3N (bottom).

If pentazole intermediates are indeed formed from the reaction of $SO_2(N_3)_2$ with N_3^-, then their instability may hinder any attempt to observe/isolate them. Since it is already established that electron withdrawing substituents destabilise pentazoles, the reaction of $PPN(N_3)$ was also tested with phosphoryl triazide ($PO(N_3)_3$), as the phosphoryl group is less electron withdrawing than the sulphonyl group. No reaction occurred however, indicating that the phosphoryl group is not sufficiently electron withdrawing to activate the azido groups. Fine tuning of substituents on either sulphonyl or phosphoryl azides may afford an azido group that is only just electron deficient enough to allow for reaction with azide ions, without compromising the stability of the resulting pentazole.

To confirm if there is any precedence for neutral diazo compounds to be precursors for pentazole compounds, diazoquinone was selected as a possible neutral precursor to the known compound 4-pentazolylphenoxide according to the scheme in Figure 6.15.
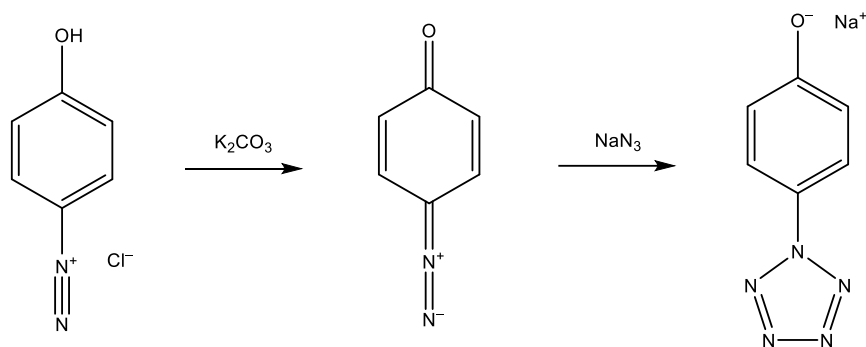
Figure 6.15. Proposed formation of sodium 4-pentazolylphenoxide via diazoquinone as an intermediate.

4-hydroxybeznenediazonium chloride was made by diazotisation of 4-aminophenol in aqueous hydrochloric acid using sodium nitrite. Neutralisation of the resulting reaction mixture affords an aqueous solution of diazoquinone. The effect of adding NaN_3 to this solution was monitored by NMR spectroscopy at -3 °C. At this temperature, a very slow reaction takes place between diazoquinone and NaN_3 to form two new compounds. These compounds are identified as sodium 4-pentazolylphenoxide and sodium 4-azidophenoxide based on the reported NMR shifts of their caesium salts.[154] Initially, the ratio of 4-pentazolylphenoxide : 4-azidophenoxide is 1.6 : 1, consistent with the known simultaneous formation of aryl-pentazoles and aryl-azides from reaction of diazonium salts with azide ions.[153] Allowing the mixture to react at room temperature for 30 minutes increased the conversion of diazoquinone, but caused visible bubbling, and the ratio of 4-pentazolylphenoxide to 4-azidophenoxide decreased to 0.9 : 1. These observations are consistent with the decomposition of 4-pentazolylphenoxide to form 4-azidophenoxide occurring alongside the formation of both species from diazoquinone. Subsequently, a small quantity of $ZnCl_2$ was added to the mixture, since $ZnCl_2$ is a known catalyst for the cycloaddition of azide to cyano compounds.[196] This did not appear to have any significant effect on reaction rate. The simultaneous formation of 4-pentazolylphenoxide and 4-azidophenoxide, combined with the lack of catalytic effect of $ZnCl_2$, suggests that the reaction between NaN_3 and diazoquinone follows the same mechanism as observed for reaction with diazonium salts. $RhCl_3(H_2O)_3$ was similarly found to have no significant effect, suggesting heavier transition metals may also have limited utility in aiding this reaction. Over time, the ratio of 4-pentazolylphenoxide to 4-azidophenoxide in the solution decreased owing to the decomposition of the former. As the reaction conversion continues,

eventually the concentration of 4-pentazolylphenoxide starts decreasing, as the rate of decomposition exceeds the rate of formation. This ultimately renders this method unsuitable for the synthesis of 4-pentazolylphenoxide, as the majority of 4-pentazolylphenoxide will have decomposed by the time conversion of diazoquinone is complete. This may explain why a previous report claims the reaction of diazoquinone with tetrabutylammonium azide in methanol produces exclusively 4-azidophenoxide.[197]

For the study of pentazolylphenoxides, a more stable derivative is desirable. The proposed stabilising effect of *ortho*-hydroxy groups on aryl-pentazoles has yet to be determined experimentally, thus it was planned to synthesise 4-pentazolyl-3,5-dihydroxyphenoxide according to the scheme outlined in Figure 6.16.
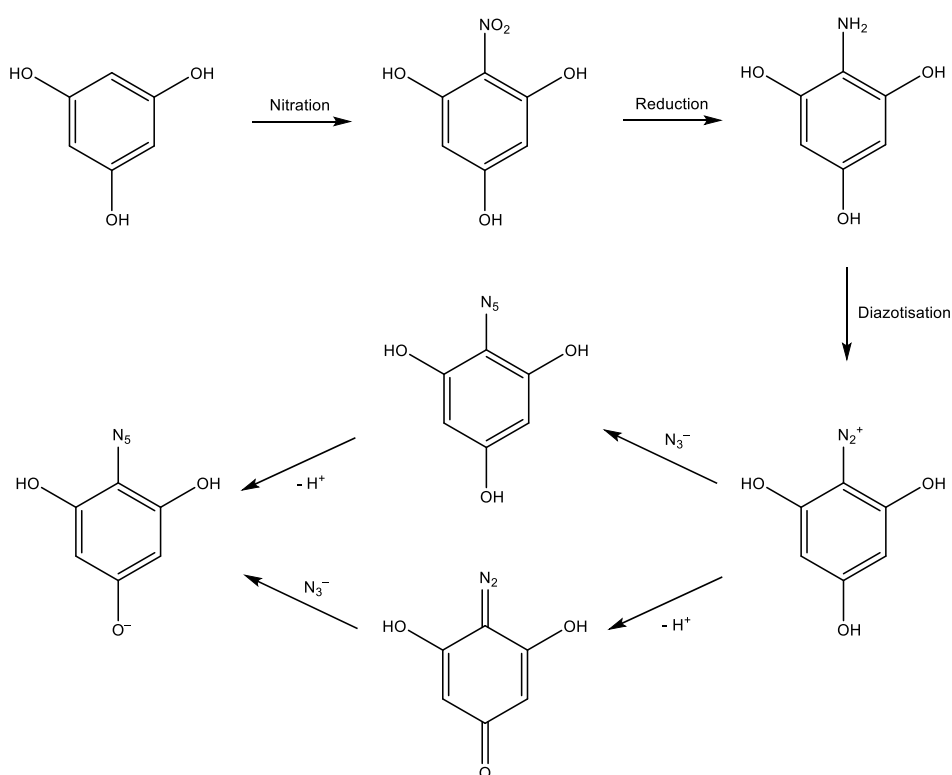
Figure 6.16. Planned scheme for the synthesis of 4-pentazolyl-3,5-dihydroxyphenoxide from phloroglucinol (1,3,5-benzenetriol).

Nitration of phloroglucinol (1,3,5-benzenetriol) using NO_2BF_4, according to the procedure used to nitrate O,O'-dimethylphloroglucinol,[198] resulted in a purple-black residue from which no pure product could be isolated. Nitration of phloroglucinol with a mixture of aqueous sulphuric acid and nitric acid[199] was found to suffer from incomplete conversion,

and repeating the nitration starting from partially-converted material did not significantly further the conversion. It is possible that some of the formed nitrophloroglucinol hydrolyses back into phloroglucinol during workup, thus higher yields would necessitate more effective workup rather than longer reaction duration. Nonetheless, pure nitrophloroglucinol can be separated from the reaction product by washing with water followed by extraction with DCM.

There is only one report of reduction of nitrophloroglucinol, which uses a mixture of zinc and hydrochloric acid to produce aminophloroglucinol hydrochloride (2,4,6-trihydroxyanilinium chloride).[200] For the purposes of synthesising a stable diazonium salt in the subsequent step, it is desirable to form the aniline as a tetrafluoroborate salt rather than as a chloride. Attempting to reduce nitrophloroglucinol to free aminophloroglucinol under non-acidic conditions in EtOH using N_2H_4 with Pd/C produced a red-brown residue that was poorly soluble in organic solvents. No pure material could be isolated from this residue. ^{13}C DEPTQ and ^{1}H-^{13}C HMBC NMR experiments were conducted on a sample of this material in d6-DMSO to determine the structure of the dominant product. These spectra confirmed the presence of CH_2 groups in the product, clearly indicating it is not aminophloroglucinol. The most likely structures based on the NMR data obtained are shown in Figure 6.17.
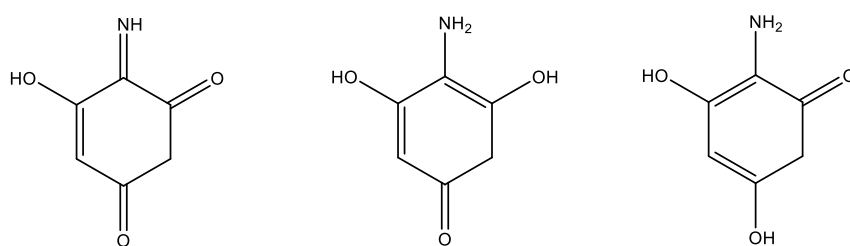
Figure 6.17. Possible structures of the major product from reaction of nitrophloroglucinol with N_2H_4 in the presence of palladium catalyst.

Distinguishing the product from its O–H and N–H proton environments was not possible due to chemical exchange with residual hydrazine content. Two of these possible structures are tautomers of aminophloroglucinol, and may thus be synthetically equivalent. However, due to the difficulty in extracting any pure material from the reaction residue, this reduction method was deemed unsuitable for the synthesis of aminophloroglucinol. $Na_2S_2O_4$ reduction of nitrophloroglucinol was also unsuccessful – when conducted in acetone,

spectra of the product mixture indicated reaction with the solvent, while in EtOH the product appears to be deprotonated nitrophloroglucinol without reduction. Considering the difficulty in isolating free aminophloroglucinol, the direct synthesis of the protonated form 2,4,6-trihydroxyanilinium tetrafluoroborate (Figure 6.18) was conducted instead. This was achieved by reduction of nitrophloroglucinol in dilute aqueous tetrafluoroboric acid using H_2 and Pd/C catalyst.
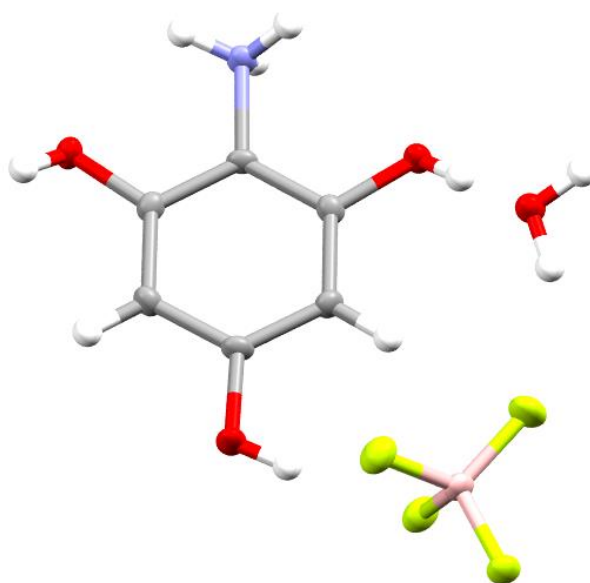
Figure 6.18. Thermal ellipsoid plot of 2,4,6-trihydroxyanilinium tetrafluoroborate monohydrate. Ellipsoids at the 50% probability level, hydrogen atoms are shown as spheres of fixed radius (0.2 Å).

Attempting to diazotise 2,4,6-trihydroxyanilinium tetrafluoroborate using isoamyl nitrite and tetrafluoroboric acid in EtOH resulted in red-brown products, which remained soluble if the solvent is replaced with Et_2O. Drying these Et_2O solutions afford residues from which no aromatic compound could be clearly identified. Toluene was found to be unable to extract any material from this residue. After attempting to extract the residue with toluene, the residues were no longer soluble in Et_2O, indicating some chemical change had occurred. Considering the intense colour of the product, and the electron-rich nature of aminophloroglucinol, it is likely that azo-bridged products are formed as shown in Figure 6.19.
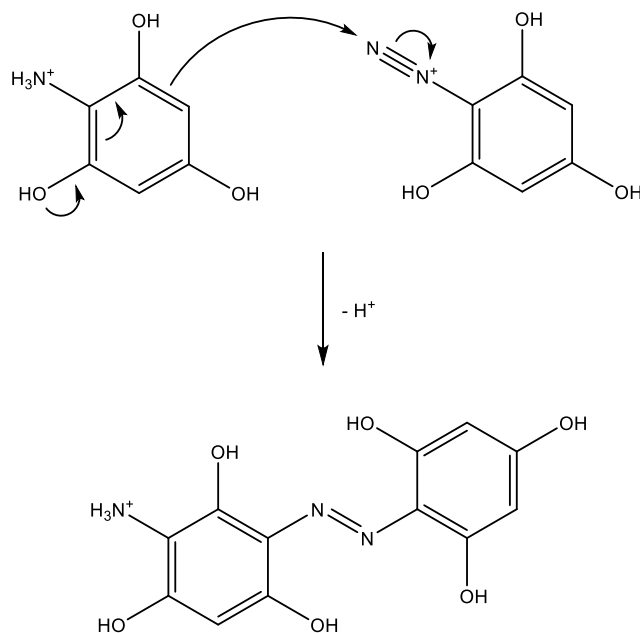
Figure 6.19. Possible azo-bridged product from reaction of 2,4,6-trihydroxybenzenediazonium with its precursor, 2,4,6-trihydroxyanilinium.

As the resulting azo-bridged product can itself be diazotised, this may eventually form polymeric species which may no longer be soluble in organic solvents. Despite the high predicted stability of pentazolylphloroglucinol, it may be that the instability of its precursor diazonium salts is a contributing factor to the absence of pentazolylphloroglucinol in the literature. Such an issue could conceivably be resolved by adding substituents to the remaining two positions of the ring, thus preventing C–N bond formation between molecules. Triaminophloroglucinol is a reported compound,[201] and could thus serve as a precursor to 2,4,6-trihydroxy-3,5-diaminobenzenediazonium salts, which could then be converted to the analogous pentazole compound. The synthesis of triaminophloroglucinol would involve the preparation of the highly explosive[202] trinitrophloroglucinol, thus the necessary safety precautions would complicate the synthesis slightly. Investigations into the synthesis of triaminophloroglucinol were not conducted due to time limitations.

6.2.3. Preliminary investigations into the synthesis of N_5O^-

As the synthesis of N_5O^- from N_2O and N_3^- is calculated to be unfeasible under ambient conditions due to a high reaction barrier, there is interest in investigating the reactivity of synthetic equivalents to N_2O towards N_3^-. Hyponitrous acid ($H_2N_2O_2$, HO–N=N–OH) is known to spontaneously decompose to release water and N_2O,[203] indicating that it may act synthetic alternative to N_2O. The spontaneous nature of the decomposition also indicates that it possesses greater thermodynamic potential than N_2O, which may make hyponitrous acid or its derivatives more effective for the formation of N_5O^-. When sodium *trans*-hyponitrite ($Na_2N_2O_2$) and $PPN(N_3)$ are mixed in the polar organic solvent HMPA, only the $PPN(N_3)$ dissolves, and no reaction occurs. After addition of two equivalents of $TsOH \cdot H_2O$, all $Na_2N_2O_2$ dissolves, indicating conversion to $H_2N_2O_2$. IR analysis of the solution shows much of the $PPN(N_3)$ has been converted to HN_3 (by comparison to a spectrum of HN_3 generated by addition of TsOH to $PPN(N_3)$ in the absence of $Na_2N_2O_2$), but there is no evidence of other reactions occurring. To make $H_2N_2O_2$ more reactive towards nucleophiles, it may be desirable to replace one of the OH groups with an effective leaving group. Thus, to a solution of $Na_2N_2O_2$ in MeCN, TsCl was added with the intention of forming tosyl hyponitrite ($TsONNO^-$). No reaction occurs, likely due to the insolubility of $Na_2N_2O_2$. However, if this reaction is conducted in the presence of 2.2 equivalents of 15-crown-5, small amounts of bubbling are observed upon addition and IR analysis of the filtered reaction solutions shows no remaining TsCl after 15 minutes. Addition of Et_2O to precipitate out the products resulted in the formation of crystals of Na(15c5)OTs, the mass of which accounts for almost all tosyl group added to the reaction. An MeCN solution of Na(15c5)OTs was prepared and found to have a near-identical IR spectrum to that of the reaction solution. Thus, the reaction of $Na_2N_2O_2$ with TsCl is selective for the decomposition of $Na_2N_2O_2$ as shown in Figure 6.20.
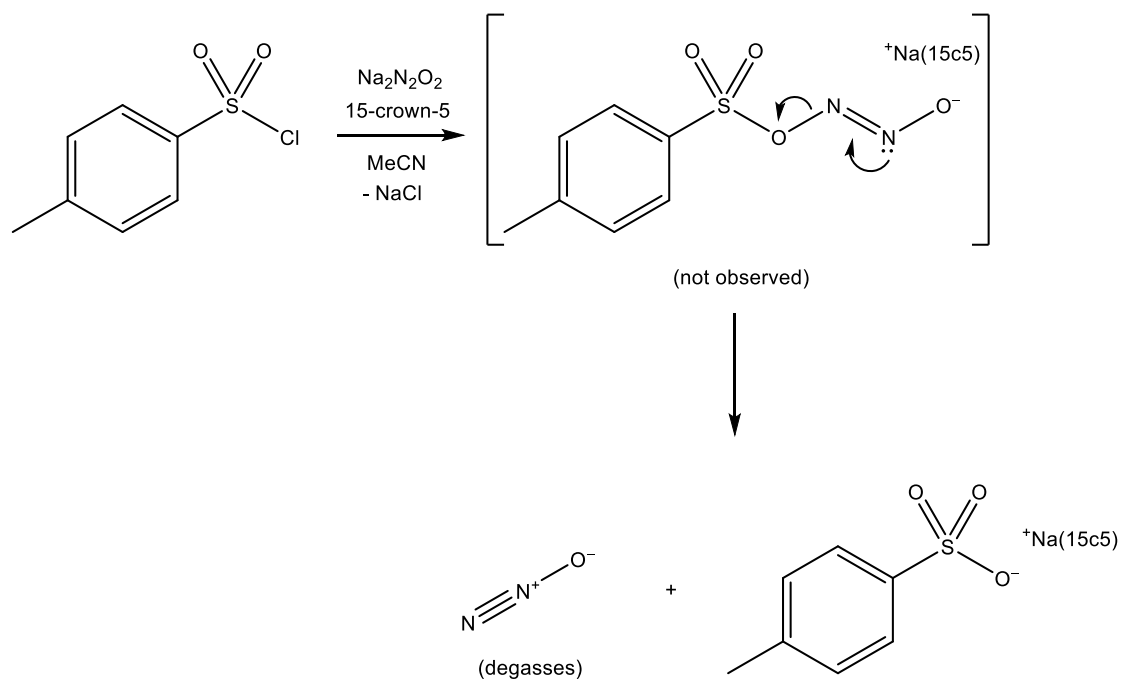
Figure 6.20. Reaction of TsCl with $Na_2N_2O_2$ in the presence of 15-crown-5 to form Na(15c5)OTs.

If this reaction is conducted with TsN_3 instead of TsCl, the reaction is significantly slower with considerable TsN_3 remaining after 10 minutes. However, after 5 hours most TsN_3 has converted to Na(15c5)OTs. The presence of both N_3^- and N_2O can be detected in this reaction solution, reinforcing the mechanism proposed in Figure 6.20. Additionally, this observation confirms that, under these conditions, N_3^- and N_2O do not react, providing some experimental evidence for the hypothesis that N_5O^- cannot be readily synthesised from N_3^- and N_2O under ambient conditions.

6.3. Conclusions

The viability of synthesising pentazoles from reaction of azide ions with various types of neutral diazo compounds has been investigated. Diazocyclopentadienides have been found to be too inert towards reaction with azide. Ru(II) and Rh(III) compounds have been found to be ineffective in catalysing this reaction, instead causing undesired reactions with diazocyclopentadienes. 2-Diazoimidazole does appear to undergo some reaction with azide based on the formation of bubbles upon addition, however the instability of 2-diazoimidazole causes inextricable precipitates to form from these reaction solutions, rendering this method ineffective. It may be that the reaction of azide with the more stable protonated form, imidazole-2-diazonium chloride, is more effective. As the protonated form of the pentazole would be less stable, this reaction would need to be conducted at low temperatures, and the resulting pentazole product could then be deprotonated to form 2-pentazolylimidazolate, which is calculated to be a relatively stable pentazole derivative,[155] and may be an effective precursor to pentazolate ions.

The reaction of PPN(N_3) with $SO_2(N_3)_2$ was found to produce $SO_2(N_3)^-$ in solution. By analogy to the literature reaction of NaN_3 with the Vilsmeier reagent, this reaction is likely to proceed via a pentazole intermediate, but this could not be isolated. In contrast, PPN(N_3) had no effect on $PO(N_3)_3$, which is attributed to the difference in electron-withdrawing capabilities of the sulphonyl and phosphoryl groups. In order to synthesise a more stable pentazole from sulphuryl azide, a less withdrawing sulphuryl group would need to be identified. Alternatively, a more withdrawing phosphoryl group may allow for a phosphoryl azide to react with azide to form a similar pentazole.

In contrast to a report in the literature, the reaction of diazoquinone with azide was found to produce 4-pentazolylphenoxide, however the rate of formation of 4-pentazolylphenoxide from this method is too slow compared to its rate of decomposition, making this an unviable synthetic strategy. This reaction does, however, demonstrate that the synthesis of pentazole derivatives from neutral diazo precursors is possible.

Attempts to synthesise the high (predicted) stability aryl-pentazole 4-pentazolyl-3,5-dihydroxyphenoxide were hindered by the apparent instability of 2,4,6-trihydroxybenzenediazonium tetrafluoroborate, which is likely spurred by its readiness to

form azo-bridged compounds. A more promising alternative which should not suffer this issue is suggested, derived from 1,3,5-triaminophloroglucinol.

Hyponitrite derivatives have been investigated as possible alternatives to N_2O for the predicted reaction of N_2O with N_3^- to synthesise N_5O^-. In HMPA, N_3^- does not react with $Na_2N_2O_2$ or $H_2N_2O_2$. Attempts to synthesise a more reactive hyponitrite, $TsONNO^-$, from $Na_2N_2O_2$ and TsCl resulted in decomposition to N_2O and TsO^-. Replacing TsCl with TsN_3 affords N_2O and N_3^-, incidentally proving that N_2O and N_3^- do not react in MeCN under ambient conditions. Other conditions may still allow for the reaction of N_2O or $H_2N_2O_2$ with N_3^-, but such conditions have yet to be found. It is notable that the solvents tested here are aprotic organic solvents. As the reaction involves zwitterionic and charged species, water or other protic solvents may facilitate this reaction by stabilising the charges with hydrogen bond interactions.

7. Summary

7.1. Precursors to low-valent silicon azides

Numerous potential precursors for the synthesis of low-valent silicon azides have been developed. The first class of these are hydrido(azido)silicon compounds, which are expected to be viable precursors to low-valent silicon azides based on the known conversion of hydrido(chloro)silanes to low-valent silicon chlorides.[50, 60] The most significant of these developments is the establishment of a procedure for synthesising triazidosilane ($HSi(N_3)_3$), as this compound is directly analogous to the species used to synthesise many low-valent silicon chlorides, trichlorosilane ($HSiCl_3$). The synthesis involves treating $HSiCl_3$ with the aluminium azide reagent sodium tetraazidoaluminate tetrakis(THF) in (deuterated) benzene. It has been demonstrated that the previously-discovered issue of $HSi(N_3)_3$ disproportionation can be avoided with careful control of reaction conditions. Unfortunately, the sensitivity of $HSi(N_3)_3$ towards disproportionation still poses an issue towards the reliability of the synthesis developed here. The synthesis and simultaneous disproportionation of $HSi(N_3)_3$ has been monitored spectroscopically from the reaction of $HSiCl_3$ with $TMS(N_3)$ in C_6D_6, affording NMR spectroscopic data on all species of the form $HSiX_3$, H_2SiX_2 and H_3SiX (X = Cl, N_3). For compounds of these species with at least one azido group, this represents the first NMR data on these compounds, thus enabling identification of these species in future studies. It has also been demonstrated that $HSi(N_3)_3$ can be synthesised from the reaction of $LiAlH_4$ with $Si(N_3)_4$, however this yield of $HSi(N_3)_3$ is far too low for this to be a viable preparative method. In addition to $HSi(N_3)_3$, hydrido(azido)silicon complexes have been synthesised. Substantial improvements to the synthesis of the known complex $(^{Dipp}NCN)SiH(N_3)_2$[73] have been made, improving the isolated yield of its synthesis to 71% (up from the reported yield of 19%). The improved methods have been applied to the synthesis of two new amidinato silicon complexes, $(^{tBu}NCN)SiH(N_3)_2$ and $(^{TMS}NCN)SiH(N_3)_2$. The former of these complexes has been shown to react with $LiN(TMS)_2$ to afford another hydrido(azido)silicon complex, $(^{tBu}NCN)SiH(N_3)(N(TMS)_2)$. This reactivity matches that of $(^{Dipp}NCN)SiH(N_3)_2$ and is contrary to the observed reactivity of $(^{tBu}NCN)SiHCl_2$, confirming that the previously observed difference in reactivity between $(^{Dipp}NCN)SiH(N_3)_2$ and $(^{tBu}NCN)SiHCl_2$ can be attributed to the difference between chloro and azido groups rather

than a difference in amidinato ligand. A neutral hexacoordinate hydrido(azido)silicon complex, (^{Dipp}NCN)$_2$SiH(N$_3$), has also been synthesised by reaction of (^{Dipp}NCN)SiH(N$_3$)$_2$ with Na(^{Dipp}NCN). While working with silicon complexes of ^{Dipp}NCN, a new homoleptic azido silicon species, Si(N$_3$)$_5^-$, has been synthesised as a salt with (^{Dipp}NCN)H$_2^+$.

(Ar = 4-tertbutylphenyl-)
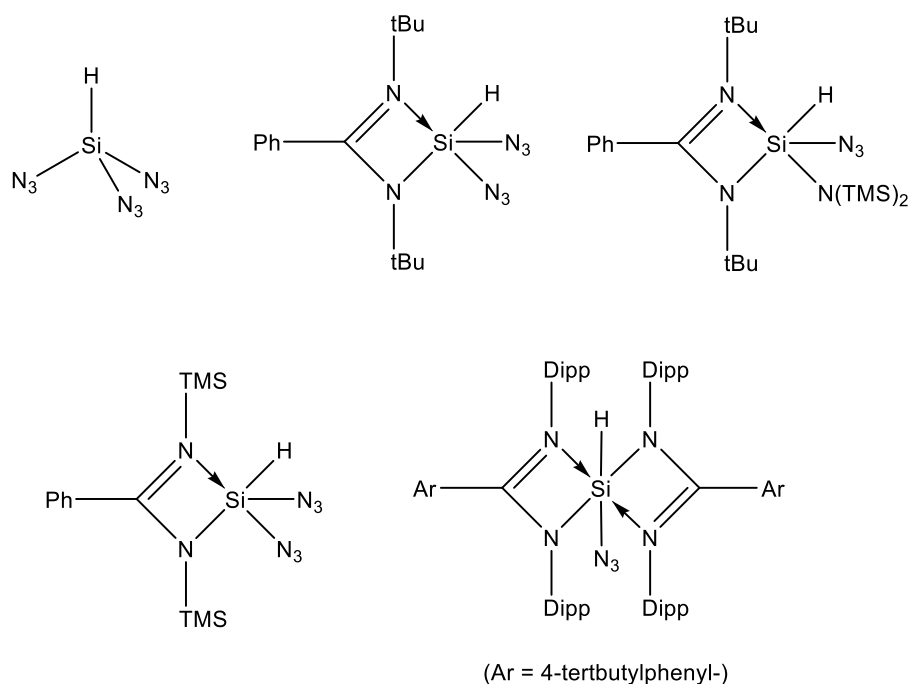
Figure 7.1. Hydrido(azido)silicon compounds developed in this work.

The second class of low-valent silicon azide precursor developed in this work are complexes involving a tridentate ligand coordinated to SiCl$_2$. The previously-reported complex IPrSiCl$_2$ has been demonstrated to undergo de-coordination of the IPr ligand from the silicon when treated with the azide transfer reagents PPN(N$_3$) or NaAl(N$_3$)$_4$(THF)$_4$. As such, the tridentate ligand 2,6-bis(N-(2,6-diisopropylphenyl)acetimino)pyridine (BIP) was considered as an alternative to IPr. BIP does not react with SiCl$_4$ or Si(N$_3$)$_4$ even at elevated temperatures. BIP only reacts with HSiCl$_3$ at elevated temperatures, and the reaction is too unselective to isolate any products. Three complexes containing the SiCl$_2$ motif were identified from the reaction of BIP with Si$_2$Cl$_6$. In all three cases, modifications to the ligand occurred. In one of these cases, the modification to the ligand does not significantly disrupt the electronic structure of the ligand, thus affording the first isolated silicon complex with a bis(imino)pyridine-type ligand. 2,2';6',2''-terpyridine was also found to react with Si$_2$Cl$_6$ to afford an adduct of SiCl$_2$, also with modification to the ligand. Reaction of BIP with HSi(N$_3$)$_3$ affords a dimerised complex containing SiH$_2$ functionalities with no remaining azido groups,

believed to be the result of reaction of BIP with $H_2Si(N_3)_2$ (a disproportionation product of $HSi(N_3)_3$). These results are summarised in Figure 7.2.
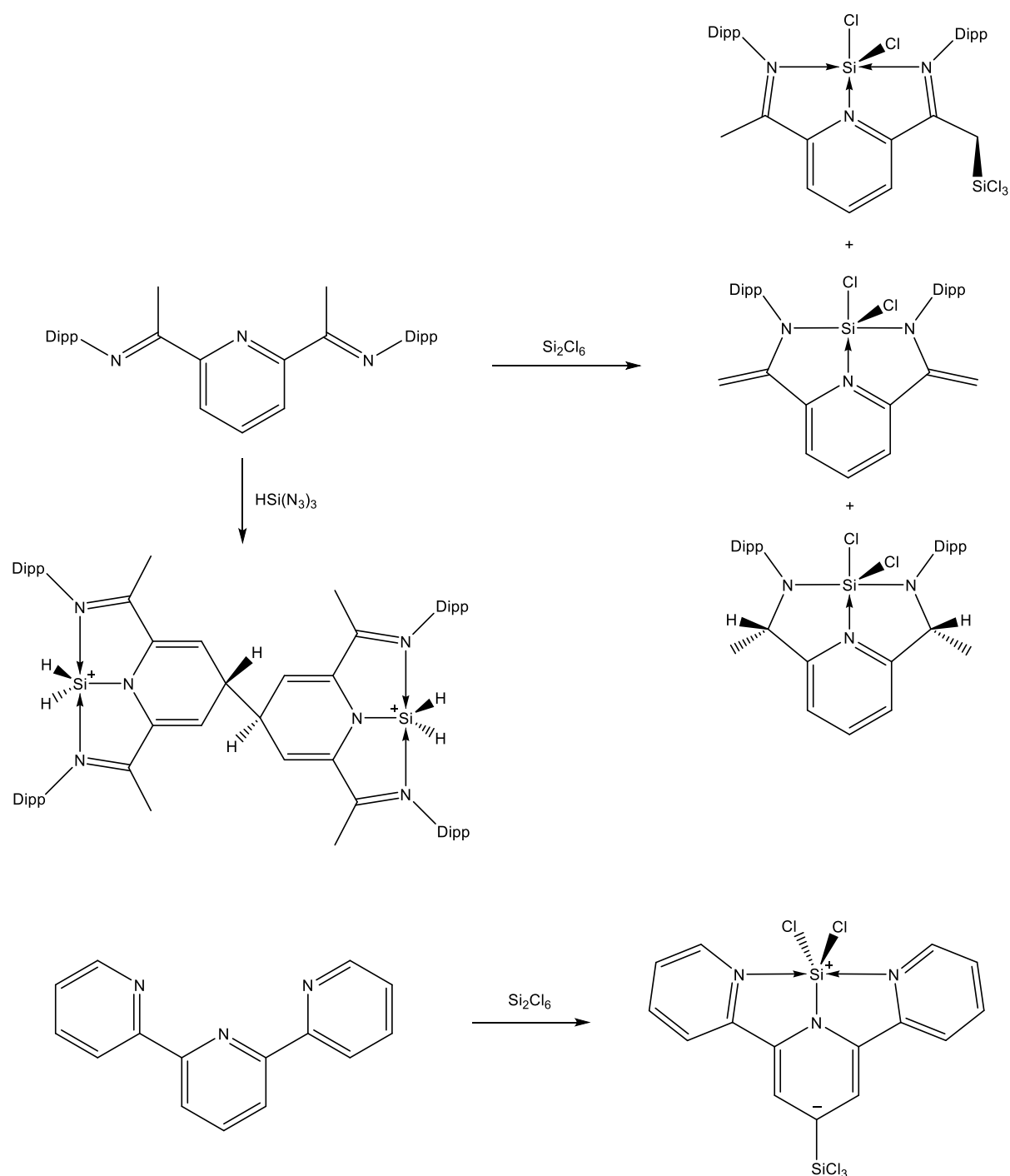
Figure 7.2. Simplified reaction diagrams for the formation of five new silicon complexes bearing tridentate ligands, showing the approximate geometry of the products.

The third class of low-valent silicon azide precursor developed in this work are salts of trichlorosilanide ($SiCl_3^-$). This anion has been previously detected *in-situ*[138] and proposed as

a reaction intermediate,[33] but not isolated. Numerous methods to generate $SiCl_3^-$ *in-situ* have been tested, largely from reaction of Si_2Cl_6 with a variety of nucleophiles. Of these reactions, it has been found that reaction of $LiN(TMS)_2$ with Si_2Cl_6 in THF or DME selectively forms $LiSiCl_3$ in solution. Unfortunately, attempts to isolate this compound out of solution result in decomposition to afford LiCl. The reaction of potassium metal with Si_2Cl_6 in the presence of 18-crown-6 affords the $K(18c6)^+$ salt of the known anion $Si_6Cl_{14}^{2-}$. This is a new route towards this ion, which has previously only been synthesised by reaction of Si_2Cl_6 with tetraorgano phosphonium/ammonium chlorides (PR_4Cl or NR_4Cl). The resulting $[K(18c6)]_2[Si_6Cl_{14}]$ may also be a potential precursor to low-valent silicon species.

7.2. Reduction of silicon azides and synthesis of nitrido-silicon compounds

The reaction between $(^{Dipp}NCN)SiH(N_3)_2$ and ItBu has previously been reported to afford $[ItBuH][(^{Dipp}NCN)SiH(N_3)_3]$.[73] Based on reaction stoichiometry, it has been speculated that this reaction may also afford a low-valent silicon azide, $(^{Dipp}NCN)Si(N_3)$. This has now been disproven, as the other product clearly contains an Si−H bond based on NMR data, with the most likely product being a silyl-substituted N-heterocyclic carbene derived from ItBu.

Multiple other routes towards low-valent silicon azides have been attempted. The reduction of silicon azides with the silanide reagent $(THF)_3LiSi(TMS)_3$ affords selective reduction of azido groups rather than the silicon centre. This has resulted in the isolation of two silaimines and a cyclodisilazane (Figure 7.3). This cyclodisilazane, 2,2,4,4-tetraazido-1,3-bis(tris(trimethylsilyl)silyl)cyclodisilazane (TABTC), contains a four-membered Si_2N_2 ring in which both silicon atoms are bound only to nitrogen atoms, and both nitrogen atoms are bound only to silicon atoms. As such, it can be seen as a form of azido(nitrido)silicon compound and may offer insight into the structural motifs within silicon nitrides.
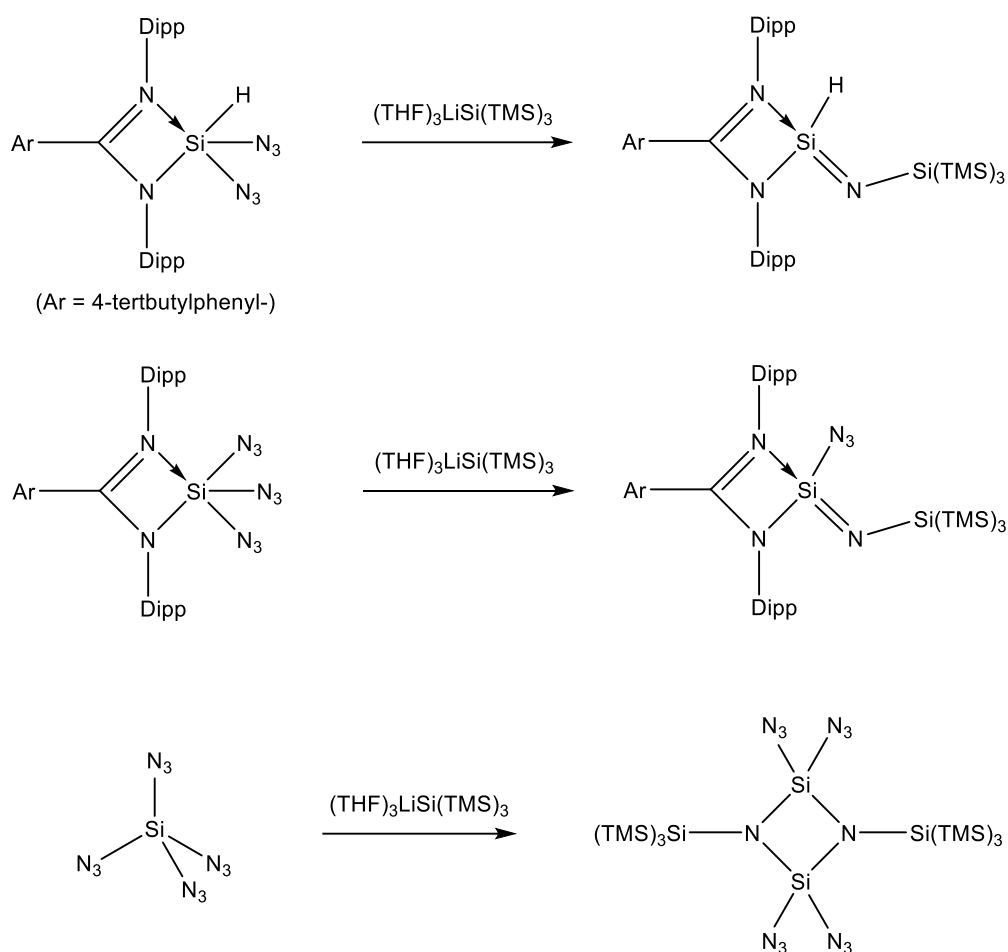
Figure 7.3. Reduction of an azido group from (^{Dipp}NCN)SiH(N$_3$)$_2$, (^{Dipp}NCN)Si(N$_3$)$_3$ and Si(N$_3$)$_4$ by (THF)$_3$LiSi(TMS)$_3$.

The reduction of Si(N$_3$)$_4$ with alkali metals predominantly afforded species that no longer contain azido groups. The major product is postulated to be elemental silicon, based on appearances and the known formation of silicon from alkali metal reduction of SiCl$_4$.[101, 102] In one case, where the amount of alkali metal was not quite enough for complete reduction to elemental silicon, traces of an insoluble substance with a broad IR absorption at 2175 cm^{-1} was observed.

As mentioned in Chapter 7.1, the addition of PPN(N$_3$) to the already reduced silicon species IPrSiCl$_2$ results in decomposition of azido groups. The insoluble residue produced by this reaction was found to still contain azido groups by IR analysis. The resulting azide absorption bands are broad, suggesting a polymeric material that is likely the result of SiX$_2$ (X = N$_3$, Cl) decomposition, since free IPr ligand is identified as the only major soluble product.

The most intense IR absorption from the residue of reaction between $IPrSiCl_2$ and $PPN(N_3)$ is a broad absorption at 2168 cm^{-1}. The formation of material with a broad absorption band around 2170 cm^{-1} has been observed multiple times throughout this work, and is attributed to an amorphous polymer with the formula $[Si(N)(N_3)]_n$. The reactions that form material with this absorption are either reactions where the formation of the (likely) unstable species $Si(N_3)_2$ is predicted, or are reactions which were deliberately attempting to synthesise $Si(N)(N_3)$. The most important of these reactions are a series of thermal decomposition reactions of $(^{Dipp}NCN)SiH(N_3)_2$. These decomposition reactions predominantly afford quantitative amounts of $(^{Dipp}NCN)H$, so the formation of $Si(N_3)_2$ (or its decomposition products) is predicted by stoichiometry. Analysis of the residues of these decompositions show two insoluble products, formed in different ratios by different decomposition experiments, with broad IR absorption bands. Analysis of the gaseous products in two of these decomposition reactions shows the evolution of N_2 (and only N_2), indicating these products must have the empirical formulae SiN_{6-x}. With assistance from these observations, gravimetric analysis indicates that one of these products (with an IR absorption band around 2259 cm^{-1}) has an empirical formula of SiN_2, while the other product (with an IR absorption band around 2172 cm^{-1}) has an empirical formula of SiN_4. The presence of an azide absorption in the IR spectrum of this latter product indicates that it still contains azido groups, and thus given the tentative formula $[Si(N)(N_3)]_n$. A summary of the reactions that have been observed to form this material is given in Figure 7.4.
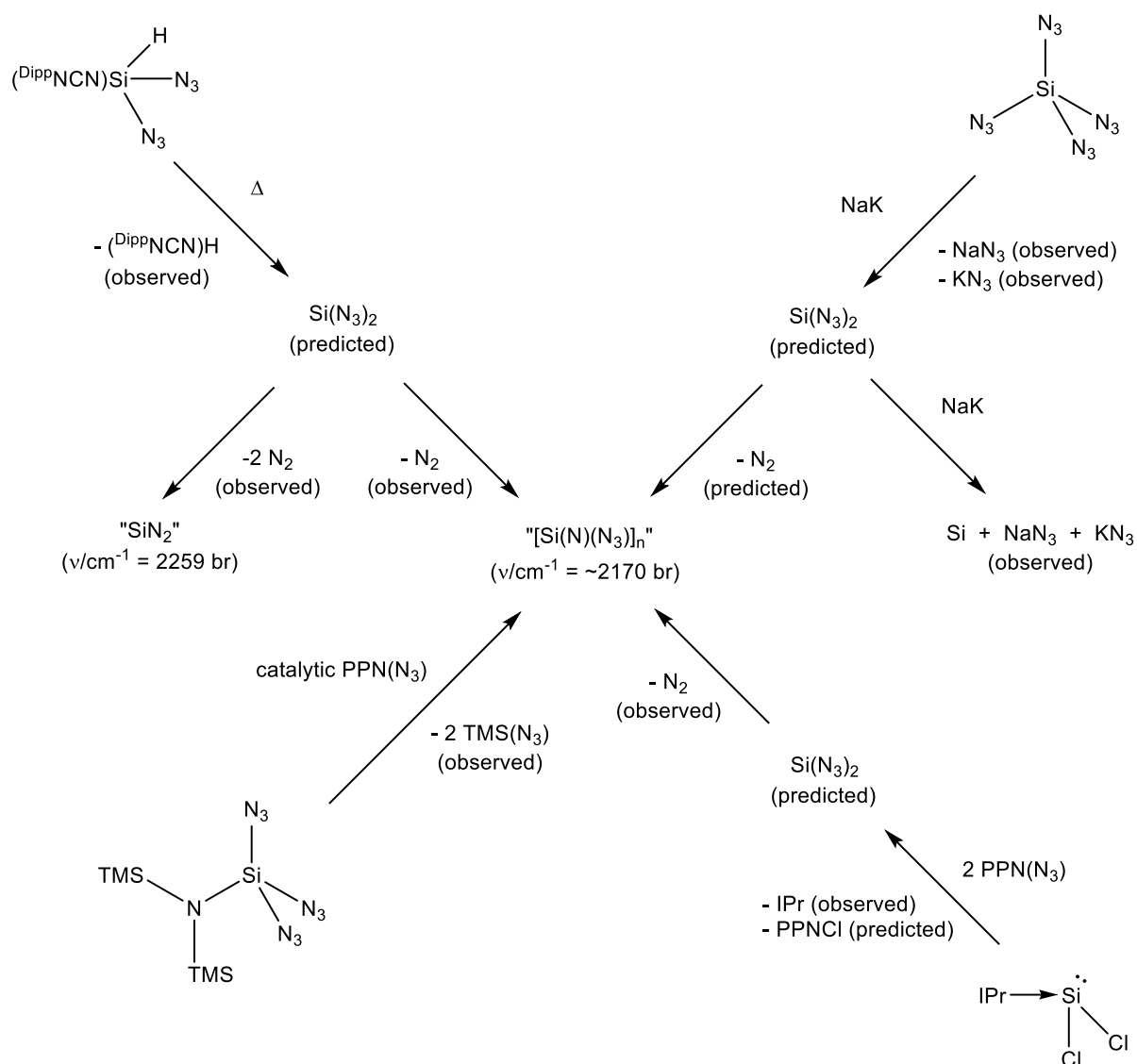
Figure 7.4. Reactions in this work that have been observed to afford a silicon-nitrogen material with a broad IR absorption around 2170 cm^{-1}, hypothesised to be [Si(N)(N$_3$)]$_n$ based on indirect evidence from these reactions.

7.3. Investigating alternative synthetic routes towards pentazoles

As an alternative all-nitrogen functional group to the azido group, the synthesis of compounds containing the pentazolyl group have been investigated. Currently, the lack of a reliable source of the pentazolate ion hinders the study of silicon pentazoles, so investigations have been conducted with a focus on developing alternative precursors for pentazolate synthesis.

The hypothesised reaction of diazocyclopentadiene (CpN$_2$) with azide ions to form pentazolylcyclopentadienide was found to be inaccessible, as CpN$_2$ was found to be unreactive towards multiple azide sources (PPN(N$_3$), HN$_3$, NaAl(N$_3$)$_4$(THF)$_4$, RhCp*(N$_3$)$_2$PPh$_3$). A substituted derivative of CpN$_2$, tetramethyldiazocyclopentadiene (Cp^{x}N$_2$) has been synthesised, however it similarly shows a lack of reactivity towards sources of azide ions. FeCl$_2$ was found to have no catalytic effect to aid this reaction, while rhodium and ruthenium complexes were found to decompose the diazo group of Cp^{x}N$_2$.

2-diazoimidazole was found to react with NaN$_3$, based on the evolution of gasses on addition. Unfortunately, 2-diazoimidazole appears to decompose to an insoluble black solid, the formation of which prevented adequate investigation of the products of this reaction.

The reaction of diazoquinone with NaN$_3$ was found to generate the known pentazolyl derivative, 4-pentazolylphenoxide (previously synthesised from deprotonation of the parent 4-pentazolylphenol[154]). This reaction demonstrates that neutral diazo compounds can be viable precursors towards pentazolyl compounds. In this case, however, the decomposition of 4-pentazolylphenoxide competes with its formation, making this particular reaction unfeasible as a preparative method.

The synthesis of pentazolylphloroglucinol (2-pentazolyl-1,3,5-beznenetriol) was attempted, as this compound has been predicted to have remarkably high stability for an aryl-pentazole.[151] The necessary diazonium precursor, 2,4,6-trihydroxybenzenediazonium has been found to be unstable, which may make pentazolylphloroglucinol inaccessible.

Sulphuryl diazide (SO$_2$(N$_3$)$_2$) has been found to react with PPN(N$_3$) to afford SO$_2$(N$_3$)$^-$ in solution by decomposition on an azido group. This is hypothesised to proceed via a pentazole intermediate, but this could not be proven. The same mode of reactivity has also been observed when azide is generated *in-situ* by the substitution of one of the SO$_2$(N$_3$)$_2$ azido groups by amines. By contrast, PO(N$_3$)$_3$ does not react with PPN(N$_3$), indicating the more strongly withdrawing sulphonyl group is necessary for the observed reactivity of a covalent azide with azide ions. Attempted syntheses of pentazolyl compounds from reaction of neutral diazo and azido compounds with azide ions are summarised in Figure 7.5.
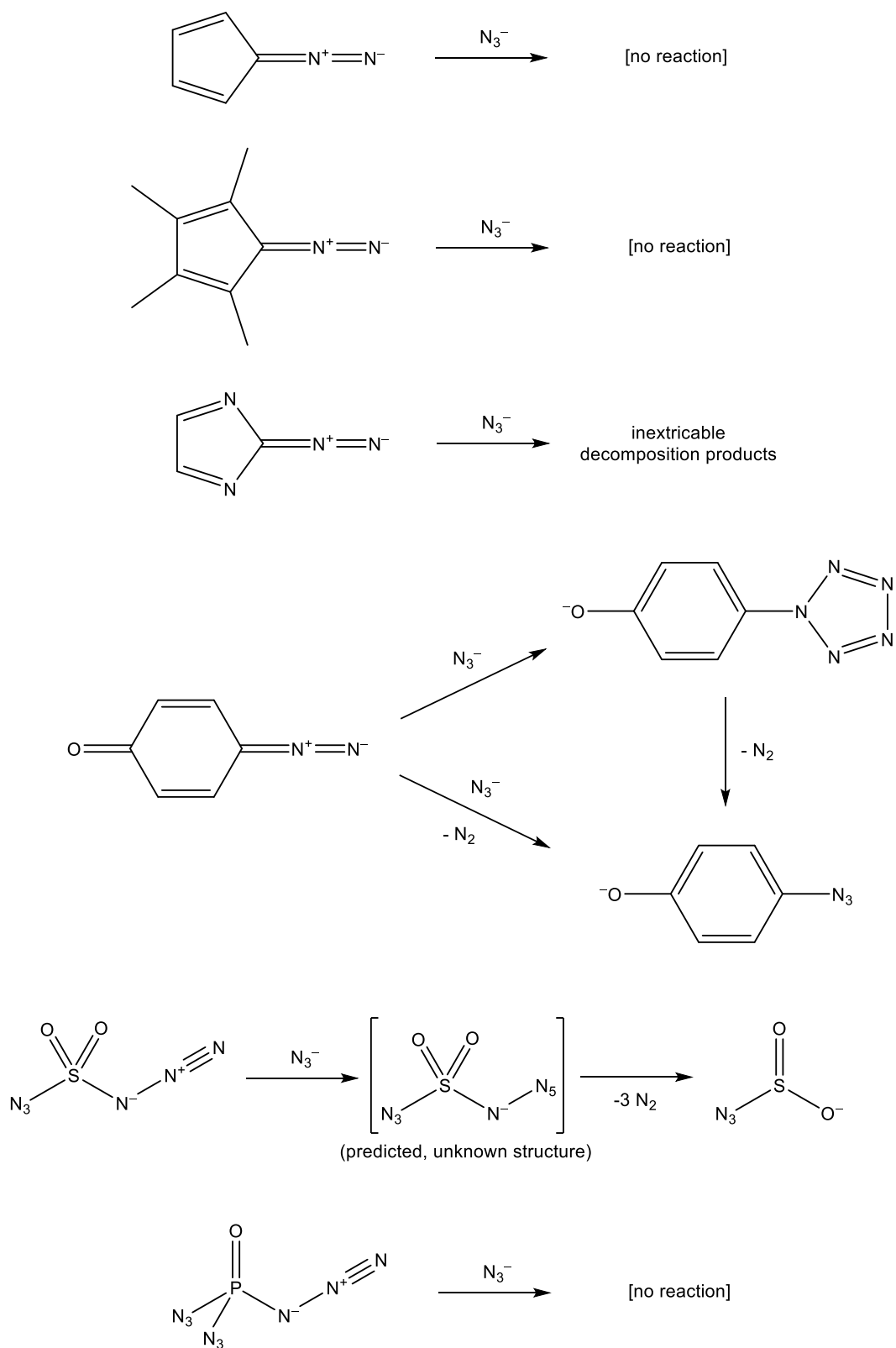
Figure 7.5. Attempted reactions of diazo and azido compounds with azide ions, and their observed outcomes.

8. Experimental details

8.1.1. General experimental procedures

Unless otherwise stated, all procedures outlined were conducted with strict exclusion of air using Schlenk-line and Glovebox techniques under an atmosphere of argon (Glovebox specifications: MBraun UNIlab, maintained at < 0.1 ppm H_2O, < 0.1 ppm O_2). Reactions were conducted at room temperature (20 °C ± 5 °C) unless otherwise specified. Stirring is achieved using a magnetic stirrer bar added to the reaction vessel, typically coated with Teflon. In reactions involving alkali metals, organolithium reagents, or $(THF)_3LiSi(TMS)_3$, glass-coated stirrer bars were instead used to avoid reaction of these reagents with Teflon. Sonication is achieved using an Ultrawave U300H Ultrasonic Bath filled with water. Unless otherwise stated, filtrations were carried out through glass microfibre filter paper dried in an oven at 80 – 120 °C prior to use. In other cases, "glass frit" refers to a fine sintered glass filter with pore size of 10 – 16 μm (porosity grade 4), and "Celite" refers to commercial Celite 545, which has been dried at 200 °C for 3 days and stored under argon to exclude moisture. "Vacuum" refers to a vacuum manifold maintained by a rotary vane oil pump, with a typical absolute vacuum pressure of 10^{-2} – 10^{-1} mbar. "High vacuum" refers to a vacuum manifold maintained by a turbo pump, with a typical absolute vacuum pressure of 10^{-5} – 10^{-4} mbar.

Infrared (IR) spectra were acquired using a Bruker Tensor 27 FT-IR spectrometer, typically using a resolution of 2 cm^{-1} with 16 scans. Spectra were recorded using the OPUS software package and analysed using the MestReNova software package. Solid samples were recorded with a wavenumber range of 4000 – 500 cm^{-1}, with a crushed powder sample suspended in paraffin oil (referred to as a Nujol mull), held between a pair of NaCl windows. This paraffin oil is kept dry by storing over sodium under an atmosphere of argon. Samples are backgrounded against the empty windows, and therefore display the spectrum of the paraffin oil in addition the sample. A spectrum of the paraffin oil used to make Nujol mulls is available in the electronic appendix for reference. Solution phase samples were recorded with a wavenumber range of 4000 – 1100 cm^{-1}, using a cell composed of CaF_2 windows separated by a Teflon spacer. Samples are backgrounded against the same cell filled with the relevant solvent. All air-sensitive samples were prepared under an atmosphere of argon.

As the spectrometer is not housed in an inert atmosphere, traces of sample degradation due to air exposure occurs in some cases. For this experimental chapter, isolated compounds (with recorded IR data) have all prominent signals reported. For crude reaction products, only signals in the diagnostic region of 2300 – 1900 cm^{-1} are reported in the interest of clarity. Original spectra can be found as part of the electronic appendix as OPUS output files.

Nuclear Magnetic Resonance (NMR) spectra were acquired at 298 K (25 °C) unless otherwise stated. Unless otherwise stated, spectra were recorded using a Bruker Avance III HD 400 MHz spectrometer. In a handful of cases, data was recorded using a Bruker Avance III HD 500 MHz spectrometer. Both instruments collect data using the TopSpin 3.6 software package. ^{14}N spectra are referenced externally to 90% CH_3NO_2 in $CDCl_3$, spectra of other nuclei are referenced externally to the respective IUPAC recommended standards.[204] Where possible, ^{1}H and ^{13}C spectra are calibrated to the residual signal of the dominant solvent according to reported literature.[205] Unless otherwise stated, other spectra are calibrated according to the default calibration of the instrument. ^{13}C spectra are recorded with proton decoupling, spectra of other nuclei are recorded without decoupling. NMR analysis of samples in non-deuterated solvents were conducted with the addition of a sealed capillary containing either d6-DMSO or D_2O for locking. Data processing was performed on either TopSpin 3.6 or TopSpin 4.3 software. All air-sensitive NMR samples were prepared under an atmosphere of argon in air-tight NMR tube fitted with a J. Young Teflon valve. For this experimental chapter, isolated products have their chemical shift values reported along with coupling information (where applicable), integral ratios and assignments. Signals corresponding to solvents are not reported except in cases where an isolated compound forms as a solvate. All ^{27}Al and ^{29}Si spectra contain a broad signal corresponding to the glass of the sample tube. Original spectra can be found as part of the electronic appendix as Topspin output folders.

Single Crystal X-Ray Diffraction (SCXRD) analysis was conducted using Bruker SMART, Kappa and Venture diffractometers (details in Table 8.1). Crystals were mounted on MiTiGen Micromount loops after selection under paraffin oil and cooled to 100 K using an Oxford Cryosystems Cryostream cooler.

Diffractometer	Radiation type	Radiation wavelength	Detector type
SMART	Mo-Kα	0.71073 Å	CCD
Kappa	Mo-Kα	0.71073 Å	CCD
Venture	Cu-Kα	1.54178 Å	PHOTON CMOS

Table 8.1. Summary of diffractometer radiation wavelengths and detector types used.

Data was collected and integrated using Bruker APEX3 software. Structures were then solved and refined using Shelxt and Shelxl respectively, within the Olex2 software package.[206, 207] Full details on data collection, crystal properties and structure refinement for each structure can be found as part of the electronic appendix as .cif files.

8.1.2. Reagents used

Table 8.2 outlines the source and quoted reagent grade (where available) of the reagents used. Locally-synthesised reagents and reagents of unknown origin were found to be of acceptable purity by NMR analysis prior to use. All air-sensitive reagents, or reagents to be used in reactions involving air-sensitive reagents, were stored under an atmosphere of argon. Benzonitrile, 15-crown-5 and diisopropylamine were dried over activated 3 Å molecular sieves. Anthracene, 2,2'-bipyridine, 18-crown-6, and naphthalene were dried by sublimation under open vacuum. Diisopropylethylamine and triethylamine were dried over CaH$_2$, then distilled. Sodium azide was dried under high vacuum at 100 °C. Anhydrous sodium *trans*-hyponitrite was obtained by drying sodium *trans*-hyponitrite hydrate under high vacuum until no water content was detected by IR analysis. Lithium granules were washed by sonication suspended in Et$_2$O, discarding all material that did not float. Clean sodium granules were obtained by melting and resolidifying sodium chunks suspended in toluene. Potassium chunks were cleaned by cutting off the outer surfaces. Potassium tert-butoxide was purified by dissolving in THF, repeatedly filtering the resulting solution until it stayed clear, then removing the THF under vacuum. Sulphonyl chloride was degassed under vacuum shortly prior to use. The actual concentration of methyllithium was determined by titration shortly before use, using 2,2'-bipyridine as an indicator and tert-butanol as a titrant. All other reagents were used as purchased without further purification. The 3 Å molecular

sieves were activated by initially heating under air at 240 °C for 1 week, followed by 1 day at 240 °C under vacuum.

Table 8.2 (below). List of reagents used in this experimental work, with their respective sources and purity grades.

Reagent	Abbreviation / formula	Supplier / synthesised by	Reagent grade
Acetic acid	AcOH	Fluka	≥99.8%
Aluminium trichloride	$AlCl_3$	Fluka	≥99.0%
2-aminoimidazole hemisulphate		Fluorochem	
4-aminophenol hydrochloride		Sigma Aldrich	
Anthracene		Fluka	≥90%
Benzeneruthenium dichloride dimer	$[(C_6H_6)RuCl_2]_2$	Aldrich	
1,3,5-benzenetriol	Phloroglucinol	Fluorochem	
Benzonitrile	PhCN	Sigma Aldrich	≥99%
2,2'-bipyridine	Bpy	Sigma Aldrich	≥99%
Bis(2,6-diisopropylphenyl)carbodiimide	DippNCNDipp	Fluorochem	
Di-tert-butylcarbodiimide	tBuNCNtBu	Aldrich	99%
1,3-di-tert-butylimidazol-2-ylidene	ItBu	Peerless[73]	
Bis(triphenylphosphine)iminium chloride	PPNCl	Aldrich	97%
Bromobenzene	PhBr	Aldrich	99%
1-bromo-4-tert-butylbenzene		Alfa Aesar	97%
15-crown-5	15c5	Aldrich	98%
18-crown-6	18c6	Fluorochem	
Dicyclopentadiene	$(CpH)_2$	Fisher	95%
Diisopropylamine	$HNiPr_2$	Sigma Aldrich	99.5%
2,6-diisopropylaniline	$DippNH_2$	Alfa Aesar	90+%
Diisopropylethylamine	DIPEA	[unknown]	
Dipicolinic acid		Aldrich	99%
Glyoxal in water		Sigma Aldrich	40% wt. in H_2O
Hexachlorodisilane	Si_2Cl_6	TCI	>98.0%
Hydrazine hydrate	N_2H_4 H_2O	Sigma Aldrich	98%
Hydrazoic acid in diethyl ether	HN_3	Smallwood[140]	1.7M in Et_2O
Hydrochloric acid 37%	HCl	Sigma Aldrich	≥37%

Iron(II) chloride	$FeCl_2$	Aldrich	98%
Isopentylnitrite	Isoamylnitrite	Sigma Aldrich	96%
Lithium aluminium hydride	$LiAlH_4$	Sigma Aldrich	95%
Lithium bis(trimethylsilyl)amide	$LiN(TMS)_2$	Sigma Aldrich	97%
Lithium granules	Li	Sigma Aldrich	99%
Lithium tri(tert-butoxy)aluminium hydride	$LiAl(OtBu)_3H$	Aldrich	97%
Magnesium sulphate (dried)	$MgSO_4$	Fisher	62-70%
Magnesium turnings	Mg	Alfa Aesar	99+%
Methyllithium in diethyl ether	MeLi	Aldrich	1.6M in Et_2O
Naphthalene		Alfa Aesar	99.6%
Nitric acid 68%	HNO_3	VWR	68%
Palladium on activated carbon	Pd/C	Aldrich	10% Pd
Paraformaldehyde		Aldrich	"Reagent grade"
Pentamethylcyclopentadienyl rhodium diazide triphenylphosphine adduct	$RhCp*(N_3)_2PPh_3$	[unknown]	
Phosphoryl chloride	$POCl_3$	Alfa Aesar	99%
Potassium carbonate	K_2CO_3	VWR	100%
Potassium chunks	K	Aldrich	98%
Potassium tert-butoxide	KOtBu	Thermo Scientific	98+%
Potassium tri(3,5-dimethyl-1-pyrazolyl)borohydride	KTp*	Acros Organics	99%
p-toluenesulphonic acid monohydrate	$TsOH.H_2O$	Aldrich	98.50%
Rhodium trichloride hydrate	$RhCl_3(H_2O)_3$	Aldrich	38-40% Rh
Silicon tetrachloride	$SiCl_4$	Alfa Aesar	99%
Sodium chunks	Na	[unknown]	
Sodium amide	$NaNH_2$	Aldrich	95%
Sodium azide	NaN_3	Sigma Aldrich	≥99.5%
Sodium carbonate	Na_2CO_3	VWR	100%
Sodium dithionite	$Na_2S_2O_4$	Fisher	≥85%
Sodium granules	Na	Sigma Aldrich	99%
Sodium hydride	NaH	Aldrich	95%
Sodium nitrite	$NaNO_2$	Fluka	≥99.0%
Sodium trans-hyponitrite hydrate	$Na_2N_2O_2$	Chem Cruz	
Sulfuryl chloride	SO_2Cl_2	Sigma Aldrich	97%

Sulphuric acid 95%	H_2SO_4	Fisher	≥95%
Tert-butyllithium in pentane	tBuLi	Aldrich	1.7M in pentane
Tetrafluoroboric acid 50%	HBF_4	Alfa Aesar	ca. 50% w/w in H_2O
Tetrafluoroboric acid diethyl ether complex	$HBF_4·Et_2O$	Aldrich	
tetrakis(trimethylsilyl)silane	$Si(TMS)_4$	Nicks[208]	
1,2,3,4-tetramethyl-1,3-cyclopentadiene	Cp^xH	Thermo Scientific	85%
Tetraphenylphosphonium azide	PPh_4N_3	Peerless[73]	
Tetraphenylphosphonium chloride	PPh_4Cl	Alfa Aesar	98%
2,2';6',2"-terpyridine	Terpy	Acros Organics	96%
Tert-butanol	tBuOH	Sigma Aldrich	≥99%
4-tert-butylpyridine		Fluorochem	97%
Tosyl chloride	TsCl	Acros Organics	99+%
Trichlorosilane	$HSiCl_3$	Alfa Aesar	98%
Triethylamine	Et_3N	Sigma Aldrich	≥99%
Trimethylsilyl azide	$TMS(N_3)$	[unknown]	
Trimethylsilyl chloride	TMSCl	Alfa Aesar	98%
2,4,6-tri(tert-butyl)-1-bromobenzene	Mes*Br	Fluorochem	
Xantphos		Aldrich	97%
Zinc chloride	$ZnCl_2$	Alfa Aesar	98+%

8.1.3. Solvents used

Table 8.3 outlines the supplier and quoted reagent grade of the solvents used. MeCN, Et_2O, DME, THF, toluene, CD_3CN, CD_2Cl_2 and d8-toluene were dried over CaH_2, then distilled under reduced pressure. HMPA, hexane, C_6D_6 and d8-THF were degassed under vacuum, then dried over activated 3 Å molecular sieves. Other solvents were used as purchased without further purification. Dried solvents were stored over activated 3 Å molecular sieves under an atmosphere of argon.

Solvent	Abbreviation / formula	Supplier	Solvent grade
Acetonitrile	MeCN	Fisher	≥99.9%
Acetone		Fisher	≥99%
Benzene (anhydrous)	C_6H_6	Sigma Aldrich	99.8%
Chloroform	$CHCl_3$	Fisher	≥99.8%
Dichloromethane	DCM	Fisher	≥99.8%
Diethyl ether (BHT stabilised)	Et_2O	Sigma Aldrich	≥99.8%
Dimethyoxyethane	DME	Aldrich	≥99.9%
Ethanol	EtOH	Fisher	≥99.8%
Ethyl acetate	EtOAc	Fisher	≥99.5%
Hexamethylphosphoramide	HMPA	Fluorochem	98%
Hexane		Sigma Aldrich	≥99%
Methanol	MeOH	Fisher	≥99.8%
Pentane (mixed isomers)		Fisher	≥95%
Tetrahydrofuran	THF	Fisher	≥99.8%
Toluene		Fisher	≥99.8%
Acetone-d6		Sigma Aldrich	99.9 atom % D
Acetonitrile-d3	CD_3CN	Aldrich	99.8 atom % D
Benzene-d6	C_6D_6	Sigma Aldrich	99.6 atom % D
Chloroform-d	$CDCl_3$	VWR	99.80 atom % D
Deuterium oxide	D_2O	Aldrich	99.9 atom % D
Dichloromethane-d2	CD_2Cl_2	Sigma Aldrich	99.9 atom % D
Dimethyl sulfoxide-d6	d6-DMSO	Sigma Aldrich	99.9 atom % D
Methanol-d4		Aldrich	99.8 atom % D
Tetrahydrofuran-d8	d8-THF	Sigma Aldrich	99.5 atom % D
Toluene-d8	d8-toluene	Sigma Aldrich	99.6 atom % D

Table 8.3. List of solvents used in this experimental work, with their respective sources and purity grades.

8.2 Experimental Procedures (Chapter 2)

8.2.1 – 8.2.13 (Chapter 2.2.1)

8.2.1. Reaction of HSiCl$_3$ with NaN$_3$ in MeCN

NaN$_3$ (1.927 g, 29.6 mmol) was suspended in MeCN (15 mL) in a Schlenk tube. To this, HSiCl$_3$ (0.3 mL, 2.95 mmol) was added via syringe. The mixture was stirred vigorously for 24 hours, then filtered. IR (reaction solution in MeCN) v/cm^{-1} = 2110 s.

8.2.2. Reaction of HSiCl$_3$ with TMS(N$_3$) in C$_6$D$_6$

To an NMR tube, C$_6$D$_6$ (0.5 mL) and TMS(N$_3$) (0.2 mL, 1.5 mmol) were added and mixed. To this solution, HSiCl$_3$ (20 mg) was added. The solution was shaken to mix, and promptly inserted into an NMR spectrometer for analysis. ^{1}H, ^{14}N and ^{29}Si NMR spectra were recorded of this solution numerous times over the course of 7 days, with an additional set of spectra recorded 14 days and 76 days after reaction start. ^{1}H spectra from this sample are calibrated to the residual solvent signal of C$_6$D$_6$, set to δ = 7.17 ppm, ^{29}Si spectra are calibrated to the signal of TMS(N$_3$) set to δ = 15.7 ppm (calibration values determined from experimentally determined chemical shifts of C$_6$D$_6$ and TMS(N$_3$) in solution of 0.5 mL C$_6$D$_6$, 0.2 mL TMS(N$_3$) and 0.1 mL tetramethylsilane, calibrated to tetramethylsilane δ = 0 ppm). NMR data for the observed species is shown in Table 8.4.

Compound	^1H δ/ppm	J_{Si-H} /Hz	$^{14}N(\beta)$ δ/ppm	$^{14}N(\gamma)$ δ/ppm	^{29}Si δ/ppm
$Si(N_3)_4$	–	–	-153.6	-193.0	-73.9
$HSiCl_3$	5.56	370	–	–	-9.3†
$HSi(N_3)Cl_2$	5.00	361	-152.3	-190.0	-25.7
$HSi(N_3)_2Cl$	4.55	345	-152.3	-193.0	-40.6
$HSi(N_3)_3$	4.18	324	-152.3	-195.6	-53.7
H_2SiCl_2	4.92	292	–	–	?
$H_2Si(N_3)Cl$	4.54	283	?	?	-25.3
$H_2Si(N_3)_2$	4.18	270	-149.2	-198.6	-36.9
H_3SiCl	4.23	240	–	–	?
$H_3Si(N_3)$	4.05	231	?	?	-43.8
SiH_4	3.13	203	–	–	?
TMSCl	0.23	6.8	–	–	30.4
$(TMS)_2O$	0.10	6.7	–	–	7.3
$TMS(N_3)$	0.00	6.9	-145.4	-208.6	*15.7*

Table 8.4. ^1H, ^{14}N and ^{29}Si chemical shifts (in ppm) and Si-H coupling constants (in Hz) for observed species, where distinguishable. Cases where data is not applicable are marked with a dash. Cases where the signal could not be detected are marked with a question mark. †The ^{29}Si value for $HSiCl_3$ was taken from a repeat experiment.

8.2.3. Synthesis of $NaAl(N_3)_4(THF)_4$

To a flask containing THF (80 mL), $AlCl_3$ (2.00 g, 15 mmol) was slowly added in portions. This caused significant heating of the solution. Once all $AlCl_3$ had dissolved, NaN_3 (3.9 g, 60 mmol) was added, followed by additional THF (20 mL) to wash the walls. This mixture was stirred vigorously for 20 hours. The resulting suspension was filtered into a flask containing another batch of NaN_3 (3.9 g, 60 mmol), and the mixture stirred vigorously for 21 hours. This suspension was also filtered, the solution stored in a sealed ampoule for future use. Crystalline $NaAl(N_3)_4(THF)_4$ is then obtained by concentrating an aliquot of this solution under vacuum to approximately 1/10th of the aliquot volume, followed by decanting off

the residual solution. CAUTION: evaporating to dryness may result in the elimination of THF from the crystals, which may afford explosive $NaAl(N_3)_4$ residues. It is thus also recommended to store these crystals under an atmosphere saturated in THF to prevent this loss of THF. Yield = 100 mL of approx. 0.1M solution (~10 mmol, 67%). NMR (d8-THF) ^{1}H δ/ppm = 3.61 (m, THF), 1.77 (m, THF); ^{14}N δ/ppm = -142.4 (s), -275.0 (br); ^{23}Na δ/ppm = -5.9 (s); ^{27}Al δ/ppm = 46.5 (s).

8.2.4. Synthesis of HSi(N₃)₃ in C₆D₆, followed by filtration through PPNCl

In an NMR tube, $HSiCl_3$ (20 mg, 0.15 mmol) was dissolved in C_6D_6 (0.6 mL). After recording an initial spectrum of $HSiCl_3$ (^{1}H δ = 5.40 ppm), crystalline $NaAl(N_3)_4(THF)_4$ (76 mg, 0.15 mmol) was added. The mixture was sonicated for 2 x 30 seconds with intermittent shaking. Another ^{1}H NMR spectrum was recorded, showing $HSiCl_3$ (5.43 ppm), $HSi(N_3)Cl_2$ (4.87 ppm), $HSi(N_3)_2Cl$ (4.42 ppm) and $HSi(N_3)_3$ (4.04 ppm), with a respective (molar) ratio of 0.16 : 0.07 : 0.49 : 0.28. This correlates to an average of 1.89 equivalents of azide exchanged, thus 63% conversion to $HSi(N_3)_3$. The mixture was sonicated for a further 4x 30s with intermitted shaking, affording 95% conversion. Sonication for another 4x 30s with intermittent shaking affords 98% conversion. The suspension was filtered, allowing for the recording of higher quality NMR spectrum. Identified products by ^{1}H NMR: $HSi(N_3)_2Cl$ (4.48 ppm), $HSi(N_3)_3$ (4.12 ppm), $H_2Si(N_3)_2$ (4.11 ppm), with a respective (molar) ratio of 0.04 : 0.94 : 0.01. NMR (C_6D_6) ^{27}Al δ/ppm = 66.0 (br, $Al(N_3)Cl_2$, 55.4 (br, $Al(N_3)_2Cl$), 42.1 (br, $Al(N_3)_3$).

This solution was then filtered through a plug of powdered PPNCl, and the NMR spectra re-recorded. Identified products by ^{1}H NMR: $H_2Si(N_3)_2$ (4.09 ppm, $^1J_{Si-H}$ = 273 Hz), $HSi(N_3)_3$ (4.08 ppm, $^1J_{Si-H}$ = 327 Hz), with a respective (molar) ratio of 0.27 : 0.73. ^{27}Al δ/ppm = 104.7 (s, $AlCl_4$), 96.4 (br, $AlCl_3$).

8.2.5. Synthesis of HSi(N₃)₃ in C₆D₆, followed by addition of hexane

To an NMR tube containing C_6D_6 (0.6 mL), crystalline $NaAl(N_3)_4(THF)_4$ (139 mg, 0.275 mmol) was added. This mixture was sonicated for a total of 5 minutes with intermittent shaking to break up the crystals. ^{27}Al NMR analysis of this solution shows no significant aluminium

species are dissolved at this time. To this mixture, $HSiCl_3$ (46 mg, 340 mmol) was added, and the tube shaken vigorously to mix. The mixture was left standing for 20 minutes. Shaking the solution again results in a fine white suspension with no large solids remaining. To this suspension, hexane (1.8 mL) was added, causing further precipitation. The suspension was then filtered, and NMR spectra recorded (note: due to the unconventional solvent mixture, this solution is not manually calibrated to the solvent – the residual signal of C_6D_6 appears at 7.08 ppm). Identified products by ^1H NMR: $HSi(N_3)_2Cl$ (4.70 ppm, $^1J_{Si-H}$ = 342 Hz), $HSi(N_3)_3$ (4.38 ppm, $^1J_{Si-H}$ = 322 Hz), with a respective (molar) ratio of 0.11 : 0.89. ^{27}Al δ/ppm = 66.9 (br, $Al(N_3)Cl_2$), 56.1 (br, $Al(N_3)_2Cl$). After standing for 48 hours, the signal of $H_2Si(N_3)_2$ is detected (4.37 ppm, $^1J_{Si-H}$ = 269 Hz), with an (molar) ratio $HSi(N_3)_3$: $H_2Si(N_3)_2$ of 0.99 : 0.01, corresponding to 2% disproportionation of $HSi(N_3)_3$.

8.2.6. Synthesis of $HSi(N_3)_2Cl$ in THF, followed by addition of $Na(^{Dipp}NCN)(THF)$

(See experimental for Chapter 2.2.2 for synthesis of $Na(^{Dipp}NCN)(THF)$). To an NMR tube containing $HSiCl_3$ (6 mg, 0.04 mmol), a solution of ~0.1M $NaAl(N_3)_4$ in THF (0.5 mL, 0.05 mmol) was added, resulting in a while precipitate. The mixture was then left standing for 18 hours. Identified products by ^1H NMR: $HSi(N_3)_2Cl$ (4.89 ppm, $^1J_{Si-H}$ = 339 Hz), $H_2Si(N_3)Cl$ (4.61 ppm, $^1J_{Si-H}$ = 288 Hz), with a respective (molar) ratio of 0.69 : 0.31.

To this mixture, $Na(^{Dipp}NCN)(THF)$ (23 mg, 0.04 mmol) was added, resulting in more white precipitate. This was then filtered to afford a pale-yellow solution, and 0.1 mL C_6D_6 added to act as a locking solvent for NMR. ^1H NMR spectrum recorded of this solution. $(^{Dipp}NCN)SiH(N_3)_2$ and $(^{Dipp}NCN)SiH_2(N_3)$ can be identified in the spectrum based on their $^1J_{Si-H}$ values compared to those known in C_6D_6, as $^1J_{Si-H}$ values do not change significantly in different solvents: $(^{Dipp}NCN)SiH(N_3)_2$ (5.71 ppm, $^1J_{Si-H}$ = 310 Hz), $(^{Dipp}NCN)SiH_2(N_3)$ (5.31 ppm, $^1J_{Si-H}$ = 277 Hz), in a respective (molar) ratio of 0.66 : 0.34.

8.2.7. Attempted synthesis of $HSi(N_3)_3$ in hexane

To a vial, hexane (1.0 mL) and $NaAl(N_3)_4(THF)_4$ (51 mg, 0.10 mmol) were combined and stirred vigorously. To the stirring suspension, a solution of $HSiCl_3$ (14 mg, 0.10 mmol) in hexane (0.5 mL) was added. The suspension was stirred for an additional 5 minutes, then

filtered. Identified products by ^{1}H NMR: $HSi(N_3)Cl_2$ (5.96 ppm, $^1J_{Si-H}$ = 362 Hz), $HSi(N_3)_2Cl$ (5.38 ppm, $^1J_{Si-H}$ = 352 Hz), $HSi(N_3)_3$ (4.71 ppm, $^1J_{Si-H}$ = 319 Hz), with a respective (molar) ratio of 0.54 : 0.14 : 0.32. ^{27}Al δ/ppm = 66.5 (br, $Al(N_3)Cl_2$).

8.2.8. Synthesis of $Na(15c5)Al(N_3)_4$

In a vial, 15-crown-5 (397 mg, 1.80 mmol) was dissolved in Et_2O (4 mL). To this solution, $NaAl(N_3)_4(THF)_4$ (720 mg, 1.42 mmol) was added. The mixture was stirred for 18 hours, affording a white suspension and a waxy solid residue. The suspension was decanted off the wax, then filtered to isolate the suspended precipitate. This precipitate was then washed with hexane (3 x 3 mL) and dried under vacuum. Yield = 517 mg (1.18 mmol, 83% with respect to $NaAl(N_3)_4(THF)_4$). Dissolving this material in THF followed by slow evaporation of the solvent affords crystals of $Na(15c5)Al(N_3)_4(THF)$ suitable for SCXRD.

8.2.9. Synthesis of $HSi(N_3)_3$ using $Na(15c5)Al(N_3)_4$

In a vial, $HSiCl_3$ (40 mg, 0.30 mmol) was dissolved in hexane (4 mL). To this solution, $Na(15c5)Al(N_3)_4$ (102 mg, 0.23 mmol) was added, and the resulting suspension stirred for 30 minutes. Identified products by ^{1}H NMR: $HSi(N_3)_2Cl$ (4.97 ppm, $^1J_{Si-H}$ = 335 Hz), $HSi(N_3)_3$ (4.71 ppm, $^1J_{Si-H}$ = 319 Hz), with a respective (molar) ratio of 0.40 : 0.60. Stirring for an additional 3 hours did not afford further conversion to $HSi(N_3)_3$, but did afford the formation of $H_2Si(N_3)_2$ (4.69 ppm, $^1J_{Si-H}$ = 265). No ^{27}Al NMR signal detected in solution throughout the experiment.

8.2.10. Example synthesis of $Si(N_3)_4$ solution in toluene

To a large Teflon-stoppered ampoule, NaN_3 (4.06 g, 62.5 mmol) and $AlCl_3$ (12 mg, 0.12 mmol) were added. To this, a solution of $SiCl_4$ (1.02 g, 6.00 mmol) in toluene (20 mL) was added. The mixture was stirred and heated at 100 °C for 5 days. The solution was filtered, and the residue extracted with toluene (5 mL). The filtered solution and extract were returned to the ampoule, and additional NaN_3 (4.06 g, 62.5 mmol) was added, followed by more toluene (2 mL) to wash the NaN_3 down the walls. The resulting suspension was again

stirred at 100 °C for 5 days. A small aliquot of this solution was taken for ^{14}N NMR analysis, confirming complete conversion to $Si(N_3)_4$. The aliquot was returned to the bulk suspension, the suspension then filtered, and the residue extracted with toluene (5 + 5 + 1 mL). The filtered solution and the extracts were combined to afford a total of 25.10 g of solution. IR (toluene) v/cm^{-1} = 2202 w, 2170 vs, 2133 w (HN_3), 1326 m. NMR (toluene, D_2O capillary) ^{14}N δ/ppm = -153.8 (1N, N_β), -192.8 (1N, N_γ), -320.7 (br, 1N, N_α); ^{27}Al shows no signals.

To determine the concentration of the solution, 389 mg of this solution was added to an NMR tube. To this, MeCN (16 mg) was added. Quantitative ^{1}H NMR analysis shows a MeCN : toluene ratio of 1 : 11.0. Quantitative ^{14}N NMR analysis shows an $Si(N_3)_4$: MeCN ratio of 1 : 4.47. Thus, the molar ratio of $Si(N_3)_4$: toluene is 1 : 49.2, corresponding to a percentage by weight of 4.15% (approximate molarity = 0.19 M), and thus a total yield of 5.30 mmol (88% with respect to $SiCl_4$).

8.2.11. Reaction of $Si(N_3)_4$ with NaH

In a vial, NaH (3.5 mg, 0.15 mmol) was suspended in toluene (1 mL). To this suspension, a solution of $Si(N_3)_4$ in toluene (0.14M, 1 mL, 0.14 mmol) was added. The mixture was stirred vigorously for 4 days, then filtered. No detectable products by ^{1}H NMR. ^{14}N NMR shows predominantly $Si(N_3)_4$ (δ/ppm = -153.6, -192.9, -324.5) with weak signals at -152.0 ppm, -195.3 ppm. ^{29}Si NMR shows predominantly $Si(N_3)_4$ (δ = -74.2), with a weak signal at -21.9 ppm.

8.2.12. Reaction of $Si(N_3)_4$ with LiAl(OtBu)$_3$H

A vial was charged with LiAl(OtBu)$_3$H (37 mg, 0.15 mmol). To this, a solution of $Si(N_3)_4$ in toluene (0.14M, 1 mL, 0.14 mmol) was added, and the resulting suspension was stirred for 3 hours. Half of this solution was filtered into an NMR tube, and a small amount of C_6D_6 was added to it for analysis. Major NMR signals (toluene + C_6D_6) ^{1}H δ/ppm = 4.71 (s, $^1J_{Si-H}$ = 299 Hz), 4.45 (s, $^1J_{Si-H}$ = 315 Hz), 1.21 (s, C(CH$_3$)$_3$), 1.06 (s, C(CH$_3$)$_3$), 1.05 (s, C(CH$_3$)$_3$); ^{14}N δ/ppm = -150.2 (s), -151.4 (s), -196.5 (s), -199.0 (s), -322.5 (br); ^{29}Si δ/ppm = -61.7 (d, $^1J_{Si-H}$ = 315 Hz), -80.7 (s).

8.2.13. Reaction of Si(N₃)₄ with LiAlH₄

In a vial, DME (48 mg, 0.53 mmol) was dissolved in a solution of $Si(N_3)_4$ in toluene (4.15%, 2505 mg, 0.53 mmol). The solution was stirred, and $LiAlH_4$ (5 mg, 0.13 mmol) was added, resulting in immediate bubbling that lasted less than 1 minute. Stirred for a further 1.5 hours, affording a dark grey suspension. NMR (toluene, d6-DMSO capillary) ^{1}H δ/ppm = 4.05 (s, $^1J_{Si-H}$ = 325 Hz, $HSi(N_3)_3$); ^{7}Li δ/ppm = -2.22; ^{14}N δ/ppm = -152.2 (s), -199.5 (br); ^{27}Al shows no signals; ^{29}Si δ/ppm = -54.8 (d [extremely weak], $^1J_{Si-H}$ = 322 Hz, $HSi(N_3)_3$), -85? (br [difficult to distinguish from the signal of the glass tube]).

After stirring for an additional 16 hours, the solution was filtered. The grey precipitate was washed with toluene (2 x 0.5 mL), then dried under vacuum. IR (Nujol mull) = 2178 s br, 2161 vs br, 2126 m, 2105 s, 2059 vw.

8.2.14 – 8.2.27 (Chapter 2.2.2)

8.2.14. Direct synthesis of (ᴰⁱᵖᵖNCN)SiHCl₂ (without formation of (ᴰⁱᵖᵖNCN)H)

To a Schlenk tube containing Et_2O (30 mL), lithium granules (230 mg, 33.0 mmol) were added, and the mixture cooled to 0 °C. The mixture was stirred vigorously and 1-bromo-4-tert-butylbenzene (3.356 g, 15.75 mmol) was added at once. Stirring was continued at 0 °C for 1 hour, affording a dull brown suspension with small amounts of unreacted lithium granules.

In a separate flask, bis(2,6-diisopropylphenyl)carbodiimide (5.438 g, 15.00 mmol) was dissolved in Et_2O (20 mL). The solution was cooled to 0 °C and stirred. The aforementioned dull brown suspension was filtered onto this stirred solution, affording a greenish-yellow solution. Once addition was complete, the cooling bath was removed to allow the solution to warm up to room temperature. The solution was stirred for a further 30 minutes, after which it was cooled back down to 0 °C. Whilst still stirring, $HSiCl_3$ (1.67 mL, 16.5 mmol) was added at once, resulting in a thick white suspension. The suspension was again allowed to warm to room temperature, then stirred for a further 30 minutes. All volatiles were then removed under vacuum, and the residue extracted with hexane (40 + 10 mL) to afford a pale-yellow solution. The combined extracts were evaporated under argon flow to a total

volume of 10 mL. This solution was then cooldown to -10 °C overnight, followed by -50 °C for 4 hours, affording colourless crystals. The crystals were isolated by cold filtration through a glass frit, washed with cold hexane (2 x 5 mL), and dried under vacuum. Yield = 1.642 g.

The hexane used for washing was combined with the filtrate, and additional hexane (60 mL) was added. The resulting solution was cooled to -10 °C overnight, affording further crystals, which were isolated in the same manner as above. Yield = 0.597 g. The remaining filtrate was concentrated under vacuum further to 10 mL, and left standing for 1 week, affording crystalline residue. This mixture was cooled to -20 °C overnight, then the supernatant was decanted off. The crystalline residue was then washed with cold hexane (5 mL). Yield = 0.720 g. Combined yield = 2.959 g (4.97 mmol, 33% with respect to bis(2,6-diisopropylphenyl)carbodiimide). NMR (Et$_2$O, d6-DMSO capillary) ^{1}H δ/ppm = 7.13–7.08 (m, 2H, aryl-H), 7.05–7.00 (m, 6H, aryl-H), 6.90 (d, 2H, $^3J_{HH}$ = 8.7 Hz, aryl-H), 6.29 (s, 1H, $^1J_{Si-H}$ = 355 Hz), 1.18 (d, 12H, $^3J_{H-H}$ = 6.8 Hz, CH(CH_3)$_2$), 0.79 (d, 12H, $^3J_{H-H}$ = 6.9 Hz, CH(CH_3)$_2$), some environments obscured by Et$_2$O.

8.2.15. Synthesis of (^{Dipp}NCN)H

To a Schlenk tube containing Et$_2$O (100 mL), lithium granules (800 mg, 115 mmol) were added. The mixture was stirred and 1-bromo-4-tert-butylbenzene (10.5 mL, 60.5 mmol) was added at once, resulting in sufficient heating to boil the Et$_2$O. As such, the solution was promptly placed in a water-ice bath. Stirring was continued at 0 °C for 2 hours, affording a red-brown suspension with small amounts of unreacted lithium granules.

In a separate flask, bis-(2,6-diisopropylphenyl)carbodiimide (20.0 g, 55.2 mmol) was dissolved in Et$_2$O (20 mL). The solution was cooled to -35 °C and stirred. The aforementioned red-brown suspension was filtered onto this stirred solution, affording a yellow solution. This solution was stirred at 0 °C for 1 hour, then whilst still stirring at 0 °C, water (60 mL) was added, resulting in two layers forming. The layers were separated, and the aqueous layer was extracted with DCM (2 x 100 mL). The extracts were combined with the Et$_2$O solution and dried under vacuum to afford crystals coated in a yellow oil. This material was redissolved in boiling hexane (250 mL) then cooled to -30 °C overnight, affording an off-

176

white crystalline residue. The solution was decanted, and the crystals washed with cold hexane (2 x 30 mL). This material was dried under vacuum, then sublimed at 155 °C under vacuum in two batches, affording a total of 11.974 g (^{Dipp}NCN)H as a crystalline solid (24.1 mmol, 44% with respect to bis-(2,6-diisopropylphenyl)carbodiimide).

8.2.16. Example synthesis of Na(^{Dipp}NCN)(THF)$_x$

In a Schlenk flask, (^{Dipp}NCN)H (4.318 g, 8.69 mmol) was dissolved in THF (25 mL). To this solution, NaH (418 mg 17.4 mmol) was added, resulting in a white suspension that gradually turned yellow over several minutes. The flask was stoppered with a needle to vent pressure, and stirred for 18 hours. Additional NaH (1.26 g, 52.5 mmol) was then added and stirred for 6 hours. The solution was diluted with hexane (25 mL), filtered, and the residue extracted with hexane (2 x 20 mL). The combined solution and extracts were concentrated under vacuum to approximately 5 mL, resulting in the formation of crystals of (^{Dipp}NCN)H indicating incomplete conversion. Thus, all material was redissolved by the addition of 25 mL THF, and another batch of NaH (1.26 g, 52.5 mmol) was added. The mixture was stirred for 4 days, and NMR analysis of the solution shows all (^{Dipp}NCN)H is consumed. This solution was then diluted with 25 mL hexane, filtered, and the residue extracted with hexane (2 x 10 mL). The combined solution and extracts were then concentrated under vacuum to approximately 5 mL, then cooled overnight to -40 °C affording a hard yellow solid. The solid was broken up, washed briefly with cold hexane (10 mL), then dried briefly under vacuum to afford (^{Dipp}NCN)Na with 2.3 equivalents of THF and 0.05 equivalents of (^{Dipp}NCN)H by NMR analysis. Yield = 4.579 g (6.45 mmol of Na(^{Dipp}NCN), 74% with respect to (^{Dipp}NCN)H). Note that the quantity of THF remaining varies depending on drying time. NMR (C$_6$D$_6$) ^{1}H δ/ppm = 7.54 (vbr, 2H, aryl-H), 7.05 (br, 6H, aryl-H), 6.90 (br, 2H, aryl-H), 3.76 (vbr, 4H, CH(CH$_3$)$_2$), 3.32 (m, ~9H, THF), 1.31 (m, ~9H, THF), 1.20 (vbr, 24H, CH(CH_3)$_2$), 1.05 (br, 9H, C(CH$_3$)$_3$).

8.2.17. Synthesis of (^{Dipp}NCN)SiHCl$_2$ from Na(^{Dipp}NCN)

In a Schlenk tube, Na(^{Dipp}NCN)(THF)$_{2.3}$·[(^{Dipp}NCN)H]$_{0.05}$ (2.84 g, 4.0 mmol) was dissolved in Et$_2$O (15 mL) affording a bright yellow solution, and cooled to 0 °C. To this, pre-cooled HSiCl$_3$ (596 mg 4.4 mmol) was added whilst stirring, followed by extra Et$_2$O (1 mL) to wash it down

the flask. A white suspension formed on addition. The suspension was stirred for 2.5 hours, then filtered and the residue extracted with 3x5 mL hexane. The combined solution and extracts were dried under vacuum, affording (^{Dipp}NCN)SiHCl$_2$ as a white powder without additional work-up being necessary. Yield = 2.267 g (3.81 mmol, 95% with respect to Na(^{Dipp}NCN)). NMR (C$_6$D$_6$) ^{1}H δ/ppm = 7.21 (d, 2H, $^3J_{H-H}$ = 8.6 Hz), 7.14–7.05 (m, 6H, aryl-H), 6.95 (s, 1H, $^1J_{Si-H}$ = 356 Hz), 6.79 (d, 2H, aryl-H), 3.60 (sept, 4H, $^3J_{H-H}$ = 6.8 Hz, CH(CH$_3$)$_2$), 1.40 (d, 12H, $^3J_{H-H}$ = 6.8 Hz, CH(CH_3)$_2$), 0.97 (d, 12H, $^3J_{H-H}$ = 6.9 Hz, CH(CH_3)$_2$), 0.77 (s, 9H, C(CH$_3$)$_3$).

8.2.18. Synthesis of PPN(N$_3$)

In a flask under air, water (120 mL) was added and heated to 60 °C. To this, PPNCl (8.02 g, 14.0 mmol) was dissolved. To this solution, a pre-heated solution of NaN$_3$ (13.65 g, 210 mmol) in water (35 mL) was added with stirring, resulting in immediate precipitation. The solution was allowed to gradually cool to room temperature whilst stirring over the course of 1 hour, then it was cooled to 0 °C. The resulting suspension was filtered, and the residue washed with cold water (30 mL). The residue was then extracted with acetonitrile (50 + 20 mL). The acetonitrile was then removed under vacuum, and the residue re-extracted with acetone (35 mL). The acetone solution was slowly cooled to -30 °C for 3 days, affording colourless crystals. The flask was tilted to allow the solution to decant off the crystals by gravity, and left at -30 °C for 1 day. The solution was then removed, and the crystals dried under high vacuum. The removed solution was allowed to slowly evaporate under air over the course of 4 days to approximately 1 mL volume remaining, affording large colourless crystals. The solvent was decanted and the crystals briefly washed with acetone (0.5 mL) and Et$_2$O (2 x 2 mL). The leftover solution used for washing was then left to evaporate under air until dryness, affording more large crystals, which were briefly washed with acetone (3 x 5 mL) and dried under vacuum. The three batches of crystals were combined. These crystals were found to contain significant water content (by ^{1}H NMR), so the material was crushed up using a glass rod and heated in an oven at 115 °C for 5 days, followed by transfer *via* vacuum port into an argon-filled glovebox (whilst still hot) to prevent accumulation of moisture. Combined yield of PPN(N$_3$) = 6.846 g (11.79 mmol, 84% with respect to PPNCl). NMR analysis was conducted with Bu$_4$NBr as an additive to determine PPN : N$_3$ ratio by comparing ^{1}H and ^{14}N integrals of PPN$^+$ and N$_3^-$ against Bu$_4$N$^+$. PPN : N$_3$ ratio was

determined to be approximately 1 : 1.03, confirming full conversion. NMR (d6-acetone) ^{1}H δ/ppm = 7.77–7.67 (m, 18H, PPN$^+$), 7.61–7.56 (m, 12H, PPN$^+$); ^{14}N δ/ppm = -129.8 (s, 1N), -277.6 (s, 2N); ^{31}P δ/ppm = 20.9 (s, PPN$^+$); ^{35}Cl shows no signals.

8.2.19. Synthesis of (^{Dipp}NCN)SiH(N$_3$)$_2$ according to Peerless' method

To a Schlenk tube, (^{Dipp}NCN)H (3.936 g, 7.94 mmol) and LiN(TMS)$_2$ (1.325 g, 7.92 mmol) were combined as solids. These were then dissolved by the addition of Et$_2$O (40 mL). The solution was stirred for 1 hour, then all volatiles were removed under vacuum. The residue was then redissolved in Et$_2$O (40 mL), and the solution stirred. To the stirred solution, HSiCl$_3$ (1.4 mL, 14 mmol) was added at once, affording an immediate white precipitate and some bubbling (likely boiling of Et$_2$O due to the heat generated). After the mixture had cooled back to room temperature, all volatiles were removed under vacuum to afford a white solid. The solid was extracted with hexane (2 x 40 mL), and the combined extracts dried under vacuum. A small sample of the solid was taken for NMR analysis, confirming it to be (^{Dipp}NCN)SiHCl$_2$. To the remaining solid, NaN$_3$ (1.94 g, 30 mmol) was added, followed by THF (40 mL). The mixture was stirred vigorously for 70 hours, then filtered onto another batch of NaN$_3$ (2.08 g, 32 mmol). This mixture was then stirred vigorously for 20 hours, filtered, and dried under vacuum to afford a white residue. This residue was suspended in a mixture of 1:1 hexane : toluene (60 mL). The suspension was concentrated under vacuum to approximately 5 mL, then cooled to -30 °C for 4 hours. This was then filtered while cold and the residue dried under vacuum to afford a white powder. NMR analysis indicates the mixture contains both (^{Dipp}NCN)H and (^{Dipp}NCN)SiH(N$_3$)$_2$ in a respective ratio of approximately 1 : 2. This material was recrystallised by redissolving in a 1:1 (by volume) mixture of hexane and toluene (150 mL), concentrating to 40 mL volume, filtering, then slow concentration to 20 mL volume. The mixture was then cooled slowly to -30 °C overnight to grow the crystals, then the supernatant suspension was decanted. The crystals were washed with hexane (2 x 1.5 mL) and dried under vacuum. Yield = 699 mg (1.15 mmol, 14% with respect to (^{Dipp}NCN)H). NMR (C$_6$D$_6$) ^{1}H δ/ppm = 7.18 (d, 2H, ^{3}J$_{H-H}$ = 8.7 Hz, aryl-H), 7.13–7.04 (m, 6H, aryl-H), 6.77 (d, 2H, aryl-H), 6.15 (s, 1H, ^{1}J$_{Si-H}$ = 311 Hz), 3.51 (sept, 4H, ^{3}J$_{H-H}$ = 6.9 Hz, CH(CH$_3$)$_2$), 1.40 (d, 12H, ^{3}J$_{H-H}$ = 6.8 Hz, CH(CH_3)$_2$), 0.96 (d, 12H, ^{3}J$_{H-H}$ = 6.9 Hz, CH(CH_3)$_2$), 0.76 (s, 9H, C(CH$_3$)$_3$); ^{29}Si δ/ppm = -98.5 (d, ^{1}J$_{Si-H}$ = 311 Hz).

8.2.20. Reaction of (^{Dipp}NCN)SiH(N$_3$)$_2$ with PPN(N$_3$) in C$_6$D$_6$

In an NMR tube, (^{Dipp}NCN)SiH(N$_3$)$_2$ (11 mg, 0.018 mmol) was dissolved in C$_6$D$_6$ (0.6 mL). A ^{1}H NMR spectrum was recorded to confirm the sample identity. To this sample, powdered PPN(N$_3$) (11 mg, 0.019 mmol) was added, and the mixture sonicated for 3 minutes to break up the solid. The mixture was left standing for 18 hours, then another ^{1}H NMR spectrum recorded. The spectrum shows (^{Dipp}NCN)H as the dominant species in solution, with no detectable (^{Dipp}NCN)SiH(N$_3$)$_2$.

8.2.21. Synthesis of (^{Dipp}NCN)SiH(N$_3$)$_2$ according to "Method 1"

In a Schlenk tube, (^{Dipp}NCN)SiHCl$_2$ (2.805 g, 4.71 mmol) was suspended in TMS(N$_3$) (25 mL, 190 mmol). The suspension was stirred for 45 minutes, then slowly cooled down over 2 hours to -40 °C. The suspension was filtered whilst cold and the residue washed with cold TMS(N$_3$) (2 x 5 mL). The residue was dried under vacuum to afford a white solid. A small sample of this solid was taken for NMR analysis and found to contain (^{Dipp}NCN)SiH(N$_3$)$_2$, (^{Dipp}NCN)SiHCl$_2$ and (^{Dipp}NCN)H in a respective ratio of 0.73 : 0.04 : 0.23. The material was then placed under high vacuum and heated to 135 °C for 44 hours to afford (^{Dipp}NCN)SiH(N$_3$)$_2$ in acceptable purity (approximately 96% by ^{1}H NMR analysis). Yield = 1.430 g (2.35 mmol, 50% with respect to (^{Dipp}NCN)SiHCl$_2$). IR (Nujol mull) v/cm^{-1} = 3439 vw, 3426 vw, 3408 w, 3071 vw, 3060 w, 3017 w, 2158 s, 2142 vs, 2117 vs, 1943 vw, 1917 vw, 1875 vw, 1808 vw, 1791 vw, 1607 m, 1590 vw, 1571 m, 1550 m, 1508 w, 1500 w, 1420 m, 1392 w, 1384 m, 1365 m, 1346 m, 1313 s, 1295 w, 1268 w, 1257 w, 1229 vw, 1200 vw, 1179 vw, 1135 w, 1112 vw, 1101 w, 1055 w, 1047 vw, 1028 vw, 1016 vw, 991 m, 937 w, 855 w, 838 w, 793 s, 783 s, 762 s, 748 s, 728 w, 697 m, 678 w, 655 vw, 633 vw, 613 vw, 591 vw, 572 w, 550 w, 528 vw, 515 m, 506 w. ^{1}H NMR matches exactly to (^{Dipp}NCN)SiH(N$_3$)$_2$ synthesised by Peerless' procedure.

8.2.22. Synthesis of (^{Dipp}NCN)SiH(N$_3$)$_2$ according to "Method 2"

In a Schlenk tube, (^{Dipp}NCN)SiHCl$_2$ (2.085 g, 3.50 mmol) was dissolved in THF (15 mL). To this solution, NaN$_3$ (569 mg, 8.75 mmol) was added, followed by AlCl$_3$(MeCN) (6 mg, 0.035 mmol). The mixture was stirred vigorously with aliquots taken periodically for ^{1}H NMR

analysis to determine degree of conversion (aliquots were returned to the mixture after analysis). After stirring for 88 hours, conversion was completed. The resulting suspension was filtered through a glass frit, and the residue extracted with THF (2 x 5 mL). The combined filtrate and extracts were dried under vacuum to afford a white solid. The solid was extracted with toluene (20 + 5 mL) affording a very pale, yellow-green solution. The solution was slowly concentrated under vacuum to 15 mL, affording colourless crystals. This mixture was cooled to -30 °C overnight to grow the crystals. The solvent was removed by filtration through a glass frit whilst cold, and the crystals washed with cold hexane (2 x 5 mL) and dried under vacuum to afford crystalline (^{Dipp}NCN)SiH(N$_3$)$_2$. Yield = 1.522 g (2.50 mmol, 71% with respect to (^{Dipp}NCN)SiHCl$_2$). ^{1}H NMR matches exactly to (^{Dipp}NCN)SiH(N$_3$)$_2$ synthesised by Peerless' procedure.

8.2.23. Synthesis of (^{Dipp}NCN)SiH(N$_3$)$_2$ according to "Method 3"

In a round-bottom flask, (^{Dipp}NCN)SiHCl$_2$ (1.490 g, 2.50 mmol) and NaN$_3$ (975 mg, 15.0 mmol) were combined as solids. To this, Et$_2$O (10 mL) was added, and the mixture stirred vigorously affording a suspension. After 5 minutes of stirring, AlCl$_3$ (7 mg, 0.05 mmol) was added. Stirring was continued for 16 hours, after which an aliquot was taken for NMR to confirm conversion had completed. The suspension was diluted with Et$_2$O (30 mL), filtered through a glass frit, and the residue extracted with Et$_2$O (3 x 5 mL). The combined filtrate and extract appeared to be saturated, so it was cooled to -20 °C overnight, affording colourless crystals. The Et$_2$O solution was decanted, and the crystals washed briefly with cold THF (5 mL) followed by cold hexane (2 x 5 mL). This only afforded 187 mg of material, indicating most of the product remained in the filtrate or filter residues. Thus, the decanted Et$_2$O was used to extract the residue from the initial filtration, and the resulting solution was concentrated to 10 mL volume, affording more crystals. This was again cooled to -20 °C overnight, and the solvent removed by filtration through a glass frit. The crystals were washed with Et$_2$O (2 x 5 mL). The combined Et$_2$O filtrate and extracts were diluted with additional Et$_2$O (30 mL), and used to extract the original filter residue again. This resulting solution was concentrated to 3 mL total volume, affording yet more crystals. The solution was again cooled to -20 °C, filtered, and the crystals washed (this time with hexane (2 x 5 mL)). Total crystalline yield = 1.067 (1.75 mmol, 70% with respect to (^{Dipp}NCN)SiHCl$_2$). [Note: The solubility of ($^{Dipp-}$

NCN)SiH(N$_3$)$_2$ in Et$_2$O appears to be very poor, and with a little dependency on temperature. The workup procedure for future syntheses can likely be simplified greatly by starting with a much larger volume of Et$_2$O (e.g. 100 mL), and crystals grown by concentrating the filtered reaction solution to near-dryness rather than using cooling methods]. ^{1}H NMR matches exactly to (^{Dipp}NCN)SiH(N$_3$)$_2$ synthesised by Peerless' procedure.

8.2.24. Synthesis of (^{tBu}NCN)SiHCl$_2$

In a Schlenk tube, PhBr (2.355 g, 15.0 mmol) was dissolved in Et$_2$O (20 mL) and the resulting solution cooled to -20 °C. To this solution, lithium granules (125 mg, 18.0 mmol) were added whilst stirring. The mixture was stirred while gradually warming up to 10 °C over the next 2 hours, resulting in all lithium being consumed and a brown suspension. Additional lithium granules (125 mg, 18.0 mmol) were added, and the mixture stirred at 10 °C for an additional 1 hour. The remaining unreacted lithium was picked out and weighed (46 mg, 6.6 mmol, consistent with complete conversion of PhBr to PhLi). The suspension was filtered through a glass frit to afford an orange solution. The residue was extracted with Et$_2$O (5 x 5 mL) and the extracts added to the filtrate. The combined solution was cooled to -30 °C and stirred. To the stirred solution, di-tert-butylcarbodiimide (2.314 g, 15.0 mmol) was added as a solid. The cooling was removed, and the solution was allowed to stir at room temperature for 1 hour, then cooled back down to -10 °C whilst still stirring. To this solution, HSiCl$_3$ (2.438 g, 18.0 mmol) was added at once, affording an immediate white precipitate. The cooling was again removed, and the mixture stirred at room temperature for 30 minutes. All volatiles were removed under vacuum, and the resulting residue was extracted with toluene (20 + 5 + 5 mL). The combined extracts were concentrated to a total volume of 20 mL, and slowly cooled to -45 °C overnight, affording a fine, white, crystalline material. The solvent was decanted off whilst cold, and the crystals washed with cold hexane (4 x 5 mL). Yield = 3.755 g (11.3 mmol, 75% with respect to PhBr). NMR (C$_6$D$_6$) ^{1}H δ/ppm = 6.91–6.86 (m, 1H, aryl-H), 6.82–6.79 (m, 0.5H, aryl-H), 6.79 (s, 1H, ^{1}J$_{Si-H}$ = 333 Hz), 6.78–6.74 (m, 2.5H, aryl-H), 1.11 (s, 18H, C(CH$_3$)$_3$); ^{29}Si δ/ppm = -96.8 (d, ^{1}J$_{Si-H}$ = 333 Hz). ^{1}H and ^{29}Si spectra show that approximately 10% of the material is a different compound with similar environments. NMR (minor product, C$_6$D$_6$) ^{1}H δ/ppm = 7.21 (s, ^{1}J$_{Si-H}$ = 331 Hz, Si-H), 1.12 (s, C(CH$_3$)$_3$); ^{29}Si δ/ppm =

-108.7 (d, $^1J_{Si-H}$ = 331 Hz). Aryl proton environments could not be identified due to overlap with the major product.

8.2.25. Synthesis of (^{tBu}NCN)SiH(N$_3$)$_2$

In a vial, (^{tBu}NCN)SiHCl$_2$ (331 mg, 1.00 mmol), NaN$_3$ (163 mg, 2.50 mmol) and AlCl$_3$(MeCN) (2 mg, 0.01 mmol) were combined as solids. THF (10 mL) was then added to the vial, and the mixture stirred for 19 hours. The resulting suspension was filtered through celite. The filtrate was dried under vacuum, affording a white microcrystalline solid. The solid was extracted with toluene (5 + 1 mL), and the combined extracts were concentrated under vacuum to approximately 1 mL total volume. This solution was then cooled slowly to -40 °C overnight, affording colourless crystals. The solvent was decanted, and the crystals washed with cold hexane (2 x 1 mL) then dried under vacuum. Yield = 249 mg (0.72 mmol, 72% with respect to (^{tBu}NCN)SiHCl$_2$). IR (Nujol mull) v/cm^{-1} = 3432 vw, 3414 vw, 3065 vw, 2150 vs, 2134 vs, 2129 vs, 2064 w, 1607 w, 1557 m, 1487 m, 1446 w, 1385 s, 1365 m, 1315 s, 1273 w, 1227 vw, 1202 m, 1085 w, 1042 vw, 1034 w, 1022 m, 930 vw, 924 vw, 881 vw, 814 vw, 800 w, 777 s, 749 m, 742 m, 709 m, 687 m, 672 w, 620 w, 612 vw, 592 vw, 552 w. NMR (C$_6$D$_6$) ^{1}H δ/ppm = 6.94–6.89 (m, 1H, aryl-H), 6.84–6.79 (m, 2H, aryl-H), 6.76–6.72 (m, 2H, aryl-H), 5.71 (s, 1H, $^1J_{Si-H}$ = 291 Hz), 0.99 (s, 18H, C(CH$_3$)$_3$); ^{13}C (DEPTQ-135) δ/ppm = 172.9 (N–C=N), 132.9 (ipso-phenyl), 130.2 (phenyl), 128.4 (phenyl), 128.0 (phenyl), 54.7 (*C*(CH$_3$)), 31.3 (C(*C*H$_3$)); ^{14}N δ/ppm = -141.7 (br, N$_\beta$), -203.0 (br, N$_\gamma$); ^{29}Si δ/ppm = -102.6 (d, $^1J_{Si-H}$ = 291 Hz).

8.2.26. Synthesis of (^{TMS}NCN)SiHCl$_2$

To a Schlenk tube, Et$_2$O (25 mL) and LiN(TMS)$_2$ (3.35 g, 20.0 mmol) were combined to afford a white suspension. The suspension was stirred, and PhCN (2.06 g, 20.0 mmol) was added to it, followed by addition Et$_2$O (5 mL). Upon completion of addition, the suspension became clear. The resulting solution was stirred for 42 hours, then cooled to 5 °C. To the cooled solution, HSiCl$_3$ (2.12 mL, 21.0 mmol) was added at once, resulting in a formation of a white suspension. The suspension was allowed to warm to room temperature and stirred for 1 hour. All volatiles were removed under vacuum, and the residue extracted with toluene (3 x 30 mL) to afford a yellow solution. This solution was concentrated to a volume of 80 mL,

affording small colourless crystals. The mixture was cooled to -40 °C overnight to grow the crystals, after which the solution was removed by filtration, and the crystals washed with cold toluene (2 x 5 mL) and dried under vacuum. Yield = 1.607 g.

The filtered solution was allowed to warm to room temperature and used to perform another extraction of the dried reaction residue. This extract was the concentrated slowly under vacuum to a volume of 20 mL, affording more colourless crystals. The mixture was cooled to -40 °C overnight to grow the crystals. The solution was removed by filtration, and the crystals washed briefly with cold toluene (2 x 5 mL) and dried under vacuum. Yield = 1.180g. Combined yield = 2.787 g (8.31 mmol, 42% with respect to PhCN). IR (Nujol mull) v/cm^{-1} = 3078 vw, 3057 vw, 3031 vw, 2208 w, 2185 vw, 2135 vw, 1605 w, 1578 vw, 1540 s, 1485 s, 1446 m, 1410 vw, 1362 vs, 1304 vw, 1261 m, 1254 s, 1200 w, 1076 w, 1055 m, 1020 w, 986 m, 930 w, 841 vs, 797 m, 781 s, 766 s, 750 m, 737 m, 708 s, 697 s, 690 m, 646 w, 569 s. NMR (C$_6$D$_6$) ^{1}H δ/ppm = 6.93–6.88 (m, 1H, phenyl-H), 6.82–6.77 (m, 2H, phenyl-H), 6.72–6.68 (m, 2H, phenyl-H), 6.52 (s, 1H, $^1J_{Si-H}$ = 355 Hz, Si-H), 0.01 (s, 18H, $^2J_{Si-H}$ = 6.9 Hz, Si(CH$_3$)$_3$); ^{29}Si δ/ppm = 5.54 (m, $^2J_{Si-H}$ = 6.9 Hz), -89.2 (d, $^1J_{Si-H}$ = 355 Hz).

8.2.27. Synthesis of (^{TMS}NCN)SiH(N$_3$)$_2$

To a vial, Et$_2$O (2 mL) and (^{TMS}NCN)SiHCl$_2$ (67 mg, 0.20 mmol) were combined, affording a white suspension. To this suspension, NaN$_3$ (78 mg, 1.20 mmol) was added, followed by AlCl$_3$ (1 mg, ~0.01 mmol) and additional Et$_2$O (1 mL). The resulting suspension was stirred for 16 hours. The suspension was filtered, and the residue was extracted with Et$_2$O (1.5 mL). The filtrate and extract were combined and dried under argon flow to afford a white crystalline residue. The crystals were washed with hexane (0.5 mL) then dried under vacuum. Yield = 42 mg (0.12 mmol, 60% with respect to (^{TMS}NCN)SiHCl$_2$). IR (Nujol mull) v/cm^{-1} = 3430 vw, 3406 vw, 3063 vw, 3056 vw, 2608 vw, 2153 vs, 2140 vs, 2121 vs, 1607 w, 1578 vw, 1543 s, 1487 s, 1447 m, 1377 vs, 1312 vs, 1263 m, 1254 s, 1206 w, 1058 m, 1014 s, 928 w, 843 vs, 795 w, 782 vs, 765 vs, 755 w, 744 w, 718 m, 703 s, 693 s, 646 w, 576 s, 555 s, 510 vw, 506 vw, 501 vw. NMR (C$_6$D$_6$) ^{1}H δ/ppm = 6.92–6.87 (m, 1H, phenyl-H), 6.82–6.77 (m, 2H, phenyl-H), 6.73–6.69 (m, 2H, phenyl-H), 5.66 (s, 1H, $^1J_{Si-H}$ = 311 Hz, Si-H), -0.06 (s, 18H, Si(CH$_3$)$_3$); ^{14}N δ/ppm = -142 (br), -202 (br); ^{29}Si δ/ppm = 4.77 (m, $^2J_{Si-H}$ = 7.0 Hz), -105.4 (d, $^1J_{Si-H}$ = 311 Hz).

The ^{1}H NMR spectrum also shows the presence of minor signals, including an Si-H environment at 5.47 ppm with $^1J_{Si-H}$ coupling of 276 Hz. This lower coupling constant value is expected for (^{TMS}NCN)SiH$_2$(N$_3$), indicating some disproportionation occurs in the synthesis.

8.2.28 – 2.2.40 (Chapter 2.2.3)

8.2.28. Synthesis of (^{tBu}NCN)SiH(N$_3$)(N(TMS)$_2$)

To an NMR tube containing a sample of (^{tBu}NCN)SiH(N$_3$)$_2$ (34 mg, 0.10 mmol) in C$_6$D$_6$ (0.5 mL), LiN(TMS)$_2$ (17 mg, 0.10 mmol) was added, and the solution inverted several times to dissolve the LiN(TMS)$_2$ and afford mixing. After 5 minutes, the solution became turbid. The solution was filtered, and the residue extracted with hexane (0.5 mL). The combined filtrate and extract were dried under argon flow, affording colourless crystals. The crystals were washed with hexane (0.2 mL) and dried under vacuum. Yield = 39 mg (0.084 mmol, 84% with respect to (^{tBu}NCN)SiH(N$_3$)$_2$). IR (Nujol mull) v/cm^{-1} = 3399 vw, 3015 vw, 2156 vw, 2136 vw, 2111 vs, 2058 w, 1612 vw, 1530 w, 1492 vw, 1478 w, 1444 w, 1388 s, 1361 m, 1305 m, 1264 w, 1258 m, 1252 w, 1229 vw, 1225 vw, 1199 m, 1180 vw, 1091 w, 1076 w, 1031 vw, 1020 vw, 954 s, 887 s, 873 s, 844 m, 829 vw, 797 w, 774 m, 753 w, 731 vw, 716 vw, 703 w, 682 vw, 672 w, 649 vw, 614 vw, 609 w, 502 vw. NMR (C$_6$D$_6$) ^{1}H δ/ppm = 6.98–6.92 (m, 3H, aryl-H), 6.90–6.85 (m, 2H, aryl-H), 5.55 (s, 1H, $^1J_{Si-H}$ = 297 Hz), 1.11 (s, 18H, C(CH$_3$)$_3$), 0.48 (s, 18H, $^2J_{Si-H}$ = 6.5 Hz, Si(CH$_3$)$_3$); ^{14}N δ/ppm = -137.9 (br, N$_β$), -209.1 (br, N$_γ$); ^{29}Si δ/ppm = 2.8 (m, Si(CH$_3$)$_3$), -97.1 (d, $^1J_{Si-H}$ = 296 Hz).

8.2.29. Reaction of (^{tBu}NCN)SiCl with NaAl(N$_3$)$_4$(THF)$_4$

To an NMR tube containing a solution of (^{tBu}NCN)SiHCl$_2$ (12 mg, 0.036 mmol) in C$_6$D$_6$ (0.5 mL), LiN(TMS)$_2$ (6 mg, 0.04 mmol) was added, followed by additional C$_6$D$_6$ (0.2 mL). The NMR tube was shaken to afford mixing, resulting in a yellow colouration and some precipitation. Over the course of an hour, the precipitate gradually changed from yellow to orange in colour. The formation of (^{tBu}NCN)SiCl was verified by NMR (^{29}Si δ = 14.2 ppm), along with HN(TMS)$_2$ (^{29}Si δ = 2.0 ppm) and small amounts of an unknown silicon-containing product (^{29}Si δ = 18.2 ppm). To this NMR sample, crystalline NaAl(N$_3$)$_4$(THF)$_4$ (9 mg, 0.02

mmol) was added, resulting in slight bubbling. The sample was sonicated for 10 x 30 seconds, with intermittent vigorous shaking to break up the crystals and afford mixing. Initial ^{1}H and ^{29}Si NMR spectra show the concentration of (^{tBu}NCN)SiCl in solution has approximately halved, HN(TMS)$_2$ is unreacted, no significant new signals detected aside from those of THF. The sample was left standing for 8 days, after which the ^{1}H NMR spectrum shows all (^{tBu}NCN)SiCl has been consumed, still no significant new signals detected.

8.2.30. NMR study of the reaction between (^{Dipp}NCN)SiH(N$_3$)$_2$ and ItBu

In an NMR tube, (^{Dipp}NCN)SiH(N$_3$)$_2$ (24 mg, 0.04 mmol) was dissolved in C$_6$D$_6$ (0.6 mL). A ^{1}H NMR spectrum of this sample was recorded. ItBu (7 mg, 0.04 mmol) was then dissolved into this solution. The solution was shaken to afford initial mixing, then left standing. ^{1}H NMR spectra recorded after 10 minutes, 45 minutes, 1 hour, 2 hours, 16 hours and 4 days. Note that the first two of these spectra were recorded at 293 K (the rest were recorded at 298 K). At the time of the '45 minutes' spectrum, some microcrystalline material had begun to precipitate. These crystals grew over the course of the next 4 days. A ^{29}Si spectrum was recorded between the '2 hours' spectrum and the '16 hours' spectrum, thus the sample was maintained at 298 K for this duration, rather than room temperature (~293 K). Shortly after recording the '4-days' spectrum, additional ItBu (14 mg, 0.08 mmol) was dissolved into the sample solution. ^{1}H NMR spectra recorded after 5 minutes, 1 hour, 2 hours and 15 hours. After a total of 19 hours had elapsed from the extra addition of ItBu, the sample was placed in an NMR instrument with the sample cooled to 10 °C. An initial ^{1}H spectrum was recorded, and further ^{1}H spectra recorded 1 hour, 2 hours and 22 hours after inserting into the cooled instrument. Note that due to a locking/shimming issue on the instrument, all signals in these spectra are split into doublets ~1.2 Hz apart. This effect is ignored for the following reported signals. Between 2 hours and 22 hours, a ^{29}Si spectrum was recorded. NMR (C$_6$D$_6$, 500 Hz, 10 °C) ^{1}H (after 22 hours at 10 °C) δ/ppm = 8.00 (s, 1H, imidazolyl-H), 7.24 (d, 2H, ^{3}J$_{H-H}$ = 8.4 Hz, aryl-H), 7.09–7.06 (m, 2H, aryl-H), 7.03–6.98 (m, 2H, aryl-H) 6.90–6.85 (m, 4H, aryl-H), 6.67 (s, 1H, ^{1}J$_{Si-H}$ = 290 Hz), 3.96 (sept, 2H, ^{3}J$_{H-H}$ = 6.8 Hz, C*H*(CH$_3$)$_2$), 3.20 (sept, 2H, ^{3}J$_{H-H}$ = ~6.6 Hz, C*H*(CH$_3$)$_2$), 1.70 (s, 9H, C(CH$_3$)$_3$), 1.69 (s, 9H, C(CH$_3$)$_3$), 1.31 (d, 6H, ^{3}J$_{H-H}$ = 6.8 Hz, CH(C*H*$_3$)$_2$), 1.14 (d, 6H, ^{3}J$_{H-H}$ = ~6.5 Hz, CH(C*H*$_3$)$_2$), 1.15 (d, 6H, ^{3}J$_{H-H}$ = 6.7 Hz, CH(C*H*$_3$)$_2$), 0.80 (d,

6H, $^3J_{H-H}$ = 6.8 Hz, CH(CH_3)$_2$). 0.78 (s, 9H, C(CH$_3$)$_3$); ^{29}Si (2 – 22 hours at 10 °C) δ/ppm = -66.6 (d, $^1J_{Si-H}$ = 290 Hz).

After 22 hours at 10 °C, the sample was allowed to warm back up to room temperature. After 1 hour at room temperature, another ^{1}H spectrum was recorded. Subsequently, the solvent was decanted off and handful of crystals isolated for SCXRD analysis. Unit cell: a = 10.41 Å, b = 12.23 Å, c = 22.81 Å, α = 85.23 °, β = 77.04 °, γ = 71.51 °, V = 2683 Å^3. This cell is a very close match to [ItBuH][(^{Dipp}NCN)SiH(N$_3$)$_3$](hexane),[73] indicating that these crystals are [ItBuH][(^{Dipp}NCN)SiH(N$_3$)$_3$](C$_6$D$_6$).

8.2.31. Synthesis of (^{Dipp}NCN)$_2$SiH(N$_3$)

In an NMR tube, (^{Dipp}NCN)SiH(N$_3$)$_2$ (30 mg, 0.050 mmol) and Na(^{Dipp}NCN)(THF) (26 mg, 0.044 mmol) were combined as solids. C$_6$D$_6$ was added to the sample, and the NMR tube was shaken to dissolve all material. ^{1}H NMR analysis indicates no initial reaction. The sample was left standing for 11 days, after which another ^{1}H NMR spectrum was recorded, also indicating no reaction. The sample was heated to 80 °C for 5 hours, still no reaction observed by ^{1}H NMR. To the sample, 15-crown-5 (22 mg, 0.10 mmol) and additional Na(^{Dipp}NCN)(THF) (35 mg, 0.066 mol) were added, followed by additional C$_6$D$_6$ (0.1 mL). The tube was shaken to mix and left standing for 20 hours. ^{1}H NMR shows (^{Dipp}NCN)SiH(N$_3$)$_2$ is still largely unconsumed, so the sample was heated to 100 °C for a total of 46 hours, affording full consumption of (^{Dipp}NCN)SiH(N$_3$)$_2$. The NMR sample was transferred to a vial and dried under vacuum. The residue was extracted with toluene (2 x 0.5 mL) and the combined extracts were concentrated slowly under argon flow to afford a few crystals of (^{Dipp}NCN)$_2$SiH(N$_3$). NMR (C$_6$D$_6$) ^{29}Si δ/ppm = -163.1 (d, $^1J_{Si-H}$ = 276 Hz).

8.2.32. Synthesis of (THF)$_3$LiSi(TMS)$_3$

In a round-bottom flask, Si(TMS)$_4$ (4.00 g, 12.5) and THF (10 mL) were combined. The Si(TMS)$_4$ only partially solvated, resulting in a suspension. The suspension was cooled to -15 °C and stirred, and to it a pre-cooled solution of MeLi in Et$_2$O (0.35M, 43 mL, 15 mmol) was added gradually over the course of 15 minutes, resulting in the solvation of (almost) all undissolved material. The mixture was warmed up to room temperature and stirred for a

further 18 hours. An aliquot was taken for NMR analysis to determine conversion, which was found to be only ~15%. The mixture was concentrated under vacuum to 25 mL total volume, then 20 mL THF was added. Stirring was continued at room temperature for 51 hours, after which ^{1}H NMR analysis shows approximately 85% conversion, however all MeLi has been consumed. Thus, additional MeLi in Et$_2$O (0.35M, 6 mL, 2 mmol) was added, and the solution stirred for a further 20 hours. The solution was dried under vacuum to afford a fluffy pale-yellow solid. To this, hexane (40 mL) and THF (1 mL) was added, which did not dissolve much of the material. On addition of further THF (3 mL), almost all solids dissolved, affording a slightly turbid yellow solution, which was filtered through a glass frit. The residue was extracted with hexane (2 x 5 mL). The filtrate and extracts were combined, and THF (3 mL) was added. The solution was the concentrated slowly under vacuum until crystals began to form. The mixture was then cooled to -20 °C overnight, affording large, colourless, plate-shaped crystals. The crystals were isolated by filtering the mixture using a pre-cooled glass frit, and the crystals were washed with cold hexane (2 x 5 mL). The crystals were dried briefly under vacuum for approximately 30 seconds (Yield = 4.078 g). The filtrate was again concentrated under vacuum until crystals began to form. Hexane (2 mL) was added, and the mixture again cooled to -20 °C overnight to afford more crystals, which were isolated by filtration on a pre-cooled glass frit, washed with cold hexane (2 x 2 mL), and dried under vacuum for 30 seconds. These crystals were added to the first batch, affording a combined yield of 5.113 g (10.86 mmol, 87% with respect to Si(TMS)$_4$). NMR (C$_6$D$_6$) ^{1}H δ/ppm = 3.54 (m, 12H, THF), 1.46 (m, 12H, THF), 0.54 (s, 27H, Si(CH$_3$)$_3$); ^{7}Li δ/ppm = 0.63; ^{29}Si δ/ppm = -5.3 (m, $^2J_{Si-H}$ = 5.8 Hz, Si(CH$_3$)$_3$), -188.8 (s, *Si*(TMS)$_3$).

8.2.33. Synthesis of (^{Dipp}NCN)Si(H)=NSi(TMS)$_3$

To an NMR tube containing a solution of (^{Dipp}NCN)SiH(N$_3$)$_2$ (30 mg, 0.049 mmol) in C$_6$D$_6$ (0.6 mL), (THF)$_3$LiSi(TMS)$_3$ (28 mg, 0.059 mmol) was added resulting in bubbling, precipitate formation, and an orange colouration of the solution. ^{1}H NMR analysis of the reaction solution indicates all (^{Dipp}NCN)SiH(N$_3$)$_2$ has been consumed to afford a single major product, and the excess LiSi(TMS)$_3$ remains unreacted. The solution was filtered, and the filtrate was dried under vacuum to afford a sticky orange residue. The residue was dissolved in hexane (0.2 mL) and cooled to -40 °C to afford orange, rectangular crystals of

($^{\text{Dipp}}$NCN)Si(H)=N(Si(TMS)$_3$). The solvent was decanted, and the crystals dried under vacuum. Yield = 27 mg (0.034 mmol, 69% with respect to ($^{\text{Dipp}}$NCN)SiH(N$_3$)$_2$). IR (Nujol mull) v/cm^{-1} = 3063 w, 2100 m, 1610 w, 1568 vw, 1531 vw, 1487 w, 1398 w, 1366 w, 1327 vw, 1295 vw, 1248 s, 1239 s, 1202 vw, 1179 vw, 1137 vw, 1114 vw, 1099 vw, 1057 vw, 1048 vw, 1025 vw, 1018 vw, 993 vw, 935 vw, 926 vw, 862 s, 836 s, 788 m, 754 vw, 745 vw, 703 w, 682 w, 645 vw, 620 vw, 561 vw, 553 vw, 515 vw. NMR (C$_6$D$_6$) ^{1}H δ/ppm = 7.21 (d, 2H, $^3J_{\text{H-H}}$ = 8.7 Hz, aryl-H), 7.13–7.10 (m, 4H, aryl-H), 7.04–7.01 (m, 2H, aryl-H), 6.74 (d, 2H, $^3J_{\text{H-H}}$ = 8.7 Hz, aryl-H), 6.32 (s, 1H, $^1J_{\text{Si-H}}$ = 256 Hz), 3.88 (sept, 2H, $^3J_{\text{H-H}}$ = 6.8 Hz, C*H*(CH$_3$)$_2$), 3.41 (sept, 2H, $^3J_{\text{H-H}}$ = 6.8 Hz, C*H*(CH$_3$)$_2$), 1.57 (d, 6H, $^3J_{\text{H-H}}$ = 6.8 Hz, CH(C*H$_3$*)$_2$), 1.33 (d, 6H, $^3J_{\text{H-H}}$ = 6.8 Hz, CH(C*H$_3$*)$_2$), 1.07 (d, 6H, $^3J_{\text{H-H}}$ = 6.9 Hz, CH(C*H$_3$*)$_2$), 0.90 (d, 6H, $^3J_{\text{H-H}}$ = 6.9 Hz, CH(C*H$_3$*)$_2$), 0.77 (s, 9H, C(CH$_3$)$_3$), 0.35 (s, 27H, $^2J_{\text{Si-H}}$ = 6.1 Hz, Si(CH$_3$)$_3$); ^{29}Si δ/ppm = -17.9 (m, $^2J_{\text{Si-H}}$ = 6.1 Hz, Si(CH$_3$)$_3$), -52.0 (d, $^1J_{\text{Si-H}}$ = 256 Hz), -52.1 (br, *Si*(TMS)$_3$).

8.2.34. Attempted synthesis of ($^{\text{Dipp}}$NCN)Si(N$_3$)$_3$ *via* Li($^{\text{Dipp}}$NCN)

In a Schlenk tube, ($^{\text{Dipp}}$NCN)H (6.622 g, 13.3 mmol) and LiN(TMS)$_2$ (2.249 g, 13.4 mmol) were combined as solids and the tube placed in an ice bath at 0 °C. To this, Et$_2$O (80 mL) was added, and the resulting solution was stirred at 0 °C for 2 hours. All volatiles were removed under vacuum to afford a porous yellow solid, assumed to be Li($^{\text{Dipp}}$NCN).

71 mg of this solid (0.14 mmol Li($^{\text{Dipp}}$NCN) if pure) was added to a stirred solution of Si(N$_3$)$_4$ in toluene (0.14 M, 1.0 mL, 0.14 mmol), affording a colourless solution and white precipitate. The solution was filtered into an NMR tube, and C$_6$D$_6$ (0.5 mL) was added to the tube for locking. NMR (2:1 toluene:C$_6$D$_6$) ^{1}H (major product) δ/ppm = 7.20 (d, 2H, $^3J_{\text{H-H}}$ = 8.6 Hz), 6.76 (d, 2H, $^3J_{\text{H-H}}$ = 8.6 Hz), 3.58 (sept, 4H, $^3J_{\text{H-H}}$ = 6.8 Hz), 1.43 (d, 12H, $^3J_{\text{H-H}}$ = 6.8 Hz), 0.91 (d, 12H, $^3J_{\text{H-H}}$ = 6.9 Hz), 0.74 (s, 9H). Some signals are obscured by the toluene. Note that these signals exactly match those of isolated ($^{\text{Dipp}}$NCN)Si(N$_3$)$_3$ synthesised later (8.2.36). ^{29}Si (all signals) δ/ppm = 15.3 (m, $^2J_{\text{Si-H}}$ = 6.9 Hz), -21.9 (m, $^2J_{\text{Si-H}}$ = 7.3 Hz), -118.1 (s).

The filtered solution was transferred into a vial with a loosely-fitted cap, and allowed to slowly evaporate under an atmosphere of argon of the course of 1 week, affording a white residue containing crystals that were identified as [($^{\text{Dipp}}$NCN)H$_2$][Si(N$_3$)$_5$] by SCXRD.

8.2.35. Dedicated synthesis of [(^{Dipp}NCN)H$_2$][Si(N$_3$)$_5$]

To a vial, a solution of Si(N$_3$)$_4$ in toluene (0.12 M, 0.50 mL, 0.06 mmol) was added. To this solution, (^{Dipp}NCN)H (31 mg, 0.06 mmol) was added, which only partially dissolved, resulting in a suspension. To this suspension, a solution of HN$_3$ in Et$_2$O (1.69 M, 42 mg, ~0.09 mmol) was added, causing the suspension to become thicker. Et$_2$O (4 mL) was added, and the suspension shaken to mix. After leaving standing for 1 hour, the supernatant was decanted. The residue was dissolved in THF (1 mL). Both the decanted supernatant and the THF solution were allowed to evaporate under argon flow, affording crystals of [(^{Dipp}NCN)H$_2$][Si(N$_3$)$_5$]. IR (Nujol mull) v/cm^{-1} = 3474 vw, 3443 vw, 3420 vw, 3379 vw, 3237 w, 3214 w, 3193 w, 3164 w, 3140 w, 3074 w, 2161 m, 2135 vs, 2119 m, 2111 s, 1610 m, 1587 w, 1557 w, 1515 vw, 1504 w, 1414 vw, 1402 vw, 1322 m, 1315 s, 1287 m, 1270 w, 1259 vw, 1206 w, 1198 vw, 1180 w, 1151 vw, 1131 vw, 1110 vw, 1103 w, 1094 w, 1059 w, 936 w, 922 w, 861 w, 836 w, 830 w, 808 m, 805 m, 784 vw, 764 w, 757 w, 750 vw, 690 w, 674 w, 636 vw, 620 vw, 591 w, 580 m, 558 w, 504 vw.

8.2.36. Synthesis of (^{Dipp}NCN)Si(N$_3$)$_3$ from Na(^{Dipp}NCN)

In a vial, a solution of Si(N$_3$)$_4$ in toluene (4.15%, 2.364 g, 0.50 mmol) was added and stirred. To the stirred solution, Na(^{Dipp}NCN)(THF)$_{2.3}$ (355 mg, 0.50 mmol) was added as a powder, affording a pale yellow suspension that decolourised after several seconds. The suspension was stirred for 90 minutes, then filtered through celite. The residue was extracted with toluene (1 + 0.5 mL), and the combined filtrate and extracts were concentrated under vacuum to 1 mL total volume. This solution was then slowly cooled to -20 °C, affording colourless crystals. The solution was decanted, and the crystals were washed with Et$_2$O (0.2 mL) then dried under vacuum. Yield = 179 mg (0.28 mmol, 56% with respect to Si(N$_3$)$_4$). NMR (d8-toluene) ^{1}H δ/ppm = 7.19 (d, 2H, ^{3}J$_{H-H}$ = 8.6 Hz, aryl-H), 7.12–7.02 (m, 6H, aryl-H), 6.76 (d, 2H, ^{3}J$_{H-H}$ = 8.6 Hz, aryl-H), 3.58 (sept, 4H, ^{3}J$_{H-H}$ = 6.8 Hz, CH(CH$_3$)$_2$), 1.43 (d, 12H, ^{3}J$_{H-H}$ = 6.7 Hz, CH(CH_3)$_2$), 0.91 (d, 12H, ^{3}J$_{H-H}$ = 6.8 Hz, CH(CH_3)$_2$), 0.73 (s, 9H, C(CH$_3$)$_3$); ^{29}Si δ/ppm = -118.0 (s).

8.2.37. Synthesis of (^{Dipp}NCN)Si(N$_3$)=NSi(TMS)$_3$

In a vial, (^{Dipp}NCN)Si(N$_3$)$_3$ (39 mg, 0.060 mmol) was dissolved in d8-toluene (0.6 mL). The solution was stirred, and crystalline (THF)$_3$LiSi(TMS)$_3$ (28 mg, 0.060 mmol) was added resulting in bubbling, precipitate formation, and an orange colouration of the solution. The resulting suspension was stirred for 5 minutes, by which point bubbling was no longer observed. The suspension was filtered into an NMR tube. ^{1}H NMR analysis shows two different ^{Dipp}NCN environments, and two different TMS environments. The solution was transferred back into a vial and concentrated under vacuum to afford a thick orange oil. A single drop of hexane was added to this oil, and crystals grew from this mixture over the next 6 hours. The mixture was then cooled to -20 °C overnight, and the solvent decanted. The crystalline residue was found to be a mixture of (^{Dipp}NCN)Si(N$_3$)=NSi(TMS)$_3$ (yellow plates) and (^{Dipp}NCN)Si(N$_3$)$_3$ (colourless blocks). NMR ((^{Dipp}NCN)Si(N$_3$)=NSi(TMS)$_3$ in d8-toluene) ^{29}Si δ/ppm = -18.4 (m, $^2J_{Si-H}$ = 6.2 Hz, Si(CH$_3$)$_3$), -52.4 (br, **Si**(TMS)$_3$), -78.0 (s, Si=N).

8.2.38. Synthesis of PhLi(Et$_2$O)(LiBr)$_{0.33}$

In a Schlenk tube, degassed PhBr (7.88 g, 50 mmol) was dissolved in Et$_2$O 60 mL. The solution was cooled to 0 °C, then lithium granules (0.833 g, 120 mmol) were added. The mixture was stirred at 0 °C for 10 minutes, after which it began to turn red and bubble slightly. Once bubbling had stopped, the mixture was allowed to gradually warm to room temperature whilst stirring over the next 1 hour. The resulting suspension was filtered to afford a bright orange solution which was dried under vacuum. The residue was extracted with hexane (100 mL), and the extract solution was cooled to -30 °C overnight affording a white crystalline solid. The supernatant was decanted, allowed to warm up to room temperature, and Et$_2$O (10 mL) was added to it. This solution was then used to extract the residue a second time, and the resulting extract solution was added to the white crystals. This mixture was then cooled to -30 °C overnight, affording more crystalline material. The solution was decanted, and the crystals washed with a 9 : 1 mixture of hexane : Et$_2$O (2 x 10 mL), followed by pure hexane (2 x 10 mL). The crystals were dried under vacuum. NMR (d8-THF) ^{1}H δ/ppm = 7.87 (d, 2H, $^3J_{H-H}$ = 6.8 Hz, phenyl-H), 6.83 (t, 2H, $^3J_{H-H}$ = 6.9 Hz, phenyl-H), 6.76–6.72 (m, 1H, phenyl-H), 3.38 (q, 4H, $^3J_{H-H}$ = 7.0 Hz, Et$_2$O), 1.11 (t, 6H, $^3J_{H-H}$ = 7.0 Hz, Et$_2$O).

8.2.39. Synthesis of (^{tBu}NCN)SiCl$_3$

In a vial, PhLi(Et$_2$O)(LiBr)$_{0.33}$ (561 mg, 3.00 mmol) was dissolved in Et$_2$O (4 mL). The solution was cooled to 0 °C and stirred. To this stirred solution, pre-cooled di-tert-butylcarbodiimide (462 mg, 3.00 mmol) was added dropwise, followed by additional Et$_2$O (1 mL) to wash it all into the reaction solution. The heat of the reaction warmed the reaction solution to approximately room temperature, and the solution was allowed to stir at room temperature for 10 minutes, then cooled back down to 0 °C over the next 30 minutes. SiCl$_4$ (561 mg, 3.30 mmol) was subsequently added dropwise to this solution, affording a white precipitate. Et$_2$O (1 mL) was added to wash the residual SiCl$_4$ into the reaction mixture, and the resulting suspension was allowed to stir at room temperature for 18 hours. The suspension was then filtered, and the residue extracted with Et$_2$O (3 + 2 + 2 mL). During the filtration and extraction, evaporation of the filtrate resulted in the formation of colourless needle crystals. The filtrate and extracts were combined, and cooled to -30 °C overnight, affording more crystals. The solution was decanted, and the crystals washed with cold Et$_2$O (1 mL) and dried under vacuum. Yield = 330 mg. The original filter residue was extracted with more Et$_2$O (5 mL), and the extract solution cooled to -30 °C overnight. This afforded more crystals, which were washed with cold Et$_2$O (2 x 2 mL) and dried under vacuum to afford an additional 97 mg yield. Total yield = 427 mg, (1.17 mmol, 39% with respect to di-tert-butylcarbodiimide). NMR (C$_6$D$_6$) ^{1}H δ/ppm = 6.94–6.89 (m, 1H, phenyl-H), 6.83–6.78 (m, 2H, phenyl-H), 6.74–6.71 (m, 2H, phenyl-H), 1.18 (s, 18H, C(CH$_3$)$_3$).

8.2.40. Reaction of (^{tBu}NCN)SiCl$_3$ with (THF)$_3$LiSi(TMS)$_3$

In an NMR tube, (^{tBu}NCN)SiCl$_3$ (37 mg, 0.10 mmol) was dissolved in C$_6$D$_6$ (0.6 mL). To this solution, (THF)$_3$LiSi(TMS)$_3$ (47 mg, 0.10 mmol) was added, causing the solution to turn orange and turbid. The tube was sealed and shaken to afford mixing. After 6 hours, the presence of (^{tBu}NCN)SiCl in the reaction mixture is confirmed by ^{29}Si analysis (δ = -14.1 ppm). After standing for 21 hours, the dried under vacuum, and the residue extracted with hexane (3 x 3 mL). The solution was concentrated under vacuum to 4 mL total volume, at which point it became turbid, so it was filtered. The filtered solution was cooled to -30 °C overnight, affording orange needle crystals. The solution was decanted, and the crystals

washed with cold hexane (5 + 1 mL) and dried under vacuum. These crystals were confirmed to be (^{tBu}NCN)SiCl by SCXRD unit cell determination. Yield = 9 mg (0.03 mmol, 30% with respect to (^{tBu}NCN)SiCl$_3$.

8.2.41 (Chapter 2.2.4)

8.2.41. General procedure for the thermal decomposition experiments of (^{Dipp}NCN)SiH(N$_3$)$_2$

Sample composition and decomposition conditions are outlined in Table 2.5. Heating was achieved by partially submerging the reaction vessel in a stirred oil bath set at the assigned temperature. In experiments where products sublimed, the sublimed material deposited on the walls of the reaction vessel slightly above the level of the oil bath, except in cases where a cold-finger was used, in which case the sublimate predominantly deposited on the cold-finger. Experiments consisting of <50 mg of (^{Dipp}NCN)SiH(N$_3$)$_2$ were conducted in Teflon-valve NMR tubes. After heating was concluded, C$_6$D$_6$ (0.5 – 0.6 mL) was added directly to the tube, and NMR spectra recorded. Experiments consisting of 50–330 mg (^{Dipp}NCN)SiH(N$_3$)$_2$ were conducted in a narrow Schlenk tube. Experiments consisting of >330 mg (^{Dipp}NCN)SiH(N$_3$)$_2$ were conducted in a large Schlenk tube containing a water-cooled cold-finger suspended in the centre of the tube. In some cases, the sublimed product was manually separated from the residue, which was then analysed by NMR by dissolving a sample in C$_6$D$_6$. The remaining contents of the Schlenk tube were then extracted with Et$_2$O. The insoluble residue is then dried for IR analysis as a Nujol mull. The extract solution is dried under vacuum, and a sample of the dried extract is dissolved in C$_6$D$_6$ for NMR analysis.

8.3. Experimental Procedures (Chapter 3)

8.3.1 – 8.3.9 (Chapter 3.2.1)

8.3.1. Synthesis of NaK

To a vial, freshly cut potassium (196 mg, 5.0 mmol) and sodium granules (115 mg, 5.0 mmol) were combined. The sodium granules were cut in half, and the cleanly cut face pressed into the potassium with a spatula. The mixture was then stirred with the spatula until it became a homogenous liquid.

8.3.2. Reaction of $Si(N_3)_4$ with sodium in toluene (Experiment 1 of Table 3.2)

In a vial, sodium granules (6 mg, 0.3 mmol) were added to a solution of $Si(N_3)_4$ in toluene (0.14 M, 1.0 mL, 0.14 mmol). The solution was stirred overnight, but no reaction appeared to have occurred (sodium granules unconsumed, solution remains clear and colourless).

8.3.3. Reaction of $Si(N_3)_4$ with NaK in toluene (Experiment 2 of Table 3.2)

In a vial, NaK (4 mg, 0.06 mmol) and toluene (1 mL) were combined. To this, a solution of $Si(N_3)_4$ in toluene (0.12 M, 1.0 mL, 0.12 mmol) was added, and the mixture was stirred. After 1 day of stirring, the NaK had solidified into flakes, which had a black tint to them. After another day, much of these flakes had been consumed, and the solution now contains a dark grey precipitate. After a total of 3 days, only trace metal remains. The precipitate was allowed to settle, and the bulk solution was decanted. IR analysis of the toluene solution shows exclusively $Si(N_3)_4$ (v/cm^{-1} = 3481 vw, 2202 w, 2171 vs, 1326 m). The residual solid was washed with toluene (2 x 2 mL). IR (Nujol mull) v/cm^{-1} = 2122 vs br (NaN_3), 2109 vs (NaN_3), 2022 s (KN_3).

8.3.4. Reaction of $Si(N_3)_4$ with NaK in toluene (Experiment 3 of Table 3.2)

In a vial, NaK (8 mg, 0.13 mmol) and toluene (1 mL) were combined. To this, a solution of $Si(N_3)_4$ in toluene (0.12 M, 1.0 mL, 0.12 mmol) was added, and the mixture was stirred. After

1 day of stirring, a black precipitate had formed. After a total of 2 days stirring, ^{14}N NMR analysis of the solution shows significant unreacted $Si(N_3)_4$ (δ/ppm = -153.7, -192.7).

Additional NaK (8 mg, 0.13 mmol) was added to the reaction solution, and the mixture stirred for a further 10 days. ^{14}N NMR analysis shows all $Si(N_3)_4$ is now consumed (no signals detected). The solution was decanted, and the residual solid washed with hexane (4 mL). IR (solid residue as Nujol mull) v/cm^{-1} = 2175 m br, 2127 s, 2039 vs.

8.3.5. Reaction of Si(N₃)₄ with NaK in HMPA (Experiment 4 of Table 3.2)

In a vial NaK (16 mg, 0.26 mmol) was added to HMPA (5 mL), partially dissolving to afford a deep blue solution. The solution was stirred and $Si(N_3)_4$ in toluene (0.12 M, 1.0 mL, 0.12 mmol) was added, changing the colour of the solution to a deep red. Over the next 5 minutes, this colour faded to a bright orange. Stirred for an additional 18 hours, affording a bright orange solution with traces of white precipitate. IR (HMPA) v/cm^{-1} = 2105 vw, 2025 m, 2015 w, 1994 s, 1981 vw.

8.3.6. Reaction of Si(N₃)₄ with NaK in HMPA (Experiment 5 of Table 3.2)

In a vial, NaK (16 mg, 0.26 mmol) was added to a solution of $Si(N_3)_4$ in toluene (0.12 M, 1.0 mL, 0.12 mmol). No initial signs of reaction. To this mixture HMPA (5 mL) was added and the mixture stirred, affording an initially deep red solution. Over the next 5 minutes, this colour faded to a bright orange, however over the subsequent 5 minutes, the solution became bright red. Stirred for an addition 18 hours, resulting in an even more intensely red solution, with traces of white precipitate. IR (HMPA) v/cm^{-1} = 2025 m, 2015 m, 1994 s, 1980 vw.

8.3.7. Reaction of Si(N₃)₄ with sodium in HMPA (Experiment 6 of Table 3.2)

In a vial, sodium flakes (11.5 mg, 0.50 mmol) were added to a solution of $Si(N_3)_4$ in toluene (0.12 M, 1.0 mL, 0.12 mmol). Shortly after, HMPA (5 mL) was added, resulting in some fuming of the solution. The mixture was stirred for 4 hours, affording a clear, deep-pink solution. IR (HMPA) v/cm^{-1} = 2025 m, 1994 s, 1980 vw.

8.3.8. Synthesis of Si(N₃)₄ in Et₂O, followed by reaction with potassium anthracenide (Experiment 7 of Table 3.2)

In a vial, NaN_3 (650 mg, 10 mmol) and Et_2O (5 mL) were combined. To this mixture, $SiCl_4$ (170 mg, 1.0 mmol) was added, and the mixture stirred vigorously for 1 hour. An aliquot of the solution was taken for IR analysis, but no $Si(N_3)_4$ was detected. Thus, to the reaction mixture, $AlCl_3(MeCN)$ (3 mg, 0.02 mmol) was added. The mixture was then stirred vigorously for an additional 24 hours, then filtered. An aliquot of the filtered solution was taken for NMR analysis, confirming complete conversion to $Si(N_3)_4$. NMR (Et_2O, d6-DMSO capillary) ^{14}N δ/ppm = -153.5 (s, 1N, N_β), -193.2 (s, 1N, N_γ), -323.6 (br, 1N, N_α); ^{27}Al shows no detectable species in solution.

Approximately 4 mL of this solution (containing ~0.8 mmol $Si(N_3)_4$) was transferred to a separate vial. To this aliquot, in order, anthracene (19 mg, 0.11 mmol), potassium chunks (31 mg, 0.79 mmol) and Et_2O (3 mL) were added, and the reaction mixture stirred for 64 hours. During this time, the mixture had dried out to afford a dull blue-grey solid. This was carefully disposed of due to the potential explosion hazard of dry $Si(N_3)_4$.

8.3.9. Reaction of Si(N₃)₄ with (THF)₃LiSi(TMS)₃ (synthesis of TABTC)

In an NMR tube, $(THF)_3LiSi(TMS)_3$ (28 mg, 0.06 mmol) was dissolved in C_6D_6 (0.2 mL). To this solution, $Si(N_3)_4$ in toluene (0.12 M, 0.5 mL, 0.06 mmol) was added. The tube was shaken to afford mixing, resulting in an immediate white precipitate. Initial NMR spectra recorded, showing one major product, as well as some minor signals. NMR (major product, 5:2 toluene:C_6D_6) ^1H δ/ppm = 0.30 (s); ^{14}N δ/ppm = -151.9 (br), -193.1 (br); ^{29}Si δ/ppm = -14.5 (m, $^2J_{Si-H}$ = 6.4 Hz, $Si(CH_3)_3$), -41.5 (br, *Si*(TMS)₃), -59.2 (s).

After 19 hours, the mixture was filtered and concentrated under vacuum to afford a turbid oil. This was cooled to -30 °C, affording colourless needle crystals, however these were of too poor quality for SCXRD. Thus, the crystalline residue was redissolved with 5 drops of hexane. Slow evaporation of the hexane solution afforded crystals of TABTC.

8.3.10 – 8.3.13 (Chapter 3.2.2)

8.3.10. Reaction of Si(N₃)₄ with 1 equivalent NaNH₂

In a vial, $NaNH_2$ (5 mg, 0.13 mmol) was suspended in toluene (1 mL). To this suspension, $Si(N_3)_4$ in toluene (0.14 M, 1.0 mL, 0.14 mmol) was added. The solution was stirred for 10 days. A small aliquot of the solution was taken for IR analysis, showing the presence of $Si(N_3)_4$. The mixture was filtered, and the filter residue also analysed by IR spectroscopy. IR (residue as Nujol mull) v/cm^{-1} = 2195 m br, 2126 s br, 2082 w br, 2046 w br, 2010 w.

8.3.11. Reaction of Si(N₃)₄ with 3 equivalents of NaNH₂

To a vial, a solution of $Si(N_3)_4$ in toluene (4.15%, 1.418 g, 0.30 mmol) was added, and stirred. To this solution, $NaNH_2$ (35 mg, 0.90 mmol) was added. Stirring was continued for 64 hours, then the resulting suspension was filtered, and the residue washed with toluene (1 + 0.5 mL). IR analysis of the solution shows the presence of $Si(N_3)_4$. By comparison of the intensity of the absorption band at 2169 cm^{-1} to that of known-concentration solutions of $Si(N_3)_4$ in toluene, it is estimated that half of the $Si(N_3)_4$ has been consumed.

The residue was dried under vacuum and found to contain a mixture of fine white powder and small white beads of roughly 1 mm diameter, which were analysed separately by IR spectroscopy. The powder appears to be predominantly NaN_3; IR (Nujol mull) v/cm^{-1} = 2195 m br, 2117 s br, 2046 w br. The beads appear to be predominantly $NaNH_2$; IR (Nujol mull, N–H stretch) v/cm^{-1} = 3257 s, 3209 s.

8.3.12. Reaction of Si(N₃)₄ with LiN(TMS)₂, followed by addition of PPN(N₃)

To a vial, a solution of $Si(N_3)_4$ in toluene (4.15%, 473 mg, 0.10 mmol) was added and stirred. To this stirred solution, a solution of $LiN(TMS)_2$ (17 mg, 0.10 mmol) in C_6D_6 (0.5 mL) was added dropwise, affording a turbid colourless solution. Additional C_6D_6 (0.1 mL) was added to wash down the $LiN(TMS)_2$, and the turbid reaction solution was stirred for an additional 15 minutes. The solution was then filtered into an NMR tube for analysis. NMR analysis shows selective formation of a single product in solution, assumed to be $(TMS)_2N–Si(N_3)_3$.

NMR (1:1 toluene:C_6D_6) ^1H δ/ppm = 0.15 (s); ^{14}N δ/ppm = -150.4 (s, 1N), -196.1 (s, 1N); ^{29}Si δ/ppm = 7.8 (m, $^2J_{Si-H}$ = 6.7 Hz), -59.9 (s).

To this NMR sample, PPN(N_3) (6 mg, 0.01 mmol) was added. The sample was sonicated for 1 minute to break up the solid. The contents of the NMR tube were analysed periodically over the next 22 days, showing the gradual consumption of $(TMS)_2N–Si(N_3)_3$ at decreasing rate, to form a single major product with signal intensity approximately matching the lost intensity of the $(TMS)_2N–Si(N_3)_3$ signals. After 22 days, a small amount of TMS(N_3) was added to the sample, which cause an increase in the product signals without the appearance of new signals, thus verifying the product's identity as TMS(N_3). NMR (product, 1:1 toluene:C_6D_6) ^1H δ/ppm = -0.07 (s, $^2J_{Si-H}$ = 6.9 Hz); ^{14}N δ/ppm = -145.2 (s, 1N), -208.2 (s, 1N), -320.5 (br, 1N); ^{29}Si δ/ppm = 15.3 (m, $^2J_{Si-H}$ = 6.9 Hz).

8.3.13. Larger scale reaction of Si(N_3)$_4$ with LiN(TMS)$_2$, followed by addition of PPN(N_3)

In a vial, LiN(TMS)$_2$ (167 mg, 1.00 mmol) was dissolved in toluene (1 mL). This solution was then added dropwise over the course of 10 minutes to a separate vial containing a stirred solution of Si(N_3)$_4$ in toluene (4.15%, 4.727 g, 1.00 mmol of Si(N_3)$_4$). The resulting white suspension was stirred for an additional 20 minutes, then filtered. The filter residue was extracted with toluene (2 x 2 mL). The filtrate and extracts were combined in a small Schlenk tube and stirred. To this stirred solution, PPN(N_3) (58 mg, 0.10 mmol) was added. This mixture was stirred for a total of 11 days, affording a colourless solution with an orange-brown residue coating the walls of the tube. 0.3 mL of this solution was decanted into an NMR tube containing 0.2 mL C_6D_6, and a ^1H NMR spectrum recorded of this sample to determine the ratio of $(TMS)_2N–Si(N_3)_3$: TMS(N_3), which was found to be 1 : 2.3.

The bulk reaction solution was decanted, and the orange-brown residue was washed with toluene (2 x 3 mL). The residue was then dried under vacuum to afford 63 mg of a waxy brown solid. IR (Nujol mull) v/cm^{-1} = ~2168 s br, 2148 s, ~2098 m br, 1992 vw, 1968 vw, 1900 vw. Air exposure of this IR sample results in a reduction of the intensity of the absorption at 2168 cm^{-1} relative to the other absorptions, and a new absorption appears at 2031 cm^{-1}.

8.4. Experimental Procedures (Chapter 4)

8.4.1 – 8.4.7 (Chapter 4.2.1)

8.4.1. Synthesis of N,N'-bis(2,6-diisopropylphenyl)-1,4-diazabutadiene

Under ambient atmosphere, in a large round-bottom flask, DippNH$_2$ (50.0 g, 282 mmol) was dissolved in MeOH (50 mL). To this solution, AcOH (0.25 mL, 4 mmol) was added, and the solution warmed to 50 °C. The solution was stirred, and to it a separately prepared solution of glyoxal in H$_2$O (40%, 18.4 g, 127 mmol) diluted with MeOH (50 mL) was added. Stirring was continued at 50 °C for 15 minutes, then the solution was allowed to cool to room temperature. A few minutes after allowing to cool down, a bright yellow precipitate began to form. The mixture was stirred at room temperature for a further 45 minutes and was then filtered. The residue was thoroughly washed with cold (-5 °C) MeOH (2 x 100 mL) to afford a bright yellow powder, which was dried under vacuum. Yield = 33.6 g (89.2 mmol, 70% with respect to glyoxal).

8.4.2. Synthesis of 1,3-bis(2,6-diisopropylphenyl)imidazolium chloride ([IPrH]Cl)

Under ambient atmosphere, in a large round-bottom flask, N,N'-bis(2,6-diisopropylphenyl)-1,4-diazabutadiene (15.06 g, 40.0 mmol) was suspended in EtOAc (250 mL). The suspension was heated to 70 °C and stirred. To the stirred suspension, a solution of TMSCl (5.33 mL, 42.0 mmol) in EtOAc (50 mL) was added slowly over the course of 20 minutes. The resulting suspension was stirred at 70 °C for a further 2 hours, affording a brown solution with an off-white precipitate. The suspension was allowed to slowly cool down to room temperature with gentle stirring over the next 1.5 hours, and was then placed in an ice box for 1.5 hours to cool it to 0 °C. Once cooled, the mixture was filtered, the residue washed with cold EtOAc (2 x 100 mL), affording a white powder with a slight pink tint to it. The powder was dried under vacuum overnight, which removed the pink discolouration. ^{1}H NMR analysis of this material shows it still contains 0.6 equivalents of EtOAc, so the material was further dried by heating to 100 °C under high vacuum until no significant mass loss was observed, which took 9 days [note: if a higher temperature is used, the necessary duration will likely be shorter]. Yield = 14.06 g (33.1 mmol, 83% with respect to N,N'-bis(2,6-diisopropylphenyl)-1,4-

diazabutadiene). NMR (d6-DMSO) ^{1}H δ/ppm = 10.22 (t, 1H, $^4J_{\text{H-H}}$ = 1.5 Hz, imidazolyl-H), 8.58 (d, 2H, $^4J_{\text{H-H}}$ = 1.5 Hz, imidazolyl-H), 7.69 (t, 2H, $^3J_{\text{H-H}}$ = 7.8 Hz, aryl-H), 7.53 (d, 4H, $^3J_{\text{H-H}}$ = 7.8 Hz, aryl-H), 2.35 (sept, 4H, $^3J_{\text{H-H}}$ = 6.8 Hz, CH(CH$_3$)$_2$), 1.26 (d, 12H, $^3J_{\text{H-H}}$ = 6.8 Hz, CH(CH_3)$_2$), 1.16 (d, 12H, $^3J_{\text{H-H}}$ = 6.9 Hz, CH(CH_3)$_2$).

8.4.3. Synthesis of 1,3-bis(2,6-diisopropylphenyl)imidazol-2-ylidene (IPr)

In a round-bottom flask, [IPrH]Cl (4.251 g, 10.0 mmol) was suspended in THF (30 mL) and stirred for 10 minutes. Whilst still stirring, KOtBu (1.178 g, 10.5 mmol) was then added at once, causing the solution colour to change from pale pink to orange. The mixture was stirred for 2.5 hours, after which all volatiles were removed under vacuum. Toluene (30 mL) was added to the residue, and stirred until it became a homogenous suspension. To this suspension, hexane (30 mL) was added, and the suspension was filtered through celite. The filter residue was extracted with toluene (2 x 10 mL) followed by hexane (20 mL). The extracts were combined with each other and filtered through celite before combining with the original filtrate. The combined filtrates were slowly concentrated under vacuum to 40 mL total volume, affording fine, colourless, needle-shaped crystals. The solution was then cooled to -40 °C overnight to afford more crystal growth. The solvent was decanted, and the crystals washed with cold hexane (10 mL) and dried under vacuum. The decanted solution and the hexane used for washing were combined, and concentrated slowly under vacuum to dryness, affording more crystals stained with an orange waxy residue. The crystals were washed with cold (0 °C) hexane (10 + 5 + 5 mL) and dried under vacuum. Combined crystalline yield = 3.425 g (8.81 mmol, 88% with respect to [IPrH]Cl). NMR (C$_6$D$_6$) ^{1}H δ/ppm = 7.32–7.27 (m, 2H, aryl-H), 7.19 (d, 4H, $^3J_{\text{H-H}}$ = 7.7 Hz), 6.62 (s, 2H, imidazolyl-H), 2.97 (sept, 4H, $^3J_{\text{H-H}}$ = 6.9 Hz, CH(CH$_3$)$_2$), 1.29 (d, 12H, $^3J_{\text{H-H}}$ = 6.8 Hz, CH(CH_3)$_2$), 1.19 (d, 12H, $^3J_{\text{H-H}}$ = 7.0 Hz, CH(CH_3)$_2$).

8.4.4. Synthesis of IPrSiCl$_2$

In a Schlenk tube, HSiCl$_3$ (291 mg, 2.15 mmol) was dissolved in toluene (40 mL) and stirred. To this stirred solution, IPr (1.671 g, 4.30 mmol) was added at once, followed by toluene (10 mL), affording a bright yellow suspension. The suspension was stirred for 17 hours, then

filtered. The filter residue was extracted with toluene (2 x 10 mL), and the combined filtrate and extracts were slowly concentrated under vacuum to dryness, affording a yellow crystalline residue. The residue was washed with hexane (10 + 5 mL) and briefly dried under vacuum to afford a yellow microcrystalline powder. Yield = 872 mg (1.79 mmol, 83% with respect to $HSiCl_3$). NMR (C_6D_6) ^1H δ/ppm = 7.22 (t, 2H, $^3J_{H-H}$ = 7.8 Hz, aryl-H), 7.07 (d, 4H, $^3J_{H-H}$ = 7.8 Hz, aryl-H), 6.37 (s, 2H, imidazolyl-H), 2.79 (sept, 4H, $^3J_{H-H}$ = 6.8 Hz, CH(CH$_3$)$_2$), 1.43 (d, 12H, $^3J_{H-H}$ = 6.7 Hz, CH(CH_3)$_2$), 1.01 (d, 12H, $^3J_{H-H}$ = 6.9 Hz, CH(CH_3)$_2$). NMR (d8-THF) ^1H δ/ppm = 7.61 (s, 2H, imidazolyl-H), 7.46 (t, 2H, $^3J_{H-H}$ = 7.8 Hz, aryl-H), 7.29 (d, 4H, $^3J_{H-H}$ = 7.8 Hz, aryl-H), 2.70 (sept, 4H, $^3J_{H-H}$ = 6.9 Hz, CH(CH$_3$)$_2$), 1.34 (d, 12H, $^3J_{H-H}$ = 6.8 Hz, CH(CH_3)$_2$), 1.15 (d, 12H, $^3J_{H-H}$ = 6.9 Hz, CH(CH_3)$_2$); ^{29}Si δ/ppm = 16.9 (s).

8.4.5. Small scale synthesis of IPrSiCl$_2$ followed by reaction with NaAl(N$_3$)$_4$(THF)$_4$

In an NMR tube, IPr (39 mg, 0.10 mmol) was dissolved in C_6D_6 (0.5 mL). To this solution, $HSiCl_3$ (6 mg, 0.04 mmol) was added, and the tube shaken to afford mixing, resulting in a yellow solution with a white precipitate. NMR analysis of this solution shows IPrSiCl$_2$ as the dominant species in solution. To this solution, NaAl(N$_3$)$_4$(THF)$_4$ (18 mg, 0.035 mmol) was added, and the mixture sonicated for 2 x 5 minutes with vigorous shaking in between to break up the solid. The reaction progress was periodically monitored by ^1H NMR spectroscopy. After a total of 28 days, the reaction appears to be complete, with three products observed in both ^1H and ^{27}Al NMR – one major product, one minor product, one trace product, with a respective ^1H integral ratio of 1.00 : 0.42 : 0.03, and a respective ^{27}Al integral ratio of 1.00 : 0.37 : 0.04. The similarity of these ratios indicate that these signals correspond to the same respective compounds. NMR (major product, C_6D_6) ^1H δ/ppm = 7.28 (t, $^3J_{H-H}$ = 7.8 Hz, aryl-H), 7.15 (d, $^3J_{H-H}$ = 7.8 Hz, aryl-H), 6.41 (s, imidazolyl-H), 2.46 (sept, $^3J_{H-H}$ = 6.9 Hz, CH(CH$_3$)$_2$), 1.41 (d, $^3J_{H-H}$ = 6.7 Hz, CH(CH_3)$_2$), 0.94 (d, $^3J_{H-H}$ = 6.9 Hz, CH(CH_3)$_2$); ^{27}Al δ/ppm = 66.2 (s). NMR (minor product, C_6D_6) ^1H δ/ppm = 7.27 (t, $^3J_{H-H}$ = 7.8 Hz, aryl-H), 7.14 (d, $^3J_{H-H}$ = 7.8 Hz, aryl-H), 6.44 (s, imidazolyl-H), 2.52 (sept, $^3J_{H-H}$ = 6.8 Hz, CH(CH$_3$)$_2$), ~1.41 (?, [obscured by THF]), 0.94 (d, $^3J_{H-H}$ = 6.9 Hz, CH(CH_3)$_2$); ^{27}Al δ/ppm = 81.3 (br). NMR (trace product, C_6D_6) ^1H δ/ppm = 6.47 (s, imidazolyl-H), 2.58 (sept, $^3J_{H-H}$ = 6.9 Hz, CH(CH$_3$)$_2$), [other signals obscured by other products]; ^{27}Al δ/ppm = 94.1 (br).

After recording spectra, the mixture was filtered, and the solution was evaporated under argon flow to afford colourless crystals and a brown residue. The crystals were determined to be $IPrAl(N_3)_3$ by SCXRD.

Note: the change in ^{27}Al chemical shift from the major product, to the minor product, then to the trace product is comparable to that observed from the substitution of azides for chlorides on aluminium azides during the syntheses of $HSi(N_3)_3$. Additionally, all species have very similar ^1H chemical shift values. It is therefore likely that the aforementioned spectra of major, minor and trace products correspond $IPrAl(N_3)_3$, $IPrAl(N_3)_2Cl$ and $IPrAl(N_3)Cl_2$ respectively, but this could not be verified.

8.4.6. Reaction of IPrSiCl₂ with PPN(N₃)

In an NMR tube, $IPrSiCl_2$ (20 mg, 0.04 mmol) was partially dissolved in d8-THF (0.5 mL). NMR spectra were recorded to confirm the stability of $IPrSiCl_2$ in THF. After 16 hours, only small amounts of the $IPrSiCl_2$ were found to have decomposed, so $PPN(N_3)$ (46 mg, 0.08 mmol) was added to the sample. The tube was sonicated for a total of 5 minutes with intermittent shaking to break up the solid. The mixture was left standing, and periodically analysed by NMR spectroscopy over the next 42 hours. The solution was then filtered. The product in solution was confirmed to be IPr by the addition of a genuine sample for reference.

The filter residue was washed with toluene (2 x 1 mL) and dried under vacuum. IR (Nujol mull) v/cm^{-1} = 2234 vw, 2220 vw br, 2168 w br, 2115 vw, 2106 w, 2006 m, 2001 m, 1994 s, 1991 vs, 1976 vw. Air exposure of the IR sample for 10 minutes resulted in a decrease of the relative intensities of the bands at 2234 cm^{-1} and 2168 cm^{-1}, and an increase in the relative intensities of the bands at 2115 cm^{-1} and 2006 cm^{-1}.

8.4.7. Reaction of IPrSi(N₃)₄ with (THF)₃LiSi(TMS)₃

In a vial, IPr (23 mg, 0.06 mmol) was dissolved in toluene (0.5 mL). This solution was then added to a stirred solution of $Si(N_3)_4$ in toluene (0.12 M, 0.5 mL, 0.06 mmol), affording a yellow suspension. After 1 hour of stirring, a solution of $(THF)_3LiSi(TMS)_3$ was added, resulting in violent bubbling for several seconds and the yellow colour of the solution

intensified. The suspension was stirred for an additional 10 minutes, then filtered. Attempts to crystallise products by concentrating under vacuum and cooling to -30 °C were unsuccessful.

8.4.8 – 8.4.20 (Chapter 4.2.2)

8.4.8. Synthesis of diethyldipicolinate

Under ambient atmosphere, in a large round-bottom flask, dipicolinic acid (16.71 g, 100 mmol) was dissolved in 200 mL EtOH. To this solution, H_2SO_4 (95%, 4 mL) and benzene (20 mL) were added. The solution was stirred and refluxed at 90 °C under a Dean-Stark apparatus for 21 hours. The solvent was then removed by opening the tap of the apparatus, allowing all volatiles to distil out of the flask. The residue was allowed to cool down to room temperature, and H_2O (50 mL) was added to it. The resulting solution was neutralised (pH = 7) by gradual addition of Na_2CO_3. This solution was then extracted with $CHCl_3$ (5 x 25 mL). The combined $CHCl_3$ extracts were then dried under vacuum to afford white crystals. Yield = 17.17 g (77 mmol, 77% with respect to dipicolinic acid). NMR ($CDCl_3$) ^1H δ/ppm = 8.26 (d, 2H, $^3J_{H-H}$ = 7.8 Hz, pyridine-H), 7.98 (t, 1H, $^3J_{H-H}$ = 7.8 Hz, pyridine-H), 4.47 (q, 4H, $^3J_{H-H}$ = 7.1 Hz, CH_2CH$_3$), 1.43 (t, 6H, $^3J_{H-H}$ = 7.1 Hz, CH$_2$CH_3).

8.4.9. Synthesis of 2,6-diacetylpyridine

To a round-bottom flask, dry EtOH (130 mL, dried over 3 Å molecular sieves) was added. To this, sodium granules (5.29 g, 230 mmol) were added, and the mixture stirred until the sodium had completely dissolved. The solution was then dried under vacuum to leave behind a residue of NaOEt. To this residue, a solution of diethyldipicolinate (11.10 g, 49.7 mmol) in EtOAc (40 mL) was added. A water condenser was attached to the flask, and the mixture was stirred and heated to reflux for 18 hours. Additional EtOAc (60 mL) was added, and the mixture was cooled down to 0 °C. Whilst stirring, aqueous HCl (37%, 33 mL) was added to the mixture dropwise. Once addition was complete, the mixture was heated to reflux and stirred for 8 hours. The solution was allowed to cool to room temperature, and H_2O was added until all solids dissolved. The EtOAc phase was separated, and the aqueous

solution extracted with $CHCl_3$ (4 x 25 mL). The extracts were added to the EtOAc solution to form a combined organic solution, which was washed with an aqueous solution of Na_2CO_3 (5%, 50 mL). Once bubbling was no longer observed in the mixture, the organic phase was separated, and the aqueous phase extracted with $CHCl_3$ (3 x 10 mL). The combined organic phase and extracts were dried over $MgSO_4$ and filtered. This filtered solution was then concentrated under vacuum at 60 °C until it appeared close to saturation, then the solution was cooled to -30 °C overnight, affording a crystalline residue. The crystals were washed with pentane (3 x 10 mL) and dried under vacuum. Yield = 4.49 g (27.5 mmol, 55% with respect to diethyldipicolinate). NMR ($CDCl_3$) ^1H δ/ppm = 8.19 (d, 2H, $^3J_{H-H}$ = 7.8 Hz, pyridine-H), 7.97 (t, 1H, $^3J_{H-H}$ = 7.8 Hz, pyridine-H), 2.78 (s, 6H, CH_3).

8.4.10. Synthesis of bis-2,6-(N-(2,6-diisopropylphenyl)acetimino)pyridine (BIP)

In a round-bottom flask, 2,6-diacetylpyridine (1.00 g, 6.13 mmol) was dissolved in toluene (35 mL). To this solution, p-toluenesulphonic acid monohydrate (71 mg, 0.37 mmol) was added, followed by 2,6-diisopropylaniline (2.6 mL, 13.9 mmol). The flask was attached to a Dean-Stark apparatus, and the solution heated to reflux for 18 hours. The solution was allowed to cool down to room temperature, and the solvent removed under vacuum. The residue was extracted with DCM, and the DCM solution allowed to slowly evaporate to dryness, affording BIP as a microcrystalline yellow powder. Yield = 1.285 g (2.67 mmol, 44% with respect to 2,6-diacetylpyridine). NMR (CD_2Cl_2) ^1H δ/ppm = 8.47 (d, 2H, $^3J_{H-H}$ = 7.8 Hz, pyridine-H), 7.96 (t, 1H, $^3J_{H-H}$ = 7.8 Hz, pyridine-H), 7.17 (d, 4H, $^3J_{H-H}$ = ~7.6 Hz, aryl-H), 7.09 (dd, 2H, $^3J_{H-H}$ = 6.9 Hz, 8.3 Hz, aryl-H), 2.77 (sept, 4H, $^3J_{H-H}$ = 6.9 Hz, CH(CH$_3$)$_2$), 2.26 (s, 6H, CH$_3$), 1.16 (t, 24H, $^3J_{H-H}$ = 6.9 Hz, CH(CH_3)$_2$). NMR (C_6D_6) ^1H δ/ppm = 8.51 (d, 2H, $^3J_{H-H}$ = 7.8 Hz, pyridine-H), 7.29 (t, 1H, $^3J_{H-H}$ = 7.8 Hz, pyridine-H), 7.23–7.20 (m, 4H, aryl-H), 7.18–7.13 (m, aryl-H), 2.92 (sept, 4H, $^3J_{H-H}$ = 6.9 Hz, CH(CH$_3$)$_2$), 2.28 (s, 6H, CH$_3$), 1.20 (d, 12H, $^3J_{H-H}$ = 6.9 Hz, CH(CH_3)$_2$), 1.16 (d, 12H, $^3J_{H-H}$ = 6.9 Hz, CH(CH_3)$_2$).

8.4.11. Reaction of BIP with SiCl$_4$

In an NMR tube, BIP (50 mg, 0.10 mmol) was partially dissolved in C_6D_6 (0.6 mL). To the resulting yellow suspension, $SiCl_4$ (19 mg, 0.11 mmol) was added. The mixture was briefly

sonicated to break up the solids. Initial ^{1}H NMR analysis shows no reaction. The sample was heated to 100 °C, causing all solids to dissolve and the solution to mix by refluxing. Heating was continued for 80 hours, then cooled down to room temperature, resulting in precipitation. ^{1}H NMR analysis shows no change. Thus, to this sample, lithium (4 mg, 0.6 mmol) and naphthalene (3 mg, 0.02 mmol) were added. The sample was heated to 100 °C, causing all solids except the lithium to dissolve. After heating for 90 hours, the solution had darkened slightly. The sample was cooled down to room temperature, again resulting in precipitation. ^{1}H NMR analysis shows no species in solution other than BIP and naphthalene.

8.4.12. Reaction of BIP with HSiCl$_3$

In an NMR tube, BIP (50 mg, 0.10 mmol) was partially dissolved in C$_6$D$_6$ (0.6 mL). To the resulting yellow suspension, HSiCl$_3$ (14 mg, 0.10 mmol) was added. The mixture was briefly sonicated to break up the solids. Initial ^{1}H NMR analysis shows no reaction. The sample was heated to 100 °C, causing all solids to dissolve and the solution to mix by refluxing. Heating was continued for 80 hours resulting in a significant darkening of the solution. ^{1}H NMR analysis shows unreacted BIP as the dominant compound in solution, with innumerous other signals which are too convoluted to adequately interpret. The sample was heated for an additional 5 days. ^{1}H NMR analysis now shows an increase in intensity of all product signals, however the most intense signals are still those of BIP.

8.4.13. Reaction of BIP with Si$_2$Cl$_6$

In an NMR tube, BIP (50 mg, 0.10 mmol) was partially dissolved in C$_6$D$_6$ (0.6 mL). To the resulting yellow suspension, Si$_2$Cl$_6$ (30 mg, 0.11 mmol) was added. The mixture was briefly sonicated to break up the solids. Initial ^{1}H NMR analysis shows no reaction. The sample was heated to 100 °C, causing all solids to dissolve and the solution to mix by refluxing. Heating was continued for 64 hours, affording a dark brown solution. ^{1}H NMR analysis shows significant quantities of unreacted BIP, as well as several sets of signals indicating the formation of multiple products. The solution was filtered and dried under vacuum. The residue was dissolved in hexane (0.5 mL), and the hexane solution allowed to slowly evaporate affording a brown residue and a few blue-black crystals identified as (^{SiCl3}BIP)SiCl$_2$

by SCXRD. The remaining residue was extracted with Et_2O (1 mL), affording a pink solution. This solution was allowed to slowly evaporate to afford colourless crystals of BIP and orange crystals identified as $(^{\pm H2}BIP)SiCl_2$ by SCXRD.

8.4.14. Reaction of Xantphos with Si_2Cl_6

In an NMR tube, Xantphos (59 mg, 0.10 mmol) was dissolved in C_6D_6 (0.5 mL). ^1H and ^{31}P NMR spectra of the Xantphos was recorded (^1H δ/ppm = 7.42–7.37 (m, 8H), 7.10 (dd, 2H), 7.06–7.02 (m, 12H), 6.84–6.81 (m, 2H), 6.76 (t, 2H), 1.36 (s, 6H); ^{31}P δ/ppm = -17.8). To this sample, Si_2Cl_6 (34 mg, 0.13 mmol) was added, causing the solution to become slightly turbid. Over the next 15 minutes, a fluffy white precipitate formed and settled at the bottom of the tube. After allowing to react for a total of 2 hours, ^1H and ^{31}P NMR analysis shows no consumption of Xantphos, while ^{29}Si analysis shows the presence of Si_2Cl_6 (δ = -6.4 ppm) and $SiCl_4$ (δ = -18.9 ppm). After allowing to react for a total of 4 days, the Xantphos remains unreacted, the Si_2Cl_6 concentration has decreased, and the $SiCl_4$ concentration has increased. After a total of 17 days, almost all Si_2Cl_6 is consumed, still no consumption of Xantphos.

8.4.15. Reaction of BIP with Si_2Cl_6 in the presence of Xantphos

In an NMR tube, Si_2Cl_6 (16 mg, 0.06 mmol) was dissolved in C_6D_6 (0.6 mL). To this sample, BIP (29 mg, 0.06 mmol) was added, which partially dissolved to afford a yellow suspension. Xantphos (3 mg, 0.005 mmol) was added to the sample, and the mixture sonicated for 10 seconds to break up the solids. The sample was heated to 60 °C to aid in the solvation of BIP, however not all material dissolved. After heating at 60 °C for 4 hours, the solution turned orange, however ^1H NMR analysis shows no significant change. Heating was continued for a total of 3 days, affording a dark red-orange suspension. ^1H NMR analysis of this solution shows predominantly unreacted BIP and Xantphos with only weak other signals, while the ^{29}Si spectrum shows the majority of Si_2Cl_6 has decomposed to afford $SiCl_4$.

8.4.16. Reaction of BIP with Si_2Cl_6 in the presence of DIPEA

In an NMR tube, Si_2Cl_6 (14 mg, 0.05 mmol) was dissolved in C_6D_6 (0.6 mL). To this sample, BIP (25 mg, 0.05 mmol) was added followed by DIPEA (1 mg, 0.01 mmol), and the sample shaken briefly to afford mixing. Initial ^1H NMR analysis shows no reaction. The sample was left standing for 14 days. ^1H NMR analysis shows no change, while ^{29}Si analysis shows only $SiCl_4$ in solution, with no remaining Si_2Cl_6.

8.4.17. Reaction of BIP with $HSiCl_3$ in the presence of DIPEA

In an NMR tube, $HSiCl_3$ (7 mg, 0.05 mmol) was dissolved in C_6D_6 (0.6 mL). To this sample, BIP (25 mg, 0.05 mmol) was added followed by DIPEA (1 mg, 0.01 mmol), and the sample shaken briefly to afford mixing. Initial ^1H NMR analysis shows no reaction. The sample was left standing for 13 days. ^1H NMR analysis shows the presence of some minor new signals, but the initial reagents are all largely unconsumed.

8.4.18. Reaction of BIP with $Si(N_3)_4$

In an NMR tube, a solution of $Si(N_3)_4$ in toluene (0.12 M, 0.5 mL, 0.06 mmol) was diluted with C_6D_6 (0.2 mL). To this solution, BIP (29 mg, 0.06 mmol) was added, and the mixture briefly sonicated to break up the solids. Initial ^1H NMR analysis shows no reaction. The sample was heated to 100 °C for 6 days. No change to the sample by ^1H NMR analysis, ^{14}N analysis shows only unreacted $Si(N_3)_4$.

8.4.19. Preparation of $HSi(N_3)_3$ followed by reaction with BIP

BIP (82 mg, 0.17 mmol) was added to an NMR tube. To this tube, an aliquot of the 3:1 hexane:C_6D_6 solution from "Synthesis of $HSi(N_3)_3$ in C_6D_6, followed by addition of hexane" was added (0.6 mL, ~0.08 mmol $HSi(N_3)_3$). The mixture was briefly sonicated to break up the solid, then left standing to react. After 1 hour, ^1H and ^{29}Si NMR analysis show the dominant Si-containing compound in solution is still $HSi(N_3)_3$, however significant quantities of $H_2Si(N_3)_2$ and $Si(N_3)_4$ are also observed (each approximately half the concentration of $HSi(N_3)_3$). After 16 hours, ^1H NMR analysis shows the concentration of

HSi(N$_3$)$_3$ has decreased somewhat, while H$_2$Si(N$_3$)$_2$ remains unchanged. The mixture was filtered, and slow evaporation of the solvent afforded a residue that contained a few crystals of (H$_2$SiBIP)$_2$[AlCl$_4$]$_2$.

8.4.20. Reaction of terpyridine with Si$_2$Cl$_6$

In a vial, Si$_2$Cl$_6$ (269 mg, 1.00 mmol) was dissolved in toluene (5 mL). To this solution, a separate solution of terpyridine (233 mg, 1.00 mmol) in toluene (1 mL) was added at once, resulting in an immediate dark green colour that rapidly darkened to near black on completion of addition. After a few seconds, the solution colour changed from dark green to dark red. The solution was briefly swirled to afford mixing then left standing for 10 days, affording a dark red solution which turns green upon even traces of air exposure, and an amorphous black residue on the walls of the vial. After standing for a further 7 days, thin, black, plate-shaped crystals grew in this residue. These crystals were identified as (^{SiCl3}Terpy)SiCl$_2$ by SCXRD.

8.5. Experimental Procedures (Chapter 5)

8.5.1 – 8.5.10 (Chapter 5.2)

8.5.1. Reaction of Si_2Cl_6 with NaN_3 and 15-crown-5

To a vial, THF (2.5 mL) and NaN_3 (1.625 g, 25.0 mmol) were combined. To this, 15-crown-5 (330 mg, 1.50 mmol) was added, followed by Si_2Cl_6 (134 mg, 0.50 mmol). The reaction mixture was shaken to mix, resulting in bubbling. The solution was stirred for 3 days. An aliquot of the supernatant was taken for ^{14}N and ^{29}Si analysis, no signals detected in either.

8.5.2. Reaction of Si_2Cl_6 with $NaAl(N_3)_4(THF)_4$ in C_6D_6

In an NMR tube, Si_2Cl_6 (46 mg, 0.17 mmol) was dissolved in C_6D_6 (0.6 mL). To this sample, $NaAl(N_3)_4(THF)_4$ (130 mg, 0.26 mmol) was added, resulting in violent bubbling. After 5 minutes, the rate of bubbling had reduced, so the tube was sealed and shaken to afford mixing. After 30 minutes, bubbling had subsided, and the sample was taken for ^{29}Si NMR analysis. The most intense signal corresponds to $Si(N_3)_4$ (δ = -74.4 ppm). Other weaker signals at -60.0 ppm and -46.6 ppm are consistent with $Si(N_3)_3Cl$ and $Si(N_3)_2Cl_2$ respectively, and very weak unknown signals at -66.0 ppm and -75.9 ppm. Comparison of the spectrum with blank ^{29}Si spectra indicates the presence of a strong broad signal superimposed on glass resonance with a chemical shift range from -31 ppm to -96 ppm. Another spectrum was recorded after 12 days, in which this broad signal was no longer present, other peaks have only had slight changes in intensity.

8.5.3. Reaction of Si_2Cl_6 with $NaAl(N_3)_4(THF)_4$ in THF

In an NMR tube, $NaAl(N_3)_4(THF)_4$ (89 mg, 0.18 mmol) was partially dissolved in THF (0.5 mL). To this mixture, Si_2Cl_6 (27 mg, 0.10 mmol) was added, resulting in bubbling. After 20 minutes, bubbling had subsided, and the sample was taken for ^{29}Si NMR analysis. The only intense signal appears at -76.1 ppm, which is attributed to $Si(N_3)_4$. Weak signals are detected at δ/ppm = -51.9 (br), -55.6 (s), -58.8 (br), -59.8 (s), -65.0 (s), =76.8 (s). Another spectrum recorded after 2.5 days shows no significant change to the sample.

8.5.4. Reaction of Si_2Cl_6 with TMS(N_3)

In an NMR tube, Si_2Cl_6 (26 mg, 0.10 mmol) was dissolved in C_6D_6 (0.3 mL). To this solution, TMS(N_3) (0.2 mL) was added. The tube was initially shaken to affording mixing, then left standing. The progress of the reaction was monitored by ^{14}N and ^{29}Si NMR spectroscopy. After 3 days, ^{14}N NMR analysis indicates the formation of several new azido-silicon species; ^{29}Si shows unreacted Si_2Cl_6 (δ = -6.4 ppm) as the dominant non-TMS compound in solution. Several weak signals are also detected, including those of $SiCl_4$ (δ = -18.9) and $Si(N_3)_4$ (δ = -74.2 ppm). After a total of 98 days, approximately one third of the Si_2Cl_6 content still remains, and its resonance is still the most intense non-TMS signal in the ^{29}Si NMR spectrum. The signal corresponding to $SiCl_4$ is no longer present, most other signals have increase slightly in intensity, including that of $Si(N_3)_4$. The ^{14}N NMR spectrum confirms that $Si(N_3)_4$ is the dominant azide-containing product of the reaction (δ/ppm = -153.5, -193.0).

8.5.5. Synthesis of 2,4,6-tri-tert-butylphenyl lithium (Mes*Li)

In a vial, 2,4,6-tri-tert-butyl-1-bromobeznene (200 mg, 0.62 mmol) was dissolved in THF (5 mL) and the solution cooled to -45 °C. To this, a pre-cooled solution of tBuLi (1.7 M, 0.75 mL, 1.3 mmol) was added at once, affording a yellow solution. The solution was stirred at -45 °C for 1 hour, after which the yellow colour had faded. The solution was then allowed to warm up to room temperature whilst stirring for 20 minutes before drying under vacuum to afford a white solid coated in a sticky orange oil. This residue was washed with hexane (2 x 2 mL) to afford a white powder. NMR analysis of the powder shows the presence of 1.5 equivalents of THF per Mes* group. NMR (Et_2O, d6-DMSO capillary) ^1H δ/ppm = 7.25 (s, 2H, aryl-H), 3.81 (m, 6H, THF), 1.92 (m, 6H, THF), 1.51 (s, 18H, $C(CH_3)_3$), 1.39 (s, 9H, $C(CH_3)_3$).

8.5.6. Reaction of $HSiCl_3$ with Mes*Li(THF)$_{1.5}$

In an NMR tube, Mes*Li(THF)$_{1.5}$ (25 mg, 0.07 mmol) was dissolved in THF (0.5 mL). A d6-DMSO capillary was added for locking purposes, and a ^1H NMR spectrum of this solution was recorded to compare the reaction products against. This solution was cooled to -30 °C, then $HSiCl_3$ (13 mg, 0.10 mmol) was added to it. The solution was allowed to warm to room

temperature and left standing for 1 hour before being analysed by NMR spectroscopy. ^{1}H NMR analysis shows all Mes*Li has been consumed, being replaced by an approximately equal quantity of 1,3,5-tri-tert-butylbenzene (assigned based on integral ratio and chemical shift relative to Mes*Li – the absolute ^{1}H chemical shift cannot be determined reliably due to the mixture having no reliable signal to calibrate to). Considerable excess $HSiCl_3$ is also observed in this spectrum. After 1 day, no change to the ^{1}H NMR spectrum is observed. [29]Si δ/ppm = 29.6 (s, $SiCl_3^-$), -9.9 (d, $^1J_{Si-H}$ = 380 Hz, $HSiCl_3$), -18.1 (t, $^1J_{Si-H}$ = 312 Hz, H_2SiCl_2), -39.3 (s, unknown), -138.6 (s, unknown). After 10 days, the signal corresponding to $SiCl_3^-$ has decreased to approximately one seventh of the intensity, two new signals are observed – δ/ppm = -31.0 (d, $^1J_{Si-H}$ = 358 Hz), -39.0 (s).

8.5.7. Preparation of a mixture of $HSi(N_3)_2Cl$ and $HSi(N_3)_3$ in hexane, followed by reaction with Mes*Li(THF)$_{1.5}$

In an NMR tube, $Na(15c5)Al(N_3)_4$ (45 mg, 0.10 mmol) and hexane (0.6 mL) were combined. The mixture was sonicated for 5 x 5 minutes, with vigorous shaking in between, to break up the solid. To the resulting mixture, $HSiCl_3$ (10 mg, 0.07 mmol) was added. The mixture was shaken to afford mixing for 5 minutes, then a sealed capillary containing d_6-DMSO was added for NMR locking. ^{1}H NMR analysis shows multiple products, indicating incomplete conversion. The spectrum is poor quality, likely due to the presence of suspended material, thus preventing detailed analysis. 40 minutes after the addition of $HSiCl_3$, the sample was filtered, and more NMR spectra recorded. The ^{1}H NMR spectrum shows the presence of both $HSi(N_3)_2Cl$ and $HSi(N_3)_3$ in equal quantities. The ^{27}Al NMR spectrum shows no signals.

This filtered NMR sample was cooled to -40 °C, and Mes*Li(THF)$_{1.5}$ (20 mg, 0.06 mmol) was added to it. The sample was shaken gently to mix whilst cold. No initial signs of reaction. The sample was thus allowed to warm up to room temperature. Upon warming to room temperature, the previously colourless solution turned pale orange, and the previously fluffy solid (Mes*Li) turned into a fine powder. NMR analysis conducted on the sample 10 minutes after warming to room temperature. NMR (hexane, d_6-DMSO capillary) [1]H (significant aromatic and Si-H environments) δ/ppm = 7.41 (s, major product), 7.18 (s, minor product), 5.54 (s, major product, $^1J_{Si-H}$ = 263 Hz), 5.20 (s, minor product, $^1J_{Si-H}$ = 228 Hz); [14]N

δ/ppm = -146 (br, minor product), -148.6 (s, major product), -198.8 (s, major product), -204 (br, minor product); ^{29}Si δ/ppm = -37.9 (d, $^1J_{Si-H}$ = 263 Hz), -40.8 (t, $^1J_{Si-H}$ = 228 Hz). Due to the long duration of the ^{14}N and ^{29}Si experiments, another ^{1}H spectrum was recorded after they had finished (17 hours after reaction start), showing no significant change compared to the spectrum after 10 minutes.

The NMR sample was filtered and allowed to slowly evaporate under argon for a week, affording orange crystals of (Mes*)N=N(Mes*).

8.5.8. General procedure for the reaction of Si$_2$Cl$_6$ with nucleophiles

The chosen nucleophile is dissolved in the chosen solvent. In cases where the quantity of solvent is ≤ 0.6 mL, this is done in an NMR tube, otherwise it is done in a vial. To this solution, Si$_2$Cl$_6$ is added, and the mixture is briefly shaken to afford mixing. This mixed solution is then left standing. In cases where the reaction is conducted in a vial, the solution is filtered into an NMR tube shortly prior to recording spectra. To the NMR tube, a capillary containing either D$_2$O or d6-DMSO is added to enable locking. A ^{29}Si NMR spectrum of the sample is then recorded over a certain time period after the mixing of reagents. Reagent quantities and conditions are summarised in Table 8.5. Observed signals in the ^{29}Si NMR spectra are listed in Table 5.1.

Reagent	Reagent quantity	Si_2Cl_6 quantity	Solvent	Spectrum time period / h
tBuLi 1.7 M in hexane	74 mg (0.12 mL, 0.20 mmol)	54 mg (0.20 mmol)	THF (0.5 mL)	0 – 15
PPh$_4$Cl	150 mg (0.40 mmol)	269 mg (1.00 mmol)	CD$_2$Cl$_2$ (0.5 mL)	2 – 3
KTp*	71 mg (0.41 mmol)	102 mg (0.42 mmol)	THF (0.55 mL)	0 – 2
(THF)$_3$LiSi(TMS)$_3$	24 mg (0.05 mmol)	17 mg (0.06 mmol)	C$_6$D$_6$ (0.6 mL)	0 – 15
LiN(TMS)$_2$	33 mg (0.20 mmol)	54 mg (0.20 mmol)	THF (0.45 mL) d8-THF (0.15 mL)†	2 – 17
LiN(TMS)$_2$	84 mg (0.50 mmol)	134 mg (0.50 mmol)	THF (0.5 mL)	1 – 8
LiN(TMS)$_2$	168 mg (1.00 mmol)	270 mg (1.00 mmol)	DME (3.5 mL)	0 – 2
KOtBu 18-crown-6	22 mg (0.20 mmol) 58 mg (0.22 mmol)	54 mg (0.20 mmol)	Toluene (2.0 mL)	7 – 18
K(18c6)OtBu 18-crown-6	22 mg (0.20 mmol) 53 mg (0.20 mmol)	54 mg (0.20 mmol)	DME (1.0 mL)	9 – 16

Table 8.5. Reagent quantities and conditions for the reactions of Si_2Cl_6 shown in Table 5.1. †In this reaction, Si_2Cl_6 was pre-dissolved in 0.15 mL d8-THF, which was added to the solution of LiN(TMS)$_2$ in 0.45 mL THF.

8.5.9. Synthesis of (TMS)$_2$N–SiCl$_3$ for NMR spectroscopic reference

To an NMR tube, SiCl$_4$ (27 mg, 0.20 mmol) was dissolved in DME (0.6 mL). To this solution, LiN(TMS)$_2$ (33 mg, 0.20 mmol) was added. The tube inverted several times to afford mixing resulting in the formation of a white precipitate. A capillary containing D$_2$O was added, and NMR data is then recorded of the solution. ^{29}Si δ/ppm = 9.9 (m, $^3J_{H-H}$ = 6.8 Hz), -27.4 (s).

8.5.10. Synthesis of [K(18c6)]$_2$[Si$_6$Cl$_{14}$]

In a small Schlenk tube, potassium chunks (78 mg, 2.0 mmol) and DME (5 mL) were combined and cooled to -40 °C. After a few minutes, the DME had turned bright orange. To this mixture, 18-crown-6 (529 mg, 2.00 mmol) was added. The mixture was stirred at -30 °C for 5 minutes, and the solution turned dark green. To this solution, a pre-cooled solution of Si_2Cl_6 (269 mg, 1.00 mmol) was added dropwise over the course of 15 minutes, causing the

solution to become turbid and change colour to intense orange. The solution was stirred at -30 °C for a further 15 minutes before allowing it to warm to room temperature and stir for an additional 1 hour. The mixture was filtered, and the residue extracted with DME (1 mL). The filtrate and extract were combined, affording a dark orange solution. The unreacted potassium that had been filtered off was found to have a mass of 52 mg (1.3 mmol). The combined filtrate and extract were concentrated under vacuum to a volume of 3 mL. 30 minutes after this, a fine precipitate began to form. The mixture was left standing for 3 months, resulting in the precipitate being replaced by large colourless crystals. Approximately one third of the crystals were taken for SCXRD analysis, identifying them as $[K(18c6)]_2[Si_6Cl_{14}]$. The solvent was decanted from the remaining crystals, and these were washed with DME (2 mL) and dried under argon flow. Yield (excluding those taken for SCXRD) = 34 mg (0.046 mmol, 5% with respect to potassium (added), 14% with respect to potassium (consumed), 14% with respect to Si_2Cl_6).

8.6. Experimental Procedures (Chapter 6)

8.6.1 – 8.6.22 (Chapter 6.2.1)

8.6.1. Synthesis of cyclopentadiene

To a round-bottom flask under ambient atmosphere, dicyclopentadiene (~40 mL) was added, followed by iron powder (~1 g). The flask was connected to a distillation setup with a collecting flask cooled in ice water. The flask containing the dicyclopentadiene was heated to 160 °C to afford the formation and distillation of cyclopentadiene. Once the temperature of the vapour exceeded 45 °C, heating was stopped. To the cyclopentadiene in the collecting flask, activated molecular sieves (3Å) were added, and the flask was stoppered and stored at -20 °C for 2 days before using in the synthesis of LiCp.

8.6.2. Synthesis of lithium cyclopentadienide (LiCp)

In a large round-bottom flask, THF (250 mL) was cooled to 0 °C. The solution was stirred, and cyclopentadiene (25 g, 380 mmol) was added, followed by lithium granules (3.43 g, 494 mmol). The flask was fitted with a bubbler, and the mixture was stirred at 0 °C for 30 minutes, during which time gas generation was observed along with the formation of a sky-blue suspension. The lithium appeared to passivate, so additional lithium granules (0.79 g, 114 mmol) and THF (50 mL) was added. The mixture was further stirred at 0 °C for 1.5 hours, after which no further gas formation was observed. Additional THF was added (300 mL), and the mixture was filtered through a large glass frit. The filtered solution was concentrated under vacuum to a volume of 20 mL to afford an off-white powder. The remaining solution was decanted, and the solid was washed with 1:1 THF:Et_2O (10 + 5 mL). Yield = 11.567 g (161 mmol, 42% with respect to cyclopentadiene). NMR (CD_3CN) ^1H δ/ppm = 5.50 (s).

8.6.3. Synthesis of tosyl azide (TsN$_3$) solution in Et$_2$O

In a Schlenk tube, TsCl (9.533 g, 50.0 mmol) was dissolved in THF (25 mL). To this solution, NaN_3 (4.226 g, 65.0 mmol) was added, followed by additional THF (15 mL). The resulting mixture was stirred vigorously for 2.5 hours, affording a white suspension. To the suspension, Bu_4NBr (1.612 g, 5.00 mmol) was added as a phase transfer catalyst, followed

by additional THF (10 mL). The mixture was stirred vigorously for 24 hours. The solution was concentrated under vacuum to a total volume of 20 mL, then filtered to afford a pale orange solution. This solution was then carefully concentrated under vacuum to afford a non-volatile oil. This oil was diluted with Et_2O to a total solution volume of 50 mL. The addition of Et_2O resulted in a white precipitate, presumed to be Bu_4NBr. Quantitative ^{1}H NMR analysis indicates a concentration of TsN_3 of 17.8% by mass (0.735 M by volume). Yield = 50 mL of 0.735 M solution (36.75 mmol, 74% with respect to TsCl). Note: NMR analysis also indicates 0.01 molar equivalents of Bu_4NBr still present in the solution as an impurity. NMR (Et_2O, d6-DMSO capillary) [1]H δ/ppm = 7.70 (d, 2H, $^3J_{H-H}$ = 8.1 Hz, aryl-H), 7.31 (d, 2H, $^3J_{H-H}$ = 8.1 Hz, aryl-H), 2.33 (s, 3H, CH_3).

8.6.4. Example synthesis of diazocyclopentadiene (CpN_2) solution in Et_2O

In a vial, LiCp (27 mg, 0.37 mmol) was suspended in Et_2O (0.5 mL). This vial was immersed in a bath at room temperature, and the suspension was stirred. To the stirred suspension, a solution of TsN_3 in Et_2O (0.735 M, 0.50 mL, 0.37 mmol), diluted with additional Et_2O (0.5 mL), was added dropwise. The mixture was stirred vigorously for 1 hour, affording a dark brown suspension. The suspension was filtered to afford a deep yellow solution. Quantitative ^{1}H NMR analysis indicates a concentration of CpN_2 of 2.2% by mass (~0.17 M by volume). Yield = 1.0 mL of 0.17 M solution (0.17 mmol, 46% with respect to LiCp). NMR (Et_2O, d6-DMSO capillary) [1]H δ/ppm = 6.74 (m, 2H), 5.92 (m, 2H).

8.6.5. Example synthesis of diazocyclopentadiene (CpN_2) solution in MeCN

In a vial, a solution of TsN_3 in Et_2O (0.50 mL, 0.77 M, 0.39 mmol) was stirred. To this stirred solution, a solution of LiCp (28 mg, 0.39 mmol) in MeCN (3 mL) was added dropwise over the course of 30 minutes. The resulting mixture was stirred for 20 hours, then filtered to afford a dark orange solution. Quantitative ^{1}H NMR analysis indicates a concentration of CpN_2 of 1.0% by mass. Filtering the solution through activated charcoal removes the dark colouration, affording a deep yellow solution, however this does not have any significant effect on the NMR spectra. Yield = 2.310 g of 1.0% solution (23 mg CpN_2, 0.25 mmol, 65%

with respect to LiCp). NMR (MeCN, D_2O capillary) ^1H δ/ppm = 6.84 (m, 2H), 5.97 (m, 2H); ^{13}C δ/ppm = 119.8 (s), 119.1 (s).

8.6.6. Reaction of CpN$_2$ (solution in MeCN) with PPN(N$_3$)

In an NMR tube, PPN(N$_3$) (81 mg, 0.14 mmol) was added to a solution of CpN$_2$ in CD$_3$CN (0.14 mmol in 0.5 mL), followed by additional CD$_3$CN (0.2 mL). Bubbling was briefly observed on addition. The tube was inverted several times to afford mixing. Over the next few minutes, the solution darkened and a dark brown precipitate formed. ^1H NMR analysis after 15 minutes indicates an unknown impurity has reacted, but no CpN$_2$ has been consumed. The sample was left standing for 17 hours, after which the solution had turned dark wine-red, and a black precipitate had formed. ^1H NMR analysis still indicates no reaction with CpN$_2$. The solution was filtered, and the residue washed with MeCN (0.5 mL) then Et$_2$O (0.5 mL). The residue was then dried and analysed by IR spectroscopy as a Nujol mull; v/cm^{-1} = 2178 vw br (unknown), 2100 w (unknown), 2005 vw (PPN(N$_3$)).

8.6.7. Reaction of CpN$_2$ (solution in MeCN) with HN$_3$ (solution in Et$_2$O)

In an NMR tube, a solution of HN$_3$ in Et$_2$O (1.7 M, 10 mg, ~0.022 mmol) was added to a solution of CpN$_2$ in MeCN (~0.5%, 378 mg, ~0.022 mmol). The tube was inverted several times to afford mixing, and a capillary containing D$_2$O was added for NMR locking. The solution was left standing for 4 hours, after which ^1H NMR analysis shows no reaction with CpN$_2$. Another ^1H NMR spectrum was recorded 6 hours later, showing no change compared to the previous spectrum.

8.6.8. Reaction of CpN$_2$ (solution in 3:2 Et$_2$O:MeCN) with NaAl(N$_3$)$_4$(THF)$_4$

In an NMR tube, a crystal of NaAl(N$_3$)$_4$(THF)$_4$ (3 mg, 0.006 mmol) was dissolved in a solution of CpN$_2$ in 3:2 Et$_2$O:MeCN (0.013 mmol in 1 mL). After 10 minutes, ^1H and ^{27}Al NMR spectra so no significant consumption of CpN$_2$ and NaAl(N$_3$)$_4$ respectively. The solution was left standing for 12 days, affording brown precipitate. NMR analysis affords an identical ^1H spectrum to the one recorded after 10 minutes, however the ^{27}Al signal for NaAl(N$_3$)$_4$ has

decreased in intensity to approximately one tenth of the previous spectrum. No new products observed in either of the ^{1}H or ^{27}Al spectra.

8.6.9. Reaction of CpN$_2$ (solution in Et$_2$O) with NaAl(N$_3$)$_4$(THF)$_4$

To an NMR tube containing a solution of CpN$_2$ in Et$_2$O (0.08 mmol in 0.5 mL), 15-crown-5 (11 mg, 0.05 mmol) was added followed by NaAl(N$_3$)$_4$(THF)$_4$ (10 mg, 0.02 mmol). The tube was shaken and sonicated for a few seconds to afford mixing, resulting in a sticky white precipitate that gradually turned brown over the next 5 minutes. The mixture was left standing for an additional 10 minutes, then ^{1}H and ^{14}N NMR spectra were recorded, confirming no significant consumption of CpN$_2$. A ^{27}Al NMR spectrum was also recorded, however no signals were detected (NaAl(N$_3$)$_4$ is poorly soluble in Et$_2$O). After standing for 5 days, another ^{1}H NMR spectrum was recorded, showing no change to the solution.

8.6.10. Synthesis of lithium tetramethylcyclopentadienide (LiCp^x)

In a Schlenk tube, 1,2,3,4-tetramethyl-1,3-cyclopentadiene (2.445 g, 20.0 mmol) was dissolved in hexane (8 mL) and cooled to -20 °C. The solution was stirred, and to it a pre-cooled solution of tBuLi in pentane (1.7 M, 12 mL, 20 mmol) was added, affording a white precipitate. The solution was allowed to warm to room temperature and stirred for 2 hours. Additional hexane (12 mL) was added, and the mixture filtered. The precipitate was washed with hexane (3 x 10 mL) then dried under vacuum. Yield = 2.091 g (16.3 mmol, 82% with respect to 1,2,3,4-tetramethyl-1,3-cyclopentadiene).

8.6.11. Synthesis of tetramethyldiazocyclopentadiene (Cp^{x}N$_2$) (and notes for future syntheses)

In a vial, a solution of TsN$_3$ in Et$_2$O (0.77 M, 2.60 mL, 2.0 mmol) was cooled to -30 °C and stirred. To this, a pre-cooled suspension of LiCp^x (256 mg, 2.00 mmol) in Et$_2$O (3 mL) was added, followed by additional Et$_2$O (2 x 1 mL) to wash the residual LiCp^x into the reaction mixture. The mixture was stirred whilst gradually warming to room temperature over the course of 90 minutes, then filtered to afford a bright orange solution and considerable

amounts of beige residue. The solution was concentrated to 1 mL total volume. The residue was extracted with hexane (2 x 1 mL). The extracts were added to the Et_2O solution, resulting in the precipitation of additional beige solid. As such, this mixture was filtered again. The filtrate was dried under vacuum to afford a yellow solid and traces of an orange oil. The yellow solid was analysed by IR spectroscopy as a Nujol mull and found to contain TsN_3 (v = 2123 cm^{-1}) and a diazo compound (v = 2060 cm^{-1}), however the bulk of isolated material is the beige filter residue. This material contains no azide or diazo absorptions by IR analysis. Based on this observation, and its insolubility in hexane, this residue is assumed to be lithium tosyl(tetramethylcyclopentadienyl)triazenate, a predicted intermediate in the reaction. As such, all beige solids were recombined and suspended in Et_2O (5mL) and stirred at room temperature for 18 hours, affording a bright orange solution and a yellow precipitate. A small aliquot of this solution was analysed by IR spectroscopy as a solution and found to now contain a diazo compound (v = 2062 cm^{-1}). As such, the bulk solution was filtered and dried under vacuum to afford an orange wax and a pale-yellow powder. These solids were extracted with hexane (5 + 1 mL), and the hexane extracts dried to afford 35 mg of crude Cp^xN_2 as a non-volatile orange-red liquid (note: this liquid freezes at 15–20 °C, so it may solidify depending on ambient temperature). IR (Et_2O solution) v/cm^{-1} = 2062 s, 1444 s. NMR (C_6D_6) ^1H δ/ppm = 1.84 (s, 6H), 1.80 (s, 6H); ^{13}C (DEPTQ 135 & HMBC) δ/ppm = 125.9 (s, C–CH$_3$), 120.2 (s, C–CH$_3$), 72.7 (s, C=N$_2$), 11.0 (s, CH$_3$), 9.7 (s, CH$_3$); ^{14}N δ/ppm = -97.3 (s).

Due to the poor yield, the residue not extracted by hexane was resuspended in Et_2O (8 mL) and stirred at room temperature for longer. After 1 day of stirring, the suspension is now orange. This colour remained unchanged until the 4th day, at which point the suspension colour changed to a bright reddish pink. This colour remained for the following day, after which point the mixture was filtered, affording an intense orange solution and a purple-pink residue (note: the identity of the pink residue is unclear, but its sudden appearance only after 4 days of reaction may provide an indicator of reaction completion for future syntheses). The solution was concentrated under vacuum to a volume of 0.2 mL affording an orange-red liquid, containing red crystals whilst still cold from the evaporation. These crystals melted on warming to room temperature. The pink filter residue was extracted with hexane (4 mL). The hexane extract was added to the orange-red liquid, and the resulting solution concentrated under vacuum to afford 103 mg of crude Cp^xN_2 (note: evacuation was

continued until the rate of mass loss became constant, indicating all hexane had been removed. The rate of mass loss never reaches zero, indicating that Cp^xN_2 is slightly volatile and thus yield is lost during this step. Using more volatile solvents will allow for solvent removal with less loss of Cp^xN_2). Total (crude) yield of Cp^xN_2 = 138 mg (0.51 mmol, 26% with respect to $LiCp^x$).

8.6.12. Reaction of Cp^xN_2 with PPN(N_3) and TMS(N_3) in C_6D_6

To an NMR tube containing a solution of Cp^xN_2 in C_6D_6 (0.07 mmol in 0.5 mL), PPN(N_3) (22 mg, 0.04 mmol) was added followed by additional C_6D_6 (0.2 mL). The mixture was sonicated for 2 x 30 seconds to break up the solids, and the mixture left standing. ^1H NMR spectra recorded after 15 minutes and again after 24 hours show no reaction occurring. Subsequently, TMS(N_3) (240 mg, 0.21 mL, 2.08 mmol) was added (note: this TMS(N_3) contains traces of diglyme). ^1H NMR analysis shows some PPN^+ ions in solution, but no other change. Another ^1H spectrum recorded after 4 days shows still no change, so the sample was heated to 60 °C for 4 days. Again, no significant change to the ^1H spectrum was observed.

8.6.13. Reaction of Cp^xN_2 with PPh_4(N_3) and $FeCl_2$ in d_6-acetone

To an NMR tube containing a solution of Cp^xN_2 in d_6-acetone (0.05 mmol in 0.7 mL), PPh_4(N_3) (19 mg, 0.05 mmol) was added. The mixture was sonicated for 2 x 30 seconds to break up the solids, and the mixture left standing. ^1H NMR spectra recorded after 10 minutes, 24 hours and 5 days show no reaction occurring. Anhydrous $FeCl_2$ (3 mg, 0.03 mmol) was added, however this did not dissolve. To improve the solubility of the $FeCl_2$, pyridine (20 mg, 0.25 mmol) was added, and the mixture sonicated for 4 x 30 seconds with intermittent shaking to break up the solids. ^1H NMR spectra, recorded after 15 minutes and 18 hours, show no reaction of Cp^xN_2. The pyridine is exhibiting paramagnetic deshielding, indicating interaction with Fe(II): ^1H δ/ppm = 28.49 (vbr, 2H), 14.07 (br, 2H), 9.17 (s, 1H). The mixture was heated at 60 °C for 7 hours, resulting in a darkening of the solution and precipitate to orange-brown. After cooling to room temperature, ^1H NMR analysis shows a broadening of all signals, likely

due to the solvation of more paramagnetic Fe(II) species, but no consumption of Cp^xN_2. On cooling to room temperature, crystals of an iron complex $(PPh_4)_2[FeCl_3(N_3)]$ formed.

8.6.14. Reaction of Cp^xN_2 with $PPh_4(N_3)$ and $((C_6H_6)RuCl_2)_2$ in d_4-methanol

In an NMR tube, $PPh_4(N_3)$ (19 mg, 0.05 mmol) was dissolved in d_4-methanol (0.6 mL). To this, crude Cp^xN_2 was added (11 mg, 0.05 mmol of Cp^xN_2). ^1H NMR analysis shows no significant consumption of Cp^xN_2 after 1 hour. $((C_6H_6)RuCl_2)_2$ (13 mg, 0.05 mmol of Ru) was subsequently added followed by d_4-methanol (0.2 mL), affording bubbling. The mixture was sonicated for a few seconds to break up the solids. ^1H NMR spectra recorded after 1 hour and 8 hours indicate the conversion of Cp^xN_2 to a new product: ^1H δ/ppm = 2.14 (s, 6H), 2.04 (s, 6H). Another spectrum recorded after 18 hours shows no significant further change. Attempts to crystallise the product(s) of reaction by concentrating and cooling toluene, THF, d_4-methanol and aqueous solutions of the product mixture were unsuccessful.

8.6.15. Reaction of Cp^xN_2 with $PPN(N_3)$ and $RhCl_3(H_2O)_3$ in $CDCl_3$

To an NMR tube containing a solution of Cp^xN_2 in $CDCl_3$ (0.06 mmol in 0.5 mL), $PPN(N_3)$ (35 mg, 0.06 mmol) was added, which dissolved completely. ^1H NMR spectra recorded after 10 minutes and again after 1 hour show no reaction of Cp^xN_2. A ^{14}N spectrum recorded between these times also confirms no reaction. $RhCl_3(H_2O)_3$ (3 mg, 0.01 mmol) was added, but this remained completely insoluble even after brief sonication to break up the solid. MeCN (0.5 mL) was added which did not initially improve the solubility. After leaving overnight, the solids had dissolved to afford an orange-red solution. ^1H NMR analysis indicates no significant consumption of Cp^xN_2. Another spectrum recorded after 17 days shows no significant change.

8.6.16. Reaction of Cp^xN_2 with HN_3 in Et_2O

In an NMR tube, crude Cp^xN_2 (6 mg, 0.03 mmol of Cp^xN_2) was dissolved in Et_2O (0.5 mL), and a capillary containing D_2O was added for NMR locking. To this solution, a solution of HN_3 in

Et$_2$O (1.7 M, 13 mg, 0.03 mmol) was added. ^{1}H NMR spectra recorded after 5 minutes and again after 6 days indicate no reaction occurred.

8.6.17. Reaction of CpN$_2$ with RhCp*(N$_3$)$_2$(PPh$_3$)

To an NMR tube containing a solution of CpN$_2$ in MeCN (0.025 mmol in 0.5 mL), RhCp*(N$_3$)$_2$(PPh$_3$) (15 mg, 0.025 mmol) was added, followed by additional MeCN (0.1 mL). The mixture was sonicated for a few seconds and inverted several times to afford mixing. NMR spectra recorded over the course of 10 days show a very slow consumption of both CpN$_2$ and RhCp*(N$_3$)$_2$(PPh$_3$). To speed the reaction up, the mixture was heated to 60 °C, resulting in partial solvation of the residual solids. NMR spectra indicate conversion completed after 4 hours at 60 °C. 3 days into the room-temperature reaction, orange crystals formed in the tube, which were identified by SCXRD as RhCp*(N$_3$)$_2$(PPh$_3$)·(MeCN). Following the completion of the reaction, attempts to crystallise the reaction product(s) by evaporation, and by addition of toluene to an MeCN solution, were unsuccessful.

8.6.18. Reaction of RhCl$_3$(H$_2$O)$_3$ with NaN$_3$, followed by addition of Cp^{x}N$_2$

In a vial, RhCl$_3$(H$_2$O)$_3$ (26 mg, 0.10 mmol) was added to MeCN (1.0 mL). The rhodium complex did not dissolve, so 4-tert-butylpyridine (41 mg, 0.30 mmol) was added, resulting in partial solvation of the rhodium complex to afford a brick-red solution. To this solution, NaN$_3$ (39 mg, 0.60 mmol) was added. The resulting mixture was stirred for 16 hours, affording a light orange-brown suspension. The suspension was diluted with MeCN (1.0 mL) and filtered to afford an orange filtrate that quickly became turbid again after filtering. The residue was extracted with MeCN (1.0 mL), and the combined filtrate and extract were filtered again, this time through celite, affording a bright orange solution was that still slightly turbid. This afforded 1.942 mg of solution with a rhodium concentration of ~0.04 M, of which 105 mg was taken for IR analysis: v/cm^{-1} (azide bands) = 2138 w, 2033 s, 1618 m. 166 mg of the solution was taken for evaporation to grow crystals, however this afforded an oil.

500 mg of the above solution (0.026 mmol of Rh) was transferred to a separate vial. To this solution, Cp^{x}N$_2$ (4 mg, 0.03 mmol) was added. Upon addition, traces of white precipitate

were observed. The solution did not change colour. The mixture was stirred for 80 minutes, after which an aliquot was taken for IR analysis. IR indicates the solution is an unreacted mixture of the added rhodium solution and Cp^XN_2. After the mixture was left stirring for 3 days, another aliquot was taken for IR analysis which again shows only the rhodium solution and Cp^XN_2.

8.6.19. Reaction of Cp^XN_2 with $((C_6H_6)RuCl_2)_2$

In an NMR tube, crude Cp^XN_2 (12 mg, 0.05 mmol Cp^XN_2) was dissolved in d_4-methanol (0.3 mL). To this solution, $((C_6H_6)RuCl_2)_2$ (27 mg, 0.11 mmol of Ru) was added followed by additional d_4-methanol (0.3 mL). Bubbling was observed upon addition, which subsided after 5 minutes. NMR analysis shows all Cp^XN_2 consumed, with a major and several minor products observed. [1]H (major product) δ/ppm = 1.74 (s, 6H), 1.62 (s, 6H). After the mixture was left standing for 19 hours, ^{1}H analysis shows the minor products have almost entirely decomposed and the signals of the major product have decreased somewhat as well. The mixture was heated to 60 °C for 15 minutes and slowly cooled to room temperature over 3 hours to grow crystals, however this was unsuccessful. Subsequent ^{1}H NMR analysis shows that heating of the sample further decomposed the major product of the reaction.

8.6.20. Reaction of Cp^XN_2 with $RhCl_3(H_2O)_3$ in d_4-methanol

In an NMR tube, crude Cp^XN_2 (17 mg, 0.09 mmol Cp^XN_2) was dissolved in d_4-methanol. A ^{1}H NMR spectrum of Cp^XN_2 in d_4-methanol was recorded after 5 minutes and again after 1 hour, to confirm that Cp^XN_2 does not react with the methanol (δ/ppm = 2.03 (s, 6H), 1.84 (s, 6H)). $RhCl_3(H_2O)_3$ (24 mg, 0.09 mmol) was added to the NMR sample, resulting in bubbling and a brick-red suspension. Bubbling subsided after 10 minutes, after which NMR analysis shows all Cp^XN_2 has been consumed, no significant new products observed by ^{1}H NMR in solution. Upon leaving the sample overnight, the brick-red precipitated turned dark brown, and was thus deemed to have decomposed.

8.6.21. Reaction of Cp^{x}N$_2$ with RhCl$_3$(H$_2$O)$_3$ in MeCN

In a vial, crude Cp^{x}N$_2$ (2 mg, 0.01 mmol) was dissolved in MeCN (0.3 mL). To this solution, RhCl$_3$(H$_2$O)$_3$ (3 mg, 0.01 mmol) was added. The solids were crushed up with a spatula, and the mixture swirled for 10 minutes. IR analysis of the solution shows no signs of reaction. 4-tert-butylpyridine (6 mg, 0.04 mmol) was added, and the mixture left standing for 1 hour. IR analysis of the solution shows all Cp^{x}N$_2$ has been consumed. IR (major product(s)) ν/cm^{-1} = 2974 s, 1618 s, 1500 m, 1275 m, 1229 m, 1205 w. Evaporation of the solution did not afford crystals for SCXRD analysis.

8.6.22. Synthesis of 2-diazoimidazole and subsequent reaction with NaN$_3$

In a large vial, 37% HCl (390 mg, 4.0 mmol) was diluted with water (4 mL) and cooled to 0 °C. Into this solution, 2-aminoimidazole hemisulphate (264 mg, 2.00 mmol) was dissolved. The resulting solution was stirred at 0 °C, and NaNO$_2$ (152 mg, 2.20 mmol) was added in small portions over the course of 10 minutes, affording a bright orange solution. The solution was stirred in the dark for an addition 5 minutes, during which time it was slowly bubbling. To this solution, a pre-cooled solution of K$_2$CO$_3$ (691 mg, 5.00 mmol) in water (1 mL) was added dropwise over the course of 7 minutes, affording a dark brown solution with some precipitate. The solution was stirred for an additional 5 minutes, then an aliquot of 0.5 mL was transferred to an NMR tube containing 0.05 mL D$_2$O, pre-cooled to 0 °C. NMR (1:10 D$_2$O:H$_2$O, 0 °C) ^{1}H δ/ppm = 7.33 (s); ^{13}C (DEPTQ135) δ/ppm = 165.5 (C=N$_2$), 140.7 (C–H); ^{14}N δ/ppm = -101 (vbr), -136.5 (br).

The solution and NMR sample were left standing at 0 °C for 1.5 hours, during which no significant change to ^{1}H NMR was observed, however significant amounts of black precipitate have formed in both, affording a paste that is no longer fluid. To the main reaction solution, a pre-cooled solution of ZnCl$_2$ (123 mg, 0.90 mmol) and NaN$_3$ (130 mg, 2.00 mmol) in water (1 mL) was added dropwise. After just a few drops, the reaction solution foamed up considerably, preventing the addition of the remaining solution. THF (4 mL) was added, which dissolved the foam, allowing for the remainder of the ZnCl$_2$ and NaN$_3$ solution to be added. After addition was complete, a 0.5 mL aliquot of the solution was transferred to an NMR tube containing 0.05 mL D$_2$O, precooled to 0 °C. NMR analysis was

conducted at 0 °C. ^{1}H NMR spectrum has no significant signals other than H_2O and THF. ^{14}N NMR spectrum has no significant signals other than NaN_3. ^{13}C (DEPTQ135) δ/ppm = 163.8 (0H or 2H environment).

8.6.23 – 8.6.36 (Chapter 6.2.2)

8.6.23. Synthesis of sulphuryl diazide ($SO_2(N_3)_2$) solution in MeCN

In a vial, SO_2Cl_2 (54 mg, 0.40 mmol) was dissolved in MeCN (4.0 mL). To this solution, NaN_3 (104 mg, 1.60 mmol) was added. Trace bubbling was observed (believed to be due to reaction of NaN_3 with Cl_2 impurity). The resulting mixture was stirred for 16 hours, then filtered. The residue was extracted with MeCN (2 x 2 mL), and the extracts combined with the filtrate, affording 6.373 g (8 mL) of 0.9% (0.05 M) $SO_2(N_3)_2$ solution (assuming full conversion). IR (MeCN solution) v/cm^{-1} = 2160 m, 2143 s. A medium intensity signal at 2017 cm^{-1} is also observed, corresponding to $SO_2(N_3)^-$ which forms from reaction of N_3^- with SO_2 impurity in the SO_2Cl_2.

8.6.24. Reaction of SO_2Cl_2 with NaN_3, 15-crown-5 and $TMS(N_3)$ in toluene

In a vial, SO_2Cl_2 (7 mg, 0.05 mmol) was dissolved in toluene (0.57 mL). To this solution, in order, NaN_3 (20 mg, 0.31 mmol), 15-crown-5 (22 mg, 0.10 mmol) and $TMS(N_3)$ (0.57 mL, 4.36 mmol) were added. The resulting mixture was stirred overnight. An aliquot of the solution was concentrated to an oil. The oil was mixed with paraffin for IR analysis: v/cm^{-1} = 2105 w, 2056 w, 2030 m, 2014 m.

8.6.25. Attempted reaction of TsN_3 with $TMS(N_3)$ in Et_2O

To an NMR tube containing a solution of TsN_3 in Et_2O (0.77 M, 0.55 mL, 0.42 mmol), $TMS(N_3)$ (47 mg, 0.41 mmol) was added. A ^{1}H NMR spectrum recorded after 2 hours shows unreacted TsN_3 and $TMS(N_3)$. Another ^{1}H NMR spectrum recorded after 5 days shows no change.

8.6.26. Reaction of SO$_2$Cl$_2$ with PPN(N$_3$) in MeCN

In a vial, PPN(N$_3$) (232 mg, 0.40 mmol) was dissolved in MeCN (1 mL). The resulting solution was stirred, and to it a solution of SO$_2$Cl$_2$ (14 mg, 0.10 mmol) in MeCN (1 mL) was added, resulting in vigorous bubbling. The bubbling lasted approximately 2 minutes, after which the solution had turned pale yellow-green. IR (MeCN solution) v/cm^{-1} = 2016 s (SO$_2$(N$_3$)$^-$), 2005 s (PPN(N$_3$)).

8.6.27. Synthesis of SO$_2$(N$_3$)$_2$ in MeCN, followed by reaction with PPN(N$_3$)

In a vial, SO$_2$Cl$_2$ (14 mg, 0.10 mmol) was dissolved in MeCN (1.0 mL). To this solution, NaN$_3$ (23 mg, 0.35 mmol) was added. The resulting mixture was stirred for 16 hours, then filtered. 0.1 mL of the solution was taken for IR analysis, v/cm^{-1} = 2160 m, 2144 s, 2018 w.

The residue was extracted with MeCN (1.0 mL), and the extract was added to the filtrate. To this combined solution, a solution of PPN(N$_3$) (52 mg, 0.09 mmol) in MeCN (0.5 mL) was added, resulting in precipitated formation and gradual bubbling. The solution was left standing for 24 hours, then filtered. The residue was extracted with MeCN (1.5 mL), and the extract was added to the filtrate. This combined solution was then concentrated under vacuum to a volume of ~1 mL to approximately match the concentration of the IR sample of SO$_2$(N$_3$)$_2$. An aliquot of this solution was taken for IR analysis: v/cm^{-1} = 2017 s, 2006 m (note: the absorption at 2017 cm^{-1} is approximately 9 times more intense than the absorption at 2018 cm^{-1} in the SO$_2$(N$_3$)$_2$ solution).

8.6.28. Reaction of SO$_2$(N$_3$)$_2$ with diisopropylamine in MeCN

To a vial containing a solution of SO$_2$(N$_3$)$_2$ in MeCN (0.9%, 820 mg, 0.05 mmol), diisopropylamine (11 mg, 0.11 mmol) was added under ambient atmosphere. The vial was capped, and the resulting solution was stirred for 10 minutes. An aliquot of the solution was taken for IR analysis, which shows the majority of the SO$_2$(N$_3$)$_2$ has been consumed, and the concentration of SO$_2$(N$_3$)$^-$ has increased significantly. A weak band is observed at 2109 cm^{-1}, which was previously only a trace. The IR sample was left standing (sealed) for 40 minutes, and another IR spectrum was recorded showing further consumption of SO$_2$(N$_3$)$_2$ and

further increase in the concentrations of $SO_2(N_3)^-$ and the compound giving rise to the absorption at 2109 cm^{-1}.

8.6.29. Reaction of $SO_2(N_3)_2$ with triethylamine in MeCN

To a vial containing a solution of $SO_2(N_3)_2$ in MeCN (0.9%, 820 mg, 0.05 mmol), Triethylamine (11 mg, 0.11 mmol) was added. The resulting solution was swirled for 10 minutes, then an aliquot was taken for IR analysis. The IR spectrum shows the appearance of triethylamine absorption bands,[209] and other new bands are observed at 1242 cm^{-1} and 1102 cm^{-1}. The intensity of $SO_2(N_3)_2$ absorption bands have decreased relative to the 0.9% solution. The IR sample slowly bubbled over time. The reaction solution was left standing, and another aliquot was taken for IR analysis after a total elapsed time of 140 minutes. Relative to the previous spectrum, this spectrum shows a slight increase in the intensity of the absorptions at 1242 cm^{-1} and 1102 cm^{-1}, and a significant decrease in the concentration of $SO_2(N_3)_2$. After a total of 18 hours, a final aliquot was taken for IR analysis, indicating complete consumption of $SO_2(N_3)_2$ as well as a further increase in the intensity of the absorptions at 1242 cm^{-1} and 1102 cm^{-1}.

8.6.30. Synthesis of phosphoryl triazide ($PO(N_3)_3$) solution in MeCN

In a vial, $POCl_3$ (30 mg, 0.20 mmol) was dissolved in MeCN (2 mL). To this solution, NaN_3 (78 mg, 1.2 mmol) was added, and the mixture stirred for 16 hours. The resulting suspension was filtered, and the residue extracted with MeCN (2 mL). The filtrate and extract were combined to afford a total of 3.276 g (4 mL) of 1.1% (0.05 M) $PO(N_3)_3$ solution. IR (MeCN solution) v/cm^{-1} = 2197 w, 2174 vs, 2122 vw, 1304 w, 1256 m.

8.6.31. Reaction of $PO(N_3)_3$ with $PPN(N_3)$ in MeCN

To a vial containing a solution of $PO(N_3)_3$ in MeCN (1.1%, 782 mg, 0.050 mmol), $PPN(N_3)$ (29 mg, 0.050 mmol) was added. The resulting solution was swirled for 5 minutes, then an aliquot was taken for IR analysis. The IR spectrum shows predominantly $PO(N_3)_3$ and $PPN(N_3)$, with weak absorption bands at 2141 cm^{-1} and 2122 cm^{-1}. The reaction solution was

stirred for 17 hours, and another aliquot taken for IR analysis. This IR spectrum is identical to the one recorded after 5 minutes.

8.6.32. Synthesis of diazoquinone, followed by monitoring of its reaction with NaN₃

In a large vial, 37% HCl (390 mg, 4.0 mmol) was diluted with water (5.0 mL) and cooled to 0 °C. Into this solution, 4-aminophenol hydrochloride (291 mg, 2.00 mmol) was dissolved. The resulting solution was stirred at 0 °C, and $NaNO_2$ (152 mg, 2.20 mmol) was slowly added in portions over the course of 10 minutes, affording a dark violet solution. Stirring was continued for an additional 6 minutes, then a pre-cooled solution of K_2CO_3 (691 mg, 5.00 mmol) in water (1.6 mL) was added dropwise over the course of 15 minutes, turning the solution brown. Subsequently, stirring was continued for an additional 5 minutes, then a pre-cooled solution of NaN_3 (137 mg, 2.10 mmol) in D_2O (1.0 mL) was added dropwise over the course of 2 minutes, affording a slightly turbid orange-brown solution. This solution was stirred for an additional 10 minutes (still at 0 °C), before an aliquot of the solution was transferred to a pre-cooled NMR tube for analysis. Initial ^{1}H, ^{13}C and ^{14}N NMR spectra of this solution are consistent with a mixture of diazoquinone and NaN_3. NMR (500 MHz, H_2O, -3 °C) ^{1}H δ/ppm = 7.69 (d, 2H, $^{3}J_{H-H}$ = 9.4 Hz), 6.31 (d, 2H, $^{3}J_{H-H}$ = 9.4 Hz); ^{13}C (DEPTQ135) δ/ppm = 181.8 (C=N_2), 165.6 (C=O), 134.2 (C–H), 123.2 (C–H); ^{14}N δ/ppm = -133.3 (s), -281.6 (br). Trace signals attributable to 4-pentazolylphenoxide and 4-azidophenoxide are observed in the ^{1}H spectrum (*vide infra).*

The NMR sample was left at -3 °C for one hour. ^{1}H NMR analysis at this time shows slight conversion of diazoquinone to 4-pentazolylphenoxide: NMR (500 MHz, H_2O, -3 °C) ^{1}H δ/ppm = 7.55 (d, 2H, $^{3}J_{H-H}$ = 8.8 Hz), 6.50 (d, 2H, $^{3}J_{H-H}$ = 8.8 Hz). Conversion to 4-azidophenoxide is also observed: NMR (500 MHz, H_2O, -3 °C) ^{1}H δ/ppm = 6.61 (d, 2H, $^{3}J_{H-H}$ = 8.7 Hz), 6.46 (d, 2H, $^{3}J_{H-H}$ = 8.7 Hz). Ratio of 4-pentazolylphenoxide : 4-azidophenoxide is approximately 1.6 : 1 at this time.

The NMR sample was allowed to warm to room temperature, resulting in slight bubbling. After 30 minutes at room temperature, more diazoquinone has been consumed, resulting in an increase in concentration for both 4-pentazolylphenoxide and 4-azidophenoxide,

however the ratio of 4-pentazolylphenoxide : 4-azidophenoxide decreased to 0.9 : 1. Unreacted diazoquinone is still the dominant signal in the ^{1}H NMR spectrum.

$ZnCl_2$ (4 mg, 0.02 mmol) was added to the NMR sample, and the sample left standing at -3 °C for 1 hour. Only a slight increase in conversion observed by ^{1}H NMR analysis. The sample was thus allowed to react at room temperature for 2 hours. This resulted in considerable consumption of diazoquinone to form 4-azidophenoxide, however the concentration of 4-pentazolylphenoxide has decreased.

After a total of 6 hours at 0 °C, another aliquot was taken from the main reaction solution, and added to a pre-cooled NMR tube. A ^{1}H NMR spectrum was recorded to determine degree of conversion, then $RhCl_3(H_2O)_3$ (5 mg, 0.02 mmol) was added. After 1 hour at 0 °C, very little change to the ^{1}H NMR spectrum is observed.

8.6.33. Synthesis of nitrophloroglucinol

To a round bottom flask, under ambient atmosphere, water (40 mL) was added, and the flask placed in a water bath maintained at 20 °C. The water in the flask was stirred, and to it 95% H_2SO_4 (40 mL) was added. Of the resulting 80 mL of solution, 20 mL was taken out and placed in a separate flask. To this 20 mL solution, 68% HNO_3 (6.0 mL, 97 mmol) was added. To the remaining 60 mL solution, phloroglucinol (4.00 g, 31.7 mmol) was added, and the mixture stirred for 5 minutes. Then, the HNO_3-containing solution was added dropwise to the phloroglucinol mixture over the course of 5 minutes, affording a brown solution. This solution was stirred at 20 °C for a further 55 minutes to afford a red-brown suspension. The suspension was poured into a beaker containing crushed ice (80 g), and the contents of the beaker were swirled for 5 minutes before filtering through a glass frit. The filter residue was mixed with ice-water (30 g) and left standing for 10 minutes, by which time most of the ice had melted. The resulting mixture was filtered again. A sample of this residue was taken for NMR analysis, showing the presence of both nitrophloroglucinol and phloroglucinol in a respective ratio of 0.8 : 1.

To afford further conversion, another round bottom flask was prepared. To this flask, in order, water (40 mL), 95% H_2SO_4 (40 mL) and 68% HNO_3 (5 mL) were added. To this solution, the filter residue from the previous step was added, and the solution was stirred at 20 °C for

2 hours. The resulting suspension was poured onto crushed ice, filtered and washed as before. A sample of this residue was taken for NMR analysis, showing the presence of both nitrophloroglucinol and phloroglucinol in a respective ratio of 1.4 : 1.

This residue was extracted with DCM (7 x 400 mL), and the DCM extracts were dried under vacuum to afford nitrophloroglucinol as an orange powder. Yield = 1.586 g (9.27 mmol, 29% with respect to phloroglucinol). NMR (d_6-DMSO) ^{1}H δ/ppm = 10.49 (s, 2H, OH), 10.03 (s, 1H, OH), 5.89 (s, 2H, CH).

8.6.34. Synthesis of 2,4,6-trihydroxyanilinium tetrafluoroborate monohydrate

Under ambient conditions, a three-necked round-bottom flask (referred to as the reaction flask) and a two-necked round-bottom flask (referred to as the hydrogen flask) were connected via a short length of tubing with a tap in between. To the reaction flask, nitrophloroglucinol (490 mg, 2.86 mmol) and water (10 mL) was added. To the hydrogen flask, magnesium turnings (2.40 g, 100 mmol) and water (80 mL) was added. The water in both flasks was deoxygenated by 5 cycles of evacuation and re-pressurisation with argon. From this point onwards, these flasks are kept under anoxic atmosphere. The hydrogen flask was fitted with a dropping funnel containing 95% H_2SO_4 (7 mL). The H_2SO_4 was degassed by 1 cycle of evacuation and re-pressurisation with argon. This dropping funnel was pressurised with argon (0.15 bar overpressure). 10% palladium on activated carbon (100 mg) was added to the reaction flask, and the reaction flask fitted with an oil bubbler. The hydrogen flask was cooled in a water-ice bath, and the contents of both flasks were stirred. Several drops of H_2SO_4 were admitted to the hydrogen flask, to enable H_2 generation. The generated H_2 is allowed to pass into the reaction flask, where the rate of gas generation can be monitored from the oil bubbler (1 bubble is approximately 0.2 mL volume). H_2SO_4 was very slowly added dropwise to the hydrogen flask to maintain an H_2 generation rate of approximately 2 bubbles per second for 10 minutes. After this, H_2 generation was halted by stopping the addition of H_2SO_4. The reaction flask was purged with argon flow for 5 minutes, then 50% aqueous HBF_4 (523 mg, 3.00 mmol) was added to it. H_2 generation was then resumed by addition of H_2SO_4 to the hydrogen flask at a rate of approximately 1 drop every 25 seconds, resulting in a bubbling rate of approximately 1 bubble every 1.5 seconds. After 4 hours, all

H$_2$SO$_4$ had been added, and the entire setup was purged with argon flow for 5 minutes. The contents of the reaction flask were filtered to afford a colourless solution. The filtered solution was dried under vacuum, affording 2,4,6-trihydroxyanilinium tetrafluoroborate monohydrate as a white crystalline solid with traces of pink discolouration. Yield = 585 mg (2.37 mmol, 82% with respect to nitrophloroglucinol). This material gradually turns pink over time, but this does not appear to significantly affect its spectroscopic purity. NMR (H$_2$O, D$_2$O capillary) ^{1}H δ/ppm = 6.01 (s); ^{13}C (cpd & HMBC) δ/ppm = 156.9 (C–NH$_3$), 151.7 (*2,6*-C–OH), 99.5 (*4*-C–OH), 94.9 (C–H).

8.6.35. First attempted synthesis of 2,4,6-trihydroxybenzenediazonium tetrafluoroborate

In a small Schlenk tube, EtOH (1.5 mL) was degassed by concentrating under vacuum to 1 mL volume. To the degassed EtOH, 2,4,6-trihydroxyanilinium tetrafluoroborate monohydrate (247 mg, 1.0 mmol) was added under argon and dissolved. This solution was cooled to 0 °C, then 50% HBF$_4$ (350 mg, 2.0 mmol) was added to it. The solution was stirred at 0 °C for 5 minutes, before isoamyl nitrite (182 mg, 1.5 mmol) was added dropwise over the course of 5 minutes. Stirring was then continued at 0 °C for 1 hour. To isolate the product, Et$_2$O (8 mL) was added to the reaction solution, and the solution cooled to -25 °C overnight. However, this did not afford any precipitation or crystallisation. As such, the solution was concentrated under vacuum to afford a sticky, red-brown residue. This was redissolved in Et$_2$O (2 mL). Cooling this Et$_2$O solution to -78 °C did not afford any precipitation or crystallisation, so the solution was dried under vacuum affording a pink-brown solid. A sample of this solid was dissolved in D$_2$O for NMR analysis. The ^{1}H NMR spectrum shows only one significant signal that may be associated with an aromatic environment, at 6.06 ppm. This signal is much weaker than those of the isoamyl environments and is no longer present after 6 hours. Toluene was found to not extract any material from the pink-brown solid. After this attempted extraction, the solid was found to no longer dissolve in Et$_2$O.

8.6.36. Second attempted synthesis of 2,4,6-trihydroxybenzenediazonium tetrafluoroborate

In a small Schlenk tube, EtOH (1.0 mL) was degassed by concentrating under vacuum to 0.5 mL volume). To the degassed EtOH, 2,4,6-trihydroxyanilinium tetrafluoroborate monohydrate (248 mg, 1.0 mmol) was added under argon and dissolved. This solution was cooled to 0 °C, then $HBF_4 \cdot Et_2O$ (0.275 mL, 2.0 mmol) was added to it. The solution was stirred at 0 °C for 5 minutes, before isoamyl nitrite (180 mg, 1.5 mmol) was added dropwise over the course of 5 minutes. Stirring was then continued at 0 °C for 2 hours. Et_2O (8 mL) was added to the reaction solution. This only resulted in traces of precipitate formation, so the solution was concentrated under vacuum to afford a damp solid that would not readily dry further. A sample of this solid was dissolved in d_4-methanol for NMR analysis. The ^1H NMR spectrum shows two significant signals that may be associated with an aromatic environment, at 6.05 ppm and 5.95 ppm. The signal at 6.05 ppm is 5 times more intense than the one at 5.95 ppm, however it is significantly weaker than those of the isoamyl environments. Both signals lost most of their intensity after 3 hours. The dominant isoamyl environment was confirmed to be different to isoamyl nitrite by addition of a genuine sample to the NMR tube (the dominant isoamyl environment is therefore likely isoamyl alcohol). ^1H-^{13}C HMBC analysis shows two ^{13}C environments associated with the proton signal at 6.05: δ/ppm = 174.7 (proximity), 96.5 (adjacent).

8.6.37 – 8.6.42 (Chapter 6.2.3)

8.6.37. Preparation of HN₃ 0.03 M solution in HMPA for spectroscopic reference

In a vial, $PPN(N_3)$ (35 mg, 0.06 mmol) was added to HMPA (2.0 mL). To this mixture, $TsOH \cdot H_2O$ (11 mg, 0.06 mmol) was added. The solution was warmed to 50 °C to aid in the dissolution of the $PPN(N_3)$ and swirled until all solids had dissolved. An IR spectrum of the solution was recorded, with strong IR absorptions at v/cm^{-1} = 3500 (H_2O), 3451 (H_2O), 2120 (HN_3), 1651 (H_2O), 1117 (PPN^+).

8.6.38. Reaction of Na$_2$N$_2$O$_2$ hydrate with PPN(N$_3$) and TsOH

In a vial, a 0.03 M solution of PPN(N$_3$) in HMPA was prepared by dissolving PPN(N$_3$) (87 mg, 0.15 mmol) in HMPA (5.0 mL). This solution gains a slight orange tint after a short while. IR (HMPA) v/cm^{-1} = 2025 w, 1994 vs, 1116 m.

An aliquot of this PPN(N$_3$) solution in HMPA (1 mL, 0.03 mmol) was added to a vial containing Na$_2$N$_2$O$_2$ hydrate (6 mg, ~0.03 mmol). The Na$_2$N$_2$O$_2$ did not dissolve. After 10 minutes, IR analysis of the solution shows only unreacted PPN(N$_3$). Subsequently, TsOH·H$_2$O (6 mg, 0.03 mmol) was dissolved into the solution. The slight orange discolouration was removed, but otherwise no visible changes were observed. After 10 minutes, another batch of TsOH·H$_2$O (6 mg, 0.03 mmol) was dissolved into the solution. The mixture was swirled for 5 minutes, causing the Na$_2$N$_2$O$_2$ to dissolve. IR analysis of this reaction solution shows that the PPN(N$_3$) (v = 1994 cm^{-1}) has now been largely replaced by HN$_3$ (v = 2120 cm^{-1}). The spectrum shows no other significant changes compared to the spectrum taken before addition of acid, other than an increase in the intensity of the H$_2$O absorptions (note that the IR absorptions of the tosyl group are obscured by the solvent). Another IR spectrum of the solution was recorded after 3 hours, showing no further change.

8.6.39. Reaction of Na$_2$N$_2$O$_2$ with TsCl in MeCN

In a vial, anhydrous Na$_2$N$_2$O$_2$ (5 mg, 0.05 mmol) was suspended in MeCN (0.5 mL). To this suspension, TsCl (10 mg, 0.05 mmol) was added. The solids were crushed and mixed around with a spatula for 15 minutes. An aliquot of the supernatant solution was taken for IR analysis, which was found to contain only TsCl by comparison to a genuine sample.

8.6.40. Synthesis of Na(15c5)OTs for spectroscopic reference

In a vial, TsOH·H$_2$O (38 mg, 0.20 mmol) was dissolved in EtOH (1 mL). To this solution, NaHCO$_3$ (17 mg, 0.20 mmol) was added. No initial signs of reaction, and the NaHCO$_3$ did not dissolve. To solvate the NaHCO$_3$, MeOH (1 mL) was added, and the resulting mixture sonicated for 1 minute, affording near-complete solvation of the solids. The resulting solution was dried under high vacuum. A sample of this was dissolved in MeCN for IR

analysis. IR (MeCN) ν/cm^{-1} = 2995 w, 2990 vw, 2961 w, 2939 m, 2928 m br, 2882 m, 1354 m, 1294 vw, 1277 vw, 1251 w, 1231 m, 1217 m, 1203 m, 1188 m, 1122 s, 1118 s, 1102 m.

8.6.41. Reaction of Na$_2$N$_2$O$_2$ with TsCl and 15-crown-5 in MeCN

In a vial, 15-crown-5 (242 mg, 1.10 mmol) was dissolved in MeCN (2 mL). To this solution, anhydrous Na$_2$N$_2$O$_2$ (53 mg, 0.50 mmol) was added, followed by TsCl (95 mg, 0.50 mmol). The solution warmed up and bubbled slightly on addition of TsCl. This reaction mixture was stirred for 15 minutes. 25 mg of the resulting suspension (~1% of the total mixture) was decanted off, diluted by a factor of 4 with MeCN, then analysed by IR spectroscopy. The IR spectrum is an almost perfect match to a reference sample of Na(15c5)OTs in MeCN, but with an additional weak signal at 2228 cm^{-1}, assigned to N$_2$O based on reported literature.[210]

The remainder of the reaction suspension was filtered and concentrated under vacuum to afford a colourless liquid that does not readily concentrate further. To this liquid, Et$_2$O (2 mL) was added, resulting in the formation of white crystals identified as Na(15c5)OTs by SCXRD. The crystals were washed with Et$_2$O (2 x 0.5 mL) and dried under vacuum. Yield = 175 mg (0.42 mmol, 84% with respect to TsCl).

8.6.42. Reaction of Na$_2$N$_2$O$_2$ with TsN$_3$ and 15-crown-5 in MeCN

In a vial, 15-crown-5 (220 mg, 1.00 mmol) was dissolved in MeCN (1 mL). To this solution, anhydrous Na$_2$N$_2$O$_2$ (53 mg, 0.50 mmol) was added, and the mixture stirred.

In a separate vial, TsCl (95 mg, 0.50 mmol) was dissolved in MeCN (1 mL). To this solution, NaN$_3$ (65 mg, 1.0 mmol) was added, and the mixture stirred for 18 hours. The resulting suspension was filtered, and the filtrate added dropwise to the stirred mixture of 15-crown-5 and Na$_2$N$_2$O$_2$. The resulting reaction mixture continued stirring, and aliquots of the supernatant were taken for IR analysis after 10 minutes, 5 hours and 24 hours. After 10 minutes, the reaction solution still contains largely unreacted TsN$_3$ (ν/cm^{-1} = 2134 cm^{-1}), with two weaker absorptions in the azide asymmetric stretch region at 2032 cm^{-1} and 2005 cm^{-1}. After 5 hours, both these signals have increase in intensity significantly, whilst the TsN$_3$ has been largely consumed. Additionally, a medium intensity absorption at 2228 cm^{-1},

attributed to N_2O, is detected. After 24 hours, the absorptions at 2032 cm^{-1} and 2005 cm^{-1} have further increased in intensity, whilst TsN_3 has been almost entirely consumed. The N_2O absorption has decreased in intensity, suspected to be the result of N_2O degassing out of solution.

9. References

1.   R. Huszank, L. Csedreki, Z. Kertész and Z. Török, *Journal of Radioanalytical and Nuclear Chemistry*, 2015, **307**, 341-346.

2.   D. W. Freitag and D. W. Richerson, *Opportunities for Advanced Ceramics to Meet the Needs of the Industries of the Future*, U.S. Advanced Ceramics Association, Oak Ridge National Laboratory, 1998.

3.   Y. Nishi and R. Doering, *Handbook of Semiconductor Manufacturing Technology*, Marcel Dekker, Inc., New York, 2000.

4.   F. L. Riley, *Journal of the American Ceramic Society*, 2000, **83**, 245-265.

5.   A. C. Filippou, P. Portius and G. Schnakenburg, *Journal of the American Chemical Society*, 2002, **124**, 12396-12397.

6.   P. Portius, A. C. Filippou, G. Schnakenburg, M. Davis and K.-D. Wehrstedt, *Angewandte Chemie International Edition*, 2010, **49**, 8013-8016.

7.   C. Domene, P. Portius, P. W. Fowler and L. Bernasconi, *Inorganic Chemistry*, 2013, **52**, 1747-1754.

8.   E. Wiberg and H. Michaud, *Zeitschrift für Naturforschung B*, 1954, **9**, 500-500.

9.   T. Curtius, *Berichte der deutschen chemischen Gesellschaft*, 1890, **23**, 3023-3033.

10.   W. Wislicenus, *Berichte der deutschen chemischen Gesellschaft*, 1892, **25**, 2084-2087.

11.   J. Thiele, *Berichte der deutschen chemischen Gesellschaft*, 1908, **41**, 2681-2683.

12.   S. Bräse and K. Banert, *Organic Azides Syntheses and Applications*, John Wiley & Sons, Ltd., 2010.

13.   S. B. Hendricks and L. Pauling, *Journal of the American Chemical Society*, 1925, **47**, 2904-2920.

14.   L. K. Frevel, *Journal of the American Chemical Society*, 1936, **58**, 779-782.

15.   G. Leibeling, S. Demeshko, B. Bauer‑Siebenlist, F. Meyer and H. Pritzkow, *European Journal of Inorganic Chemistry*, 2004, **2004**, 2413-2420.

16.   E. A. Betterton, *Critical Reviews in Environmental Science and Technology*, 2010, **33**, 423-458.

17.   E. F. V. Scriven and K. Turnbull, *Chemical Reviews*, 1988, **88**, 297-368.

18.   T. Curtius, *Journal für Praktische Chemie*, 1894, **50**, 275-294.

19.   A. Rauk and P. F. Alewood, *Canadian Journal of Chemistry*, 1977, **55**, 1498-1510.

20.   L. Horner and A. Christmann, *Angewandte Chemie International Edition in English*, 1963, **2**, 599-608.

21.   H. Staudinger and J. Meyer, *Helvetica Chimica Acta*, 1919, **2**, 635-646.

22.   Y. G. Gololobov and L. F. Kasukhin, *Tetrahedron*, 1992, **48**, 1353-1406.

23.   J. H. Boyer, *Journal of the American Chemical Society*, 1951, **73**, 5865-5866.

24.   R. Huisgen, *Angewandte Chemie International Edition in English*, 1963, **2**, 565-598.

25. R. M. Pike, N. Sobinski and P. J. McManus, *Journal of Organometallic Chemistry*, 1983, **253**, 183-216.

26. E. Ettenhuber and K. Rühlmann, *Chemische Berichte*, 1968, **101**, 743-750.

27. J. W. Connolly and G. Urry, *Inorganic Chemistry*, 1962, **1**, 718-719.

28. I. Langmuir, *Journal of the American Chemical Society*, 1919, **41**, 868-934.

29. C. A. Coulson, *Valence*, Oxford University Press, 2nd edn., 1961.

30. J. Hine, *Journal of the American Chemical Society*, 1950, **72**, 2438-2445.

31. M. Faraday, *Philosophical Transactions of the Royal Society of London*, 1821, **111**, 47-74.

32. H. Schäfer and J. Nickl, *Zeitschrift für anorganische und allgemeine Chemie*, 1953, **274**, 250-264.

33. R. S. Ghadwal, R. Azhakar and H. W. Roesky, *Accounts of Chemical Research*, 2012, **46**, 444-456.

34. M. Schmeisser and P. Voss, *Zeitschrift für anorganische und allgemeine Chemie*, 1964, **334**, 50-56.

35. J. Berzelius, *Kongliga Vetenskapsakademiens Handlingar*, 1824, 46-98.

36. L. M. Dennis and H. L. Hunter, *Journal of the American Chemical Society*, 1929, **51**, 1151-1154.

37. C. Winkler, *Journal für Praktische Chemie*, 1886, **34**, 177-229.

38. M. Pelletier, *Annales de chimie*, 1792, **1**.

39. J. W. Mellor, Longmans, Green and Co. LTD., 1927, vol. Volume VII, ch. Chapter XLVI Tin, pp. 276-483.

40. A. Libavius, *Praxis alchymiæ*, 1604.

41. J. W. Mellor, Longmans, Green and Co. LTD., 1927, vol. Volume VII, ch. Chapter XLVII Lead, pp. 484-888.

42. W. W. Fisher, *Journal of the Chemical Society, Transactions*, 1879, **35**, 282-285.

43. J. R. Koe, D. R. Powell, J. J. Buffy, S. Hayase and R. West, *Angewandte Chemie International Edition*, 1998, **37**, 1441-1442.

44. J. Teichmann and M. Wagner, *Chemical Communications*, 2018, **54**, 1397-1412.

45. P. Jutzi, D. Kanne and C. Krüger, *Angewandte Chemie International Edition in English*, 1986, **25**, 164-164.

46. M. Denk, R. Lennon, R. Hayashi, R. West, A. V. Belyakov, H. P. Verne, A. Haaland, M. Wagner and N. Metzler, *Journal of the American Chemical Society*, 1994, **116**, 2691-2692.

47. M. Kira, S. Ishida, T. Iwamoto and C. Kabuto, *Journal of the American Chemical Society*, 1999, **121**, 9722-9723.

48. M. Driess, S. Yao, M. Brym, C. van Wüllen and D. Lentz, *Journal of the American Chemical Society*, 2006, **128**, 9628-9629.

49. C.-W. So, H. W. Roesky, J. Magull and R. B. Oswald, *Angewandte Chemie International Edition*, 2006, **45**, 3948-3950.

50. R. S. Ghadwal, H. W. Roesky, S. Merkel, J. Henn and D. Stalke, *Angewandte Chemie International Edition*, 2009, **48**, 5683-5686.

51. E. Amberger, R. Römer and A. Layer, *Journal of Organometallic Chemistry*, 1968, **12**, 417-423.

52. H. Gilman and C. L. Smith, *Journal of Organometallic Chemistry*, 1968, **14**, 91-101.

53. P. Jutzi, A. Mix, B. Rummel, W. W. Schoeller, B. Neumann and H.-G. Stammler, *Science*, 2004, **305**, 849-851.

54. E. Lieber, C. N. R. Rao, T. S. Chao and C. W. W. Hoffman, *Analytical Chemistry*, 1957, **29**, 916-918.

55. D. I. Hoult and B. Bhakar, *Concepts in Magnetic Resonance*, 1997, **9**, 277-297.

56. H. Reich, Hans Reich's Collection. NMR Spectroscopy., https://organicchemistrydata.org/hansreich/resources/nmr/?page=07-multi-04-quadrupolar%2F).

57. (29Si) Silicon NMR, https://chem.ch.huji.ac.il/nmr/techniques/1d/row3/si.html, (accessed 20/09/2023).

58. R. S. Drago, *Physical Methods for Chemists*, Surfside Scientific Publishers, 1992.

59. A. P. Singh, R. S. Ghadwal, H. W. Roesky, J. J. Holstein, B. Dittrich, J.-P. Demers, V. Chevelkov and A. Lange, *Chemical Communications*, 2012, **48**.

60. S. S. Sen, H. W. Roesky, D. Stern, J. Henn and D. Stalke, *Journal of the American Chemical Society*, 2009, **132**, 1123-1126.

61. T. Böttcher, S. Steinhauer, B. Neumann, H. G. Stammler, G. V. Röschenthaler and B. Hoge, *Chem. Commun.*, 2014, **50**, 6204-6206.

62. G. Maier, J. Glatthaar and H. P. Reisenauer, *Chemische Berichte*, 1989, **122**, 2403-2405.

63. G. Maier, H. P. Reisenauer and J. Glatthaar, *Organometallics*, 2000, **19**, 4775-4783.

64. G. Maier and J. Glatthaar, in *Organosilicon Chemistry I: From Molecules to Materials*, eds. N. Auner and J. Weis, VCH Verlagsgesellschaft, Weinheim, 1994, pp. 131-138.

65. A. Kuhn and W. Sander, *Organometallics*, 1998, **17**, 248-254.

66. A. I. Al-Mansour, S. S. Al-Showiman and I. M. Al-Najjar, *Spectrochimica Acta Part A: Molecular Spectroscopy*, 1988, **44**, 643-646.

67. A. I. Al-Mansour, S. S. Al-Showiman and I. M. Al-Najjar, *Inorganica Chimica Acta*, 1987, **134**, 275-278.

68. J. B. Tice, C. J. Ritter, A. V. G. Chizmeshya, B. Forrest, L. Torrison, T. L. Groy and J. Kouvetakis, *Applied Organometallic Chemistry*, 2008, **22**, 451-459.

69. H.-W. Lerner, N. Wiberg and K. Polborn, *Zeitschrift für Naturforschung B*, 2002, **57**, 1199-1206.

70. U. Wachtler, W. Malisch, E. Kolba and J. Matreux, *Journal of Organometallic Chemistry*, 1989, **363**, C36-C40.

71. P. Hädinger and A. Hinz, *European Journal of Inorganic Chemistry*, 2022, **2022**.

72. W. T. Reichle, *Inorganic Chemistry*, 1964, **3**, 402-406.

73. B. Peerless, Doctor of Philosophy, The University of Sheffield, 2017.

74. J. Glatthaar, Justus Liebig University Giessen, 2002.

75. C. Zhang, P. Patschinski, D. S. Stephenson, R. Panisch, J. H. Wender, M. C. Holthausen and H. Zipse, *Phys. Chem. Chem. Phys.*, 2014, **16**, 16642-16650.

76.   E. A. V. Ebsworth and J. J. Turner, *Transactions of the Faraday Society*, 1964, **60**, 256-263.

77.   V. M. Vorotyntsev, G. M. Mochalov and O. V. Nipruk, *Russian Journal of Applied Chemistry*, 2001, **74**, 621-625.

78.   H. Sussek, F. Stowasser, H. Pritzkow and R. A. Fischer, *European Journal of Inorganic Chemistry*, 2000, **2000**, 455-461.

79.   Bis(2,6-diisopropylphenyl)carbodiimide, https://www.tcichemicals.com/GB/en/p/B2756, (accessed 23/05/2023).

80.   1-Bromo-4-tert-butylbenzene, https://www.fishersci.co.uk/shop/products/1-bromo-4-tert-butylbenzene-97-thermo-scientific-1/10082850, (accessed 23/05/2023).

81.   M. Jones, MChem, The University of Sheffield, 2022.

82.   N. Wiberg, P. Karampatses, E. Kühnel, M. Veith and V. Huch, *Zeitschrift für anorganische und allgemeine Chemie*, 1988, **562**, 91-101.

83.   P. P. Samuel, R. Azhakar, R. S. Ghadwal, S. S. Sen, H. W. Roesky, M. Granitzka, J. Matussek, R. Herbst-Irmer and D. Stalke, *Inorganic Chemistry*, 2012, **51**, 11049-11054.

84.   F. M. Mück, A. Ulmer, J. A. Baus, C. Burschka and R. Tacke, *European Journal of Inorganic Chemistry*, 2015, **2015**, 1860-1864.

85.   F. M. Mück, J. A. Baus, A. Ulmer, C. Burschka and R. Tacke, *European Journal of Inorganic Chemistry*, 2016, **2016**, 1660-1670.

86.   M. K. Bisai, V. Sharma, R. G. Gonnade and S. S. Sen, *Organometallics*, 2021, **40**, 2133-2138.

87.   Y.-L. Shan, B.-X. Leong, Y. Li, R. Ganguly and C.-W. So, *Inorganic Chemistry*, 2017, **56**, 1609-1615.

88.   W. R. Carpenter, *Applied Spectroscopy*, 1963, **17**, 70-72.

89.   R. H. Nuttall, E. R. Roberts and D. W. A. Sharp, *Spectrochimica Acta*, 1961, **17**, 947-952.

90.   D. Gau, R. Nougué, N. Saffon‑Merceron, A. Baceiredo, A. De Cózar, F. P. Cossío, D. Hashizume and T. Kato, *Angewandte Chemie International Edition*, 2016, **55**, 14673-14677.

91.   T. Sheradsky, in *The chemistry of the azido group*, ed. S. Patai, Interscience Publishers, London, 1971, DOI: 10.1002/SERIES1078, ch. 6, pp. 331-395.

92.   H. Bretschneider and H. Hörmann, *Monatshefte für Chemie*, 1953, **84**, 1021-1032.

93.   R. Adams and D. C. Blomstrom, *Journal of the American Chemical Society*, 1953, **75**, 3405-3408.

94.   G. Barger and A. J. Ewins, *J. Chem. Soc., Trans.*, 1910, **97**, 2253-2261.

95.   P. A. S. Smith, J. H. Hall and R. O. Kan, *Journal of the American Chemical Society*, 1962, **84**, 485-489.

96.   M. O. Forster and K. A. N. Rao, *J. Chem. Soc.*, 1926, **129**, 1943-1951.

97.   I. Ugi, H. Perlinger and L. Behringer, *Chemische Berichte*, 1958, **91**, 2330-2336.

98.   H. Rathsburg, *Berichte der deutschen chemischen Gesellschaft, B: Abhandlungen*, 1921, **54**, 3183-3184.

99.   M. Tamm, S. Randoll, T. Bannenberg and E. Herdtweck, *Chemical Communications*, 2004, DOI: 10.1039/b401041h.

100. M. Denk, R. K. Hayashi and R. West, *Journal of the American Chemical Society*, 1994, **116**, 10813-10814.

101. D. Arquier, G. Calleja, M. Granier, G. Cerveau and R. J. P. Corriu, *Comptes Rendus Chimie*, 2008, **11**, 1277-1282.

102. S.-G. Lee, B.-Y. Lee, M. Hwang, H. Cho, H.-C. Kim and H. Sohn, *Journal of the Chosun Natural Science*, 2011, **4**, 282-288.

103. D. Y. Zhinkin, Y. M. Varezhkin and M. M. Morgunova, *Russian Chemical Reviews*, 1980, **49**, 1149-1980.

104. H. Zhu, Z. Yang, J. Magull, H. W. Roesky, H.-G. Schmidt and M. Noltemeyer, *Organometallics*, 2005, **24**, 6420-6425.

105. H. W. Lerner, M. Bolte, K. Schurz, N. Wiberg, G. Baum, D. Fenske, J. W. Bats and M. Wagner, *European Journal of Inorganic Chemistry*, 2006, **2006**, 4998-5005.

106. P. J. Wheatley, *J. Chem. Soc.*, 1962, **0**, 1721-1724.

107. P. Kosse and E. Popowski, *Zeitschrift für anorganische und allgemeine Chemie*, 1992, **613**, 137-148.

108. W. Clegg, U. Klingebiel, C. Krampe and G. M. Sheldrick, *Zeitschrift für Naturforschung B*, 1980, **35**, 275-281.

109. A. Rammo, *Journal of Organometallic Chemistry*, 2011, **696**, 1445-1449.

110. M. V. Und and A. Rammo, *Phosphorus, Sulfur, and Silicon and the Related Elements*, 1997, **123**, 75-87.

111. M. Veith, A. Rammo and M. Gießelmann, *Zeitschrift für anorganische und allgemeine Chemie*, 1998, **624**, 419-424.

112. D. Mootz, J. Fayos and A. Zinnius, *Angewandte Chemie*, 1972, **84**, 27-28.

113. H. Rosenberg, T.-T. Tsai, W. W. Adams, M. T. Gehatia, A. V. Fratini and D. R. Wiff, *Journal of the American Chemical Society*, 1976, **98**, 8083-8087.

114. J. Schneider, E. Popowski, K. Junge and H. Reinke, *Zeitschrift für anorganische und allgemeine Chemie*, 2001, **627**, 2680-2692.

115. B. Jaschke, R. Herbst-Irmer, U. Klingebiel, P. Neugebauer and T. Pape, *Journal of the Chemical Society, Dalton Transactions*, 1998, DOI: 10.1039/a806267f, 2953-2954.

116. B. Tecklenburg, U. Klingebiel, M. Noltemeyer and D. Schmidt-Base, *CSD Communication*, 1994.

117. T. Müller, Y. Apeloig, I. Hemme, U. Klingebiel and M. Noltemeyer, *Journal of Organometallic Chemistry*, 1995, **494**, 133-142.

118. F. W. Bergstrom and W. C. Fernelius, *Chemical Reviews*, 1933, **12**, 43-179.

119. SDBSWeb, https://sdbs.db.aist.go.jp/sdbs/cgi-bin/landingpage?sdbsno=5295, (accessed 16/09/2023).

120. B. Lyhs, D. Bläser, C. Wölper, S. Schulz, R. Haack and G. Jansen, *Inorganic Chemistry*, 2013, **52**, 7236-7241.

121. D. Enright, S. Gambarotta, G. P. A. Yap and P. H. M. Budzelaar, *Angewandte Chemie International Edition*, 2002, **41**, 3873-3876.

122. S. C. Bart, K. Chłopek, E. Bill, M. W. Bouwkamp, E. Lobkovsky, F. Neese, K. Wieghardt and P. J. Chirik, *Journal of the American Chemical Society*, 2006, **128**, 13901-13912.

123. A. P. Singh, H. W. Roesky, E. Carl, D. Stalke, J.-P. Demers and A. Lange, *Journal of the American Chemical Society*, 2012, **134**, 4998-5003.

124. R. S. Ghadwal, K. Pröpper, B. Dittrich, P. G. Jones and H. W. Roesky, *Inorganic Chemistry*, 2010, **50**, 358-364.

125. M. Novák, H. Hošnová, L. Dostál, B. Glowacki, K. Jurkschat, A. Lyčka, Z. Ruzickova and R. Jambor, *Chemistry - A European Journal*, 2017, **23**, 3074-3083.

126. G. P. A. Yap and S. Gambarotta, *CSD Communication*, 1999.

127. J. I. Schweizer, M. G. Scheibel, M. Diefenbach, F. Neumeyer, C. Würtele, N. Kulminskaya, R. Linser, N. Auner, S. Schneider and M. C. Holthausen, *Angewandte Chemie*, 2016, **128**, 1814-1818.

128. F. Meyer-Wegner, A. Nadj, M. Bolte, N. Auner, M. Wagner, M. C. Holthausen and H.-W. Lerner, *Chemistry - A European Journal*, 2011, **17**, 4715-4719.

129. L. Troost and P. Hautefeuille, *Annales de chimie et de physique*, 1876, **5**, 452-476.

130. L. Gattermann and K. Weinlig, *Berichte der deutschen chemischen Gesellschaft*, 1894, **27**, 1943-1948.

131. J. W. Mellor, Longmans, Green and Co. LTD., 1930, vol. Volume VI, ch. Chapter XL Silicon, pp. 135-992.

132. K. Naumann, G. Zon and K. Mislow, *Journal of the American Chemical Society*, 1969, **91**, 7012-7023.

133. R. C. Taylor, B. A. Scott, S. T. Lin, F. LeGoues and J. C. Tsang, *MRS Proceedings*, 1986, **77**.

134. R. C. Taylor and B. A. Scot, *MRS Proceedings*, 1987, **105**.

135. J. Tillmann, L. Meyer, J. I. Schweizer, M. Bolte, H.-W. Lerner, M. Wagner and M. C. Holthausen, *Chemistry - A European Journal*, 2014, **20**, 9234-9239.

136. J. Tillmann, M. Moxter, M. Bolte, H.-W. Lerner and M. Wagner, *Inorganic Chemistry*, 2015, **54**, 9611-9618.

137. R. A. Benkeser, K. M. Voley, J. B. Grutzner and W. E. Smith, *Journal of the American Chemical Society*, 1970, **92**, 697-698.

138. H. Oehme and H. Weiss, *Journal of Organometallic Chemistry*, 1987, **319**, C16-C18.

139. B. Peerless, T. Keane, A. J. H. M. Meijer and P. Portius, *Chemical Communications*, 2015, **51**, 7435-7438.

140. Z. Smallwood, Doctor of Philosophy, The University of Sheffield, 2019.

141. Y. Le Page, E. J. Gabe, Y. Wang, L. R. C. Barclay and H. L. Holm, *Acta Crystallographica Section B Structural Crystallography and Crystal Chemistry*, 1980, **36**, 2846-2848.

142. J. B. Lambert, J. L. Pflug, A. M. Allgeier, D. J. Campbell, T. B. Higgins, E. T. Singewald and C. L. Stern, *Acta Crystallographica Section C Crystal Structure Communications*, 1995, **51**, 713-715.

143. CCDC WebCSD Structure Search, https://www.ccdc.cam.ac.uk/structures/WebCSD/StructureSearch).

144. A. Hantzsch, *Berichte der deutschen chemischen Gesellschaft*, 1903, **36**, 2056-2058.

145. J. Lifschitz, *Berichte der deutschen chemischen Gesellschaft*, 1915, **48**, 410-420.

146. T. Curtius, A. Darapsky and E. Müller, *Berichte der deutschen chemischen Gesellschaft*, 1915, **48**, 1614-1634.

147. R. Huisgen and I. Ugi, *Angewandte Chemie*, 1956, **68**, 705-706.

148. R. Huisgen and I. Ugi, *Chemische Berichte*, 1957, **90**, 2914-2927.

149. I. Ugi and R. Huisgen, *Chemische Berichte*, 1958, **91**, 531-537.

150. I. Ugi, H. Perlinger and L. Behringer, *Chemische Berichte*, 1958, **91**, 2324-2329.

151. P. Carlqvist, H. Östmark and T. Brinck, *The Journal of Physical Chemistry A*, 2004, **108**, 7463-7467.

152. C. Zhang, C. Sun, B. Hu and M. Lu, *Journal of Energetic Materials*, 2015, **34**, 103-111.

153. R. N. Butler, A. Fox, S. Collier and L. A. Burke, *Journal of the Chemical Society, Perkin Transactions 2*, 1998, DOI: 10.1039/a804040k, 2243-2248.

154. S. Ek, S. Rehn, L. Y. Wahlström and H. Östmark, *Journal of Heterocyclic Chemistry*, 2013, **50**, 261-267.

155. A. Hammerl, T. M. Klapötke and P. Schwerdtfeger, *Chemistry - A European Journal*, 2003, **9**, 5511-5519.

156. A. Hammerl and T. M. Klapötke, *Inorganic Chemistry*, 2002, **41**, 906-912.

157. Y. Bi, W. Liao, G. Xu, R. Deng, M. Wang, Z. Wu, S. Gao and H. Zhang, *Inorganic Chemistry*, 2010, **49**, 7735-7740.

158. K. Banert and T. Pester, *Angewandte Chemie International Edition*, 2020, **59**, 12315-12320.

159. M. T. Nguyen, M. A. McGinn, A. F. Hegarty and J. Elguéro, *Polyhedron*, 1985, **4**, 1721-1726.

160. M. T. Nguyen and T.-K. Ha, *Chemical Physics Letters*, 2001, **335**, 311-320.

161. M.-T. Nguyen, M. Sana, G. Leroy and J. Elguero, *Canadian Journal of Chemistry*, 1983, **61**, 1435-1439.

162. M. N. Glukhovtsev, P. v. R. Schleyer and C. Maerker, *The Journal of Physical Chemistry*, 1993, **97**, 8200-8206.

163. M. Rahm and T. Brinck, *Chemistry - A European Journal*, 2010, **16**, 6590-6600.

164. A. Vij, J. G. Pavlovich, W. W. Wilson, V. Vij and K. O. Christe, *Angewandte Chemie International Edition*, 2002, **41**, 3051-3054.

165. H. Östmark, S. Wallin, T. Brinck, P. Carlqvist, R. Claridge, E. Hedlund and L. Yudina, *Chemical Physics Letters*, 2003, **379**, 539-546.

166. L. Belau, Y. Haas and S. Zilberg, *The Journal of Physical Chemistry A*, 2004, **108**, 11715-11720.

167. B. Bazanov, U. Geiger, R. Carmieli, D. Grinstein, S. Welner and Y. Haas, *Angewandte Chemie International Edition*, 2016, **55**, 13233-13235.

168. B. Bazanov, U. Geiger, D. Grinstein, S. Welner and Y. Haas, *The Journal of Physical Chemistry A*, 2017, **121**, 6727-6731.

169. C. Zhang, C. Sun, B. Hu, C. Yu and M. Lu, *Science*, 2017, **355**, 374-376.

170. Y. Shao, G. Wang, P. Wang, X. Zhang, Z. Jiang and M. Lu, *Chinese Journal of Energetic Materials*, 2018, **26**, 925-930.

171. Y. Xu, L. Ding, F. Yang, D. Li, P. Wang, Q. Lin and M. Lu, *Chemical Engineering Journal*, 2022, **429**.

172. S. Jiang, Q. Du, Y. Xu, Q. Lin, M. Lu and P. Wang, *Crystal Growth & Design*, 2022, **22**, 7062-7073.

173. F. Shang, R. Liu, J. Liu, P. Zhou, C. Zhang, S. Yin and K. Han, *The Journal of Physical Chemistry Letters*, 2020, **11**, 1030-1037.

174. *France Pat.*, 2023.

175. C. Yang, C. Zhang, Z. Zheng, C. Jiang, J. Luo, Y. Du, B. Hu, C. Sun and K. O. Christe, *Journal of the American Chemical Society*, 2018, **140**, 16488-16494.

176. L. Tian, Y. Xu, Q. Lin, P. Wang and M. Lu, *Chemistry – An Asian Journal*, 2019, **14**, 2877-2882.

177. Y. Xu, J. Zhou, D. Li, P. Wang, Q. Lin and M. Lu, *Crystal Growth & Design*, 2023, **23**, 811-819.

178. L. P. Cheng and X. Q. Li, *Journal of Molecular Modeling*, 2006, **12**, 805-811.

179. M. Noyman, S. Zilberg and Y. Haas, *The Journal of Physical Chemistry A*, 2009, **113**, 7376-7382.

180. I. Kang, S. G. Cho, H. W. Lee and K. Yang, *Bulletin of the Korean Chemical Society*, 2017, **38**, 1474-1480.

181. M. Begtrup and P. Vedsø, *J. Chem. Soc., Perkin Trans. 1*, 1995, DOI: 10.1039/p19950000243, 243-247.

182. V. M. Vinogradov, I. L. Dalinger, B. I. Ugrak and S. A. Shevelev, *Mendeleev Communications*, 1996, **6**, 139-140.

183. G. Frison, G. Jacob and G. Ohanessian, *New J. Chem.*, 2013, **37**, 611-618.

184. Z. Xu, S. Jiang, T. Hou, X. Zhang, M. Lu and Y. Xu, *New Journal of Chemistry*, 2023, **47**, 5616-5620.

185. W. v. E. Doering and C. H. DePuy, *Journal of the American Chemical Society*, 1953, **75**, 5955-5957.

186. R. Sexton, A. E. Porter, S. Littlejohns and S. C. Thain, *Annals of Botany*, 1995, **75**, 337-342.

187. L. J. Aarons, J. A. Connor, I. H. Hillier, M. Schwarz and D. R. Lloyd, *Journal of the Chemical Society, Faraday Transactions 2*, 1974, **70**.

188. S. Roy, L. Rangasamy, A. Nouar, C. Koenig, V. Pierroz, S. Kaeppeli, S. Ferrari, M. Patra and G. Gasser, *Organometallics*, 2021, **40**, 2716-2723.

189. F. Ramirez and S. Levy, *The Journal of Organic Chemistry*, 1958, **23**, 2036-2037.

190. J. Zhang, M. Gandelman, L. J. W. Shimon and D. Milstein, *Organometallics*, 2008, **27**, 3526-3533.

191. X. Chen, Q. Jin, L. Wu, C. Tung and X. Tang, *Angewandte Chemie International Edition*, 2014, DOI: 10.1002/anie.201408422, n/a-n/a.

192. X. Zeng, H. Beckers, E. Bernhardt and H. Willner, *Inorganic Chemistry*, 2011, **50**, 8679-8684.

193. K. O. Christe, J. A. Boatz, M. Gerken, R. Haiges, S. Schneider, T. Schroer, F. S. Tham, A. Vij, V. Vij, R. I. Wagner and W. W. Wilson, *Inorganic Chemistry*, 2002, **41**, 4275-4285.

194. D. A. Judelson, Doctor of Philosophy, Brandeis University, 1981.

195. V. P. Nazaretyan and L. M. Yagupol'skii, *Zhurnal Organicheskoi Khimii*, 1978, **14**, 207.

196. F. Himo, Z. P. Demko, L. Noodleman and K. B. Sharpless, *Journal of the American Chemical Society*, 2003, **125**, 9983-9987.

197. V. Benin, P. Kaszynski and G. Radziszewski, *The Journal of Organic Chemistry*, 2002, **67**, 1354-1358.

198. C. L. Dwyer and C. W. Holzapfel, *Tetrahedron*, 1998, **54**, 7843-7848.

199. S. V. Dubiel and S. Zuffanti, *The Journal of Organic Chemistry*, 1954, **19**, 1359-1362.

200. H. Leuchs and G. Theodorescu, *Berichte der deutschen chemischen Gesellschaft*, 1910, **43**, 1239-1251.

201. G. Quadbeck and E. Röhm, *Chemische Berichte*, 1956, **89**, 1645-1648.

202. Y.-C. Liu, H.-L. Zhou, Y. Tang, Y. Li, J. Zhai, J.-C. Jiang, Z.-X. Xing and A.-C. Huang, *Journal of Thermal Analysis and Calorimetry*, 2022, **148**, 5039-5049.

203. M. N. Hughes, *Quarterly Reviews, Chemical Society*, 1968, **22**, 1-13.

204. R. K. Harris, E. D. Becker, S. M. Cabral de Menezes, R. Goodfellow and P. Granger, *Pure and Applied Chemistry*, 2001, **73**, 1795-1818.

205. G. R. Fulmer, A. J. M. Miller, N. H. Sherden, H. E. Gottlieb, A. Nudelman, B. M. Stoltz, J. E. Bercaw and K. I. Goldberg, *Organometallics*, 2010, **29**, 2176-2179.

206. G. M. Sheldrick, *Acta Crystallographica Section A Foundations of Crystallography*, 2008, **64**, 112-122.

207. O. V. Dolomanov, L. J. Bourhis, R. J. Gildea, J. A. K. Howard and H. Puschmann, *Journal of Applied Crystallography*, 2009, **42**, 339-341.

208. J. Nicks, MChem, The University of Sheffield, 2017.

209. SDBSWeb, https://sdbs.db.aist.go.jp/sdbs/cgi-bin/landingpage?sdbsno=1288, (accessed 05/09/2023).

210. M. E. Chacón Villalba, C. A. Franca and J. A. Güida, *Spectrochimica Acta Part A: Molecular and Biomolecular Spectroscopy*, 2017, **176**, 189-196.